TESIS DE LA UNIVERSIDAD DE ZARAGOZA

2021

50

Alejandro Calle Calderón

Phenology and fruit quality in sweet cherry (Prunus avium L.). Genetics, QTL analysis and marker assisted selection

Departamento
Bioquímica y Biología Molecular y Celular

Director/es
Wunsch Blanco, Ana

ISSN 2254-7606

Prensas de la Universidad
Universidad Zaragoza

ISSN 2254-7606

Universidad Zaragoza
1542

Tesis Doctoral

PHENOLOGY AND FRUIT QUALITY IN SWEET CHERRY (PRUNUS AVIUM L.). GENETICS, QTL ANALYSIS AND MARKER ASSISTED SELECTION

Autor

Alejandro Calle Calderón

Director/es

Wunsch Blanco, Ana

UNIVERSIDAD DE ZARAGOZA

Bioquímica y Biología Molecular y Celular

2019

Universidad de Zaragoza
Facultad de Ciencias

Centro de Investigación y Tecnología
Agroalimentaria de Aragón
Unidad de Hortofruticultura

DOCTORAL THESIS

PHENOLOGY AND FRUIT QUALITY IN SWEET CHERRY (*PRUNUS AVIUM* L.). GENETICS, QTL ANALYSIS AND MARKER ASSISTED SELECTION.

Presentada por Alejandro Calle Calderón para optar al grado de doctor por la Universidad de Zaragoza

Dirigida por:
Ana Wünsch Blanco

Zaragoza, Septiembre 2019

Agradecimientos

Tras cuatro años en el CITA y después de pasar tanto tiempo dedicado a esta tesis son muchas las personas a las que me gustaría agradecer su apoyo tanto en lo profesional como personal.

En primer lugar, me gustaría agradecer a la Dra. Ana Wünsch por la dirección de esta tesis. Gracias Ana por tu dedicación, paciencia, esfuerzo, trato personal, disponibilidad a aceptar mis sugerencias y ánimos durante estos años.

Gracias a la Dra. María Luisa Peleato por su atención y amabilidad como tutora.

I gratefully acknowledge Prof. Amy Iezzoni and Dr. Lichun Cai their hospitality during my stay at Michigan State University and their collaborations in the co-direction of Chapters 2, 3 and 5.

Gracias al Dr. Jérôme Grimplet por su ayuda en la implementación de las herramientas bioinformáticas, y su colaboración en la codirección del Capítulo 4.

I gratefully acknowledge to Dr. Elisabeth Dirlewanger and Dr. Loïck Le Dantec for providing the 'Regina' sweet cherry genome and annotation file used in Chapter 4.

Gracias a la Dra. Margarita López Corrales, Paco Balas y Dr. Manuel Serradilla por la colaboración en el Capítulo 5, la cesión de los datos fenotípicos y genotípicos de la población 'Ambrunés' × 'Sweetheart' y sus comentarios y sugerencias.

Gracias al Dr. Manuel Joaquín Serradilla por su la codirección del capítulo 7 y su hospitalidad durante mi estancia en el CICYTEX. Gracias también por 'convencerme' para aceptar esta beca, te estaré eternamente agradecido.

Gracias a todos los técnicos y analistas por su ayuda en el trabajo de campo y laboratorio, especialmente a Arantxa, José Ángel, Teresa y Rosa. Gracias en especial a Rosa, por su disponibilidad siempre a ayudar y por tus consejos de campo.

Gracias a todos los miembros de la Unidad de Hortofruticultura del CITA; personal de campo, laboratorio, administración e investigadores por los buenos momentos que hemos pasado.

Gracias a la Dra. Aurora Díaz por su fidelidad a la hora de comer que me ha salvado de muchos días de aburrimiento (aunque algunos días hayas acabado desmotivándome muchísimo).

Quiero también agradecer muy especialmente a todos los compañeros de la Sala de Becarias. Gracias a Paco, Lucia, Noemí y Odibert por hacerme tan fácil aquellos primeros días por aquí. Gracias también a mis post-doc favoritas, Erica, Bea, Patricia y Oreto que siempre han sabido avisarme y prepararme ante las diferentes etapas del doctorado. Gracias a Sara y Brenda por aguantarme todos estos días, por todos los momentos de risa que hemos pasado y por esos momentos a lo Ana Rosa y Susana Griso comentando los casos más morbosos de la actualidad. Gracias también al resto de compañeros y amigos de CITA y Aula Dei (Fran, Irene, Jorge, Wafa, Octavio, Yuri,

Manuel, Inés, … seguro que me falta alguno) por lo bien que nos lo hemos pasado y por compartir nuestras penas y alegrías.

Gracias a Álvaro y Daniel, que a pesar de que ninguno de los dos son mis amigos, uno porque yo no quiero y el otro por él no quiere, nos lo hemos pasado muy bien tanto dentro como fuera del CITA, la mayoría de veces haciendo lo que más nos gusta 'criticar' (pero en el buen plan).

Gracias a mis compañeros de piso por esas noches de ludopatía, momentos post-cena y batallas de laser tag.

Y por último, gracias a mis padres por haberme apoyado siempre y guiarme por el camino del esfuerzo.

Este trabajo ha sido financiado mediante los proyectos INIA RTA2012-00103-00-00, RTA2015-00027-00-00, RFP2012-00029-C03-01 y RFP2015-00015-00-00, los Grupos de Investigación Reconocidos por el Gobierno de Aragón 'Biología del desarrollo y material vegetal en frutales' (2015-2017) y 'Fruticultura. Caracterización, adaptación y mejora genética' (2017-2019) y un contrato de investigador predoctoral concedido a Alejandro Calle Calderón en la convocatoria de 'Subvenciones destinadas a la contratación de personal investigador en formación 2015-2019' del Departamento de Innovación, Investigación y Universidad del Gobierno de Aragón.

INDEX

RESUMEN

La cereza (*Prunus avium* L.) es una fruta muy apreciada, con un alto valor nutricional y de interés económico, cuyo cultivo ha aumentado durante los últimos años. Para poder proporcionar nuevos cultivares adaptados a las demandas de los productores y consumidores, y que puedan hacer frente a desafíos como el calentamiento global, es necesario desarrollar herramientas que puedan ayudar a optimizar el proceso de mejora. Con este propósito, el objetivo de este trabajo es investigar la genética de algunos caracteres fenológicos y de calidad de fruto de interés en cerezo y avanzar en el conocimiento de los mecanismos biológicos que los regulan. Para alcanzar este objetivo se han utilizado siete familias intra-específicas de cerezo que derivan de polinizaciones cruzadas y autopolinizaciones de material vegetal local ('Cristobalina' y 'Ambrunés') que proporcionan variabilidad fenotípica adicional para éstos caracteres. Estas familias se genotiparon utilizando las plataformas genómicas 'RosBREED cherry 6K y/o 15 SNP Illumina® Infinium', lo que permitió desarrollar cinco mapas genéticos de alta densidad, que fueron utilizados para analizar la sintenia entre cerezo y melocotonero (*P. persica*), y para análisis de QTLs. Las siete familias fueron además fenotipadas para caracteres fenológicos (fecha de floración, período de desarrollo de fruto y fecha de maduración), y caracteres de calidad del fruto [firmeza, tamaño, color, contenido en sólidos solubles, acidez titulable y contenido en polifenoles (antocianinas y ácidos fenólicos)]. Estos datos se utilizaron para realizar análisis anuales y/o multianuales de QTLs utilizando diferentes estrategias de mapeo, el análisis de familias únicas se realizó utilizando MapQTL®, y el análisis de varias familias de manera combinada se realizó utilizando FlexQTL™. Estos análisis permitieron identificar QTLs principales y menores para todos los caracteres investigados, validar algunos QTLs previamente descritos para los mismos caracteres, identificar nuevos QTLs para caracteres estudiados por primera vez, e identificar nuevas variantes de QTLs de interés para la mejora. Se identificaron QTLs principales en los grupos de ligamientos (GL) 1 y 2 para fecha de floración, en el GL4 para el período de desarrollo de fruto y fecha de maduración, en los GL 1 y 2 para tamaño de fruto, en los GL 1 y 4 para firmeza, en el GL4 para el contenido en sólidos solubles, en GL6 para acidez titulable, en GL3 para color de fruto y contenido en antocianinas, y en GL1 para el contenido en ácidos fenólicos. Haplotipos de interés para la mejora en estos QTLs principales fueron identificados en algunos cultivares, como en los GL 1 y 2 de 'Cristobalina' para bajos requerimientos de frío y floración temprana, en el GL4 de 'Cristobalina' y 'Burlat' para período de desarrollo de fruto corto y fecha de maduración temprana, y en el GL1 de 'Ambrunés' para tamaño y firmeza. El período de desarrollo de fruto destacó como un carácter esencial para la fenología y la calidad del fruto, ya que la fecha de maduración, la firmeza y el contenido de sólidos solubles están correlacionados con el desarrollo de fruto y se asociaron a los mismos QTLs. La identificación de QTLs principales permitió proponer y confirmar genes candidatos para estos caracteres en estos QTL, y los genes candidatos para fecha de floración fueron investigados. Utilizando la secuencia del genoma de 'Regina', genes candidatos para requerimientos de frío y fecha de floración, *PavDAM*, ortólogos a los genes *DAM* de *P. persica* y *P. mume*, fueron identificados y caracterizados en el QTL principal de fecha de floración en GL1. La comparación de secuencias de los genes *PavDAM* de varios cultivares de cerezo con diferentes requerimientos térmicos y fechas de floración, permitió detectar polimorfismos que pueden estar asociados a las diferencias fenotipicas, y una deleción en el promotor de los *PavDAM* (DPD) en 'Cristobalina' que está asociado a floración temprana. También se desarrolló un marcador de ADN para esta mutación, que puede ser usado para la selección asistida por marcadores de floración temprana en 'Cristobalina'.

SUMMARY

Sweet cherry (*Prunus avium* L.) is a very appreciated fruit, with a high nutritional value and economic interest, which cultivation has increased during last years. In order to provide new cultivars adapted to producer and consumer demands, and that confront challenges like global warming, is necessary to develop tools that can help optimizing the breeding process. For this purpose, the objective of this work is to investigate the genetics of some relevant phenology and fruit quality traits of sweet cherry and to advance in the understanding of the biological mechanisms that regulate them. To achieve this goal, seven sweet cherry intraspecific populations that derive from cross- and self-pollinations of local plant material ('Cristobalina' and 'Ambrunés'), and that provide additional phenotypic variation for these traits, were used. These populations were genotyped with the whole genome RosBREED cherry 6K and/or 15K Illumina® Infinium SNP arrays, which allowed developing five high-density genetic maps that were then used for analyzing synteny between sweet cherry and peach (*P. persica*) and for QTL analyses. The seven populations were also phenotyped for phenology traits (bloom time, fruit development period and maturity date), and for fruit quality traits [firmness, size, color, solid soluble content, titratable acidity and polyphenols (anthocyanins and phenolic acids) content]. These data were used to perform single and/or multi-year QTL analysis, using different mapping strategies, which included single bi-parental analysis with MapQTL®, or combined multi-parental populations using FlexQTL™. These analyses allowed identifying major and minor QTLs for all the traits investigated, validating some QTLs previously reported for the same traits, reporting new QTLs for newly investigated traits, and identifying new QTLs variants of breeding interest. Major QTLs were identified on linkage groups (LGs) 1 and 2 for bloom time, on LG4 for fruit development period and maturity date, on LGs 1 and 2 for fruit size, on LGs 1 and 4 for fruit firmness, on LG4 for solid soluble content, on LG6 for titratable acidity, on LG3 for fruit color and anthocyanins content, and on LG1 for phenolic acids content. Relevant QTL haplotypes for breeding purposes were identified in these major QTLs in some cultivars, like for low chilling and early blooming in 'Cristobalina' LGs 1 and 2, for short development period and early maturity date in 'Cristobalina' and 'Burlat' LG4, and in 'Ambrunés' LG1 for size and firmness. Fruit development period reveal itself as an essential trait for phenology and fruit quality, as maturity date, firmness and soluble solids contents were correlated with fruit development and were associated to the same QTLs. The identification of major QTLs allowed proposing and confirming candidate genes for these traits at these QTLs, and candidate genes for bloom time were investigated. Using the 'Regina' sweet cherry genome sequence, candidate genes for chilling requirements and bloom time, *PavDAM* genes, orthologous to *P. persica* and *P. mume DAM* genes, were identified and characterized in the major bloom time QTL on LG1. Sequence comparison of *PavDAM* genes of various sweet cherry cultivars with different chilling requirements and bloom times allowed detecting sequence polymorphisms that may be associated to their phenotypic differences, and a deletion in the 'Cristobalina' *PavDAM* promoter (DPD) that is associated to early blooming. A DNA marker for this mutation, that can be used for marker-assisted selection of early blooming from 'Cristobalina', was also developed.

CHAPTER 1

INTRODUCTION

SWEET CHERRY

Taxonomy

Sweet cherry (*Prunus avium* L.) is a stone fruit crop belonging to Rosaceae family. Sweet cherry trees are mainly cultivated for their edible fruits, although wild types, or mazzards, are also used for timber production and ornamental practices (Webster, 1996). Sweet cherry belongs to the *Prunus* genus, which includes more than 200 species divided into six different subgenus: *Amygdalus*, *Cerasus*, *Laurocerasus*, *Lithocerasus*, *Padus* and *Prunus* (Potter et al., 2007). Within the *Prunus* genus, other species of economic relevance are almond (*Prunus amygdalus* Batsch) and peach (*Prunus persica* L.) belonging to *Amygdalus* subgenus, and apricot (*Prunus armeniaca* L.) and plums (*Prunus domestica* L. and *Prunus salicina* Lind), both belonging to *Prunus* subgenus. Cherries belong to the *Cerasus* subgenus. Other than sweet cherry, these include sour cherry (*Prunus cerasus* L.), which fruits are mainly used for transformation, Santa Lucía cherry (*Prunus mahaleb* L.) that has been traditionally used as sweet cherry rootstock, and *Prunus fructicosa* Pall. that is considered an ancestor of sweet and sour cherries (Fogle, 1975).

Sweet cherry has a basic chromosome number of x = 8. This specie presents a diploid genome (2n = 2x = 16) although triploid and tetraploid forms are found (Fogle, 1975). *Prunus cerasus* L. and *Prunus fruticose* Pall. are tetraploid (2n = 4x = 32).

Botany

Sweet cherry is a vigorous deciduous tree that can reach 20 meters in height. It presents smooth reddish-brown bark that frequently peels off on old trees. Leaves are simple, oval with short tip, large (6 to 15 cm of length and 3 to 7 cm of width) and characterized by coarse and irregular toothing (Webster, 1996). The leaf stalk length is about 3 cm and presents red glands near the lamina. Flowers are hermaphrodite and form singly in the axis of one-year wood or grouped (up to five) on older wood. Flowers have a white corolla of approximately 2.5 cm in diameter, with five sepals and five petals, from 30 to 36 stamens and a hairless pistil. The species exhibits gametophytic self-incompatibility (Herrero et al., 2017). Fruits are spherical drupes (approximately 2.0-3.5 cm in diameter), hairless and present a bright skin that range from yellow to black, although

vast majority of cultivars present red-mahogany color. The pit is globose and smooth, approximately of one third of the total fruit size.

Origin and distribution

Sweet cherry is believed to be originated in the region of Caspian and Black Seas that comprises northern Iran, Ukraine and countries south of Caucasus Mountains (Hedrick et al., 1915). Cherries are found all around Europe and it is believed that dissemination from the center of origin to Europe took place by birds prior to human migrations (Webster, 1996). Theoprastus, in 300 BC, reports first written references of cherry cultivations in the '*History of Plants*', although evidences of cherry consumption 4000 to 5000 years BC have been reported based on cherry pits found on prehistoric caves (Brown et al., 1996).

Cherries were initially cultivated by Albanians before Greek civilization that used it for wood and fruit production but the Romans, who regularly consumed cherries in their diet, facilitated cherry distribution through Europe including the Iberian Peninsula (Hedrick et al., 1915). The Roman writer Varro already described in the 1st century various grafting techniques and cherry cultivars. However, little is known about cherry development from Roman period up to 16th century, when cultivations increased especially in central Europe (Watkins, 1976). Following this growth, cherry cultivation was spread through Western Europe and individuals adapted to the climatic and agronomic condition of each growing area were selected in the different regions (Iezzoni et al., 2017). A few cultivars were taken to America in 19th century, and spread through the country by earlier settlers from east to the west coast (Brown et al., 1996; Faust and Surányi, 1997). Nowadays, more than 300 sweet cherry varieties are cultivated in more than 40 countries from temperate to subtropical regions (Quero-García et al., 2017).

Economic interest

World sweet cherry production has increased over 30% in the last two decades, reaching 2.4 M tons (in 416,000 ha) in 2017 (FAOSTAT, 2019). Sweet cherry is a relevant fruit crop, as it is the fourth largest stone fruit cultivated worldwide behind peach, plum and apricot. Turkey is the world leader sweet cherry producer (26%) followed by the USA, Iran, Uzbekistan, Chile, Italy and Spain, that all together represent the 40% of global production.

Spain is the seventh largest sweet cherry producer in the world and reached 114,433 tons in 2017 (MAPA, 2019). Cultivated area of sweet cherry was 27,600 ha in 2017, being the second cultivated stone fruit after peach, with mean yields of 4,146 kg/ha. Extremadura (7,523 ha; 40,503 tons) and Aragón (8,486 ha; 36,353 tons) are the two main producing regions. The Jerte Valley in Extremadura and Valdejalón and Caspe in Aragón concentrate almost 70% of national production. Other regions of relevant production in Spain are Cataluña, Comunidad Valenciana or Andalucia.

Sweet cherry cultivation in Spain

Sweet cherry cultivation in Spain began on calcareous terraces of mountain areas under dry conditions, resulting in trees having low production but good fruit quality (Negueroles, 2005). During the last decades, irrigation systems were introduced to increase yield, with a total amount of irrigated water that range from 2,500 to 5,500 m^3/ha depending on regions and growing season (Iglesias et al., 2016). The planting density is usually 4 × 3 to 5 × 3 m with approximately 600 trees/ha. The 'Spanish bush', which consists on induction of three or four separated branches by 90-120º from approximately 35 cm above the ground, is the most popular training system (Negueroles, 2005; Iglesias et al., 2016). This system results in trees that do not overlap, of about 2.5 m in height and exhibit good production and early yields. Sweet cherries are regularly grafted in 'Santa Lucía 64' (*Prunus mahaleb*) and 'Adara' (*Prunus cerarifera*), which are the most common rootstocks for their adaptation to soil condition of main cherry producing areas and for the promotion of early yields.

An important varietal renewal was carried out in Spain with the introduction of new varieties obtained from breeding programs of Canada, USA, France, Italy or Hungary (Iezzoni, 2008). These varieties have replaced the traditional cultivars in most orchards, except in some region such as the Jerte Valley (Cáceres) where local varieties ('Ambrunés', 'Pico Colorado', 'Pico Negro' and 'Pico Limón') are still used for production. Bred cultivars from early to late maturity date have been progressively introduced in Spain to widen the ripening period. Main used early maturity cultivars are 'Early Bigy', 'Early Lory' and 'Burlat' (Iglesias et al., 2016). 'Frisco', 'Chelan', 'Brooks', 'Giant Red', 'Celeste', '13S3-13', 'Samba', '4-84', 'Cristalina', 'Summit', 'Sunburst', and

'Sonata' are the main cultivars of medium season, while 'Skeena' and 'Sweetheart' are the two most important cultivars of late ripening.

SWEET CHERRY BREEDING

History

Until 1767, cherries were locally consumed and only the selection of local varieties propagated by seed was used (Brown et al., 1996). It was not until the beginning of the 20th century that cherry breeding started (Hedrick et al., 1915). First cherry breeding program were initiated in Geneva (USA) by 1911, and some years later, programs in Vineland and Summerland stations (Canada) were started. In Europe, first breeding programs were carried out at John Innes Institute by 1925 (Faust and Surányi, 1997). Today sweet cherry breeding is carried out in various private and public institutions and new cultivars are continuously being released. As a result, more than 230 new sweet cherry cultivars were released in the last two decades, most of them in Europe, North America and Asia (Sansavini and Lugli, 2008).

Breeding objectives

Several traits are targeted as sweet cherry breeding objectives in the different breeding programs (Dirlewanger et al., 2009; Quero-García et al., 2017; Wünsch, 2017; Dondini et al., 2018; Quero-García, 2019). Regular yields, superior fruit quality and self-compatible cultivars are considered main objectives in sweet cherry breeding (Dondini et al., 2018). Other relevant objectives like shortening juvenility period or the reduction of excessive tree vigor, by growing compact cultivars that will allow intensive growing are also considered (Bargioni, 1996; Kappel et al., 2012). Phenology related traits, mainly early and late cultivars, that enable the reduction of cherry seasonality, are also primary objectives in many breeding programs (Dondini et al., 2018). Cultivars with low chilling requirements are also gaining special attention in the recent years, in order to adapt cherries to current warming temperatures (Campoy et al., 2019), and to extend the growing area to regions with warmer winters.

Fruit quality traits like fruit size, firmness, color, sweetness and flavor are also main priority traits considered by breeders (Dirlewanger et al., 2009). Within these, fruit firmness and fruit size are the most important traits due to their relationship with consumer acceptance and post-harvest aptitude (Zheng et al., 2016). Relevant progress has been achieved regarding fruit size and firmness, with cultivars of outstanding fruit size (more than 12 g) and large firmness (Quero-García et al., 2017). Reduction of economic losses derived from fruit cracking is also a main objective of breeding programs. Despite the complexity of this phenomenon, different studies have been carried out to determine cracking susceptibility in cherry collections (Christensen, 1972; Meland et al., 2014). Although cultivars with total resistance to cracking are not known, cultivars as 'Regina' and 'Fermina' present low susceptibility and are potential parental for new cultivars highly resistance to cracking.

Resistance to biotic stresses are also fundamental traits considered by sweet cherry breeders (Quero-García et al., 2017; Dondini et al., 2018). Regarding tolerance or resistance to diseases, breeding has been limited because of the narrow genetic diversity and therefore low number of resistance alleles (Stegmeir et al., 2014). The most serious diseases and pests of sweet cherry are bacterial canker (caused by *Pseudomonas* spp.), brown rot (caused by *Monilinia* spp.), fruit fly (*Rhagoletis* spp.), black cherry aphid (*Myzus cerasi* Fab.) and the *Drosophila suzukii*.

Other traits relevant for the selection of new sweet cherry cultivars have been considering in the recent years, some of these are: stemless cultivars, double fruit reduction, postharvest behavior, content of bioactive compounds, or tree architecture (Quero-García et al., 2017).

Germplasm

Sweet cherry adaptation to different regions due to a large geographical distribution has resulted in landraces with different phenological and fruit quality characteristics (3,688 of sweet cherry and 1,553 of sour cherry accessions in European *Prunus* Database; Dondini et al., 2018). Despite this large number of local diversity, studies concerning commercial cultivars, advanced selections and landraces have shown a narrow genetic diversity in commercial varieties (Iezzoni et al., 1990; Choi and Kappel, 2004). Thus, local germplasm represents a valuable resource for sweet cherry breeding, especially for those traits related

to environment adaptation, and also fruit quality improvement (Badenes and Zuriaga, 2016).

In Spain, local germplasm is a potential source for breeding for relevant traits like self-compatibility, low chilling requirements, fruit quality and maturity date (Wünsch, 2019). This plant material includes local self-compatible varieties like 'Cristobalina', 'Talegal Ahim' or 'Son Miro' (Wünsch and Hormaza, 2004; Cachi and Wünsch, 2014). In addition, the low chilling requirements of 'Cristobalina' (<800 h; Tabuenca, 1983) compared with other sweet cherry cultivars, make it highly interesting for breeding to extend sweet cherry cultivation to warmer areas and adapt the crop to current global warming. This cultivar also has a very early maturity date, which make it of interest to wide ripening period and reduce cherry seasonality. High fruit quality and good postharvest aptitude is found in cultivars like 'Ambrunés', from the Jerte Valley, which has been used for breeding for firmness, postharvest aptitude, late ripening date and the possibility of stemless harvest (Manzano et al., 2014).

GENETICS, GENOMICS AND MARKER ASSISTED SELECTION IN SWEET CHERRY

Linkage maps

In sweet cherry, several linkage maps have been constructed from cross-pollinated populations and inter-specific crosses with related species (Clarke et al., 2009). Initially, partial linkage maps with a low number of mapped markers were developed. More than 20 years ago, Stockinger et al. (1996) developed the first sweet cherry linkage map using RAPDs markers of a microspore-derived callus culture population of the cultivar 'Emperor Francis'. The 89 RAPD markers and 2 allozymes used were then mapped in 10 linkage groups (LGs). Another partial map using isoenzymes was obtained from the inter-specific crosses of sweet cherry 'Emperor Francis' with *Prunus incisa* and *Prunus nipponica* cultivars (Boškovic and Tobutt, 1998). Subsequently, simple sequence repeat (SSR) markers were used for linkage map construction in a population of sweet cherry cultivars 'Regina' × 'Lapins' (Dirlewanger et al., 2004), and in a reciprocal cross of 'Emperor Francis' × 'New York 54' (Olmstead et al., 2008). A consensus linkage map of 'Regina'

× ‘Lapins’, ‘Emperor Francis’ × ‘New York 54’, ‘Namati’ × ‘Summit’ and ‘Natami’ × ‘Krupnoplodnaya’ populations was also developed using 268 markers (SNP and SSR) that grouped in 8 LGs (Cabrera et al., 2012). The development of a sweet cherry SNP array (RosBREED cherry 6K Illumina Infinium® SNP array v1; Peace et al., 2012), allowed he construction of high-density linkage maps in the species. This array was used for the construction of maps from two unrelated sweet cherry populations (Klagges et al., 2013), which considerably increase marker density compared with earlier SSR linkage maps (723 SNPs in ‘Black Tardarian’ × ‘Kordia’ and 687 in ‘Regina’× ‘Lapins’). Other NGS technologies such as Genotyping by Sequencing (GBS) and Specific-Locus Amplified Fragment (SLAF) were also recently used to develop high-saturated linkage maps in the species (Guajardo et al., 2015; Wang et al., 2015). More recently, three sweet cherry populations were used to construct a consensus high-density linkage map using double-digest restriction site-associated DNA sequencing that includes 2,382 markers (Shirasawa et al., 2017).

Genome sequences

New genomic technologies have contributed to the release of various Rosaceae genome sequences in the last years (Genome Database for Rosaceae (GDR); Jung et al., 2019). The sweet cherry genome sequence was published for the cultivar ‘Satonishiki’ (Shirasawa et al., 2017). This sequence has a total length of 272 Mbp covering the 80% of estimated genome size (338 Mbps; Arumuganathan and Earle, 1991), with 43,349 predicted protein-encoding genes. More recently, the genome sequence of sweet cherry cultivar ‘Regina’ has also been sequenced *de novo* using long reads sequencing and optical mapping (Le Dantec et al., 2019). This genome covers 279 Mbp, 83% of estimated cherry genome, and it is divided in 92 scaffolds. Structural annotation of predicted genes for the ‘Regina’ genome sequence is ongoing (Dirlewanger, personal communication). The partial draft genome of another sweet cherry cultivar, ‘Karina’, as a tool for genomic studies has also been reported (Cáceres-Molina et al., 2019). Low coverage was observed for ‘Karina’ genome in some regions and new sequencing data, in particular long sequences, are being introduced to improve the assembly contiguity (Cáceres-Molina et al., 2019).

Quantitative Trait Loci

In sweet cherry, most agronomical and fruit quality traits are quantitative (Iezzoni et al., 2017). During the recent decades, numerous studies have focused on the identification of quantitative trait loci (QTL) that explain the phenotype variation of these traits. Below, we resume the main detected QTLs in the species in the recent years.

QTLs related to bloom time (BT) and flowering-related traits such as chilling and heat requirements (CR and HR) have been conducted in sweet cherry. Dirlewanger et al. (2012) were the first that reported bloom time QTLs in the species; two major QTLs on LGs 1 and 4 of the population 'Regina' × 'Lapins' were reported. Latter, Castède et al. (2014) using two sweet cherry populations and data from various years found major BT, CR and HR QTLs overlapping on a syntenic region of main BT QTL detected by Dirlewanger et al. (2012) on LG4. Additional, BT QTL analysis were done for sour cherry (Wang et al., 2000; Cai et al., 2018) and high significant and stable QTLs were also detected on syntenic regions of LGs 1 and 4. These results provided the identification of candidate genes involved in the control of BT. Within this, *Dormancy Associated* MADS-box (*DAM*), *ARP4*, *EMF2*, *NUA*, *PIE1*, *GA2ox* or *KS* genes have been proposed as potential candidates for BT control in sweet cherry (Castède et al., 2015). As well as for BT, maturity date QTL analyses were conducted in sweet cherry. Dirlewanger et al. (2012) identified a major and stable maturity date QTL on LG4, and two additional minor QTLs on LGs 1 and 5 of the 'Regina' × 'Lapins' population. The same major maturity date QTL on LG4 was identified in the analysis of 'Beniyutaka' × 'Benikirari' population explaining almost 50% of phenotype variation (Isuzugawa et al., 2019). A *NAC* transcription factor has been reported as the candidate gene for maturity date in the syntenic region of peach genome (Pirona et al., 2013).

Several studies have been conducted to investigate the genetics of fruit size, a quantitative trait highly influenced by environmental conditions. Zhang et al. (2010) carried QTL analysis of fruit weight, size and diameter in the 'New York' × 'Emperor Francis' population and reported QTLs on LGs 2 and 6. Rosyara et al. (2013) performed a multifamily analysis ('New York 54' × 'Emperor Francis'; 'Regina' × 'Lapins'; 'Namati' × 'Summit'; 'Namati' × 'Krupnoplodnaya') of fruit weight, which allowed the validation of two main fruit size QTLs detected by Zhang et al. (2010) on LGs 2 and 6, and reported new minor QTLs on LGs 1, 2, 3 and 6. More recently, Campoy et al. (2015) used 'Regina'

× ‘Lapins’ and ‘Regina’ × ‘Garnet’ populations to detect a major fruit weight QTL on the bottom region of LG5. The cell number regulator (*CNR*) genes overlapping within QTL regions were reported to be the strongest candidate genes controlling fruit size in sweet cherry (De Franceschi et al., 2013).

Fruit firmness has been also taken special attention during the last years as a result of its relevance in consumer acceptability and postharvest aptitude in sweet cherry. Two firmness QTL analysis in sweet cherry are published up to date. Campoy et al. (2015) were the first that reported a firmness QTL in the species for the populations of ‘Regina’ × ‘Lapins’ and ‘Regina’ × ‘Garnet’ that were phenotyped during 7 and 4 years, respectively. A stable and most significant QTL was found on LG2, although various minor QTLs were also reported on all LGs (except LG7). Recently, a large fruit firmness QTL analysis was conducted in plant material that include wild cherry, landraces and modern cultivars (‘Fercer’ × ‘X’ population, the INRA sweet cherry germplasm collection and RosBREED pedigreed population; Cai et al., 2019). This study allowed the identification of a major firmness QTL on LG4 that accounted up to 84.6% of the phenotypic variation. Minor QTLs overlapping with those previously detected by Campoy et al. (2015) were also detected in this study.

QTL for other important agronomical and fruit quality related traits have been also reported in sweet cherry. A major fruit color QTL was located on LG3 explaining up to 87.1 and 94.7% of phenotype variation of skin and flesh color, respectively (Sooriyapathirana et al., 2010). Similarly, two stable QTLs on LG5 of ‘Regina’ and ‘Lapins’ cultivars were associated with rain-induced cracking susceptibility (Quero-García et al., 2014). Regarding cherry resistance to diseases, QTL analysis was performed for cherry leaf spot, which allowed the identification of a QTL mapped on LG4 associated with the resistance to this disease (Steigmer et al., 2014). Finally, Wang et al. (2015) conducted a trunk diameter QTL analysis in the ‘Wanhongzhu’ × ‘Lapins’ population reporting two QTLs on LGs 7 and 8.

Major genes, DNA tests and Marker Assisted Selection

Marker assisted selection (MAS) is an essential tool in sweet cherry breeding. The development of DNA-test for major genes and QTLs identified in sweet cherry can increase breeding efficiency giving information about the best parental available in the

germplasm to develop the crosses and to discard undesirable seedling in early stages of development (Dirlewanger et al., 2009). Despite the advances in genetic control of several traits, up to date, only few quantitative and qualitative traits of breeding interest are routinely implemented in MAS programs.

A few traits of breeding interest are known to be controlled by major genes, being self-incompatibility, determined by the *S*-locus, the most studied trait. DNA PCR markers are available to determinate cross compatibility between cultivars [reviewed in Herrero et al. (2017) and Iezzoni et al. (2017)]. DNA tests for this purpose are based in PCR length polymorphisms associated to the different *S*-locus genes alleles, namely *S-RNase* and *SFB.* These genes determine self-incompatibility specificity in sweet cherry (reviewed in Herrero et al., 2017). Self-compatibility is also a relevant trait in sweet cherry breeding and molecular markers to determinate this trait have also been developed. Ikeda et al. (2004) developed a DNA marker to identify the four base pair deletion in the $S_{4'}$*-SFB* allele, the most common source of self-compatibility in sweet cherry. A microsatellite in the mutated S_5 allele of 'Kronio', conferring the self-compatibility in this cultivar, was also reported to select for self-compatibility (Marchese et al., 2007). Self-compatibility from 'Cristobalina' is not linked to the *S*-locus but it is located on chromosome 3. Marker assisted selection for this trait can be done using the linked SSR EMPaS02 (Cachi and Wünsch, 2011) or more efficiently by primers that amplify the insertion in *MGST* gene associated to self-incompatibility in this cultivar (Ono et al., 2018).

The most common DNA marker for a quantitative trait was developed for main fruit size QTL on LG2. Zhang et al. (2010) reported two polymorphic SSR markers that were used to define the fruit size QTL haplotypes. This QTL must be associated with cherry domestication as most modern cultivars are homozygous or heterozygous for the allele associated with larger fruit size. More recently, a DNA marker for the main fruit firmness QTL found on LG4 was developed using five SNP markers from the RosBREED cherry 6K SNP array v1 (Cai et al., 2019). For the 13 haplotypes observed in this QTL region in a wide pool of cherry cultivars, they identified 5 firm and 8 soft haplotypes mainly found on wild and landrace cherry cultivars.

Cherry skin and flesh color have been reported to be a quantitative trait (Sooriyapathirana et al., 2010). The identification of a major QTL on LG3 explaining most of phenotype variation and co-localized with *PavMYB10*, a transcription factor associated

with the anthocyanin pathway, allowed the identification of a SSR marker for the routine identification of mahogany or blush color in sweet cherry fruits (Sanderful et al., 2016). In addition, a genetic test to detect resistance to cherry leaf spot was developed based on four SSR that spanned the major QTL controlling this disease (Stegmeir et al., 2015).

OBJECTIVES

The objective of this work is to investigate the genetics of some relevant phenology and fruit quality traits in sweet cherry, with the aim of providing tools that allow to improve the breeding process for these traits, and to advance in the understanding of the biological mechanisms that regulate them. For this purpose, sweet cherry populations derived from local plant material, 'Cristobalina' and 'Ambrunés' that provide additional phenotypic variation for these traits, were used. This general aim is divided into four main objectives:

Objective 1. Genotyping and high-density linkage mapping

To genotype several sweet cherry populations (cross- and self-pollinations), derived from local germplasm, using whole-genome SNP arrays developed in sweet cherry and to develop high-density linkage maps useful for genetic and QTL analysis.

Objective 2. Phenotyping and genetic analysis

To phenotype and evaluate phenology (bloom time, fruit development period and maturity date) and fruit quality (firmness, size, solid soluble content, titratable acidity, color and polyphenols content) traits in these populations, in order to investigate their behavior in these plant materials.

Objective 3. QTLs analyses and candidate genes

To identify and validate QTLs associated to these phenology and fruit quality traits, using single and multi-family QTL mapping approaches using the genotypic and phenotypic data generated, and to identify candidate genes in these major QTLs.

Objective 4. Haplotype analyses and marker assisted selection

To identify most relevant QTL alleles to implement marker assisted selection of these traits from these plant materials, and to identify polymorphisms in candidate genes that can be associated to the phenotypic variation to develop specific markers for marker assisted selection.

CHAPTER 2

HIGH-DENSITY LINKAGE MAPS CONSTRUCTED IN SWEET CHERRY USING CROSS- AND SELF-POLLINATION POPULATIONS REVEAL CHROMOSOMAL HOMOZYGOZITY IN INBRED FAMILIES AND NON-SYNTENIC REGIONS WITH THE PEACH GENOME*

* Calle A, Cai L, Iezzoni A, Wünsch A (2018). High-density linkage maps constructed in sweet cherry (*Prunus avium* L.) using cross- and self-pollination populations revealed chromosomal homozygosity in inbreed families and non-syntenic regions with the peach genome. Tree Genetics & Genomes 14:37. (Appendix I).

INTRODUCTION

Sweet cherry (*Prunus avium* L.), a diploid species (2n = 2x = 16) in the Rosaceae, is mainly cultivated for its fruit. World sweet cherry production has increased over 30% during the last two decades, reaching 2.2 M tons in 2014 (FAOSTAT, 2018). The increase in sweet cherry consumption, combined with challenges posed by climate change, and grower and consumer demands require breeding and production improvements. New genomic technologies and physical and genetic linkage maps generated contribute to an increase in knowledge that can lead to an improvement in breeding efficiency. In the Rosaceae family, various genome sequences have been published in recent years [Genome Database for Rosaceae (GDR); Jung et al., 2008]. Verde et al. (2013) sequenced the peach genome, the first *Prunus* genome sequenced, and, just recently, a sweet cherry genome was published (Shirasawa et al., 2017). Next generation sequencing (NGS) technologies have also allowed the identification of single nucleotide polymorphisms (SNPs) along the genome and the development of SNP array platforms for Rosaceae crops. This is the case for peach (Verde et al., 2012), sweet and sour cherry (Peace et al., 2012), strawberry (Bassil et al., 2015), and apple (Chagné et al., 2012a; Bianco et al., 2014 and 2016). These arrays have enabled the development of highly saturated linkage maps in the different species (Klagges et al., 2013; Di Pierro et al., 2016; Mahoney et al., 2016; Lambert et al., 2016). Linkage maps are a useful tool for the identification of quantitative trait loci (QTL), genomic regions associated with variation for quantitative traits. QTL for traits of breeding and production interest can be further used for marker-assisted selection or to identify candidate genes responsible for these traits.

Numerous linkage maps have been constructed in sweet cherry (reviewed in Salazar et al., 2014; Iezzoni et al., 2017). The first sweet cherry linkage maps were constructed using RAPDs (Stockinger et al., 1996) and isoenzymes (Boškovi and Tobutt, 1998). Later, maps were developed using SSR markers (Dirlewanger et al., 2004; Olmstead et al., 2008; Clarke et al., 2009) and SNP markers (Cabrera et al., 2012). High-density maps have been developed more recently (Klagges et al., 2013) using the RosBREED cherry 6K Illumina Infinium® SNP array v1 (Peace et al., 2012), Genotyping By Sequencing (GBS; Guajardo et al., 2015), and Specific-Locus Amplified Fragment (SLAF; Wang et al., 2015). Most recently, an integrated consensus linkage map containing 2,317

SNPs and 65 SSRs spanning 1,165 cM, from three crosspollination populations (Shirasawa et al., 2017), was constructed using double-digest restriction site-associated DNA sequencing (ddRAD-Seq).

All linkage maps developed in sweet cherry to date have been constructed from F_1 populations from interspecific or intraspecific crosses. Sweet cherry is a natural outcrossing species that exhibits a gametophytic self-incompatibility system controlled by the *S* locus. Pollen tube growth expressing an *S* allele that matches one of the two *S* alleles expressed in the diploid style is inhibited (Tao and Iezzoni, 2010). As a result of gametophytic self-incompatibility, self-fertilization is not possible in this species. F_1 mapping populations developed in sweet cherry have been made between cross-compatible parents. However, selfcompatible mutants do exist in sweet cherry. The selfcompatible mutant most widely used in breeding is a mutation that was induced using irradiation that renders S_4 pollen compatible in an S_4 containing style (Lewis, 1949). Therefore, any sweet cherry that carries this S_4 mutant, termed $S_{4'}$, is self-compatible. However, natural selfcompatible mutants have been found in local germplasm, including the landrace cultivars 'Cristobalina' (Wünsch and Hormaza, 2004), 'Talegal Ahim', 'Son Miro' (Cachi and Wünsch, 2014), and 'Kronio' (Marchese et al., 2007).

These cultivars, and any cultivar with $S_{4'}$, can be used to develop populations from self-pollination. Self-pollinated populations are useful for the genetic dissection of quantitative traits, especially in species with a low level of heterozygosity, because genetic effects (additive and dominant) can be estimated, and therefore, these population types are frequently used in fine mapping of QTLs (Zhang, 2012). In the genus *Prunus*, linkage maps have been developed using F_1 and F_2 populations, and these maps have been used for QTL analyses for traits of interest. In peach, most linkage maps come from F_2 populations [Genome Database for Rosaceae (GDR); Jung et al., 2008], but in other *Prunus* species that are self-incompatible, like almond or sweet cherry, all genetic maps have been developed in F_1 populations. In apricot, in which some cultivars are self-compatible, F_2 linkage maps have also been developed (Vilanova et al., 2003; Soriano et al., 2008). In breeding of sweet cherry, use of these self-compatible mutants makes it possible for the breeder to do self-pollinations or sib-matings that were previously not possible, raising the question of whether an associated increase in homozygosity in this naturally cross-pollinated crop could lead to inbreeding depression.

‘Cristobalina’, a landrace cultivar from Eastern Spain, specifically, a mountain area (Sierra de Espadán, Castellón) near the Mediterranean coast, offers many opportunities for sweet cherry breeding. This cultivar has a very low chilling requirement (<800 h), compared with other sweet cherry cultivars, such as ‘Van’ or ‘Napoleon’ (> 1100 h), that have large chilling requirements (Tabuenca, 1983). This trait makes ‘Cristobalina’ an important cultivar for breeding for low chilling, looking to extend the area of production to areas with warmer winters. This cultivar also has a very early maturity date, which makes it of interest for breeding early maturing cultivars. In addition, ‘Cristobalina’ has compact growth and medium to small size fruit (4–5 g) with dark red skin. Another relevant aspect is that ‘Cristobalina’ is self-compatible (Wünsch and Hormaza, 2004) due to a mutation located on linkage group (LG) 3 and therefore unlinked to the *S*-locus that is on LG6 (Cachi and Wünsch, 2011). Thus, it is an alternative source for breeding for self-compatibility. Being self-compatible, ‘Cristobalina’ also offers the possibility to use F_2 populations for genetic analysis of these important production traits and to investigate the possibility of inbreeding depression in this naturally cross-pollinated species. In this work, we used three sweet cherry families that have ‘Cristobalina’ as a parental cultivar, two of which are self-pollinations, to develop genetic maps using the RosBREED Cherry 6K SNP array v1. These maps were compared with previous sweet cherry linkage maps and with sweet cherry and peach physical maps (Shirasawa et al., 2017; Verde et al., 2017) to estimate the degree of similarity and synteny. The two self-pollinated populations derived from ‘Cristobalina’ were further used to investigate extent of homozygosity exhibited by the self-pollinated progeny.

MATERIALS AND METHODS

Plant material

Three sweet cherry families were used for linkage map construction that all include ‘Cristobalina’ (*S_3S_6*, *Mm*) in the parentage or ancestry. ‘Cristobalina’ has the *S* locus genotype *S_3S_6*; however, it is self-compatible because it is heterozygous for a self-incompatibility modifier locus (*Mm*) on LG3 (Cachi and Wünsch, 2011; Ono et al., 2018). All self-compatible ‘Cristobalina’ pollen has the *m* allele and either *S_3* or *S_6* (Cachi and

Wünsch, 2011; Ono et al., 2018). These three families were an F_1 family from the cross of cultivars 'Vic' (*S_2S_4*, *MM*) × 'Cristobalina' (V×C; N = 161), an F_2 family from the self-pollination of 'Cristobalina' (C×C, N = 97), and an F_2 family derived from the self-pollination of a progeny (*S_6S_9*, *Mm*) of the cross of 'Brooks' (*S_1S_9*, *MM*) × 'Cristobalina' (B×C2, N = 67). These trees come from crosses and self-pollinations made from 2008 to 2010 and are grown at the experimental orchards of CITA de Aragón in Zaragoza (Spain). All the parental cultivars belong to the CITA de Aragón sweet cherry cultivar collection. 'Vic' (Dickson, 1959) is a cultivar, derived from the cross of 'Bing' × 'Schmidt', with late blooming and maturity dates and dark large fruits. 'Brooks' is a cultivar from the cross of 'Rainier' and 'Burlat', which shows early blooming and maturity dates and dark red and firm fruits (Hansche et al., 1988). Progeny from three additional sweet cherry populations from the crosses 'Lambert' (*S_3S_4*, *MM*) × 'Cristobalina' (L × C, N = 14), 'Ambrunés' (*S_3S_6*, *MM*) × 'Cristobalina' (A×C, N = 40), and 'Brooks' (*S_1S_9*, *MM*) × 'Cristobalina' (B×C, N = 33) were genotyped using the 6K RosBREED cherry array and used to perform SNP clustering.

SNP genotyping

Genomic DNA was obtained from lyophilized leaves using DNeasy® Plant Mini Kit (Qiagen, MD, USA). Genomic DNA was extracted from the parental cultivars and all the progeny individuals. A duplicate genotype was included in each 96-plate as a quality control to evaluate reproducibility. Initial genomic DNA quantification was carried out using Nanodrop® (Thermo Fisher Scientific, Waltham, MA, USA). Genome-wide SNP genotyping of the three families and the parental cultivars was done using the RosBREED Cherry 6K Illumina Infinium® SNP Array v1 (Peace et al., 2012). Information about the SNP array, including the name, SNP type, position on the peach genome, Gbrowse link, and flanking sequence for the SNPs, can be downloaded from the Genome Database for Rosaceae (https://www.rosaceae.org/species/prunus/cherry) (Jung et al., 2008). Genotyping was carried out at CEGEN-PRB2-ISCIII (Madrid, Spain) by quantification with Quant-iT™ PicoGreen® (Invitrogen Ltd., Paisley, UK) and array scanning with Illumina iSCAN System® (Illumina Inc., San Diego, CA, USA).

SNP genotypes were analyzed using the Genotyping Module (v1.9.4) of GenomeStudio™ (v2011.1; Illumina Inc., San Diego, CA, USA) software. Manifest file

providing a description of the SNP and probe content on the array was used for the SNP genotype calling. In order to maximize allelic diversity, SNP clustering was performed by GenomeStudio™ using 480 sweet cherry genotypes. This sample included 325 genotypes corresponding to the three mapping progenies, 45 cultivars from the CITA sweet cherry cultivar collection previously genotyped with the same array (Martínez-Royo and Wünsch, 2014), 87 individuals from the remaining three families described previously, and 23 genotypes including the parents and technical duplicates. Only samples that had GenCall scores above 0.15 were initially clustered using the GenomeStudio™ build-in algorithm *Gentrain2*. Clustering for all the SNPs was also visually checked and adjusted manually if needed. Duplicated genotypes in each plate were tested for reproducibility using the GenomeStudio™ *Replicate* analysis function. GenomeStudio™ *parent–parent–child* (P-P-C) analysis function was used to test progenies and marker heritability in all the progenies. Further SNP quality filtering and data formatting for input in JoinMap were carried out using ASSIsT 1.0 (Di Guardo et al., 2015) with default parameters for each of these three populations.

To confirm homozygous LGs, a selected sample of eight individuals from C×C that collectively exhibited homozygosity for all LGs with the RosBREED Cherry 6K Illumina Infinium® SNPArray v1, was also genotyped with the recently developed RosBREED Cherry 15K Illumina Infinium® SNP array. Genotyping and SNP analysis was carried out as described previously, but SNP clustering was performed using a smaller sample (183 individuals) of sweet cherry populations and cultivars from CITA orchards. As the additional SNPs on the 15K array had not yet been placed on the linkage map generated from the C×C family, the SNP positions used were the physical positions of each SNP indicated in the array Manifest file.

Linkage map construction

Linkage map construction was performed using JoinMap 4.1® (Kyazma B.V., Netherlands; van Ooijen, 2006). All individuals with more than 5% missing data and all SNPs with more than 10% missing data were excluded from map construction.

For V×C, a cross-pollination, a *Two-step method* (Klagges et al., 2013; Tavassolian et al., 2010), was used. In the first mapping step, only heterozygous markers in each parent

were used to develop parental linkage maps. Minimum independence of LOD (= 10.0) was used for marker grouping. All informative markers were included in the parental map construction in the first mapping round. In the second round, markers showing segregation distortion ($p<0.01$) were excluded if they were not surrounded by other segregation distorted markers. A recombination frequency threshold of 0.6 was selected to prevent suspect linkages. False double recombination events were checked using *Genotype Probabilities* option with a threshold of 2.0 [−Log10 (P)]. The Maximum Likelihood mapping algorithm with default parameters was used for LG construction (van Ooijen, 2006), and recombination frequency was converted into genetic distance (centiMorgan, cM) using Kosambi's mapping function (Kosambi, 1944). In the second mapping step, heterozygous markers for both parents as well as all the markers previously mapped in each parental map were used to create the V×C consensus map. SNP markers with identical segregation were included in the linkage maps using the function *Assign identical loci to their groups*.

For the construction of the C×C and B×C2 linkage maps, in both segregating as F_2 populations, a *One-step method* was carried out using JoinMap 4.1. This method consisted of a single mapping step using all heterozygous markers of the parental tree. Minimum independence of LOD (= 10), a recombination frequency of 0.6, and maximum likelihood mapping algorithm were used for linkage map construction. As described for V×C mapping, markers showing segregation distortion ($p<0.01$) were excluded when not surrounded by other markers exhibiting segregation distortion. MapChart v2.2 was used to draw linkage maps (Voorrips, 2002). Deviation from expected Mendelian segregation was evaluated in the three families by Chi-square goodness-of-fit at $p<0.001$ to avoid false positives, using JoinMap 4.1. In addition, for each progeny individual, marker data was evaluated to identify chromosomes with just monomorphic markers, and these chromosomes were presumed to be homozygous.

Comparative mapping

The genetic positions of the SNPs placed on the genetic maps constructed were compared with their physical positions in the cherry genome PAV_r1.0 (Shirasawa et al., 2017). SNP flanking sequences were searched against the cherry genome PAV_r1.0 using

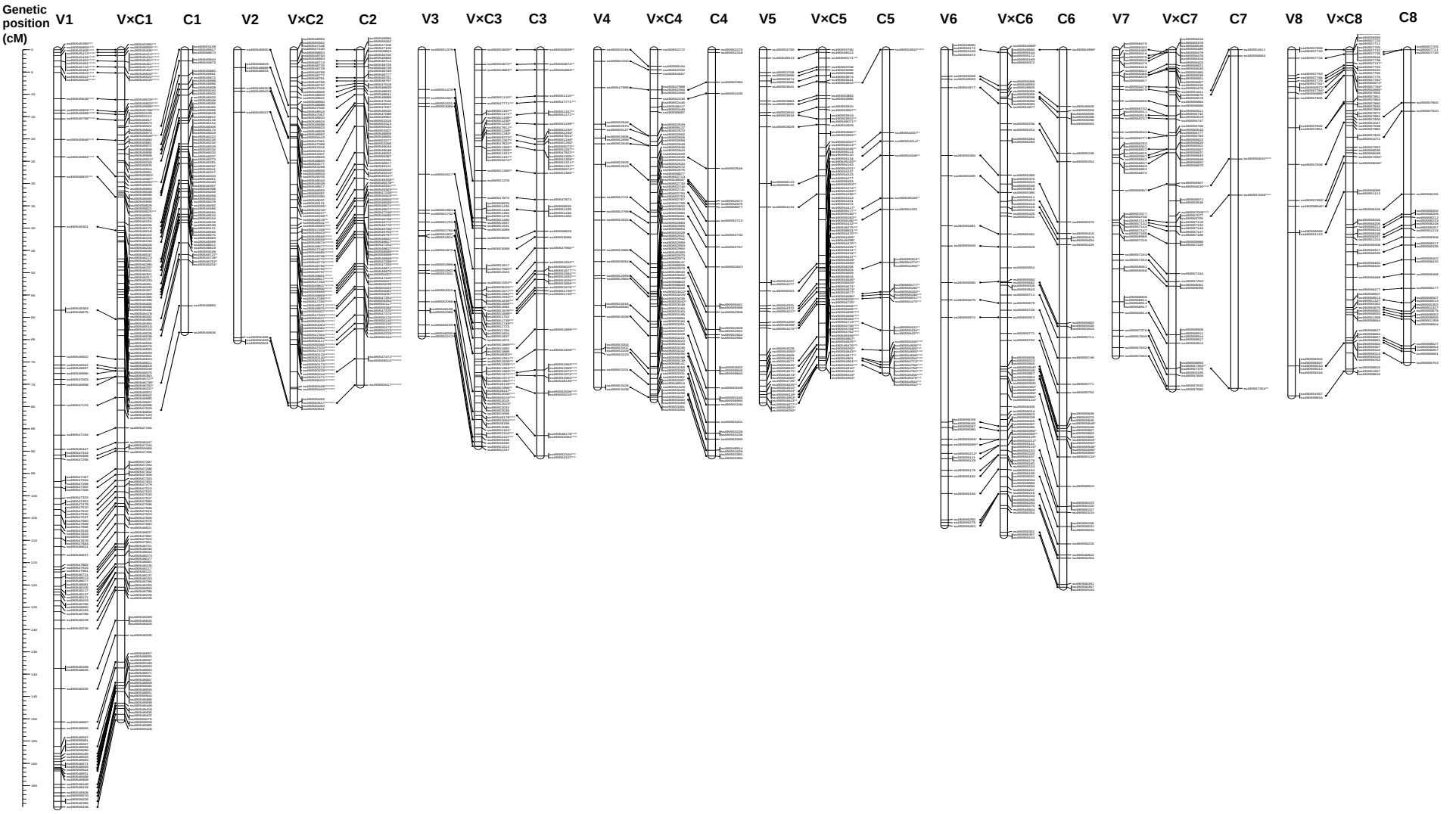

Figure 2.1 'Vic' (V), 'Cristobalina' (C), and V × C consensus (V×C) linkage maps. Asterisks indicate deviation from expected Mendelian segregation (*p < 0.1; **p < 0.05; ***p < 0.01; ****p < 0.005; *****p < 0.001; ******p < 0.0005)

the BLAST function at the Genome Database for Rosaceae (GDR, www.rosaceae.org; Jung et al., 2008), and only the best matching sequence was included as a result (Sup Table 2.1).

The SNPs mapped in the three maps were also aligned with their physical position in the peach genome v2.0.a1 (Verde et al., 2017), and the peach physical and cherry linkage map positions were compared. When discrepancies between genetic and physical order occurred, the genetic marker order was used, and physical positions for the new marker locations were extrapolated using the physical positions of flanking markers in the peach genome v2.0.a1 (Campoy et al., 2016). Using this method, the chromosomes of C×C, B×C2, 'Vic' (V), and 'Cristobalina' (C) maps (this work) and those of 'Regina' (R), 'Lapins' (L), 'Black Tartarian' (BT), and 'Kordia' (K) (Klagges et al., 2013) were drawn using MapChart v2.2 (Voorrips, 2002).

RESULTS

SNP genotyping and linkage map construction

SNP genotyping of V×C revealed 842 SNPs (14.8%) that were polymorphic in the parental cultivars and segregating in the family. The remaining SNPs were either monomorphic (4,201 SNPs, 73.7%), showed unexpected segregation (11 SNPs, 0.2%), or failed detection (642 SNPs, 11.3%) and were, therefore, discarded. From the 842 segregating SNPs, 483 (8.5%) were heterozygous in 'Vic' and 526 (9.2%) were heterozygous in 'Cristobalina' with 167 SNPs heterozygous in both cultivars. Using these markers, parental linkage maps of 'Vic' and 'Cristobalina' were constructed that each had the expected eight LGs (Table 2.1; Fig 2.1; Sup Table 2.1). The 'Vic' map has 313 SNPs covering 707.2 cM, with an average distance between markers of 3.1 cM. For 'Cristobalina', 370 SNPs were mapped, spanning 659.6 cM, with an average distance between markers of 4.0 cM. The largest numbers of markers were mapped to 'Vic' LG1 (100 SNPs) and 'Cristobalina' LG2 (95 SNPs), while 'Vic' LG2 (10 SNPs) and 'Cristobalina' LG7 (5 SNPs) were the LGs with least numbers of markers. The V×C consensus linkage map has 816 markers distributed along 726.0 cM and an average distance between markers of 0.9 cM (Table 2.1; Fig 2.1; Sup Table 2.1).

In the C×C family, of 526 SNPs heterozygous in 'Cristobalina', 511 were mapped to the eight LGs. This map covered 634.1 cM with an average distance between markers of 1.7 cM (Table 2.1; Fig 2.2; Sup Table 2.1). Like in the 'Cristobalina' parental map, the largest and lowest numbers of markers were mapped to LG2 (105) and LG7 (9 SNPs), respectively. As expected, the 'Cristobalina' linkage map generated from the two populations (V×C and C×C) was highly similar and mostly collinear (Fig 2.2); however, more SNPs were placed on the C×C map than the 'Cristobalina' V×C parental map. This difference occurred due to different criteria used for including markers in map construction. For C×C, all heterozygous markers in 'Cristobalina' could potentially be used for linkage map construction. However, the 'Cristobalina' parental map from V×C was constructed using only markers heterozygous for 'Cristobalina' and not with those that were heterozygous in both parental cultivars ('Cristobalina' and 'Vic'), as these were only used in the construction of the consensus V×C map. This effect is evident in the different size observed at the top of LGs 5 and 7 and bottom of LGs 2 and 3, where heterozygous SNPs in 'Cristobalina' were only used in C×C map construction but not in the 'Cristobalina' parental map. Other differences are also observed between both maps. For example, the last SNP (ss490557364) mapped at the bottom of LG7 of 'Cristobalina' was not present in the C×C map since this marker exhibited a high level of segregation distortion and was therefore excluded from the C×C map. Therefore, a big gap spanning 26.4 cM at the bottom of LG7 in the 'Cristobalina' parental map was not detected in the C×C map (Fig 2.2). Both maps have similar genetic length in total, and thus, the larger number of SNPs mapped in the C×C family resulted in a denser map although the average marker distances vary between LGs (Table 2.1).

SNP genotyping of the parent that was self-pollinated to generate the B×C2 family identified 589 (10.3%) heterozygous SNPs, 4,725 (82.9%) homozygous SNPs, and 382 (6.7%) that failed detection. From genotyping the B×C2 family, a linkage map was constructed from 552 SNPs. The resulting map covered a total genetic length of 622.4 cM, with a marker density of 1.2 cM (Table 2.1; Fig 2.3; Sup Table 2.1). Like in 'Vic', the largest number of markers and larger genetic length was observed for LG1 (133 SNPs, 124.7 cM), and like in the other two maps, LG7 had the lowest number of markers (51). Large gaps (>10 cM) were identified on the 'Vic' parental map for all LGs, except in LG4

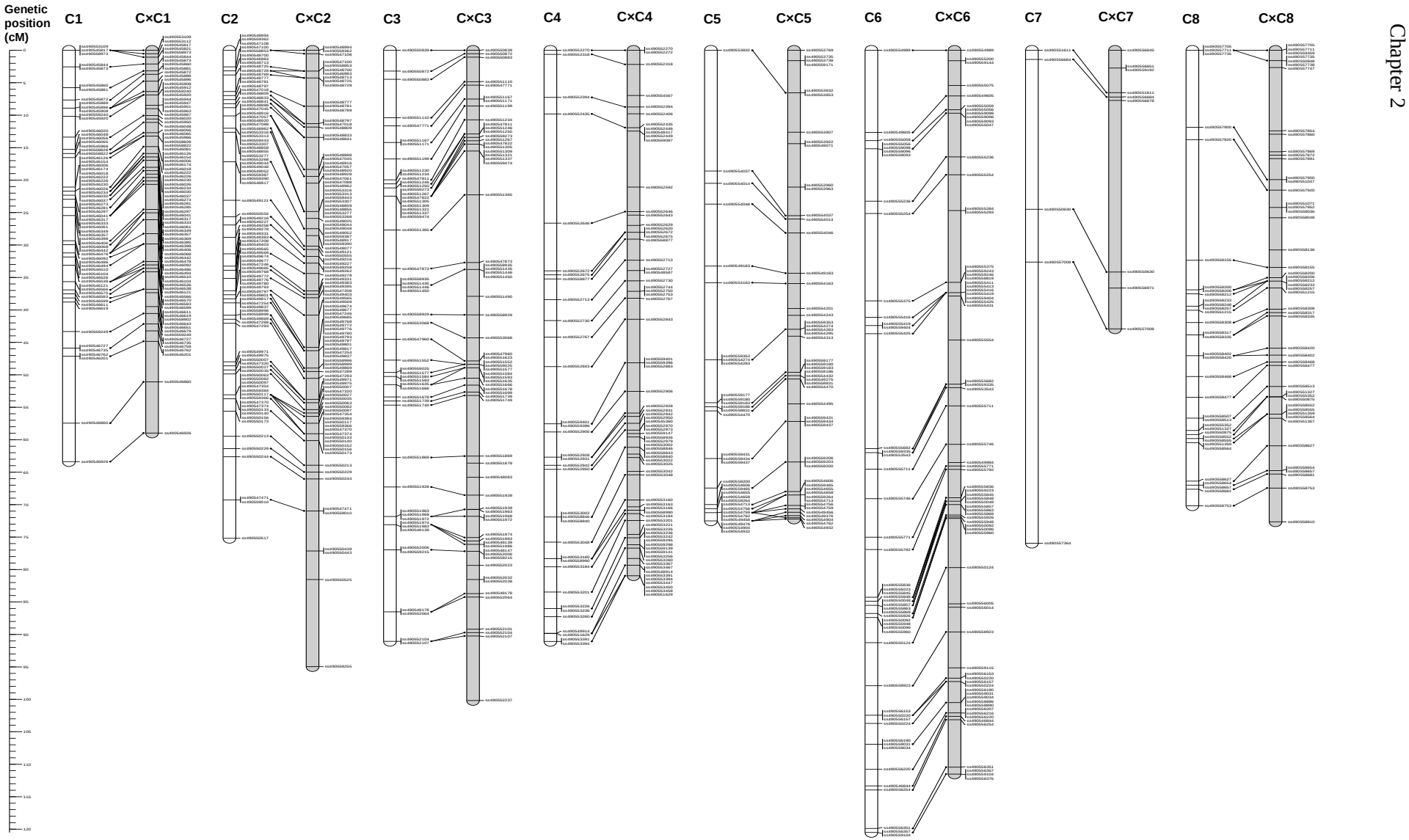

Figure 2.2 ‘Cristobalina’ parental map (white) and C×C linkage map (gray)

and LG7 (Table 2.1; Fig 2.1). The maximum gap on the 'Vic' map spanned 50.7 cM and was located on LG2. For 'Cristobalina', large gaps were detected on six of the eight linkage groups (LG1, 4–8), with the largest gap of 43.3 cM found on LG7. Fewer large gaps were observed on the V×C, C×C, and B×C2 maps compared to the 'Vic' and 'Cristobalina' maps. Additionally, the largest gaps were smaller in these maps than in the parental maps, revealing the generation of denser maps from consensus and the F_2 populations compared to the F_1 parental maps.

SNP markers showing distortion from the expected Mendelian segregation ratios ($p<0.001$) were identified in all the maps constructed except in the 'Vic' parental map. The number of skewed markers ranged from 32 in the V×C consensus map to 56 in C×C, being most frequent on LG2 and LG3 (Table 2.1). These markers were grouped in segregation distortion regions (SDRs; Fig 2.4), such as the bottom of LG2 (26.96–27.58 Mbp) for 'Cristobalina' and C×C maps and the bottom of LG3 (16.41–25.38 Mbp) for the C×C and B×C2 maps, where the 'Cristobalina' self-compatibility locus is located (Cachi and Wünsch, 2011). Segregation distortion also occurred in the C×C map, but not in the other maps, at the lower region of LGs 5 and 8 and in B×C2 at the lower part of LG1. Segregation distortion in SDRs showed distortion against one homozygous class.

Comparative mapping

Comparison of the SNPs placed on the three linkage maps with their physical position in the sweet cherry genome PAV_r1.0 (Shirasawa et al., 2017) revealed agreement in LG assignment and marker order for most of the SNPs (82%; Sup Table 2.1).Within each LG, only a few markers were mapped to orders that differed from that of the sweet cherry genome. However, some inverted regions were observed. These regions were located at the bottom of chromosome 1 and top of chromosomes 5, 6, and 7 (Sup Table 2.1). Additionally, 5% of the SNPs were mapped to different LGs than predicted by the sweet cherry genome sequence (Sup Table 2.2). Specifically, regions of chromosomes 2, 3, and 4 were mapped to different LGs for all maps (Sup Table 2.2).

Comparison of the genetic positions of the sweet cherry genetically mapped SNPs and their physical location in the peach genome v2.a.01 (Verde et al., 2017) revealed high collinearity (Sup Fig 2.1). However, SNPs mapped in different orders within a LG or to

different LGs compared to the peach genome v2.0.a1 were observed. SNPs mapped in different orders within LGs were observed in all maps at different positions, but the number of inconsistencies was highest at the top of LG5, where an inverted region was observed for the 'Vic', V×C, and B×C2 maps compared to the peach physical map (671,433–2,722,392 bp; Sup Fig 2.1). Some SNPs were also mapped to different LGs compared to the peach genome; some of these occurred in more than one map (Sup Table 2.3).

Table 2.1 Number of SNP markers, genetic length, average distance between markers, maximum gap size and number of markers with expected Mendelian segregation distortion (SD) ($p<0.001$) per linkage group (LG) in 'Vic' (V), 'Cristobalina' (C), V×C, C×C and B×C2 maps.

		LG1	LG2	LG3	LG4	LG5	LG6	LG7	LG8	Total
Number of markers	**V**	100	10	23	28	44	29	54	25	**313**
	C	67	95	54	34	32	49	5	34	**370**
	V×C	185	111	89	100	92	95	68	76	**816**
	C×C	85	105	66	75	51	71	9	49	**511**
	B×C2	133	75	70	56	48	66	51	53	**552**
Genetic length (cM)	**V**	169.8	65.3	64.2	75.7	79.2	106.7	68.7	77.6	**707.2**
	C	63.4	75.2	91.1	91.1	72.5	120.5	75.9	70.2	**659.9**
	V×C	150.3	79.8	89	78.5	71.3	108.9	76.1	72.1	**726.0**
	C×C	58.9	94.9	100.2	80.9	72.2	111.5	42.9	72.6	**634.1**
	B×C2	124.7	73.1	52.6	71.8	68.5	86.8	70.4	74.5	**622.4**
Average marker distance (cM)	**V**	1.7	7.2	2.9	2.8	1.8	3.8	1.3	3.2	**3.1**
	C	0.9	0.7	1.7	2.8	2.3	2.5	18.9	2.1	**4.0**
	V×C	0.8	1.2	1.0	0.8	0.8	1.1	1.1	0.9	**0.9**
	C×C	0.7	0.9	1.5	1.0	1.4	1.6	5.3	1.5	**1.7**
	B×C2	0.9	0.9	0.7	1.3	1.4	1.3	1.4	1.4	**1.2**
Largest gap size (cM)	**V**	18.7	50.7	15.2	8.1	16.9	23.5	7.4	29.9	**50.7**
	C	10.3	6.6	9.5	16.8	11.9	17.7	43.3	18.6	**43.3**
	V×C	6.8	5.4	6.1	6.7	7.9	7.6	10.9	5.9	**10.9**
	C×C	7.8	13.4	10.4	8.6	6.7	11.1	26.4	9.7	**26.4**
	B×C2	7.5	16.2	3.8	11.8	6.4	9.1	12.7	12.4	**16.2**
Number of markers with SD ($p<0.001$)	**V**	-	-	-	-	-	-	-	-	**0**
	C	-	36	-	-	-	-	-	-	**36**
	V×C	-	32	-	-	-	-	-	-	**32**
	C×C	-	4	32	-	12	1	1	6	**56**
	B×C2	15	-	30	-	-	1	-	1	**47**

The physical positions of the RosBREED cherry 6K SNPs in the peach genome v2.a.01 were compared to the genetic positions from the maps in this work and previous linkage maps using other cultivars (Klagges et al., 2013). This analysis allowed the visualization of the chromosomal regions covered by the mapped SNPs in the different

sweet cherry maps (Sup Fig 2.2). For the ‘Cristobalina’ and C×C maps, large regions of chromosomes 1 and 7 did not have any segregating markers. These regions could be homozygous as no heterozygous markers were detected. Thus, large presumably homozygous regions were observed in these maps for these regions. Similarly, ‘Vic’ was predicted to be homozygous at the top of chromosomes 2 and 3. The other cultivars also showed various regions of suspected homozygosity. This was most noticeable at the top and/or bottom of LG2 in ‘Vic’, ‘Black Tartarian’, ‘Kordia’, and ‘Lapins’; in LG4 for ‘Black Tartarian’ and ‘Kordia’; the top of LG5 in ‘Cristobalina’ and ‘Kordia’; and the top of LG7 in ‘Kordia’.

Homozygosity

Progeny individuals with presumably homozygous LGs based on the absence of any heterozygous SNPs on these LGs were identified in the two populations derived from self-pollination, C×C and B×C2 (Sup Fig 2.3). For C×C, 38 individuals (38%) had one homozygous LG, 13 (13%) had two homozygous LGs, and three (3%) had three homozygous LGs. Overall, more than half of the progeny (54 individuals, 54%) had at least one homozygous LG. For C×C, LG7 was the LG most often homozygous (28 individuals), followed by LG1 and LG5 being homozygous in 12 individuals. This is consistent with ‘Cristobalina’ being homozygous for the majority of LGs 1 and 7 and a portion of LG 5 (Sup Fig 2.2). In B×C2, a similar proportion, nearly half of the family (32 individuals; 48%), had trees with homozygous LGs. Of these, 23 had one homozygous LG, eight had two homozygous LGs, and one individual had four homozygous LGs. The LG most frequently homozygous was LG3, occurring for 12 individuals, while the least frequent homozygous LG was LG6 in both families.

To confirm the homozygosity of these LGs, eight individuals of C×C (Table 2.2) that collectively exhibited homozygosity for all LGs with SNPs from the RosBREED Cherry 6K array were also genotyped with the 15K RosBREED Cherry Illumina Infinium® SNP array. A larger number of heterozygous SNPs could be scored with the 15K array in each LG (Table 2.2). The assay revealed that of the 16 presumably homozygous LGs in the eight trees, seven are likely homozygous after the analysis with the 15K array, as no heterozygous markers were assigned to these LGs. Furthermore, presumably homozygous linkage groups were confirmed in all LGs, except 3, 6, and 7

(Table 2.2). The results show that increasing the number of genotyped SNPs reduced the number of homozygous LGs, but that homozygosity was confirmed in about half of them. In the LGs that were homozygous with the 6K array and not with the 15K array, few heterozygous markers were detected indicating that large regions of homozygosity are present for these LGs. In LG7, a large number of presumably homozygous LGs were detected in the RosBREED cherry 6K array; however, this seems to be due to the low number of markers mapped to this LG with this array, as this was not the case after the analysis with the 15K array.

Table 2.2 Heterozygous SNPs identified for eight C×C progeny individuals with RosBREED cherry 6K SNP array and the 15K SNP array (6K/15K).

	LG1	**LG2**	**LG3**	**LG4**	**LG5**	**LG6**	**LG7**	**LG8**
CC05	85/168	71/142	25/55	**0/0**	11/30	27/95	9/51	14/26
CC22	85/162	**0/0**	58/148	**0/7**	26/58	26/83	5/35	28/76
CC36	19/48	49/93	20/59	52/124	38/80	**0/11**	9/36	16/26
CC43	**0/8**	104/193	53/138	55/143	13/30	17/55	**0/25**	**0/0**
CC50	85/167	42/72	**0/1**	75/171	**0/0**	12/56	**0/13**	5/16
CC52	**0/0**	**0/0**	20/62	44/87	19/40	35/108	8/48	**0/0**
CC79	10/25	2/11	52/142	0/2	44/106	40/131	**0/17**	5/22
CC91	71/133	15/33	29/87	51/124	**0/2**	38/134	**0/17**	49/10

DISCUSSION

Linkage maps

The three populations and linkage maps constructed in this work will be used for future QTL analysis for chilling requirement, bloom and maturity time, and fruit size. The understanding of the map coverage and regions of segregation distortion and low marker density gained from the maps generated will be critical for interpreting the forthcoming QTL results. In general, the maps developed in this work and those previously constructed using the same SNP array revealed similar numbers of markers, genetic lengths, average distances between markers, and gap sizes (Klagges et al., 2013). However, for LG7 from 'Cristobalina' and C×C and LG2 from 'Vic', very few markers were heterozygous and met the criteria for use in linkage map construction, resulting in regions with large distances

between markers. This was noticeable for the 'Cristobalina' parental map when compared with the C×C map, due to the use of different mapping strategies for the F_1 and F_2 populations (Tavassolian et al., 2010). In general, the use of all heterozygous markers to develop F_2 and consensus maps resulted in higher marker density maps in the F_2 populations and in the consensus maps from the F_1 crosses, than in the parental maps.

The linkage maps constructed also identified regions that are presumably homozygous in the parental cultivars and therefore would be uninformative for QTL discovery. For example, 'Vic' is presumably homozygous for the top of LGs 2 and 3 and, therefore, homozygous for any QTL alleles that fall in these regions. Likewise, 'Cristobalina' is presumably homozygous for large portions of LGs 1 and 7, and, therefore, QTL analysis would not identify any loci in these regions. In this case, the population B×C2 will be particularly useful as it will allow an investigation of 'Cristobalina' derived alleles for regions that are not segregating in the V×C and C×C populations. Since the B×C2 population resulted from self-pollination, it will be possible to compare the effects of all three allele classes for SNPs homozygous in 'Cristobalina' (i.e., AA, AB, and BB).

Comparison with the sweet cherry and peach physical maps

Comparisons of the linkage maps developed herein, with the sweet cherry genome sequence PAV_r1.0 (Shirasawa et al., 2017), supported the genetic position and marker order of most of the markers mapped. However, because almost 30% of the sweet cherry genome was not anchored to any chromosome (Shirasawa et al., 2017), a large portion of mapped SNPs were not assigned to any chromosome and temporarily located to the cherry scaffold identified as Chr_0. In addition, some inconsistencies between linkage maps and scaffold positions could be due to minor misassembles in the cherry genome or the possibility that our use of the best matching marker position on the cherry scaffolds for each SNP did not provide an accurate comparison.

Comparison between sweet cherry linkage maps and the peach genome v2.0.a1 revealed extensive collinearity, but some markers mapped in different orders. Most noticeable was a group of markers that mapped in inverse order at the top of LG5 in the 'Vic' and B×C2 maps. This apparent inversion between the sweet cherry linkage maps and

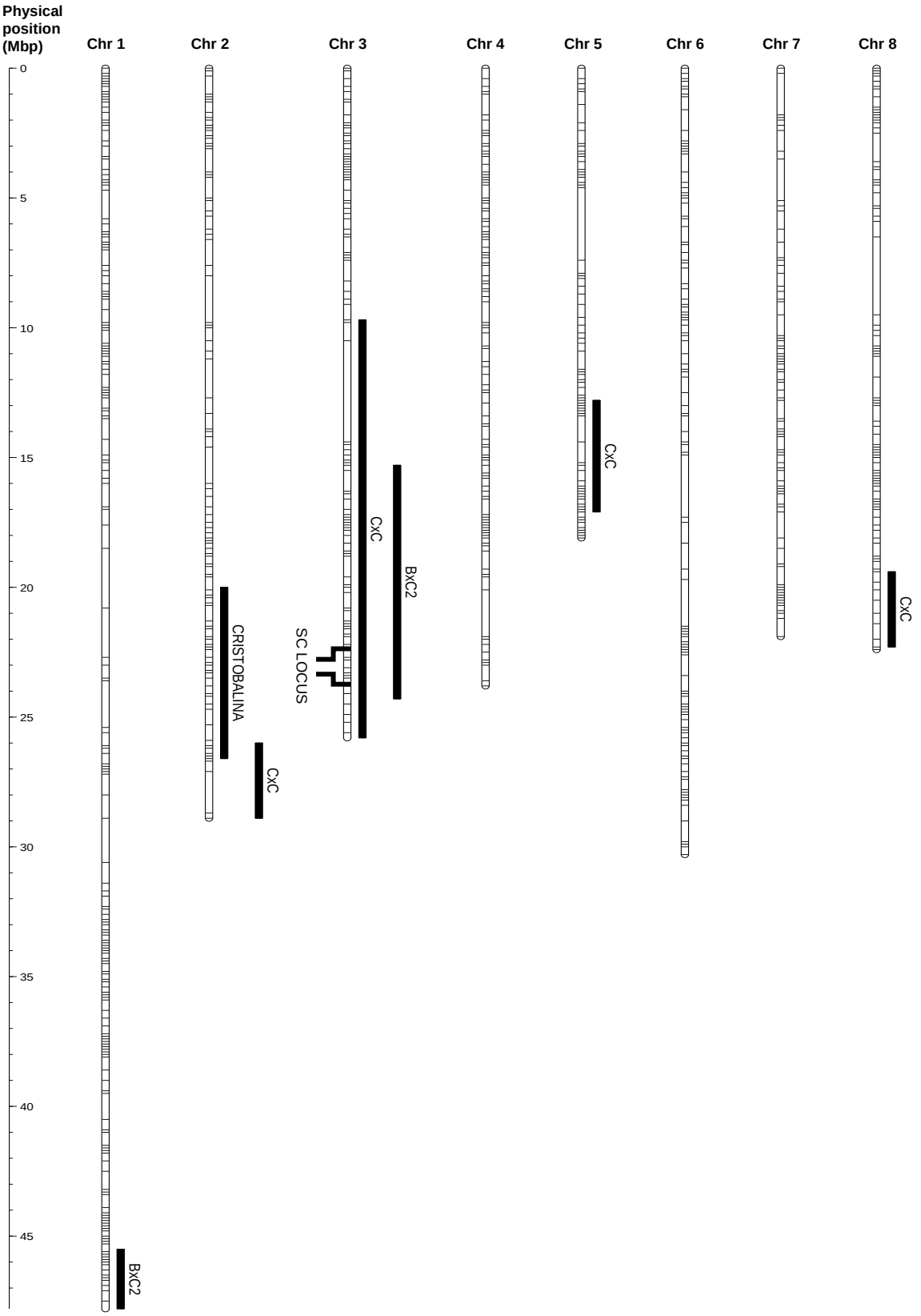

Figure 2.4 Physical positions of RosBREED cherry 6K SNP array v1 markers on the peach genome v2.0.a1 where segregation distortion ($p<0.001$) was identified in 'Vic', 'Cristobalina', C×C, and B×C2 linkage maps. (SC Locus: Self-Compatibility Locus).

peach physical map was also observed in the 'Black Tartarian' and 'Rainier' maps (Klagges et al., 2013; Guajardo et al., 2015). For the 'Cristobalina' and 'Kordia' maps, this LG5 region is presumably homozygous, and therefore, these parental maps were uninformative for this region. When the physical positions of these inverted markers were aligned with the sweet cherry genome scaffolds (Shirasawa et al., 2017), the region was not inverted. This indicates that this region may not be inverted in the cherry genome when compared to the peach genome. However, the fact that this region appears inverted in four genetic maps from unrelated sweet cherry individuals may also indicate a real inversion that has not been correctly assembled with the sweet cherry sequence.

In the maps developed herein, some SNPs were mapped to different LGs than expected based on their positions in the peach genome sequence. Similar inconsistencies were also detected in other sweet cherry linkage maps developed using the same genotyping platform (two SNPs in 'Black Tartarian', three SNPs in 'Lapins', and six SNPs in 'Regina') (Klagges et al., 2013). The presence of markers mapped in different LGs based on peach genome may indicate regions that are translocated from one genome to the other or duplicated (Dirlewanger et al., 2004; Fresnedo-Ramírez et al., 2013). The position of these markers could not be confirmed due to poor alignment with the current sweet cherry genome sequence. However, if these differences between the cherry and peach genome are eventually verified, they may mark species-specific genomic regions that contributed to the evolutionary differences between cherry and peach.

Segregation distortion

Skewed markers detected in this work were grouped in segregation distortion regions (SDRs). SDRs have also been detected in other species like barley (Li et al. 2010), eucalyptus (Myburg et al., 2004), oak (Bodénès et al., 2016), maize (Lu et al., 2002), or rice (Xu et al., 1997). SDRs detected in this work were also found in other sweet cherry maps. A SDR at the lower end of LG1 in B×C2 was also detected in 'Black Tartarian', 'Kordia', 'Regina', 'Lapins', and *Prunus davidiana* linkage maps (Foulongne et al., 2003; Klagges et al., 2013). Similarly, a SDR at the lower end of LG2 in 'Cristobalina' and C×C was also found in the 'Emperor Francis' and 'New York 54' maps (Olmstead et al., 2008), and a SDR at the lower region of LG8 for C×C was also detected in the 'Emperor Francis'

linkage map. The presence of these SDRs in different cherry maps for LGs 1, 2, and 8 may indicate the presence of lethal and/or sub-lethal alleles in these regions that reduce viability or survival (Ward et al., 2013). The SDR identified on LG2 in this study overlaps with a QTL hotspot containing fruit and bloom time traits important for sweet cherry breeding (Cai et al., 2017); therefore, understanding the basis for segregation distortion at this region would be of interest.

Other regions with segregation distortion identified herein were specific for individual linkage maps constructed in this work. This includes the lower part of LG3 in C×C and B×C2 maps, where distorted segregation results from the pollen-expressed self-incompatibility modifier locus that is heterozygous in 'Cristobalina' that maps to this region (Cachi and Wünsch, 2011; Ono et al., 2018). Only pollen containing the self-fertile allele at this locus will be able to achieve fertilization in a self-pollination, and as a result, only the self-compatible allele is inherited and segregation distortion is observed in this region. The markers with maximum distortion in this region are ss490552038, ss490552032, ss490548178, and ss490552064 in C×C (Fig 2.2; Fig 2.4) and are expected to map to the location of the self-incompatibility modifier locus that leads to self-compatibility. An additional region where segregation distortion was observed exclusively in C×C was the bottom region of LG5. In this region, one homozygous class was favored over the other, and therefore, for this region, deleterious recessive alleles may be selected against.

Self-pollination and chromosomal homozygosity

Sweet cherry evolved as an obligate outcrossing species due to the presence of a gametophytic self-incompatibility system. The 'Cristobalina'-derived C×C and B×C2 populations, both resulting from self-pollination, will provide a unique opportunity to investigate the impact of self-pollination on this heterozygous species. In C×C and B×C2, compared to V×C (F_1 population), a large number of individuals with one to four presumably homozygous LGs were identified in both F_2 populations, and, presumably, completely homozygous LGs were identified for all LGs in both populations. Recently, a *next-generation* RosBREED Cherry 15K Illumina Infinium® SNP Cherry Array was developed that was designed to fill gaps previously identified with the use of the 6K array (Illumina, San Diego, CA). This array was used in this work to test whether the degree of

homozygosity detected with the 6K array was also confirmed after analyzing a larger number of SNPs. This test revealed that the number of homozygous LGs in C×C and B×C2 was overestimated with the 6K array but confirmed the presence of large homozygous regions and homozygous LGs in the families. The finding that LG6 had the lowest level of homozygosity when considering both the C×C and B×C2 self-pollinated populations is consistent with the presence of the *S* locus on LG6. It suggests that there may be a high genetic load of presumably deleterious recessive alleles linked to the *S* locus. Taken together, these results reveal that high levels of homozygosity (up to four presumably homozygous LGs) can be tolerated in sweet cherry. The finding that 'Cristobalina' is presumably homozygous for large regions on LGs 1 and 7 and a smaller region on LG5 suggest that it may be derived from self-pollination. If 'Cristobalina' is the result of self-pollination (S_2), then the S_2 population (C×C) would be an S_3.

Selfing in naturally outcrossing species leads to an increase in homozygosity, which may result in a decrease in fitness and fitness-related traits, characterized as inbreeding depression (Charlesworth and Charlesworth, 1999). Phenotypic observations of individuals from the three mapping populations suggest that inbreeding in sweet cherry can be associated with a loss of vigor and fertility (data not presented). Trees in the C×C population are generally weak and exhibit a low vegetative vigor. The progeny only began fruiting after eight years and only 19% of the trees have fruit after 10 years. In contrast, V×C trees began fruited after five years, and 62% of trees have fruit after seven years. Furthermore, V×C is younger than C×C but shows higher vigor, measured as trunk circumference.

In conclusion, the genetic maps reported for 'Cristobalina' and its derived progeny will enable future QTL identification from this important breeding parent. In addition, the maps herein provide an opportunity to take a first look at the genome-wide impacts of self-pollination in sweet cherry. This is especially timely with the increased emphasis on the development of self-compatible cultivars using either $S_{4'}$ or naturally derived self-compatible mutations, such as the one present in 'Cristobalina'.

SUPPLEMENTARY MATERIALS CHAPTER 2

Supplementary Table 2.1 Position of RosBREED cherry 6K SNP Array v1 SNP markers mapped in 'Vic', 'Cristobalina', V×C, C×C and B×C2 linkage maps.

Document available online at http://hdl.handle.net/10532/4737. (Chapter 2 – Supplementary Table 1.xlsx).

Supplementary Table 2.2 SNP markers with genetic map positions that differed from the sweet cherry genome PAV_r1.0 (Shirasawa et al. 2017) physical map positions for 'Vic' (V), 'Cristobalina' (C), V×C, C×C and B×C2. Only the best match to the cherry genome (PAV_r1.0) sequence is included.

	Physical position PAV_r1.0		**Genetic position (cM)**					
SNP	**Chr**	**Position**	**LG**	**V**	**C**	**V×C**	**C×C**	**B×C2**
ss490546273	2	8336505	1	-	22.3	40.5	16.4	-
ss490546037	2	8367857	1	-	21.7	39.6	16.4	-
ss490546234	2	8496299	1	-	21.7	39.6	16.4	-
ss490546026	2	8506097	1		21.7	39.6	16.4	-
ss490546230	2	8508179	1	-	21.7	39.6	16.4	-
ss490546226	2	8509076	1	-	21.7	39.6	16.4	-
ss490546222	2	8526221	1	-	21.7	39.6	15.9	-
ss490546154	2	8802803	1	-	21.1	38.7	14.8	-
ss490546018	2	9046889	1	-	21.1	38.7	14.8	-
ss490546174	2	9140231	1	-	21.1	38.7	14.8	-
ss490546006	2	9338496	1	-	21.1	38.7	14.8	-
ss490550479	3	10141163	7	8.3	-	8.4	-	-
ss490551611	3	10524955	7	-	0	9.1	6.5	5.3
ss490550220	4	1781886	6	-	102.4	89.8	96.7	-
ss490556153	4	1785025	6	-	102.4	89.8	96.7	-
ss490553068	4	18009325	3	-	41.9	44.6	44.3	21.3
ss490553089	4	18622407	3	12.4	-	39.9	-	19.8
ss490553109	4	20043372	1	-	0	17.1	0	-
ss490553112	4	20073056	1	-	-	17.1	0	-
ss490545817	4	20239148	1	-	0	17.1	0.5	-
ss490545821	4	20257447	1	-	-	17.4	1	-
ss490558973	4	20260620	1	-	0	17.1	1	-
ss490553277	4	23408694	2	-	12.6	18.6	24.8	13.7
ss490548855	4	23410719	2	-	12.6	18.6	24.8	13.7
ss490553307	4	23927805	2	-	12	17	24.8	13.7
ss490553313	4	23958350	2	-	12	17	24.8	13.7
ss490553316	4	23996867	2	-	12	17	24.8	13.7

Supplementary Table 2.3 SNP markers with genetic map positions that differed from the sweet cherry genome PAV_r1.0 (Shirasawa et al., 2017) physical map positions and peach v2.0a1 (reference) physical map positions. Only the best match to the cherry genome.

	Genetic position in sweet cherry maps			Physical position in Peach Genome v2.a.01		Physical position in PAV_r1.0	
	Map	**LG**	**(cM)**	**Chr**	**bp**	**Chr**	**Bp**
ss490549697	V	1	71.3	2	21123343	0	24919707
ss490548886	V	2	3.9	4	21653711	0	7073922
ss490548917	C	2	17.2	4	24150393	1	23565595
	C×C	2	27.5				
	B×C2	2	14.4				
ss490556603	V	2	3.9	7	6257451	0	6257451
ss490551629	C	4	89.8	3	17628272	3	11621163
	C×C	4	80.9				
ss490547988	V	4	8.5	3	18327004	7	18979393
ss490554567	C×C	4	6.9	5	15968737	5	14410135
ss490548940	V	4	57.3	6	14899178	8	4698421
ss490546844	C	6	113.3	1	25136072	0	73684844
	C×C	6	102.6				
ss490550875	C	8	58.3	3	1870601	3	1008029
	C×C	8	53.4				
	B×C2	8	45.4				
ss490552915	B×C2	8	2.3	4	11102705	4	14089497
ss490553385	B×C2	8	1.5	4	22008212	4	25141013
ss490555352	C	8	57.7	6	6761904	6	6410629
	C×C	8	53.4				
	B×C2	8	44.6				

Supplementary Fig 2.1 Comparison of the genetic map and physical map constructed using all the SNPs placed on the linkage maps constructed. The SNPs were ordered according to their position in the peach genome v2.0.a1.

Document available online at http://hdl.handle.net/10532/4737. (Chapter 2 – Supplementary Figure 1.tiff)

Supplementary Fig 2.2 Comparison of physical positions of RosBREED cherry 6K SNP array v1 markers on the peach genome v2.0.a1 (PGv2) with the genetic maps of sweet cherry. 'Vic' (V), 'Cristobalina' (C), C×C and B×C2 (this work), 'Black Tartarian' (BT), 'Kordia' (K), 'Lapins' (L), and 'Regina' (R) (Klagges et al., 2013).

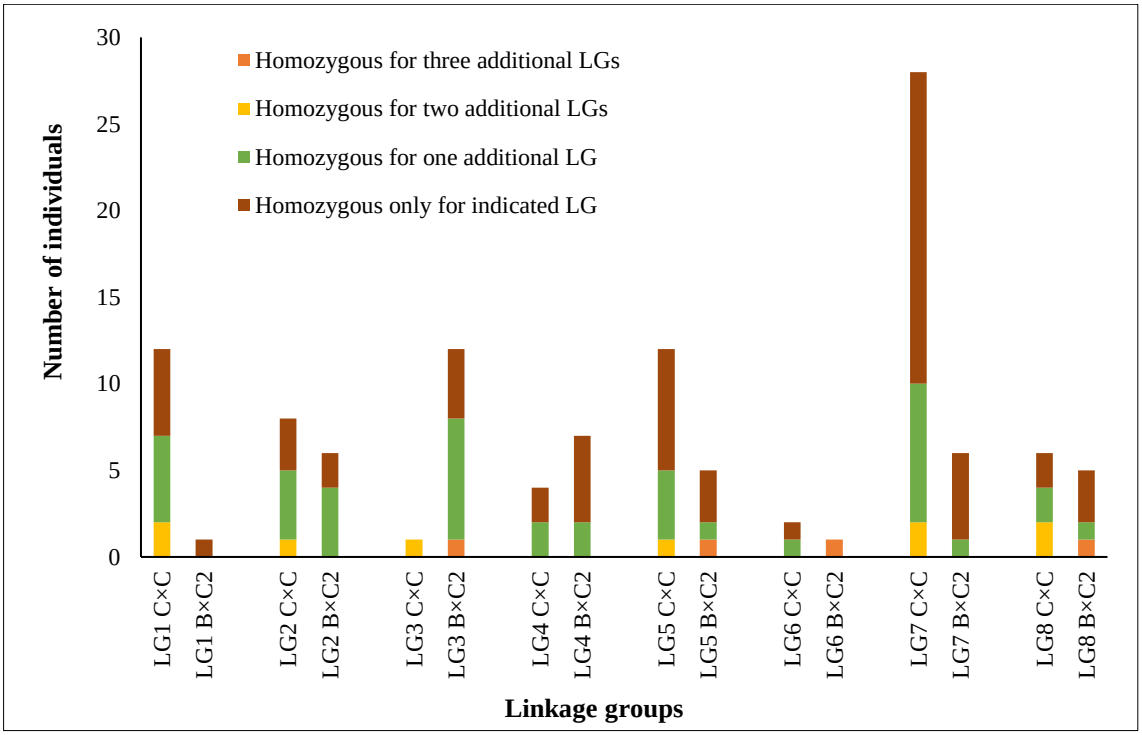

Supplementary Fig 2.3 Distribution of homozygous linkage groups (LGs) identified in self-pollinated families C×C and B×C2.

CHAPTER 3

GENETIC DISSECTION OF BLOOM TIME IN LOW CHILLING SWEET CHERRY USING A MULTI-FAMILY QTL APPROACH

INTRODUCTION

Bloom time (BT) is an important horticultural trait in temperate fruit tree species like sweet cherry (*Prunus avium* L.). Cultivar adaptation to climatic conditions in the growing area is essential for flower production and fruit set. Early blooming cultivars are susceptible to spring frost damage in cold regions (Luedeling, 2012), while late blooming cultivars can exhibit irregular floral development and low fruit set due to warm temperatures during the flowering period (Mahmood et al., 2000; Atkinson et al., 2013). The biological control of BT is complex and is known to depend on environmental signals during the winter and spring seasons (Abbott et al., 2015; Fadón and Rodrigo, 2018). Fruit trees like sweet cherry require a period of chilling temperatures followed by a period of warm temperatures to induce blooming (Lang et al., 1987). In *Prunus* species, several studies indicate that BT is more dependent on chilling than on heat requirement and that there is large variation in these requirements among individuals of the same species (Campoy et al., 2011; Okie and Blackburn, 2011; Sánchez-Pérez et al., 2012; Castède et al., 2014).

Several genetic studies in *Prunus* have focused on understanding the genetic control of chilling (CR) and heat requirements (HR) contributing to the differences in BT (reviewed in Abbott et al., 2015). BT in *Prunus* is a quantitative trait with high heritability (Anderson and Seeley, 1993; Dirlewanger et al., 2012; Castède et al., 2014), and genetic approaches have led to the identification of quantitative trait loci (QTLs) associated with this trait. BT QTLs have been identified on all *Prunus* linkage groups (LGs) (reviewed in Salazar et al., 2014; Abbott et al., 2015), but major QTLs have been found on LG1 (Fan et al., 2010; Zhebentyayeva et al., 2014; Bielenberg et al., 2015) and LG4 (Sánchez-Pérez et al., 2012; Dirlewanger et al., 2012; Castède et al., 2014) in all the *Prunus* crop species evaluated to date. In sweet and sour (*Prunus cerasus*) cherries, several QTLs have been identified for BT and CR. In sweet cherry, Dirlewanger et al. (2012) mapped two major BT QTLs on LGs 1 and 4 and three minor QTLs on LGs 5, 6 and 7. Castède et al. (2014) using three to six years data and two F_1 populations identified BT and CR QTLs in all LGs, with a major and stable QTL for both traits overlapping on LG4. Castède et al. (2014) also detected minor QTLs for both CR and BT on LGs 1 and 7, highlighting the influence of CR in BT in this species. In sour cherry, Wang et al. (2000) investigated BT QTL using an

F_1 population and 3-year data, and two major QTLs were identified on LGs 1 and 2. Another QTL study in sour cherry revealed four QTLs for BT on LGs 1, 2, 4 and 5; the most significant allele for LG4 QTL was associated with almost three days bloom delay (Cai et al., 2018).

Candidate genes have been reported for the *Prunus* BT and CR QTL that maps to LG1 (Yamane et al., 2011; Zhebentyayeva et al., 2014; Castède et al., 2015). In peach, a tandem set of six *DORMANCY ASSOCIATED MADS-BOX (DAM)* genes have been identified in this region (Zhebentyayeva et al., 2014; Romeu et al., 2014; Bielenberg et al., 2015). Studies of these genes was facilitated by the study of a peach non-dormancy mutant termed *evergrowing* peach mutant (*evg*) that has a deletion within this QTL region (Bielenberg et al., 2008). Of these genes, *DAM5* and *DAM6* were not expressed under chilling temperatures (Jiménez et al., 2010) whereas the expression of *DAM4* and *-6* were activated by short photoperiods (Li et al., 2009) suggesting that *DAM5* and *-6* are the main genes underlying this *Prunus* LG1 CR QTL (Yamane et al., 2011). For the major *Prunus* BT QTL located on LG4, genes related to temperature sensing (*ARP4, EMF2, NUA* and *PIE1*) and the gibberellin pathway (*GA2ox* and *KS* genes) have been proposed as the most promising candidates to control BT (Dirlewanger et al., 2012, Castède et al., 2015).

Most BT QTL studies in *Prunus* have been done using a single bi-parental population. This strategy is limited because only alleles present and segregating in the two parental cultivars can be detected (Bink et al., 2014). However, knowledge of the effects of these alleles in different genetic backgrounds and other loci not segregating in the bi-parental cross are needed to fully implement marker-assisted selection (MAS). The development of QTL mapping approaches based on multi-parental populations allow the identification a larger number of QTLs and QTL alleles improving the application of these results in MAS for a larger number of genetic backgrounds (Pauly et al., 2012). The Bayesian QTL mapping approach implemented by FlexQTL™ (Bink et al., 2008 and 2014) allows analyzing multiple pedigree-linked progenies at the same time; reducing the limitations derived from QTL analyses using single populations. This approach has been successfully used in recent years for QTL analyses of different traits in *Rosaceae* species, such as sweet cherry (Rosyara et al., 2013), apple (Bink et al., 2014; Guan et al., 2015; Allard et al., 2016; Di Guardo et al., 2017; Howard et al., 2018), peach (Hernández Mora

et al., 2017; Fresnedo-Ramírez et al., 2015 and 2016) and strawberry (Roach et al., 2016; Mangandi et al., 2017; Anciro et al., 2018).

Furthermore, previous QTL analyses in sweet cherry were all used cross-pollinated F_1 populations. Self-pollination is often not possible in sweet cherry due to the gametophytic self-incompatibility system operating in this species (Herrero et al., 2017). However, natural self-compatible sweet cherry mutants like 'Cristobalina' (Wünsch and Hormaza, 2004) or other self-compatible sweet cherry accessions can be used to generate F_2 populations which can be used for genetic mapping studies. The self-compatible local cultivar 'Cristobalina' and its self-compatible descendant, the selection 'BC8', were used to develop two self-pollinated populations for genetic analysis. Genetic maps of these sweet cherry populations were constructed, and their level of homozygosity was previously reported (Chapter 2). These were the first F_2 populations used for genetic map construction in this species and are now available for QTL analysis.

The Spanish cultivar 'Cristobalina' comes from the Mediterranean area, and in addition to being self-compatible (Wünsch and Hormaza, 2004; Cachi and Wünsch, 2011; Ono et al., 2018), it has a low CRs (<550 h; Tabuenca, 1983; Alburquerque et al., 2008) and extra early flowering and maturity dates. These characteristics make 'Cristobalina' an interesting breeding cultivar. Cultivars with low CRs often show early flowering (Alburquerque et al., 2008) and this low chilling requirement is of high interest for extending cherry growing to regions with warmer winters, and in the current context of global warming as a source of adaptation to low chilling. In this work, we used six related sweet cherry populations that descend from 'Cristobalina' and other sweet cherry cultivars with mid and late BTs to investigate the genetic basis of BT and low chilling in different genetic backgrounds. For this objective, we used a Bayesian QTL mapping approach implemented in FlexQTL™, and two self-pollination populations to investigate the genetic effects of the QTL alleles. The results obtained broaden the understanding of the genetic control of CR and BT in this species and will allow the implementation for MAS of these traits from this and related plant material.

MATERIALS AND METHODS

Plant materials

Six related sweet cherry full-sib families (N=406), along with six parental cultivars and five ancestor cultivars, were used in this study (Fig 3.1). Four of these families come from cross-pollinations (F_1), namely 'Vic' × 'Cristobalina' (V×C; N=158), 'Ambrunés' × 'Cristobalina' (A×C; N=40), 'Brooks' × 'Cristobalina' (B×C; N=29) and 'Lambert' × 'Cristobalina' (L×C; N=14). The remaining two populations (F_2) come from the self-pollination of 'Cristobalina' (C×C; N=97) and 'BC8' (B×C2; N=68), which is a selection from the progeny of 'Brooks' × 'Cristobalina' (Fig 3.1). All these trees derive from controlled cross- and self-pollinations made from 2008 to 2010 and are located at the experimental orchards of CITA de Aragón in Zaragoza (Spain).

Bloom time phenotyping

BT was evaluated for each progeny and the parental cultivars during four years (2015 to 2018). Blooming was observed in all the trees three days per week (every 2-3 days) during the flowering season. BT was recorded when approximately 75% of the floral buds reached stage F (full bloom; Baggiolini, 1980). BT data were converted to calendar days (CD; days from January 1st) and growing degree hours (GDH). GDH were calculated as the number of GDH accumulated from January 1st until BT using the linear model described by Richardson et al. (1974). The best linear unbiased prediction (BLUP) value among years for CD and GDH was calculated using the *lme4* package of R 3.4.1 software (Bates et al., 2015; R Core Team, 2017). All subsequent BT analyses were done using both the CD and the GDH conversions.

Mean, minimum and maximum values and the distribution of BTs were estimated in each population per year and for the BLUP values. Mean BTs were then compared between families using analysis of variance (ANOVA) and Tukey post-hoc test ($p<0.05$) for BLUP values. *Pearson* correlation coefficient of BTs between years and BLUP values were also estimated. Statistical analyses were carried out using SPSS statistics v21.0.0 software (IBM, Chicago, IL, USA).

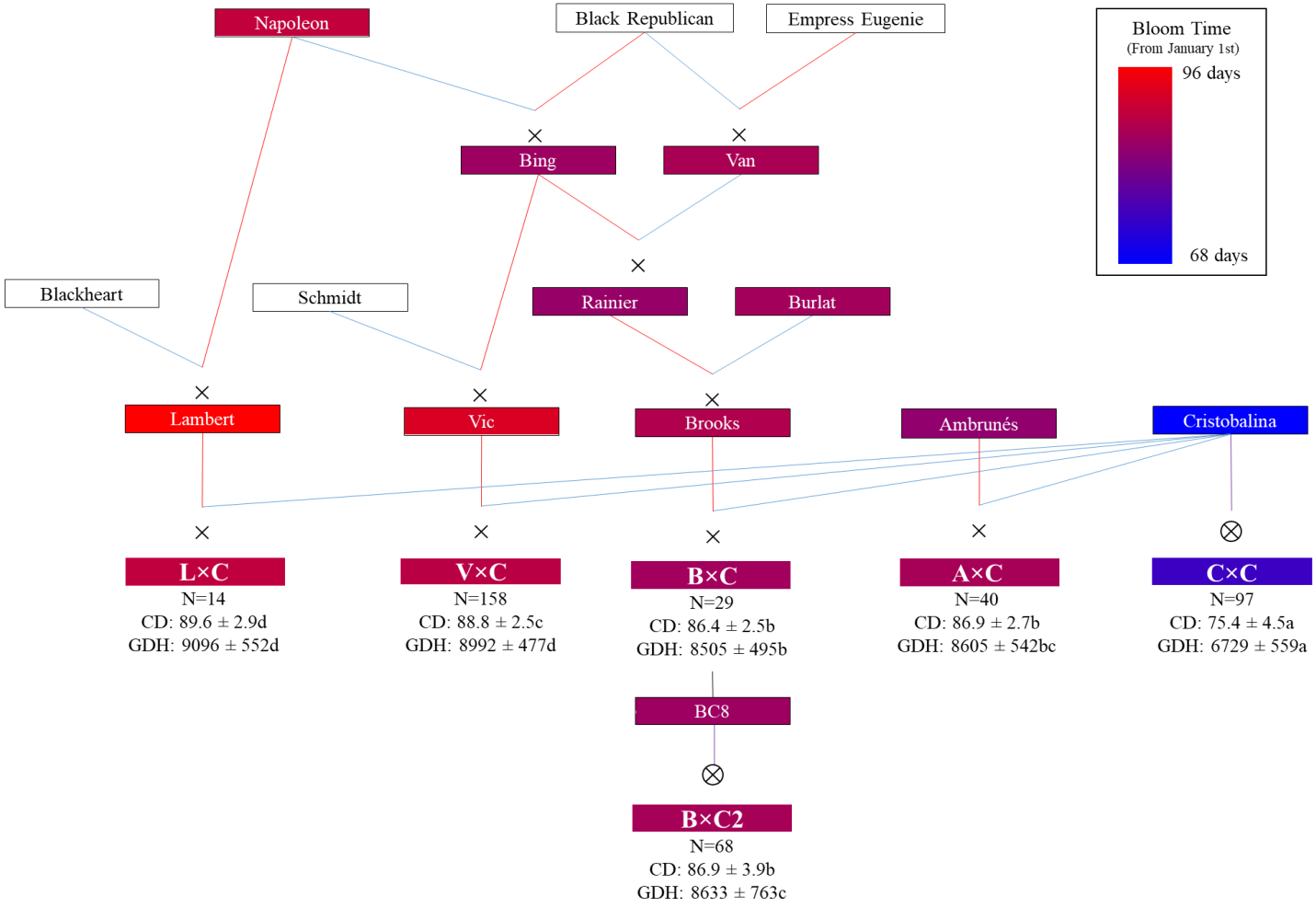

Figure 3.1 Families, parental and ancestor cultivars used in this work with their known pedigrees (Red and blue lines indicate female and male parent, respectively). Color code (from Pedimap software; Voorrips 2007) indicates the BLUP (Best linear unbiased prediction) of bloom time values expressed in calendar days (CDs). In the families, the number of individuals (N), mean value of bloom time in both CDs and growing degree hours (GDHs), and significant differences of bloom time among different families (ANOVA and Tukey Test; $P < 0.05$) are also shown

Broad-sense heritability (H^2) was calculated using the equation: $H^2 = \frac{\sigma_g^2}{\sigma_g^2 + \frac{\sigma_e^2}{n}}$, where σ_g^2 is the variance of genotype effect, σ_e^2 is the variance of the residual term and *n* is the number of years. H^2 were calculated using R v3.4.1 (R Core Team, 2017).

Genotyping and QTL analysis

Genotypes of 417 individuals that include the six populations described above, their parental and ancestor cultivars (Fig 3.1) were used for QTL analysis. All these plant material had been previously genotyped using the RosBREED Illumina cherry 6K SNP array v1 (Chapter 2). For QTL mapping using FlexQTL™ (Bink et al., 2014), the genotyped SNPs of all plant materials were previously filtered. SNPs monomorphic in all populations, that had null alleles, with MAF<0.05, with more than 5% of missing data, and showing errors in various genotypes were discarded. The selected markers were further checked by analyzing their genetic segregation using FlexQTL™ and by visual inspection when a double recombination event occurred within an interval smaller than 10 cM. A consensus genetic map from the selected SNPs was constructed. Those SNPs previously mapped in V×C (Chapter 2) were assigned their genetic position. Those SNPs not previously mapped in the V×C map were integrated in the map by using their physical position on the peach genome v2.0.a1 (Verde et al., 2017).

QTL mapping for the two parameters, CD and GDH, each year and for BLUP values, using all the plant material, was carried out using a Bayesian multiple QTL model implemented in FlexQTL™ (Bink et al., 2014). In this work, only additive effects with normal prior distribution were considered. The models were set with a prior distribution of number of QTLs of 1 and 3 in order to assess sensitivity of posterior inference to the prior assumptions. Markov chain Monte Carlo (MCMC) simulation with minimum of 500,000 iterations for each prior number of QTL were performed until at least 100 effective chain samples (ECS) were reached for overall mean (μ), the residual variance (σ_e^2), the number of QTLs (N_{QTL}) and the variance of QTLs ($_VQTL$) (Gelman and Rubin, 1992; Sorensen and Gianola, 2002). A total of 1,000 samples (500,000 iterations with thinning value of 500) were stored for further posterior inferences. The inference in the number of QTLs was estimated using twice the natural log of Bayes factors (*2lnBF*) (Kass and Raftery, 1995) obtained after a pairwise comparison of models differing by one QTL from each other.

Values of *2lnBF* higher than 2, 5 and 10 indicate positive, strong and decisive QTL evidences, respectively. Only QTLs with strong and decisive evidences were considered in this work. The percentage of variation explained (PVE) by each QTL was estimated as [(wVAt1 / PV) × 100], where wVAt1 is the weighted variance and PV is the total phenotype variation (Mangandi et al., 2017). The genomic breeding value (GBV) for each individual and parent was predicted using QTL genotype probabilities, intensity and effect size (Bink et al., 2014).

Haplotype analysis

SNP haplotypes of the two most significant QTLs detected with an average 2lnBF higher than 10, were constructed for the parental cultivars and theirs ancestors. The haplotypes were designed to span the confidence interval with 2lnBF>10 for these QTLs using BLUP model. The SNP haplotypes were estimated using SNP phase estimation of FlexQTL™ for all the cultivars, except for 'Bing' and 'Napoleon' that were estimated manually (for QTL on LG2) based on pedigree information and the availability of previously phased haplotypes (Cai et al., 2017). SNP haplotypes were also confirmed based on segregation. Mean phenotypic values of each of these QTL haplotypes and their combined effects, for CD and GDH, were estimated in each segregating class of each population. Individual progenies with recombination events within these QTL regions were excluded from the analysis. For mean comparison of the phenotypic values within each population, Kruskal-Wallis, two-tailed Student's t test and Tukey test ($p<0.01$) post-hoc analysis were used. All statistical analysis were done using SPSS statistics v21.0.0 software (IBM, Chicago, IL, USA).

RESULTS

Bloom time phenotyping, segregation and heritability

BT was evaluated in the parental cultivars and populations during four consecutive years (Fig 3.1; Sup Table 3.1). The parental cultivar 'BC8' was phenotyped only the first year as the tree was in poor health in subsequent years. 'Cristobalina' was the earliest

parental cultivar to bloom in all of the years [BLUP value: 69 CDs and 5,999 GDHs; Fig 3.1 and 3.2]. ‘Ambrunés’,‘BC8’ and ‘Brooks’ showed mid-season flowering (Fig 3.1 and 3.2), while ‘Vic’ and ‘Lambert’ exhibited late blooming with BLUP values of 95 and 97 CDs (9,841 and 10,259 GDHs), respectively (Fig 3.1 and 3.2). CR were fulfilled for ‘Cristobalina’ (550 h; Tabuenca, 1983) between mid-December to the first week of January during the four years of analysis (Sup Fig 3.1). The rest of the parental cultivars, ‘Ambrunés’, ‘Brooks’ and ‘Lambert’, all had higher CR (900 to 1,100 h; Tabuenca, 1983; Alburquerque et al., 2008). During the four years evaluated, the CR of these three cultivars were not fulfilled until mid-January to late February (Sup Fig 3.1).

The same blooming order (extra-early, mid and late blooming) was observed for the parental cultivars each year, but differences in the BTs were observed between years (Sup Table 3.1). BT was earliest in 2017 for the mid and late cultivars, which bloomed 16 to 17 days earlier than the average date of the rest of the years. However, for ‘Cristobalina’, the earliest bloom period occurred in 2016 (Sup Table 3.1), while the latest bloom period for all parental cultivars occurred in 2018 (Sup Table 3.1). In 2016, fulfilment of the CR and HR for ‘Cristobalina’ occurred early resulting in an early bloom. However, this was followed by a period of cold temperatures that delayed the flowering of the rest of the cultivars extending the blooming season (Sup Fig 3.1). In 2017, a high accumulation of chill hours during the early winter followed by a period of warmer temperatures in the beginning of February resulted in an earlier bloom for all the cultivars and a shorter blooming period (Sup Fig 3.1). In 2015 and 2018, although large amounts of chill were accumulated during the early winter, cold temperatures in February delayed bloom. Years 2017 and 2018 were colder and CR were fulfilled earlier in the year, but BT was earlier in 2016.

In the populations, different numbers of offspring were phenotyped each year, ranging from 258 (64%) in 2015 to 367 (90%) in 2018 (Sup Table 3.1). Only individuals (N=360) with phenotypic data from two or more years were used to estimate BLUP values. The bloom period varied between years and populations, from 7 to 24 days. On average A×C, B×C and L×C showed shorter bloom periods (10 to 12 days) than B×C2, C×C and V×C (16 to 18 days) (Sup Table 3.1). ‘Cristobalina’ self-pollination (C×C) was the earliest population to bloom (Fig 3.1 and 3.2), as on average, it bloomed 11 to 14 days earlier than the rest of populations (Fig 3.1 and 3.2). The mean BTs of A×C, B×C and B×C2 were

similar, while V×C and L×C were the latest populations to bloom (Fig 3.1 and 3.2). Differences in the mean BT of the populations was observed between years. For all the populations, the earliest bloom period was in 2017 and latest in 2018 (Sup Table 3.1). It was especially noticeable in 2017 when warm temperatures resulted in earlier flowering for all genotypes and the shortest bloom period (18 days) of all years. In 2016, warm temperatures in mid-February, resulted in very early bloom of some individuals from C×C population, but a cold period later on delayed the flowering of the rest of the population, resulting in the largest bloom period in all years evaluated.

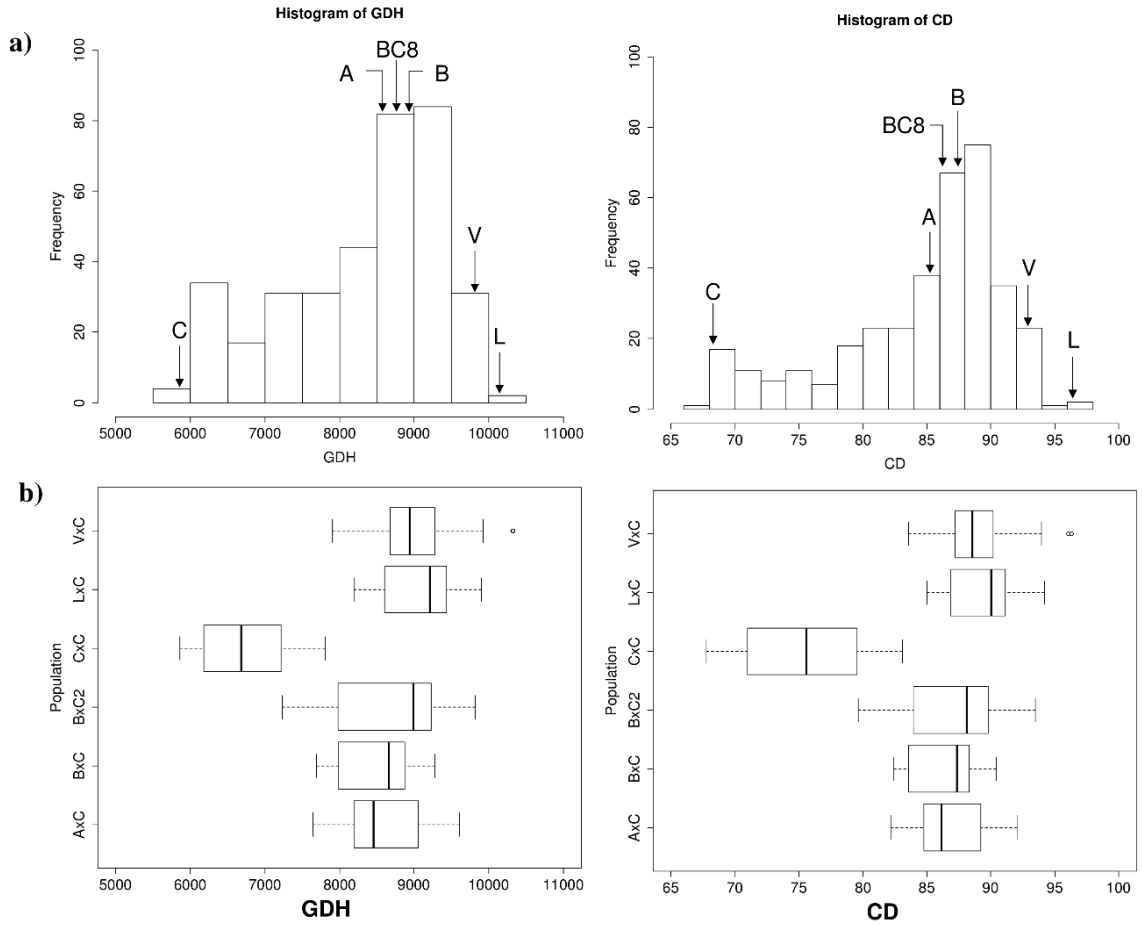

Figure 3.2 (a) Frequency distribution of bloom time BLUP values of plant materials analyzed expressed in GDHs and CDs. Letters with arrows indicate parents' bloom times; 'Ambrunés' (A), 'Brooks' (B), 'B×C-08' (BC8), 'Cristobalina' (C), 'Lambert' (L) and 'Vic' (V). (**b)** Blooming period of each population (boxes). Bold line in the boxplot indicates the median value, the left and right sides of the box represent the 25th and 75th percentile, respectively. Whiskers represent the lower and upper extreme values.

BT distribution varied between populations and years. Only the smallest populations (B×C and L×C) fitted a normal distribution for all evaluated years and for BLUP values in both models, CDs and GDHs (Shapiro-Wilk test; Prob < W: 0.083-0.263). Populations B×C2 and A×C fitted a normal distribution only two of the years also for both models (Shapiro-Wilk test; Prob<W: 0.085-0.664), whereas the remaining two populations (C×C and V×C), which are the largest, did not fit normal distributions in any of the years, neither for CD nor GDH. BT of all the progenies together also did not show normal distribution for any of the years or BLUP, or for CD or GDH (Fig 3.2). In all cases, skewed distributions towards medium and late BT were observed. In fact, only some C×C offspring were extra-early blooming, and only some B×C2 offspring were early blooming. The rest of the plant materials were medium to late blooming, even though all populations (except B×C2) had 'Cristobalina' (extra-early blooming) as one of the parental cultivar. Transgressive segregation towards late blooming was also observed in the four years and for BLUP values for all populations except L×C. On the other side, transgressive segregation towards early blooming was only observed in the self-pollinated populations (C×C and B×C2; Fig 3.2; Sup Table 3.1).

Highly significant ($p<0.01$) and positive correlations were observed for BTs between years and BLUP value ($r = 0.897$ to 0.966), and between CD and GDH data ($r = 0.984$ to 0.997; Sup Table 3.2). BT broad-sense heritability (H^2) was estimated for all populations together and for each population. H^2 was high for BT using both, GDH (0.94) and CD (0.97). In the populations, H^2 was also high, with values ranging from 0.87 to 0.96 for GDH and from 0.85 to 0.96 for CD (Sup Table 3.1).

QTL analysis

Quality filtering of the SNP markers resulted in 1,269 (22.3%) SNPs selected for map construction (Sup Tables 3.3 and 3.4) and QTL analyses. These selected SNPs covered a total genetic length of 721.98 cM with an average marker density of 0.57 cM (1 SNP per 176 kb) and a maximum gap between markers of 10.95 cM (1.43 Mbps) located on LG 7 (Sup Table 3.4).

Table 3.1 Summary of BT QTLs identified with strong evidence (2lnBF > 5) in multiyear analysis (BLUP values) for GDHs and CDs. Bold indicates decisive evidence for a QTL (2lnBF > 10).

Trait	QTL	LG[1]	cM[2]	QTL peak (cM)	Physical position* (Mbp)	Max 2lnBF	Average 2lnBF	Mean Additive effect	PVE (%)
GDH	*qP-GDH1.1*^{m}	1	4-11	8	1.73 - 3.44	9.6	7.1	272	1.6
	***qP-GDH1.2*^{m}**	**1**	**137-139**	**137**	**43.28 - 43.54**	**13.5**	**11.8**	**1403**	**50.1**
	***qP-GDH2.1*^{m}**	**2**	**73-75**	**75**	**26.96 - 29.68**	**22.0**	**22.0**	**840**	**12.8**
	qP-GDH3.1^{m}	3	37-52	45	9.41 - 15.75	9.4	7.3	290	1.9
	qP-GDH4.1^{m}	4	5-21	13	1.19 - 5.15	8.8	7.1	744	11.9
	qP-GDH5.1^{m}	5	66-71	69	16.42 - 18.10	11.8	9.3	181	0.8
CD	***qP-CD1.1*^{m}**	**1**	**137-139**	**137**	**43.28 - 43.54**	**10.9**	**9.5**	**7.4**	**32.4**
	***qP-CD2.1*^{m}**	**2**	**73-75**	**75**	**26.96 - 29.68**	**18.8**	**18.8**	**5.9**	**15.2**
	qP-CD4.1^{m}	4	4-23	19	0.92 - 5.44	5.1	4.6	3.6	6.0

[1]LG: Linkage group. [2]cM: centiMorgan. *: Physical position on Peach Genome v2.0.a1 (Verde et al., 2017)

QTL analysis using BLUP values of the four years in all the populations revealed six significant BT QTLs for GDH and three for CD (Fig 3.3). QTLs for GDH were identified on LGs 1, 2, 3, 4 and 5 (Table 3.1; Fig 3.3). For both these traits, QTLs with decisive evidences (2lnBF>10), were found on LG1 (*qP-GDH1.2*^{m}) and LG2 (*qP-GDH2.1*^{m}) (Table 3.1). *qP-GDH1.2*^{m} explained the largest percentage of phenotypic variation (PVE; 50.1%) and was associated with a mean additive effect of 1,403 GDH (Table 3.1; Fig 3.3). The other decisive QTL, *qP-GDH2.1*^{m}, had a PVE of 12.8% and an additive effect of 840 GDH (Table 3.1). Four additional QTLs with strong evidence (2lnBF>5) were detected for GDH on LGs 1, 3, 4 and 5 (Table 3.1; Fig 3.3). From these, the QTL on LG4 (*qP-GDH4.1*^{m}) showed higher PVE (11.9%) while the remaining three, showed minor effects (PVE: 1-2%; Table 3.1). For CD, the two QTLs with decisive evidence (*qP-CD1.1*^{m} and *qP-CD2.1*^{m}) had equivalent positons as those identified for GDH (Table 3.1; Fig 3.3). As for GDH, *qP-CD1.1*^{m} showed a larger PVE (32.4%) and mean additive effect (7.4 days) than *qP-CD2.1*^{m} (15.2% PVE and additive effect of 5.9 days; Table 3.1). Also a QTL on LG4 (*qP-CD4.1*^{m}) with strong evidence was identified that spanned the same region as that for GDH (Table 3.1; Fig 3.3).

In the QTL analyses for individual years, the two major QTLs detected on LGs 1 and 2 in the 4-year analysis were also detected in every year, with strong or decisive evidence, for both CD and GDH (Sup Table 3.5). However, in 2016, two of these QTLs (*qP-GDH1.2*^{m} and *qP-CD1.1*^{m}) showed lower PVE than other years. Also in 2016, the major QTL on LG2 exhibited larger PVE than the QTL on LG1 (Sup Table 3.5). The

significance of the minor effect QTLs varied between years, and were located on LGs 3, 4, 5 and 7 (Sup Table 3.5). The main difference between the 4-year and single year analyses were for the QTLs on LG4 using BLUP (*qP-GDH4.1*^{m}/*qP-CD4.1*^{m}), as they were only detected in 2017. Additionally, in 2016, a GDH QTL on LG7 (*qP-GDH7.1*) was detected that showed a high PVE (12.1%; Sup Table 3.5), but this QTL was not detected in the 4-year analysis.

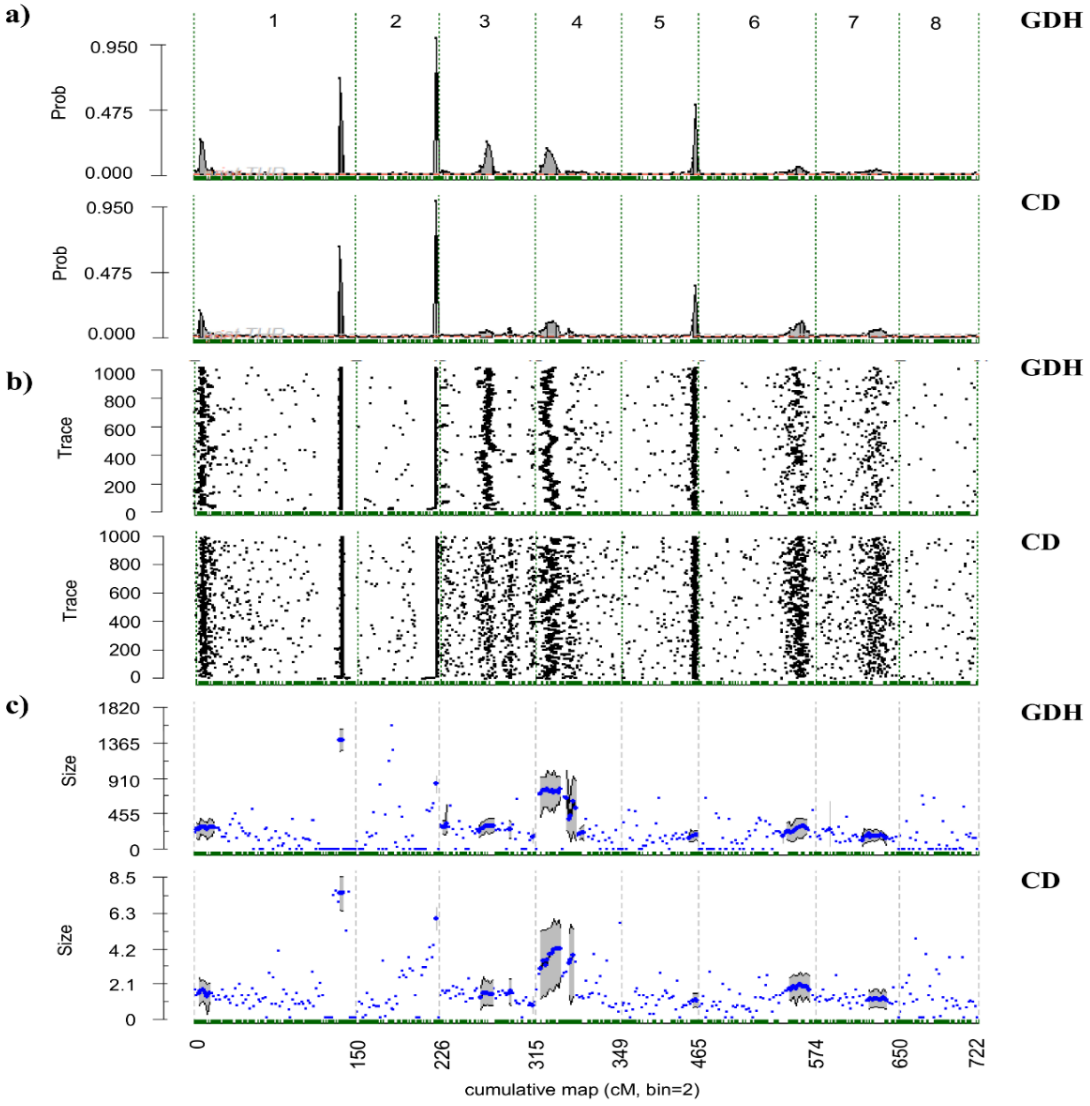

Figure 3.3 (**a**) Posterior probabilities of QTL positions along the genome with a 2 cM bin resolution. **(b)** Trace plot of Markov chain Monte Carlo samples for QTL position. (**c**) Posterior mean (*blue dots*) and 90% credible region (*gray shade*) for estimate additive QTL effects for chromosomal regions of 2 cM bins with positive evidence ($2\ln BF_{10}>2$) for QTL presence. Vertical dashed lines identify the starts and ends of chromosomes. CD: Calendar Days; GDH: Growing Degree Hours.

Estimation of QTL genotypes and genomic breeding value

QTL genotype estimation was carried out for QTL regions with either strong or decisive evidence using BLUP value (Fig 3.4) for the parental cultivars and the ancestors in the collection (Fig 3.1). For the major QTL on LG1 (*qP-GDH1.2^m/qP-CD1.1^m*) and LG2 (*qP-GDH2.1^m/qP-CD2.1^m*), 'Cristobalina' was predicted to be homozygous for alleles associated with early bloom (*qq*= low phenotype value) for the LG1 QTL and predicted to be heterozygous (*Qq*) for the LG2 QTL (Fig 3.4). 'BC8', an offspring from the cross of 'Brooks' and 'Cristobalina', was heterozygous for the early bloom allele for the LG1 QTL (*qP-GDH1.2^m/qP-CD1.1^m*). No other parental cultivar was predicted to have early BT alleles for these two QTL, instead the remaining parental cultivars were predicted to be homozygous (*QQ*) for LG1 and LG2 QTL alleles for later BT (Fig 3.4). This indicates that 'Cristobalina' is the only cultivar that contributed early BT alleles for the major QTLs in all the plant materials. For the QTL on LG4 (*qP-GDH4.1^m/qP-CD4.1^m*), only 'Rainier' and its offspring 'Brooks', were predicted to be heterozygous for early BT alleles. For the QTL on LG3, 'Burlat', 'Cristobalina' and 'Ambrunés' were predicted to be homozygous for alleles associated with early bloom, while for the QTL on LG5 (*qP-GDH5.1^m*) early bloom alleles were predicted to heterozygous in 'Cristobalina' and 'Vic' (Fig 3.4).

Differences in the predicted genotypes were used to estimate genome breeding value (GBV) of parents and ancestors (Fig 3.4). Differences of as much as 26.8 CD (4,394 GDH) between the GBV of the earliest and latest blooming cultivar were observed (Fig 3.4). All but 'Cristobalina' had GBV associated with delayed flowering. 'Cristobalina' had the lowest GVB, due to the relative abundance of alleles predicted to result in earlier flowering by 8.9 CD and 1,210 GDH. In contrast, 'Vic' and 'Lambert' cultivars had the GBV most associated with late flowering (17.0 CD/3,050 GDH and 17.9 CD/3,184 GDH, respectively; Fig 3.4).

QTL haplotype and genotype analysis

The estimation of the mean phenotypic values of these QTL haplotypes in the F_2 populations (C×C and B×C2) revealed that for the QTL on LG1 (*qP-GDH1.2^m/qP-CD1.1^m*), those individuals that were homozygous for *H1-c*, like 'Cristobalina' (*cc*), showed the earliest BTs (Fig 3.5). In C×C, this QTL was not segregating and all the

progeny were '*cc*', with a mean BT of 75 CDs (6,729 GDH). In B×C2, this QTL was segregating but segregation distortion was observed as no '*aa*' individuals were identified. In the two remaining segregating classes, individuals with the '*cc*' genotype showed a mean difference of almost 7 CDs earlier blooming that those with '*ac*' genotype (Fig 3.5).

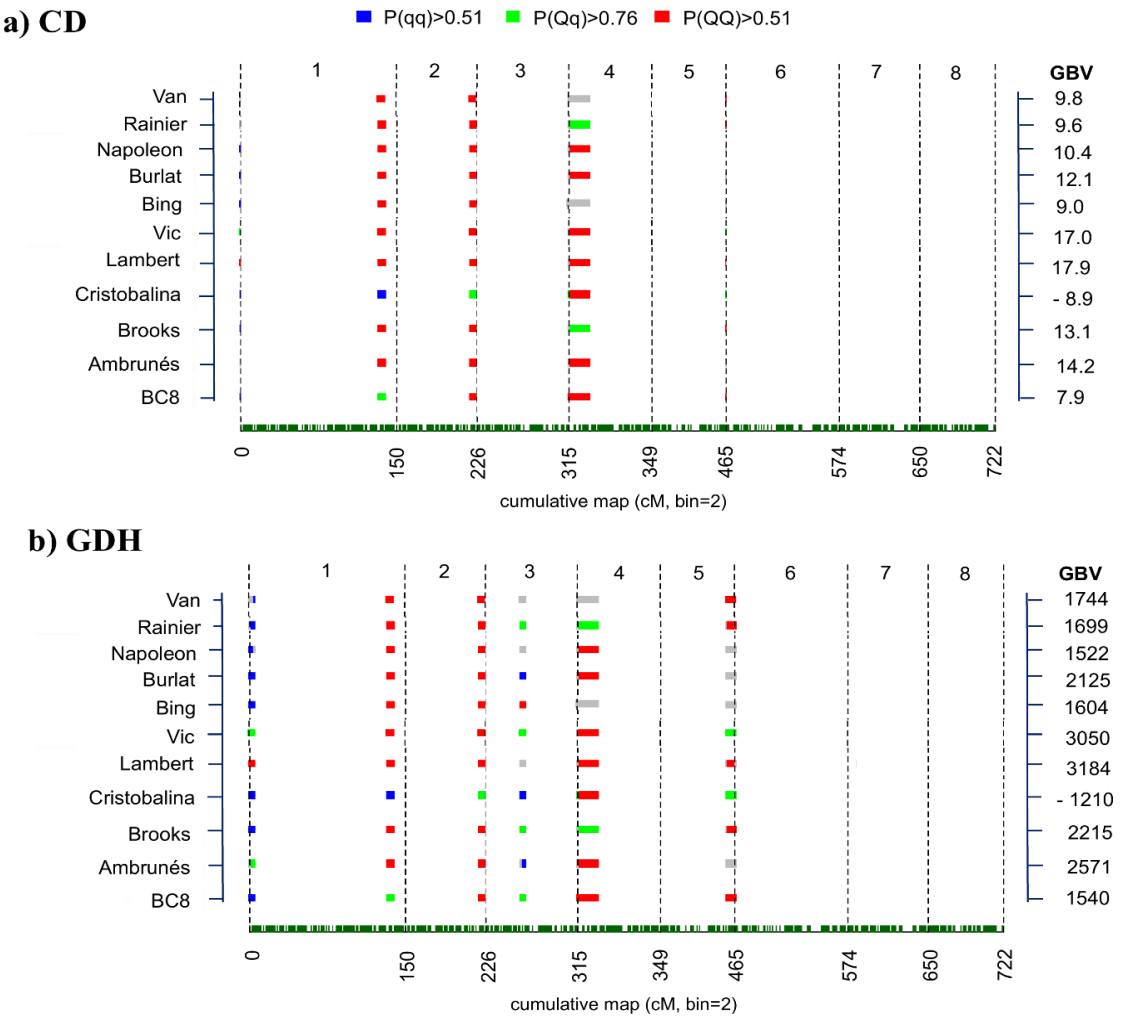

Figure 3.4 Posterior estimates of parental QTL genotype probabilities for GDH **(a)** and CD **(b)** in QTL regions with strong and decisive QTL evidences (2lnBF>5) for BLUP values. Red, green and blue colors represent positive evidence for QTL genotypes *QQ, Qq and qq* genotypes, respectevely. '*Q'* and '*q'* denote alleles with high and low phenotype values, respectively. Grey colors indicate unclear genotype estimation. Genome breeding value (GBV) for each cultivar is indicated at right.

For the QTL on LG2 (*qP-GDH2.1*^{m}/*qP-CD2.1*^{m}), *H2-f* was associated with early flowering. In C×C ('Cristobalina'; '*ef*'), this QTL segregated in three classes, with

offspring that were '*ef*' and '*ff*' flowering on average 7 CD (945 GDH) earlier that those that were '*ee*' (Fig 3.5). As no significant differences were observed between these two classes, *H2-f* appeared to be dominant to *H2-e* (Fig 3.5). B×C2 also segregated in three classes for this QTL, but no significant differences were observed among them (Fig 3.5). Since *H2-f* was not inherited in 'BC8' (*ce*), the effect of this haplotype could not be investigated in this population.

The interaction of two major QTLs on LGs 1 and 2 showed that those individuals homozygous for *H1-c* were the earliest to bloom for both populations. Within these, those that also had *H2-f* showed the earliest BT (Fig 3.5).

In the F_1 populations, for the LG1 QTL, '*ac*' genotypes were always earlier blooming (approx. 2 to 3 days that those that are '*bc*'; Sup Fig 2 and 3), indicating that *H1-a* was associated with earlier BT compared to *H1-b*. For the LG2 QTL, genotypes with *H2-f* showed earlier BT (1 to 7 CDs) compared to individuals without it. In addition, segregation distortion against *H2-f* was observed in all the populations, being most evident in B×C, as none of the progeny had this haplotype (Sup Fig 2 and 3). The genotype interaction of both QTLs in the F_1 populations showed that individuals heterozygous for *H1-a*/*H2-f*, showed earlier BT than those individuals with other genotype combinations (Sup Fig 2 and 3).

DISCUSSION

'Cristobalina', the earliest blooming parental cultivar, has a low CR (176-550 h under 7ºC; Tabuenca, 1983; Alburquerque et al., 2008); which is consistent with its native origin close to the Mediterranean coast in eastern Spain (Herrero, 1964). Plant's CR are typically correlated to the climate in the area of origin (Abbott et al., 2015). In our experimental location, which experiences a higher chilling accumulation, it is likely that the early blooming of 'Cristobalina' is due to its low CR, as earlier blooming has been observed in cultivars with lower CR (Alburquerque et al., 2008; Castède et al., 2014). 'Cristobalina' is also self-compatible (Wünsch and Hormaza, 2004) due to a single mutation affecting pollen tube growth (Cachi and Wünsch, 2011; Ono et al., 2018). Natural self-compatible mutations are rare in sweet cherry; however, this mutation may be

especially beneficial in this low chill cultivar because mating partners with overlapping flowering times would be scarce (Cachi et al., 2014).

The same BT (CD) order, early, mid- and late bloom, of the parental cultivars in the four years, independently of the year temperatures, confirms the genetic determination of this trait. As previously demonstrated, BT in cherries is a quantitative trait with high heritability (Dirlewanger et al., 2012; Castède et al., 2014; Cai et al., 2018). High heritability values for this trait were also observed in this work for the four years (0.85 to 0.96 for CD, 0.89 to 0.96 for GDH), and these values are in the same range as those estimated previously for sweet and sour cherry (0.88 to 0.96; Wang et al., 2000; Dirlewanger et al., 2012; Castède et al., 2014; Cai et al., 2018; Piaskowski et al., 2018). However, BT differences between years are highly dependent on environmental conditions and how these conditions impact CR fulfillment. For example, the coldest winters did not result in the earliest BT.

Within the populations, only individuals from F_2 populations (C×C and B×C2) showed transgressive segregation towards early blooming, whereas F_1 populations showed transgressive segregation and skewed distribution towards late flowering, revealing possible dominance of the late bloom alleles in this plant material. In sweet cherry, skewed segregation in F_1 populations towards high CR, but not late bloom, was also observed (Castède et al., 2014). This was also the case in almond, where *Late bloom* (*Lb*) is dominant (Ballester et al., 2001), and in Japanese plum and apricot F_1 populations from low CR cultivars (Campoy et al., 2011; Salazar et al., 2016; Kitamura et al., 2018). However, transgressive segregation towards both early and late blooming was observed in peach F_2 populations (Fan et al., 2010; Bielenberg et al., 2015). The effect of (recessive) alleles in the homozygous state will be possible to detect in F_2 populations (like C×C and B×C2), which may explain why transgressive segregation towards early bloom in our plant material is only observed in the F_2 populations. The extended bloom period observed in the larger populations (C×C, V×C) may also have resulted from additional climatic variation experienced during this longer BT duration. This effect was also observed by Castède et al. (2014).

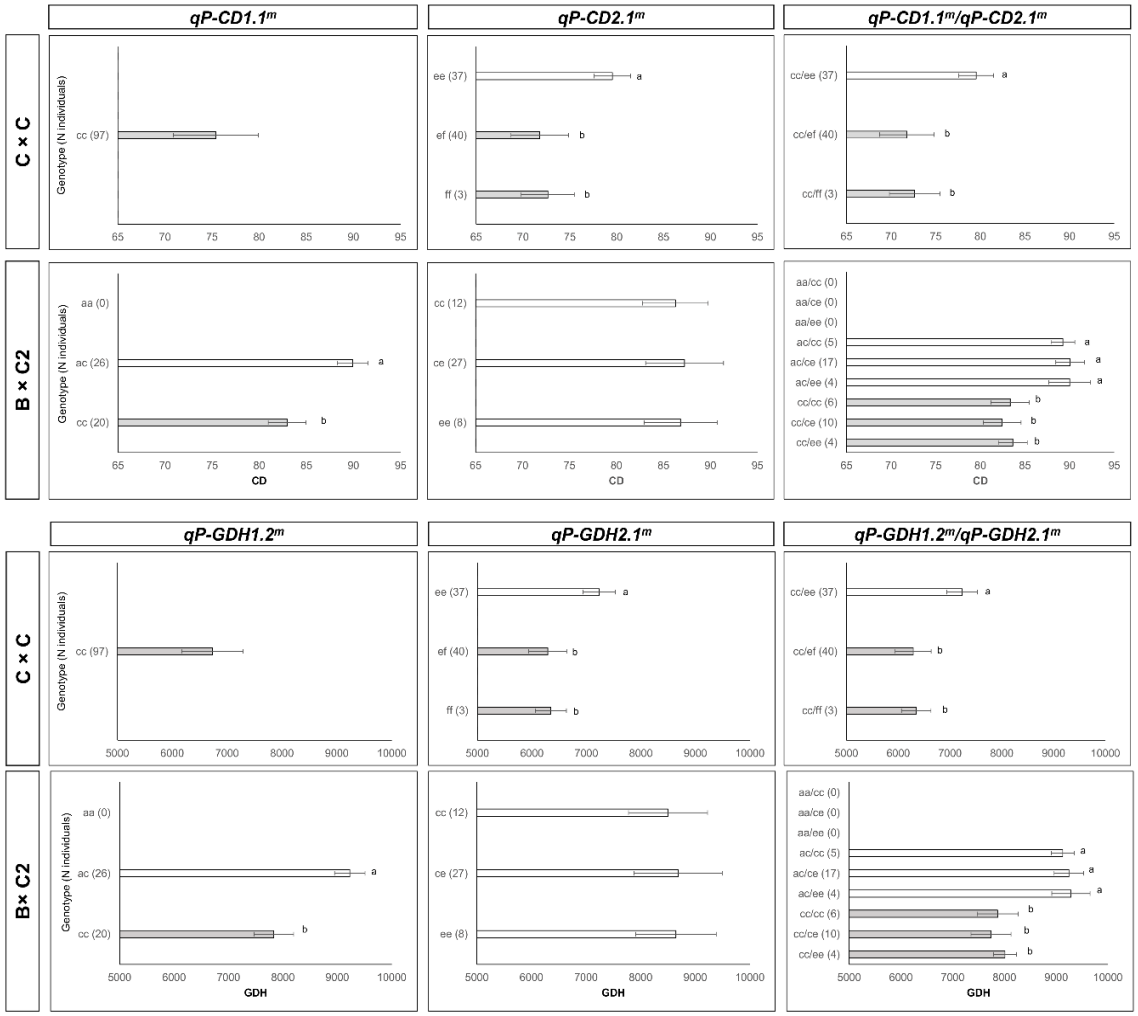

Figure 3.5 BT mean values of CD and GDH for offspring based on the haplotypes for the major QTLs detected on LG1 and LG2 individually and the two QTLs together. The offspring are from the two F_2 populations (C×C and B×C2). Significant differences between genotypes are indicated by different letters (P<0.05).

In this work, BT was evaluated using the variables CD and GDHs for QTL analysis. Both are based on the recorded BT of each individual, but differ in that CDs refer only to the recorded date while GDHs consider the temperature effect within a range (4.5 to 25 ºC; Richardson et al., 1974). As previously reported (Chavoshi et al., 2014), there is a large correlation between both parameters, suggesting that both models can be used for genetic analysis of BT. As temperature requirements for blooming are similar between years, GDHs should provide a more consistent measure of BT, whereas BT expressed as CD would be more dependent on the climatic conditions. In fact, QTL mapping results from this work were very similar for both variables, but a larger number of QTLs were detected

for GDH than for CDs. QTLs detected were more robust (higher Bayes Factor) when using GDH than when using CDs, and the same QTLs explained a larger PVE for GDH than for CD. Thus, in this work, BT expressed as GDH, provided a better ability to describe the genetic variation compared to the same bloom data expressed as CD.

Two major BT QTLs on LG1 (*qP-CD1.1^{m}/qP-GDH1.2^{m}*) and LG2 (*qP-CD2.1^{m}/qP-GDH2.1^{m}*)

The major QTL identified on LG1 (*qP-CD1.1^{m}/qP-GDH1.2^{m}*) has been previously detected in sweet cherry (Dirlewanger et al., 2012; Castède et al., 2014). However, in these works, the variation explained and additive effect of this QTL were lower than observed herein. Dirlewanger et al. (2012) first identified the LG1 QTL in 'Lapins' with a PVE ranging from 9.3 to 17.5% and an additive effect of 2.5 days. Castède et al. (2014) reported the same QTL region for two of three years for a 'Regina' × 'Garnet' population, with similar additive effect (1.4 days) and mean PVE (8%). In our work, this QTL represented 50.1 and 32.4 of PVE and has an additive effect of 1,403 GDH or 7.4 CD. These results indicate that BT of our plant material, in our environmental conditions, was determined by this QTL in a larger proportion than in earlier works in sweet cherry.

A CR QTL overlapping with this LG1 BT QTL was also identified in sweet cherry (Castède et al., 2014), confirming the correlation between both traits and the relevance of CR for BT in the species. This BT and CR QTL has also been described in other *Prunus* species like peach, apricot and almond, as a main QTL controlling these traits (Olukolu et al., 2009; Fan et al., 2010; Dirlewanger et al., 2012; Sánchez-Pérez et al., 2012; Salazar et al., 2013; Zhebentyayeva et al., 2014; Romeu et al., 2014; Bielenberg et al., 2015). In our work, the high significance and effect of this QTL in our work indicates that, in our conditions, the BT of the plant material analyzed is probably more dependent on CR than other materials analyzed in different environments.

Candidate genes of the LG1 QTL have been described in peach and sweet cherry (Bielenberg et al., 2008; Fan et al., 2010; Castède et al., 2015). The position of this QTL overlaps with the region where six *DORMANCY ASSOCIATED MADS-box* (*DAM1-6*) genes have been identified as major genes controlling CR and BT in peach (Bielenberg et al., 2008; Fan et al., 2010). In the *evergrowing* peach mutant, that lacks response to winter

cold, four of these genes are deleted and the other two are not expressed (Bielenberg et al., 2008). Castède et al. (2015) mapped two of these *DAM* genes (*DAM 5* and *6*) within the interval of this QTL in 'Lapins' sweet cherry. It is likely that the 'Cristobalina' alleles of these genes are contributing to low CR and early blooming, and the large effect of this QTL in the plant material analyzed. 'Cristobalina' contributed *H1-c* for this QTL, which was associated with earlier flowering, as BT is earliest (7 days) when *H1-c* is homozygous, as is the case for 'Cristobalina' and in all the C×C population. Previously, a large amount of homozygosity was observed in 'Cristobalina' and therefore also in the self-pollinated population (Chapter 2). More specifically, a large homozygous region at the bottom of LG1 (26.23 to 47.81 Mbp), overlapping with this BT QTL was observed (Chapter 2). A smaller difference (approx. 2 to 3 days) observed between the two remaining haplotypes (*H1-a, -b)* is in agreement with the finding that this QTL was detected at lower PVE in other works (Dirlewanger et al., 2012; Castède et al., 2014), where the allele *H1-c* was probably not present.

The second major QTL was identified on LG2 (*qP-CD2.1^{m}/qP-GDH2.1^{m}*). This QTL also overlaps with a CR and BT QTL previously described in sweet cherry (Castède et al., 2014). The PVE and additive effect of this QTL in previous work (3.6-6.5% PVE; 0.8-2.8 day; Castède et al., 2014) was also lower than observed in our study (12.8-15.2%; 5.5 CD). This QTL has also been identified in apricot and in the interspecific cross of peach and *P. davidiana*, but explained a lower PVE than herein (Quilot et al., 2004; Olukolu et al., 2009; Dirlewanger et al., 2012). *SOC1*, a MADS-box gene, has been identified as a strong candidate gene for CR and BT underlying this QTL in sweet cherry and apricot (Trainin et al., 2013; Castède et al., 2015). However, the physical position of this gene (Castède et al., 2015) is not within the interval of the QTL detected in this work. Among other candidate genes identified in this region in sweet cherry (Castède et al., 2015), only the candidate gene, *FAR-RED IMPAIRED RESPONSE 1* (*FAR1*) is within the interval of this QTL in our work. *FAR1* has been described as a negative regulator of seasonal growth and flowering time in *Arabidopsis* and the loss of function of this gene resulted in plants with early flowering (Ritter et al., 2018). Therefore, this gene seems a good candidate gene for BT regulation in the genus and further work to characterize this gene in this plant material is ongoing. A larger number of haplotypes (10) were detected for this QTL, maybe due to the haplotypes being constructed across a larger genomic region, and only *H2-f* from

'Cristobalina' was shown to associate with earlier bloom (7 days). As observed for the QTL detected on LG1, 'Cristobalina' alleles for the underlying genes are likely responsible for the higher effect of this QTL in this plant material.

Segregation distortion was observed for some populations in both major QTLs on LGs 1 and 2. Segregation distortion in these genomic regions was previously detected in these populations (Chapter 2) and in other *Prunus* species (Fan et al., 2010; Bielenberg et al., 2015). This distortion may be associated with segregation of lethal recessives alleles. However, since a relationship between seed and bud dormancy control has been reported (Leida et al., 2012; Abbot et al., 2015; Wang et al., 2016), it is possible that differences in seed dormancy may have affected seed germination and survival resulting in segregation distortion.

Other minor QTLS

Other QTLs identified by BLUP values in this work are located on LG4, for both GDH and CDs, and on LGs 1, 3 and 5 only for GDH. The QTL on LG4 (*qP-GDH4.1*^{m}, *qP-GDH4.1*^{m}) has also been previously detected in cherries (Dirlewanger et al., 2012; Castède et al., 2014; Cai et al., 2018) and other *Prunus* species (Fan et al., 2010; Sánchez-Pérez et al., 2012; Zhebentyayeva et al., 2014; Bielenberg et al., 2015; Kitamura et al., 2018). This QTL has been reported as the major QTL controlling CR and BT (17.5 to 47.2% PVE) in sweet (Dirlewanger et al., 2012; Castède et al., 2014) and sour cherry (Cai et al., 2018), almond (Sanchez-Pérez et al., 2012) and Japanese apricot (Kitamura et al., 2018). However in our work, this QTL explained a smaller part of the variation (6.0% for CD and 11.9% for GDH) (Table 3.1) and was not detected all years. Several works indicated that the LG4 QTL had a larger effect on BT of high chill cultivars (Castède et al., 2014; Kitamura et al., 2018), while in low chill cultivars, as in this work, the variation in BT is more dependent in the QTL on LG1 (Fan et al., 2010; Sanchez-Pérez et al., 2012; Zhebentyayeva et al., 2014; Salazar et al., 2016). LG1 candidate genes (*DAM1-6*) are related to CR, and therefore these genes may have a larger contribution to BT of low chilling cultivars. In contrast, BT for high CR cultivars may be less dependent on CR, and the underlying gene(s) for the LG4 QTL has yet to be determined (Zhebentyayeva et al., 2014; Castède et al., 2015).

For the remaining minor QTLs (*qP-GDH1.1*^{m}*; qP-GDH3.1*^{m}, *qP-GDH5.1*^{m}) identified by the BLUP analysis, *qP-GDH1.1*^{m} and *qP-GDH3.1*^{m} have also been reported previously in sweet cherry with small effects (Dirlewanger et al., 2012; Castède et al., 2014). However, QTL *qP-GDH5.1*^{m}, identified herein has not been previously reported in any QTL analysis of flowering time in sweet and sour cherries, but it has been described in peach (Bielenberg et al., 2015). 'Cristobalina' was the only cultivar in this work which is heterozygous for this region, and thus the identification of this QTL was probably due to the presence of this cultivar, and is probably associated with a rare allele in 'Cristobalina'. In general, the major QTLs were more stable and less influenced by the environment than minor QTLs that were detected only some years.

Breeding and genome breeding value

The predicted genotypes for the QTL identified were used to calculate breeding value. This estimation for the parental and ancestor cultivars studied offers powerful information for breeding with these cultivars. 'Cristobalina' can be used for breeding for low CR cultivars as this work shows it is the only evaluated cultivar that exhibited early flowering due to the presence of early bloom and low chill requirements alleles in the two major QTLs affecting these traits. A similar situation was observed in peach (Hernández Mora et al., 2017), where the lowest breeding values correlated with early flowering were identified in peach landraces. This highlights the benefits of introducing exotic germplasm in breeding programs to widen the range of trait variation. Specifically for breeding for low CR cultivars with 'Cristobalina', selecting for *H1-c* and *H2-f* from QTLs 1 and 2, respectively, is predicted to result in earlier blooming offspring. However, recovery of both haplotypes (*H1-c*/*H2-f*) together, may require a large number of progeny, as segregation distortion against the earlier haplotype *H2-f* was observed. At the same time, embryo rescue and *in vitro* embryo culture may be required to obtain low chilling descendants from crosses with 'Cristobalina' as the maternal parent.

If breeding for late blooming, allele *H1-b* rather than *H1-a,* should be selected for the QTL on LG1. As this QTL interval has been much narrowed in this work, and a good representation of sweet cherry breeding founders and parental cultivars is included herein, this information will also be useful for sweet cherry breeding of other plant material that do not include 'Cristobalina'. For the QTL on LG2, no conclusive evidence of late

blooming haplotypes that were sufficiently predictive to be used in breeding recommendations were observed for the haplotypes detected in the parental and ancestor cultivars. For the QTL on LG4 that had a minor effect in this work, but high effect in other plant material with higher CR, selecting in offspring from cultivars such as ‘Rainier’ and ‘Brooks’, which are heterozygous for early and late bloom alleles in this QTL, would be useful for introducing an earlier allele.

Multi-year analysis of multiple pedigree-linked populations from different genetic backgrounds that include material with low chilling requirements, has allowed the identification of robust BT QTLs that explain this highly heritable trait. BT is an essential component of cultivar adaptation to low-chill growing conditions and this trait is currently of high interest to breeders to extend sweet cherry growing to warmer areas. The analysis of F_2 populations, possible with ‘Cristobalina’, was instrumental to characterizing the haplotype effects of these QTLs. The identification of the low-chill haplotypes of these QTLs will be useful to enable marker-assisted breeding for this trait. The discovery of the major QTL on LG1 is consistent with the *DAM* gene(s) as the CR determinant in *Prunus,* and further suggests that ‘Cristobalina’ is homozygous for a unique early mutant of one or more of the *DAM* genes.

SUPPLEMENTARY MATERIALS CHAPTER 3

Supplementary Table 3.1 a) Bloom time (BT) of parental cultivars in calendar days (CD) and growing degree hours (GDH) per year. b) BT mean, standard deviation (SD), minimum (Min) and maximum (Max) values, and number of individuals phenotyped each year (N), per year and family. Broad-sense heritability (H^2) of each family for the 4 years.

a)

	'Ambrunés'		'BC8'		'Brooks'		'Cristobalina'		'Lambert'		'Vic'	
	CD	**GDH**	**CD**	**GDH**	**CD**	**GDH**	**CD**	**GDH**	**CD**	**GDH**	**CD**	**GDH**
2015	92	8748	96	9601	92	8748	74	5902	101	10546	97	9783
2016	92	9909	-	-	92	9909	58	5936	103	11810	99	11094
2017	76	7572	-	-	78	7931	64	5279	85	8851	82	8590
2018	94	9201	-	-	98	10067	78	6837	101	10394	101	10394

b)

		A×C		B×C		B×C2		C×C		L×C		V×C	
		CD	**GDH**	**CD**	**GDH**	**CD**	**GDH**	**CD**	**GDH**	**CD**	**GDH**	**CD**	**GDH**
2015	**Mean ± SD**	92.2±3.7	8769±787	93.6±3.9	9072±816	88.4±4.5	8016±894	78.0±4.4	6366±514	94.0±3.2	9178±689	92.0±3.5	8742±765
	Min	87	7576	84	7050	80	6629	71	5485	88	7815	85	7131
	Max	99	10107	100	10312	96	9601	87	7576	97	9783	102	10786
	N	36		24		28		81		13		76	
2016	**Mean ± SD**	89.1±3.2	9384±583	88.9±3.3	9343±609	90.8±4.5	9681±826	71.2±8.7	7088±765	93.4±3.6	10137±621	94.4±4.0	10318±687
	Min	82	8116	83	8255	83	8255	60	6065	88	9190	87	9033
	Max	95	10450	96	10609	98	10959	84	8410	100	11216	105	12208
	N	30		21		28		84		14		76	
2017	**Mean ± SD**	76.4±2.4	7657±419	74.5±2.6	7323±443	75.5±4.2	7493±755	67.4±2.7	5952±544	79.1±3.1	8101±488	78.5±2.4	8015±411
	Min	71	6782	70	6500	68	6053	62	5081	75	7404	73	7084
	Max	82	8590	80	8335	83	8672	74	7244	85	8851	87	9176
	N	39		24		45		90		14		141	
2018	**Mean ± SD**	92.4±3.5	8907±682	91.6±2.3	7689±438	94.4±4.7	9286±881	83.6±4.6	7437±587	94.9±3.2	9377±642	95.5±2.5	9506±499
	Min	87	7823	87	7823	86	7613	73	6326	89	8277	89	8277
	Max	99	10179	94	9201	104	10787	93	8903	100	10304	104	10787
	N	39		21		50		91		14		152	
	H^2	0.90	0.91	0.85	0.87	0.96	0.96	0.95	0.89	0.96	0.96	0.91	0.91

Supplementary Table 3.2 Pearson correlation coefficients of BT among years (2015 to 2018) and BLUP values, in CD and GDH.

	CD 15	CD 16	CD 17	CD 18	CD BLUP	GDH 15	GDH 16	GDH 17	GDH 18	GDH BLUP
CD 15	1	0.934*	0.904*	0.897*	0.962*	0.989*	0.940*	0.909*	0.891*	0.963*
CD 16		1	0.916*	0.948*	0.984*	0.904*	0.984*	0.925*	0.930*	0.965*
CD 17			1	0.938*	0.955*	0.895*	0.935*	0.997*	0.945*	0.968*
CD 18				1	0.966*	0.876*	0.945*	0.942*	0.989*	0.965*
CD BLUP					1	0.941*	0.982*	0.961*	0.955*	0.992*
GDH 15						1	0.928*	0.895*	0.882*	0.957*
GDH 16							1	0.937*	0.945*	0.983*
GDH 17								1	0.946*	0.971*
GDH 18									1	0.968*
GDH BLUP										1

* indicates significant correlation at $P<0.01$.

Supplementary Table 3.3 Number of polymorphic SNPs mapped per progeny and used for QTL analysis.

	A×C	B×C	B×C2	C×C	L×C	V×C	Total
Chr 1	231	216	135	85	211	257	**307**
Chr 2	131	126	71	99	141	140	**156**
Chr 3	77	97	57	56	85	79	**130**
Chr 4	95	107	55	72	95	98	**137**
Chr 5	66	72	47	50	53	93	**128**
Chr 6	86	97	61	59	102	110	**137**
Chr 7	69	43	48	7	50	62	**131**
Chr 8	88	75	50	44	86	74	**143**
WG*	843	833	524	472	823	913	**1269**

*WG: Whole Genome

Supplementary Table 3.4 Genetic map used for QTL analysis.

Document available online at http://hdl.handle.net/10532/4737. (Chapter 3 – Supplementary Table 4.xlsx).

Supplementary Table 3.5 Blooming time QTLs identified with strong evidence (2lnBF > 5) in single years for growing degree hours (GDH) and calendar days (CD). Bold indicates decisive evidence for a QTL (2lnBF > 10).

Trait	Year	QTL	LG[1]	cM[2]	QTL peak (cM)	Physical position* (Mbp)	Max 2lnBF	Average 2lnBF	Mean Additive effect	PVE (%)
GDH	**2015**	***qP-GDH1.2^m***	**1**	**137-141**	**139**	**42.28-43.99**	**12.2**	**10.1**	**1488**	**61.1**
	2015	***qP-GDH2.1^m***	**2**	**73-75**	**75**	**26.96-29.68**	**14.5**	**11.6**	**760**	**9.9**
	2015	*qP-GDH3.1^m*	3	39-51	47	10.02-15.76	8.7	7.4	534	5.9
	2016	***qP-GDH1.2^m***	**1**	**137-149**	**149**	**42.28-46.59**	**7.4**	**6.0**	**581**	**8.9**
	2016	***qP-GDH2.1^m***	**2**	**73-75**	**75**	**26.96-29.68**	**20.6**	**20.6**	**956**	**14.3**
	2016	*qP-GDH3.2*	3	5-11	11	21.19-36.04	6.1	5.7	776	8.7
	2016	*qP-GDH4.2*	4	53-57	55	11.47-13.03	5.9	5.8	621	2.1
	2016	*qP-GDH7.1*	7	51-57	51	17.29-18.88	5.3	5.2	1106	12.1
	2017	***qP-GDH1.2^m***	**1**	**135-139**	**137**	**43.06-43.54**	**12.9**	**9.5**	**1302**	**66.6**
	2017	***qP-GDH2.1^m***	**2**	**73-75**	**75**	**26.96-29.68**	**18.6**	**11.4**	**571**	**11.5**
	2017	*qP-GDH4.1^m*	4	11-21	15	2.56-5.23	6.6	5.7	545	4.3
	2017	*qP-GDH4.3*	4	37-49	41	7.70-10.24	8.8	7.3	346	5.6
	2017	*qP-GDH5.1^m*	5	57-69	57	13.62-17.15	8.9	7.0	170	1.2
	2017	*qP-GDH7.1*	7	45-57	51	16.68-17.45	7.8	6.7	205	1.6
	2018	*qP-GDH1.1^m*	1	5-11	7	1.95-3.46	7.6	9.4	305	2.2
	2018	***qP-GDH1.2^m***	**1**	**131-137**	**135**	**42.50-43.28**	**11.1**	**8.9**	**1453**	**57.9**
	2018	***qP-GDH2.1^m***	**2**	**73-75**	**75**	**26.96-29.68**	**18.0**	**11.2**	**743**	**14.3**
	2018	*qP-GDH4.3*	4	31-41	37	6.71-8.99	7.5	6.8	566	5.2
	2018	*qP-GDH5.1^m*	5	67-71	69	16.78-18.41	12.1	10.0	249	2.1
	2018	*qP-GDH7.1*	7	39-53	47	15.34-17.45	7.0	6.0	213	1.1
CD	**2015**	***qP-CD1.1^m***	**1**	**137-141**	**139**	**43.28-44.09**	**12.2**	**9.8**	**9.6**	**57.6**
	2015	***qP-CD2.1^m***	**2**	**73-75**	**75**	**26.96-29.68**	**19.6**	**11.8**	**5.1**	**15.0**
	2016	***qP-CD1.1^m***	**1**	**137-147**	**139**	**43.28-46.10**	**9.6**	**7.3**	**7.3**	**14.2**
	2016	***qP-CD2.1^m***	**2**	**73-75**	**75**	**26.96-29.68**	**32.8**	**32.7**	**10.8**	**23.0**
	2016	*qP-CD7.1*	7	55-61	57	17.40-18.88	5.7	5.4	6.6	3.9
	2017	***qP-CD1.1^m***	**1**	**133-139**	**137**	**42.77-43.53**	**12.3**	**9.0**	**7.3**	**25.6**
	2017	***qP-CD2.1^m***	**2**	**73-75**	**75**	**26.96-29.68**	**16.7**	**11.6**	**3.0**	**15.7**
	2017	*qP-CD4.2*	4	31-49	39	6.71-10.24	8.4	6.5	2.7	4.1
	2017	*qP-CD5.1^m*	5	54-71	69	13.08-18.41	9.0	6.3	1.0	0.4
	2017	*qP-CD7.1*	7	39-61	51	15.34-18.88	6.8	5.9	1.1	1.4
	2018	*qP-CD1.2*	1	5-21	7	2.11-6.42	9.6	6.1	1.6	2.4
	2018	***qP-CD1.1^m***	**1**	**133-139**	**135**	**42.77-46.10**	**10.6**	**9.1**	**7.6**	**60.9**
	2018	***qP-CD2.1^m***	**2**	**73-75**	**75**	**26.96-29.68**	**19.4**	**19.4**	**5.5**	**23**
	2018	*qP-CD4.2*	4	33-37	35	6.82-7.83	6.3	5.9	3.1	3.2
	2018	*qP-CD5.1^m*	5	67-71	69	16.78-18.41	12.1	10.2	1.4	2.5
	2018	*qP-CD7.1*	7	37-57	51	14.84-18.16	7.1	6.1	1.3	1.5

[1]LG: Linkage group. [2]cM: centiMorgan. *: Physical position on Peach Genome v2.0.a1 (Verde et al. 2017)

Supplementary Table 3.6 QTLs (*qP-GDH1.2*^{m}*/qP-CD1.1*^{m} and *qP-GDH2.1*^{m}*/qP-CD1.2*^{m}) haplotypes in parental cultivars and ancestors.

QTL	SNP	Haplotypes																					
		'Ambrunés'		'BC8'		'Bing'		'Brooks'		'Burlat'		'Cristobalina'		'Lambert'		'Napoleon'		'Rainier'		'Van'		'Vic'	
		H1-a	*H1-b*	*H1-a*	*H1-c*	*H1-a*	*H1-a*	*H1-a*	*H1-a*	*H1-b*	*H1-a*	*H1-c*	*H1-c*	*H1-b*	*H1-a*	*H1-a*	*H1-b*	*H1-a*	*H1-a*	*H1-a*	*H1-b*	*H1-a*	*H1-b*
***qP-GDH1.2*^{m} / *qP-CD1.1*^{m}**	ss490548667	A	B	A	B	A	A	A	A	B	A	B	B	B	A	A	B	A	A	A	B	A	B
	ss490546979	B	B	B	A	B	B	B	B	B	B	A	A	B	B	B	B	B	B	B	B	B	B
	ss490548655	B	A	B	B	B	B	B	B	A	B	B	B	A	B	B	A	B	B	B	A	B	A
	ss490548643	B	B	B	A	B	B	B	B	B	B	A	A	B	B	B	B	B	B	B	B	B	B

QTL	SNP	Haplotypes																					
		'Ambrunés'		'BC8'		'Bing'		'Brooks'		'Burlat'		'Cristobalina'		'Lambert'		'Napoleon'		'Rainier'		'Van'		'Vic'	
		H2-g	*H2-a*	*H2-c*	*H2-e*	*H2-b*	*H2-d*	*H2-d*	*H2-c*	*H2-b*	*H2-c*	*H2-e*	*H2-f*	*H2-i*	*H2-d*	*H2-d*	*H2-k*	*H2-a*	*H2-d*	*H2-a*	*H2-d*	*H2-b*	*H2-h*
***qP-GDH2.1*^{m} / *qP-CD1.1*^{m}**	ss490559076	B	B	B	B	B	A	A	B	B	B	B	B	B	A	A	B	B	A	B	A	B	B
	ss490550443	A	A	A	A	A	B	B	A	A	A	A	B	A	B	B	A	A	B	A	B	A	B
	ss490550465	A	A	A	A	B	A	A	A	B	A	A	A	A	A	A	B	A	A	A	A	B	A
	ss490550493	B	A	B	B	A	B	B	B	A	B	B	B	B	B	B	A	A	B	A	B	A	B
	ss490550497	B	B	B	B	B	A	A	B	B	B	B	B	B	A	A	B	B	A	B	A	B	B
	ss490550501	B	A	B	B	A	B	B	B	A	B	B	B	B	B	B	A	A	B	A	B	A	B
	ss490550517	B	B	B	A	B	B	B	B	B	B	A	B	B	B	B	B	B	B	B	B	B	B
	ss490550521	A	B	A	A	B	A	A	A	B	A	A	A	B	A	A	B	B	A	B	A	B	B
	ss490550529	A	B	B	A	B	B	B	B	B	B	A	B	A	B	B	B	B	B	B	B	B	A
	ss490550577	A	B	A	A	B	B	B	A	B	A	A	A	B	B	B	B	B	B	B	B	B	B
	ss490550588	B	B	B	B	B	A	A	B	B	B	B	B	B	A	A	A	B	A	B	A	B	B
	ss490550626	B	A	B	B	B	A	A	B	B	B	B	B	B	A	A	A	A	A	A	A	B	B
	ss490550731	B	B	B	B	B	A	A	B	B	B	B	B	B	A	A	A	B	A	B	A	B	B
	ss490547648	B	A	B	B	A	A	A	B	A	B	B	B	A	A	A	A	A	A	A	A	A	A

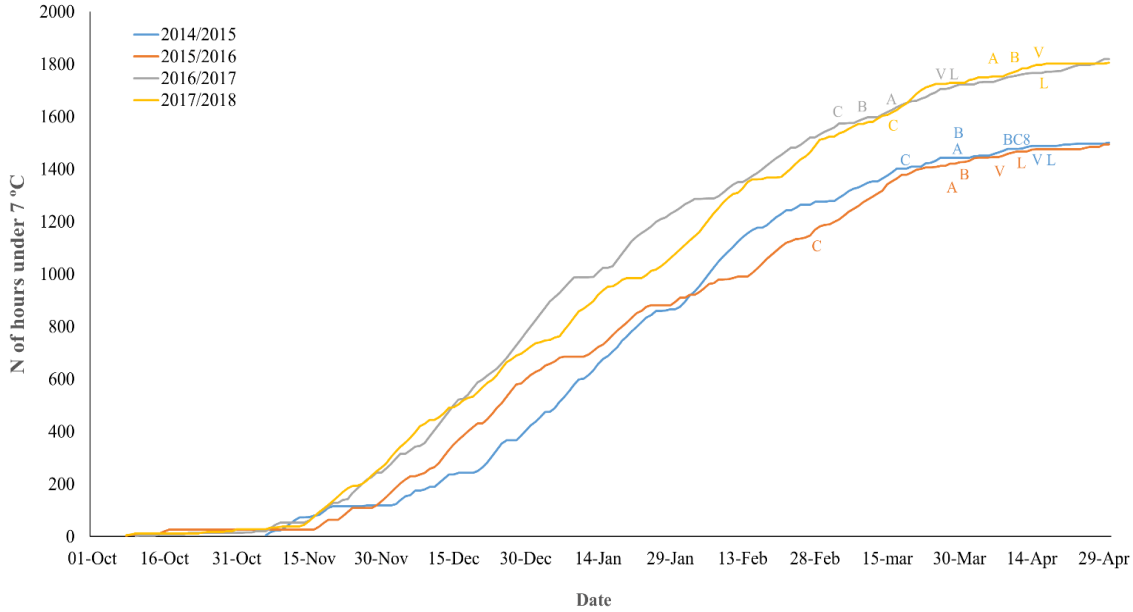

Supplementary Fig 3.1 Accumulated winter chilling (hours below 7 ºC[1]), and bloom dates of parental cultivars during the four years of analysis. 'Ambrunés' (A), 'Brooks' (B), 'Cristobalina' (C), 'Lambert' (L), 'Vic' (V) and 'BC-08' (BC8). [1]Data from: 'Estación 34-Montañana', 'Datos Meteorológicos', 'Oficina del Regante', 'Sociedad Aragonesa de Gestión Agroambiental (Sarga)', 'Gobierno de Aragón'. http://aplicaciones.aragon.es/oresa/datosMeteorologicos. inicio.do?sm= 2060

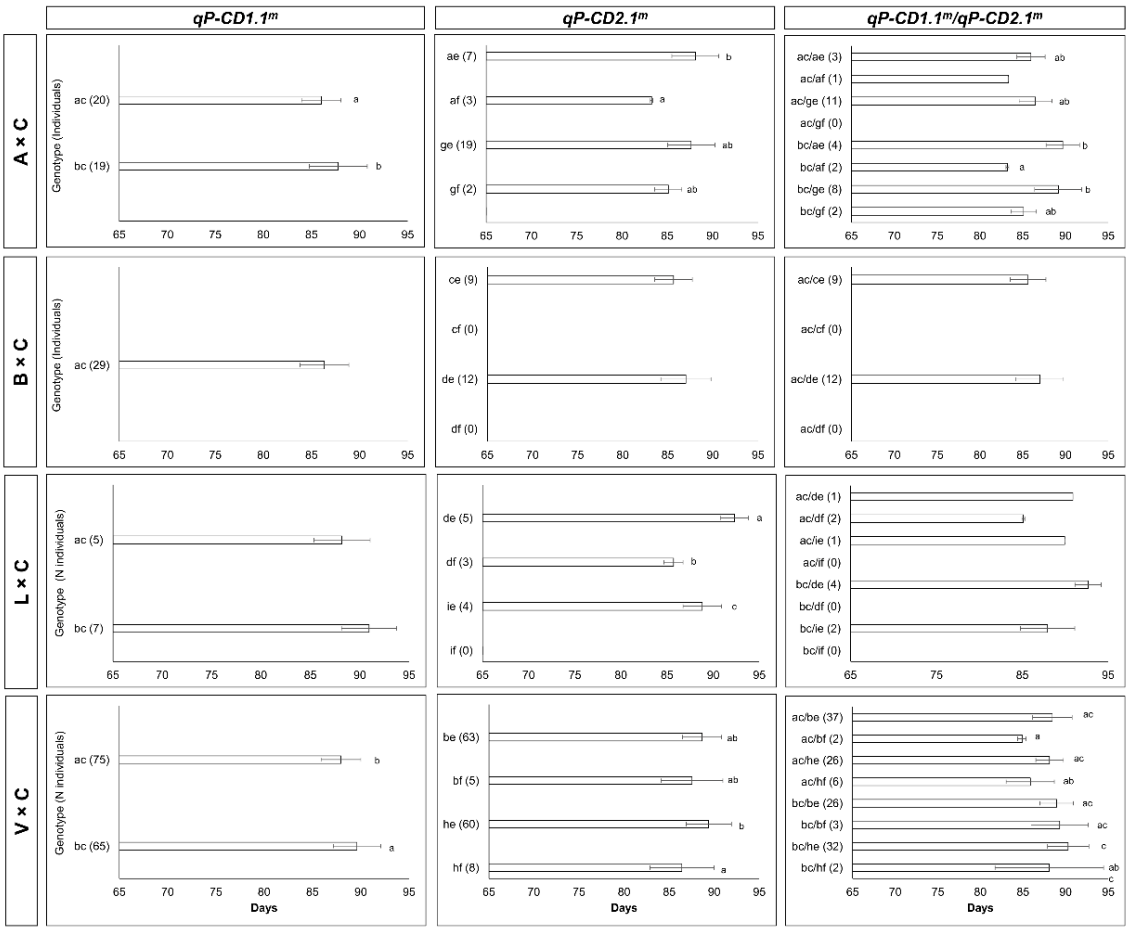

Supplementary Fig 3.2 BT (in CDs) mean genotype values of major QTLs detected and their interaction (*qP-CD1.1*^{m}, *qP-CD2.1*^{m} and both) in segregating classes of F_1 populations analysed. Significant differences between genotypes are indicated by different letters ($P<0.05$).

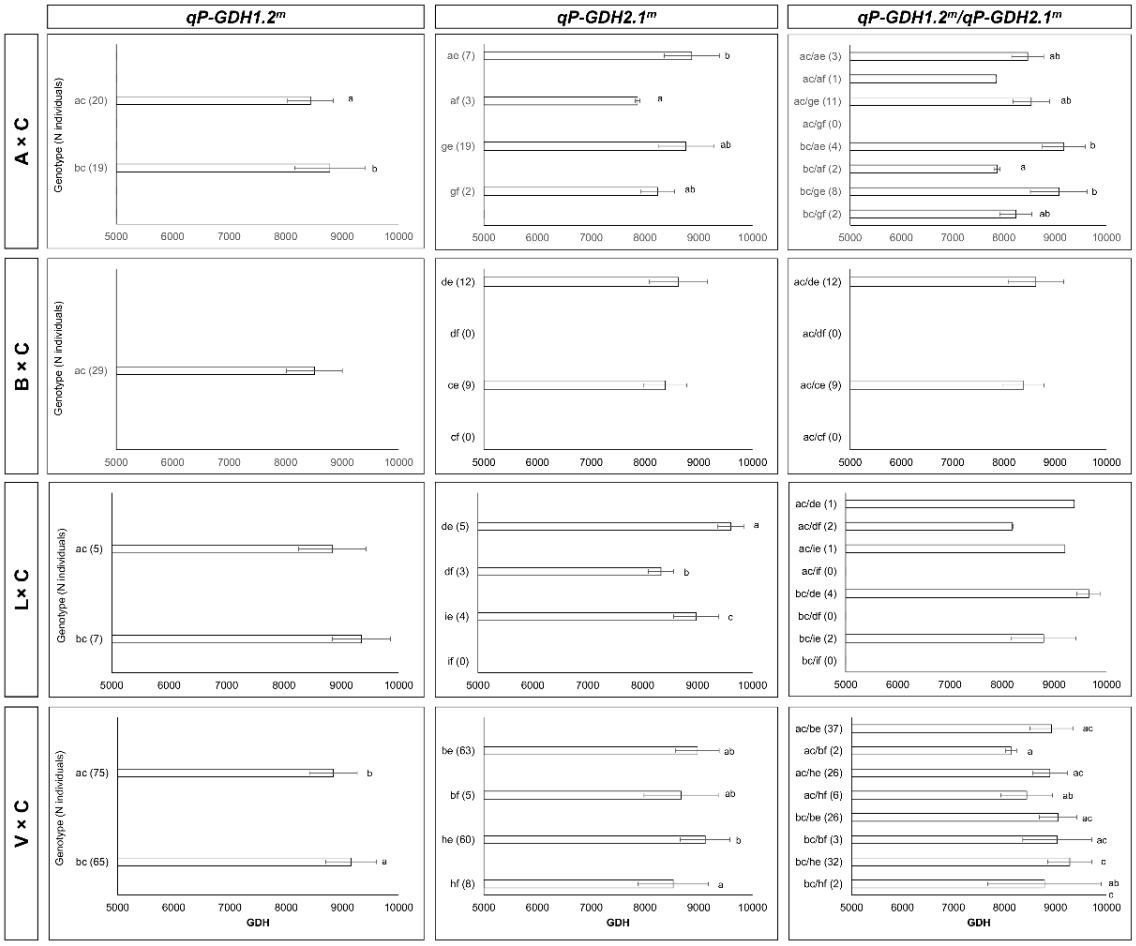

Supplementary Fig 3.3 BT (in GDHs) mean genotype values of major QTLs detected and their interaction (*qP-GDH1.2*^{m}, *qP-GDH2.1*^{m} and both) in segregating classes of F_1 populations analysed. Significant differences between genotypes are indicated by different letters ($P<0.05$).

CHAPTER 4

CHARACTERIZATION OF DORMANCY ASSOCIATED MADS-BOX GENES IN SWEET CHERRY REVEALS A PROMOTER DELETION ASSOCIATED TO EARLY BLOOMING

INTRODUCTION

Adequate blooming and pollination are essential for fruit set in sweet cherry (*Prunus avium* L.) and other fruit tree species. Temperate climate fruit trees such as sweet cherry go through a dormancy period in which meristem growth is inactive (Lang et al., 1987; Rohde and Bhalerao, 2007). This occurs before the blooming season to prevent winter damage due to frost and low temperatures. Dormancy is divided into three stages: paradormancy and endodormancy, in which bud growth is inhibited during autumn and winter seasons, and ecodormancy, in which bud growth is resumed under favorable climatic conditions in late winter and early spring (Lang et al., 1987). The length of the dormant period is dependent on the environmental temperatures since determined amounts of chill and heat [Chilling Requirements (CR) and Heat Requirements (HR)] are needed to complete endodormancy and ecodormancy before bud burst (Cooke et al., 2012). These requirements are specific of each genotype and vary depending on the environmental conditions (Alburquerque et al., 2008). Both CR and HR have influence in blooming, however several studies in *Prunus* species have reported that CR is the major determinant of bloom time (BT) (Alburquerque et al., 2008; Fan et al., 2010; Campoy et al., 2011; Castède et al., 2014).

Dormancy release, CR and BT are relevant traits for cultivar adaptation to the growing area and to ensure an adequate fruit set. Blooming at the correct time will avoid spring frosts in cold regions and will ensure pollination by overlapping BT with other cultivars. Cultivars with low CR will be useful to adapt to temperature rise in the actual climate change context, and can be used to extend cultivation to warmer areas; whereas in cold regions, cultivars with high CR should be more adapted. Several works have investigated the physiology and the genetics of these traits in sweet cherry and other fruit tree species (reviewed in Abbott et al., 2015; and Fadón and Rodrigo, 2018). In sweet cherry, genetic analysis have revealed that BT is a quantitative trait with very high heritability (Dirlewanger et al., 2012; Castède et al., 2014; Chapter 3). In this species, major quantitative trait loci (QTLs) associated to this trait have been identified on linkage group (LG) 4 (Dirlewanger et al., 2012; Castède et al., 2014), and LGs 1 and 2 (Chapter 3). In other *Prunus* species, like almond (*Prunus amygdalus* L.), peach [*Prunus persica* (L). Batsch] and Japanese apricot (*Prunus mume* L.), main BT QTLs have also been

mapped on the orthologous regions of LG1 (Fan et al., 2010; Zhebentyayeva et al., 2014; Bielenberg et al., 2015) and LG4 (Sánchez-Pérez et al., 2012; Dirlewanger et al., 2012; Kitamura et al., 2018). In the same region of LG1 stable and significant QTLs associated to CR in almond, peach and sweet cherry have also been detected (Fan et al., 2010; Sánchez-Pérez et al., 2012; Castède et al., 2014; Bielenberg et al., 2015). This LG1 QTL region overlaps with a deleted region identified in the *evergrowing* (EVG) peach mutant, which is a genotype that does not enter dormancy (Rodriguez et al., 1994). In this deleted region, a tandem repeat of six MADS-box genes, named *dormancy-associated MADS-box* (*DAM*) were identified (Bielenberg et al., 2008), reveling the potential involvement of these genes in dormancy control of *Prunus* species. In sweet cherry, *DAM5* and *-6* have also been mapped on LG1, overlapping with the main BT and CR QTL of this LG (Castède et al., 2014 and 2015). In other Rosaceous species, like apple and pear, a variable number of *DAM* gene have also been reported (Saito et al., 2013; Mimida et al., 2015), some of them overlapping with regions in which BT QTLs were found (Allard et al., 2016).

In different plant species, MADS-box transcription factors have been reported as strong candidate genes for the genetic control of blooming and temperature responses (Gramzow and Theissen, 2010). MADS-box genes play fundamental roles in pathways involved in the transition from vegetative to reproductive phases, growth, floral organ determination and other processes related to root, leaf, fruit and gametophyte development (Messenguy and Dubois, 2003; Becker and Theissen, 2003; Smaczniak et al., 2012). The *DAM* genes reported in peach and Japanese apricot belong to MIKC^{c} Type II of MADS-box and are phylogenetically related to *Arabidopsis SHORT VEGETATIVE PHASE* (*SVP*) and *AGAMOUS-LIKE 24* (*AGL24*) genes, which have been reported as main floral regulators (Jiménez et al., 2009; Sasaki et al., 2011). Analysis of *DAM* genes expression levels in these species have shown similar pattern in different years and correlation with photoperiod and temperatures changes (Falavigna et al., 2019), suggesting that these genes are main regulators of the dormancy cycle in *Prunus* species (Yamane, 2014). Maximum expression levels of *DAM1* to *-4* were observed during bud set suggesting a role in the regulation of growth cessation and bud formation in peach and Japanese apricot (Li et al., 2009; Sasaki et al., 2011; Zhang et al., 2018). On the other side, *DAM5* and *-6* showed the highest expression level in winter season during induction and maintenance of dormancy and minimal or absent expression during the budbreak and BT (Jiménez et al., 2010;

Yamane et al., 2011; Leida et al., 2012). Therefore, down-regulation of *DAM5* and *-6* during winter season, with minimum expression level when CRs are fulfilled, is compatible with the role of dormancy release repressor of *DAM* genes in *Prunus* species (Sasaki et al., 2011). Epigenetic modification and the evolution of transcript levels during dormancy were evaluated for *DAM3* and *-5* in the sweet cherry cultivar 'Bing' (Rothkegel et al., 2017), revealing the involvement of siRNAs and DNA methylations in the silencing of *DAM3* during chilling accumulation and dormancy release.

In Chapter 3, BT in sweet cherry was evaluated using a multi-family QTL approach that included populations of parental cultivars from very low to high CRs, and data from four years. The populations used derive from self- and cross-pollinations of 'Cristobalina', a cultivar with very low CR (<550 h) and extra-early flowering and maturity dates (Tabuenca, 1983; Alburquerque et al., 2008; Chapter 3). BT QTL analysis revealed that the highest percentage of phenotypic variation was explained by QTLs on LGs 1 (*qP-CD1.1*^{m}*/qP-GDH1.2*^{m}) and 2 (*qP-CD2.1*^{m}*/qP-GDH2.1*^{m}). The QTL detected on LG1 overlaps with a CR QTL previously reported on *Prunus* LG1 (Fan et al., 2010; Sánchez-Pérez et al., 2012; Castède et al., 2014; Bielenberg et al., 2015) and with *DAM* genes mapped in this region in sweet cherry, Japanese apricot and peach (Bielenberg et al., 2008; Sasaki et al., 2011; Castède et al., 2015). Moreover, haplotype analysis of this QTL showed that 'Cristobalina' was the only cultivar with alleles contributing to early blooming in the plant material evaluated (Chapter 3). Since early blooming in this plant material is believed to be due to low CR in 'Cristobalina', candidate genes for these QTLs may be involved in CR control. Following with those results, the objective of this work is to investigate candidate genes in the main BT QTL detected on LG1, *qP-CD1.1*^{m}*/qP-GDH1.2*^{m}, including *DAM* genes, in 'Cristobalina' and in other medium-late blooming cultivars with the aim of identifying polymorphisms that may be associated with low CR and early blooming of 'Cristobalina'. These results may help understanding genetic dormancy regulation and developing markers for assisted selection of this trait in sweet cherry**.**

MATERIALS AND METHODS

Candidate genes identification

The coding DNA sequences of predicted genes within a region of 326,596 bp (Chr01_49296241:49622837) were extracted from 'Regina' sweet cherry genome (Le Dantec et al., 2019). This region spans the main BT QTL (*qP-GDH1.2*^{m}/*qP-CD1.1*^{m}), identified in low and high chilling sweet cherry plant material (Chapter 3). The corresponding protein sequences of the predicted genes were blasted against the National Center for Biotechnology Information (NCBI) non-redundant protein sequences (nr) database using BLASTP algorithm to obtain the respective gene ontologies. For each gene, we searched for bibliographic evidences (annotation and predicted function) that led to any information associated with their potential involvement in BT and chilling requirements.

Validation of the structural annotation was performed using BLAST analysis and motif detection. The assigned name to predicted genes in the 'Regina' sweet cherry genome followed the nomenclature PAV0*x*_g*y*; where *x* corresponded to chromosome number and *y* to gene number in chromosome. The first predicted gene in chromosome 1 was named as PAV01_g0000001, second as PAV01_g0000011, third as PAV01_g0000021, and so on.

Phylogenetic analysis

Evolutionary analyses of sweet cherry, peach and Japanese apricot dormancy-associated MADS-box genes (*DAM1* to *6*) were conducted using MEGA X (Kumar et al., 2018). Sweet cherry *DAM* genes sequences were obtained from 'Regina' sweet cherry genome and a GFF (General File Format) annotation file containing the exon-intron structure of these genes (Le Dantec et al., 2019). These files were uploaded into the Integrative Genomics Viewers (IGV) software (Thorvaldsdóttir et al., 2012) to double-check structure with their ortholog genes in peach genome v2.0.a1 (Verde et al., 2017). Manual sequence editing was done to correct the automatic annotation if needed, conserving an adequate intron splicing prediction. Nucleotide sequences of peach (ABJ96361, ABJ96363, ABJ96364, ABJ96358, ABJ96359, ABJ96360) and Japanese apricot (BAK78921, BAK78922, BAK78923, BAK78924, BAK78920, BAH22477) *DAM*

genes used for the phylogenetic analysis were retrieved from NCBI GenBank. Multiple sequence alignment was carried out prior to tree construction using MUSCLE algorithm (Edgar, 2004). The evolutionary history was inferred by using the Maximum Likelihood method and Tamura-Nei model (Tamura and Nei, 1993). Phylogenetic analysis were estimated using a bootstrap value of 1000, and the tree with the highest log likelihood was selected. Heuristic search for initial tree was automatically obtained by using Neighbor-Join and BioNJ algorithms to a matrix of pairwise distances estimated by the Maximum Composite Likelihood (MCL) approach, and then the topology with superior log likelihood value was selected.

Cultivar sequence reads mapping on the reference genome

Sequences of 13 sweet cherry cultivars from different origins (‘Ambrunés’, ‘Brooks’, ‘Cristobalina’, ‘Ferrovia’, ‘Hedelfingen’, ‘Lambert’, ‘Napoleon’, ‘Rainier’, ‘Sam’, ‘Satonishiki’, ‘Sue’, ‘Summit’ and ‘Vic’) were used for sequence alignment. Genomic DNA-seq libraries (100 bp or 150 bp paired-end reads) of these cultivars, previously generated using the Illumina HiSeq 2500 and 4000 systems (Ono et al., 2018), were downloaded from DNA Data Bank of Japan (DDBJ; project number PRJDB6734). Genome alignment was done using the Galaxy software framework (Afgan et al., 2018). Raw sequence data was processed using SLIDINGWINDOW operation from Trimmomatic v0.36.6 (Bolger et al., 2014) to remove adapter sequences and to obtain clean sequence data. A FASTQ file for each cultivar containing clean reads was aligned to ‘Regina’ sweet cherry genome (Le Dantec et al., 2019). Whole sweet cherry genome was targeted for alignment using Bowtie 2 tool (Langmead and Salzberg, 2012) with default parameters. The consensus sequence of each cultivar was extracted from Binary Alignment Map (BAM) file using Geneious 11.1.5 software (Biomatters Ltd, Auckland, NZ).

A target region of 69,179 bp in ‘Regina’ cultivar spanning the *PavDAM* genes (1,500 bp upstream from *PavDAM1* start codon and 1,500 bp downstream from *PavDAM6* stop codon) was considered for cultivar comparison. The full-length amino acid sequence of six *DAM* genes from the aligned cultivars and reference genome (‘Regina’) were deduced and compared. Multiple amino acid sequence alignment was done using ClustalW algorithm implemented in Geneious 11.1.5 software (Biomatters Ltd, Auckland, NZ). The

percentage of identity between *DAM* genes of each cultivar was calculated as the percentage of identical amino acids between each pair of cultivars.

Promoter analysis

Genomic DNA from sweet cherry cultivars used for sequence alignment (13) and from 'Regina' was extracted from young leaves. Leaf samples were collected from trees belonging to CITA de Aragón sweet cherry germplasm and cultivar collection in Zaragoza (Spain). Genomic DNA extraction was carried out using DNeasy Plant Mini kit (Qiagen, MD, USA), and quantity and quality of extracted DNA was quantified using NanoDrop ND-1000 spectrophotometer (Thermo Scientific, DE, USA). Primers flanking a putative deletion in the promoter region of 'Cristobalina' sweet cherry *DAM* genes (DPD; *DAM* Promoter Deletion), were designed on conserved regions based on multiple cultivar alignment for this region. PCR amplification with these primers; DPDf (5' to 3': CCATCTCTCTCCCATCTCGT) and DPDr (5' to 3': TGCAGGCAAGTTGTCAATCT), was carried out for all the cultivars studied. PCR was carried out in a total volume of 20 µL as described in Cachi and Wünsch (2014). The PCR was completed using the following program: 4 min at 94ºC; 35 cycles of 45 sec at 94ºC, 45 sec 57ºC and 2 min at 72ºC; and a final step of 7 min at 72ºC. PCR products were analyzed by agarose gel electrophoresis in 1.7% TBE and stained with GelRed® Nucleic Acid Stain (Biotium, CA, USA).

Sanger sequencing of 'Cristobalina' and 'Regina' PCR products of amplification with DPDf/DPDr primers was carried out. PCR reactions were performed in a final volume of 30 µL, with the same concentrations as described above. Ten µL of the PCR reactions were visualized in an agarose gel to confirm amplification, and the remaining 20 µL were purified and sequenced by STAB VIDA (Lisbon, Portugal). Sequencing of PCR products of each cultivar ('Regina' and 'Cristobalina') was repeated three times with each primer (DPDf and DPDr). Sequences from each PCR reaction were analyzed using Geneious 11.1.5 (Biomatters Ltd, Auckland, NZ). All sequences were trimmed to eliminate low quality reading regions, and sequences from each cultivar were aligned to construct the consensus PCR fragment sequence of each cultivar. The 'Cristobalina' and 'Regina' sequences obtained were then aligned for comparison. All sequence visualizing, editing and alignments were carried out using Geneious 11.1.5 (Biomatters Ltd, Auckland, NZ).

PavDAM promoter deletion (DPD) analysis in a segregating population

Sixty-four individuals of the F_2 population B×C2 were genotyped with DPDf/DPDr primers. This family derives from the self-pollination of the selection 'BC8' ('Brooks' × 'Cristobalina') and is expected to segregate for the *DAM* gene promoter deletion (DPD) detected in 'Cristobalina'. Genomic DNA of each individual and the parental cultivar ('BC8') was extracted from young leaves using DNeasy Plant Mini kit (Qiagen, MD, USA). B×C2 genotyping with DPDf/DPDr primers was carried by PCR and agarose gel electrophoresis as described above. Deviation of marker segregation from expected Mendelian segregation was evaluated by Chi-square goodness-of-fit (χ^2). Mean phenotypic BT value of the DPD segregating classes were compared with those in the main BT QTL (*qP-GDH1.2*^{m}/*qP-CD1.1*^{m}; Chapter 3) using *Student's T* test. Statistical analysis were done using SPSS statistics v21.0.0 software (IMB, IL, USA).

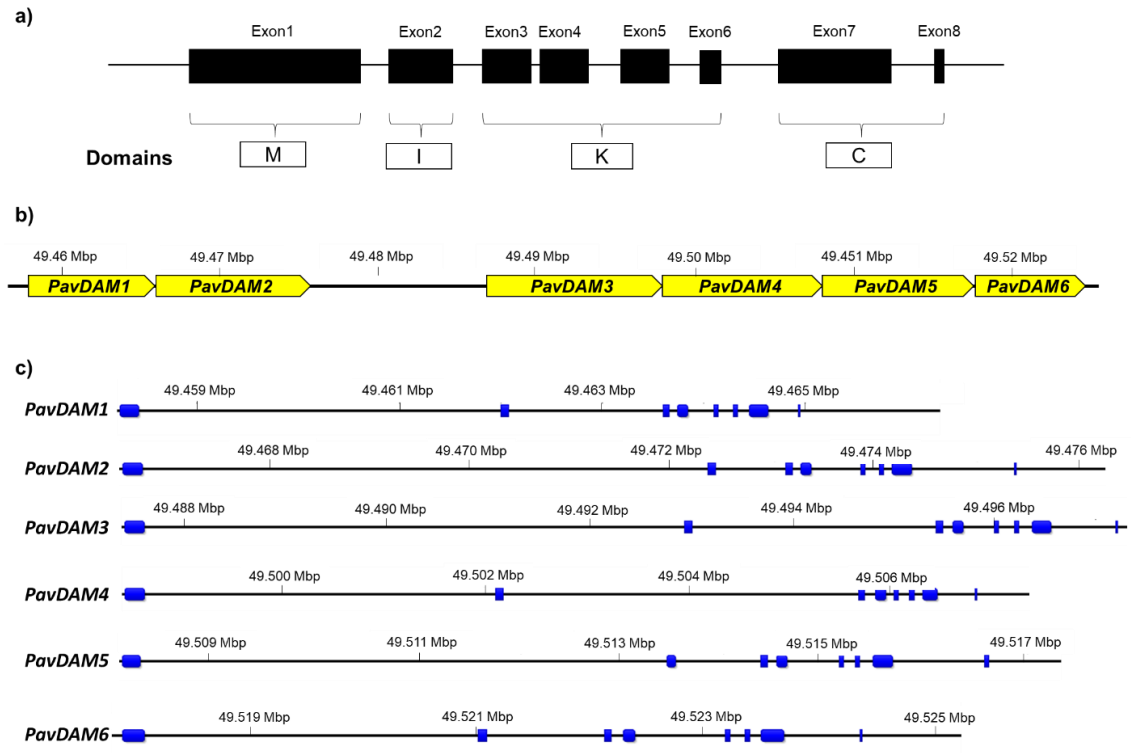

Figure 3.1 Caracterization of sweet cherry *PavDAM* genes. a) Shematic overview of intron-exon structure of MADs-box genes and M, I, K and C domains. b) Position of *PavDAM* genes in the sweet cherry genome. c) Distribution of exons (blue boxes) and introns in the six *PavDAM* genes in 'Regina' sweet cherry genome.

RESULTS

Candidate gene identification

In order to identify potential candidate genes for BT and CR, we performed functional analysis in the genomic region of LG1 corresponding to the BT QTL *qP-CD1.1*^{m}*/qP-GDH1.2*^{m} (Chapter 3). This region is located between bps 49,296,241 and 49,622,837 of chromosome 1 in 'Regina' sweet cherry genome sequence (Le Dantec et al., 2019). Forty-seven predicted genes (Sup Table 3.1) were retrieved from this sequence. From these, 7 (14.9%) deduced amino acid sequences had BLAST hits in the NCBI gene database with uncharacterized proteins and 6 (12.8%) had no significant similarity with any other sequences (Sup Table 3.1). For the rest of predicted genes (34; 72.3%), diverse amino acid sequences involved in different pathways were detected. Amongst them, 8 consecutive protein sequences were the most relevant. They were localized very close to the QTL peak and correspond to genes sequentially annotated as PAV01_g0075081, PAV01_g0075091, PAV01_g0075101, PAV01_g0075111, PAV01_g0075121, PAV01_g0075131, PAV01_g0075141 and PAV01_g0075151 (Sup Table 3.1). Using blastx, these genes matched to MADS-box proteins (query covering ranging from 51 to 99%), with percentages of similarity ranging from 86 to 100% (Sup Table 3.1). Due to their genetic similarity with type II SVP subclass of MADS-box proteins sequences, these 8 sequences may correspond to *DAM* genes in sweet cherry (*PavDAM*) and are therefore strong candidate genes for CR and BT regulation in this QTL region.

PavDAM genes structural annotation and phylogenetic analysis

Sequence inspection and MADS-box motif search in the eight candidate genes retrieved revealed incorrect annotation of the initial gene models when compared to peach gene models. Also, the expected presence and structure of MADS-box domains was not complete. Of the eight selected gene sequences, only in two of them, PAV1_g0075081 and PAV1_g0075151, the predicted proteins contained the domains MADS (M), Intervening (I), Keratin-like (K) and C-terminal (C) characteristics of type II MADS-box genes (Fig 3.1a). In another gene sequence, PAV01_g0075091, exon 3 was not annotated, and in PAV01_g0075121, two additional exons before the M domain were present. Similarly,

PAV01_g0075101 and PAV01_g0075111 were automatically annotated as two different MADS-box, although domain structure revealed that both sequences were two separated fragments of same MADS-box protein. The same was observed for PAV01_g0075131 and PAV01_g0075141 sequences, which correspond to the same MADS-box gene, but had been automatically annotated as two different gene sequences.

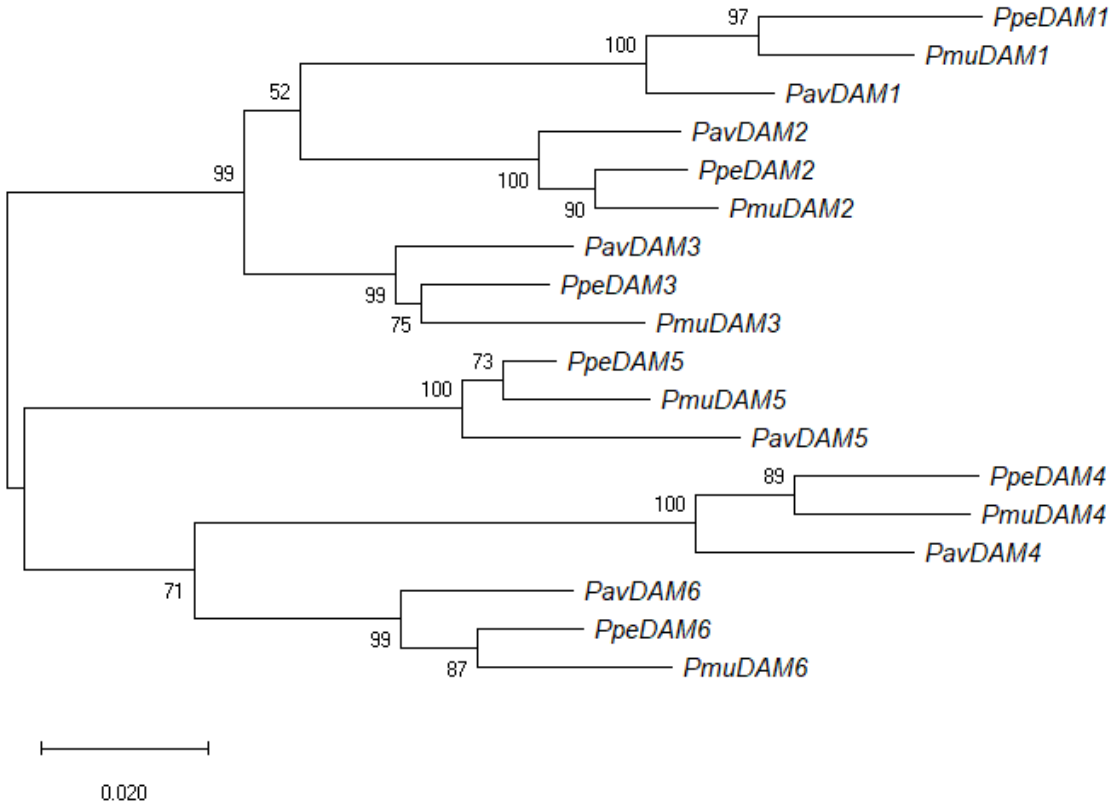

Figure 3.2 Maximum likelihood phylogenetic tree of nucleotide *DAM* sequences of sweet cherry (*PavDAM1*, *PavDAM2*, *PavDAM3*, *PavDAM4*, *PavDAM5* and *PavDAM6*) and its orthologues in Japanese apricot (*PmuDAM1*, *PmuDAM2*, *PmuDAM3*, *PmuDAM4*, *PmuDAM5* and *PmuDAM6*) and peach (*PpeDAM1*, *PpeDAM2*, *PpeDAM3*, *PpeDAM4*, *PpeDAM5* and *PpeDAM6*). The numbers at branch nodes indicate percentage of bootstrap support at 1000 replicates.

The corrected annotation of the retrieved sequences revealed six MADS-box genes instead of the eight automatically predicted in the 'Regina' sweet cherry genome (Sup Table 3.2), which is the same number of *DAM* genes reported in peach and Japanese apricot. Thus, the six MADS-box sequences were identified as PAV1_g0075081, PAV1_g0075091, PAV1_g0075101, PAV1_g0075121, PAV1_g0075131 and

PAV1_g0075151, named in this work from *PavDAM1* to *-6*, respectively (Fig 3.1; Sup Table 3.2). These genes are tandemly located in the 'Regina' sweet cherry genome (Chr01_ 49458239:49524418 bp) with a gap of 12,035 bp between *PavDAM2* and *-3* (Fig 3.1b). Gene structure analysis of the 6 genes revealed an identical structure of 8 exons and 7 introns in each gene, as well as, the conserved M, I, K and C domains (Fig 3.1c). Genomic gene length ranged from 6536 (*PavDAM6*) to 9794 nt (*PavDAM3*), whereas the predicted genes coding regions ranged from 667 (*PavDAM4*) to 730 (*PavDAM5*) nt, with variable intron size for the six sequences and conserved exon sizes (Fig 3.1c).

A phylogenetic analysis of peach, Japanese apricot (Bielenberg et al., 2008; Sasaki et al., 2011) and the sweet cherry (this work) *DAM* genes was carried out using maximum likelihood of the gene coding sequences (Fig 3.2). Orthologue *DAM* genes (*DAM1* to *DAM6*) of the three species clustered together with a high bootstrap value (99; Fig 3.2). Within these sub-clades, in all cases, peach and Japanese apricot *DAM* genes were phylogenetically closer to each other than to sweet cherry *DAM* genes (Fig 3.2). Additionally, two major clades of *DAM* orthologs were observed, one includes *DAM1, -2* and *-3*; and the other includes *DAM4*, *-5* and *6*, suggesting a common ancestor for each of them (Fig 3.2). Within these clades, *DAM1*, and *-2* were closer to each other than to *DAM3*, and *-4, and -6* were closer to each other than to *DAM5*.

Cultivar *PavDAM* sequence mapping and similarity

The whole sweet cherry genome (Le Dantec et al., 2019) was used for mapping the sequence reads of 13 sweet cherry cultivars, with CR and BT variability (Chapter 3), that had been previously sequenced (Ono et al., 2018). The complete amino acid sequence of the six *PavDAM* was deduced from the consensus sequences generated for each of the 13 cultivars (Sup Fig 3.1). Comparison of these sequences in the different cultivars revealed a high degree of conservation (Table 3.1; Sup Fig 3.1; Sup Table 3.3). The exon-intron structure was conserved in the six genes in all the cultivars. Also, the similarity between cultivars for the six *PavDAM* amino acid sequences was very high, ranging from 98.8 to 100% identity (Table 3.1). 'Cristobalina' was the cultivar with lower similarity to the rest (98.8 - 99.0%, Table 3.1). The remaining cultivars had a similarity of 99.7 to 100%.

Table 3.1 Percentage of identity between cultivars amino acid sequences of six *PavDAM* genes.

	Brooks	Cristobalina	Ferrovia	Hedelfingen	Lambert	Napoleon	Rainier	Regina	Sam	Satonishiki	Sue	Summit	Vic
Ambrunés	99.7	98.9	99.7	99.7	99.8	99.9	99.7	99.9	99.9	99.7	99.9	100	99.7
Brooks		98.9	99.7	99.9	99.8	99.8	99.9	99.8	99.8	99.9	99.8	99.7	100
Cristobalina			98.9	98.9	98.8	99.0	98.8	99.0	99.0	98.9	99.0	98.9	98.9
Ferrovia				99.7	99.7	99.8	99.7	99.8	99.8	99.7	99.8	99.7	99.7
Hedelfingen					99.8	99.8	99.8	99.8	99.8	99.9	99.8	99.7	99.9
Lambert						99.7	99.7	99.9	99.9	99.8	99.9	99.8	99.8
Napoleon							99.7	99.9	99.9	99.8	99.9	99.9	99.8
Rainier								99.7	99.7	99.8	99.7	99.7	99.9
Regina									100	99.8	100	99.9	99.8
Sam										99.8	100	99.9	99.8
Satonishiki											99.8	99.7	99.9
Sue												99.9	99.8
Summit													99.7

Complete amino acid identity (100% similarity) was observed for *PavDAM* sequences of 'Ambrunés' and 'Summit'; 'Vic' and 'Brooks'; and 'Regina', 'Sam' and 'Sue' (Table 3.1).

Alignment of the *PavDAM* amino acid sequences of all the cultivars (Sup Fig 3.1) revealed 24 polymorphisms in the form of amino acid substitutions (Sup Fig 3.1; Sup Table 3.3). Of these, 20 were unique to a specific cultivar, and the remaining 4 were common to various cultivars. 'Cristobalina' was the cultivar with the largest number of amino acid substitutions (15), of which 14 were unique in this cultivar (Sup Fig 3.1; Sup Table 3.3). 'Ferrovia', 'Lambert', 'Hedelfingen', 'Satonishiki' and 'Rainier' showed 1 to 2 unique amino acid substitutions (Sup Table 3.3). *PavDAM1* and *PavDAM4* presented the largest number of polymorphisms (Sup Fig 3.1; Sup Table 3.3). Unique amino acid substitutions were found on all domains, with a large number of unique substitutions found on domain C. Only 'Cristobalina' presented a substitution in M domain (*PavDAM2*). No INDELs were observed in the coding region of any of the cultivars (Sup Fig 3.1).

Promoter region analysis

The *PavDAM* genes promoter sequence (estimated in 1,500 bp upstream of *PavDAM1*) of the 13 sweet cherry cultivars was also analyzed. This analysis allowed to detect a putative deletion in 'Cristobalina' promoter region, revealed as a region where no sequence reads were mapped (Fig 3.3). This region spanned ~700 bp between 49,456,800 to 49,457,500 bp of chromosome 1 (Fig 3.3).

To investigate the suspected deletion in 'Cristobalina', PCR primers flanking this *DAM* promoter deletion (DPD) were used to analyze genomic DNA of all the cultivars studied, including 'Regina'. A fragment of the expected size (~1,600 bp) was amplified in all the sweet cherry cultivars, except in 'Cristobalina', in which a shorter fragment (~900 bp) was obtained (Fig 3.4). The amplification of a smaller fragment in 'Cristobalina' supports the presence of a deletion of approximately 700 bp in this region. To confirm this deletion, PCR products amplified using DPD primers in 'Cristobalina' and 'Regina' were sequenced and aligned obtaining a consensus sequence of this PCR product for each cultivar (Sup Fig 3.2 and 3.3). Comparison of both sequences revealed a deletion 'Cristobalina' of 696 bp that covered from 725 to 1,371 bp upstream of *PavDAM1* start codon in the 'Regina' sweet cherry genome (Sup Fig 3.4). Two alleles for 'Cristobalina'

and one for 'Vic' were observed in this region from the sequenced fragments (Sup Fig 3.2). A schematic representation of this deletion is shown in Fig 3.5.

Figure 3.3 Alignment of gDNA sequences of 'Cristobalina', 'Hedelfingen', 'Lambert', 'Napoleon', 'Rainier' and 'Satonishiki' to 'Regina' sweet cherry genome in the promoter region of *PavDAM* genes (49,455,295 to 49,459,399 bp).

DPD marker analysis in a segregating population

As expected, 'BC8' ('Brooks' × 'Cristobalina') analysis with DPD primers showed that this selection is heterozygous for this marker (Fig 3.6). Genotyping of 64 individuals of B×C2 population that derives from 'BC8' self-pollination, revealed, as expected, three segregating classes for this marker (Fig 3.6). These classes include genotypes homozygous for the deletion (*dd*), like 'Cristobalina'; genotypes heterozygous for the deletion (*dp*), like 'BC8'; and genotypes homozygous for the complete promoter sequence (*pp*), like 'Brooks' (Fig 3.6). Segregation of the three classes occurred in the proportion 20:24:4 (*dd*:*dp*:*pp*), which significantly differs from expected 1:2:1 ratio (χ^2=21.33; Sup Table 3.4).

DPD genotypes identified herein and QTL (*qP-CD1.1*^{m}*/qP-GDH1.2*^{m}) genotypes previously reported for same individuals (Chapter 3) were compared (Sup Table 3.4). Comparison revealed that individuals with QTL haplotypes *cc*, *ac* and *aa* (Chapter 3) were the same as those belonging to DPD segregating classes *dd, dp* and *pp*, respectively. (Sup Table 3.4). These results confirm that DPD marker is valid for identifying the different QTL haplotypes. Additionally, DPD genotyping allowed identifying the genotype in this region of 17 individuals that are recombinant for the QTL haplotypes. DPD marker analysis revealed that of the 17 recombinants, 8 individuals corresponded to genotype *dd*, and 9 to *dp* (Sup Table 3.4).

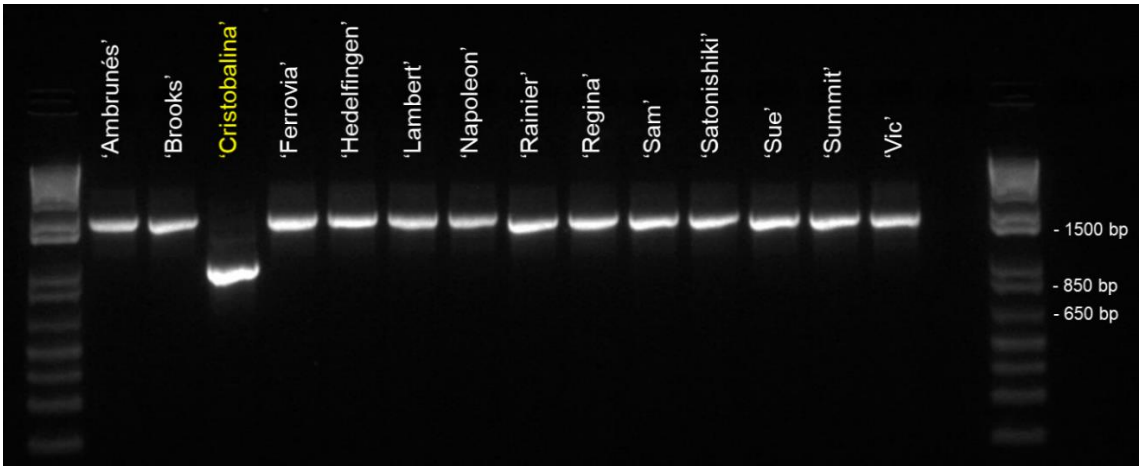

Figure 3.4 DPD analysis in 13 sweet cherry cultivars.

Estimation of the mean BT phenotypic value, in CD and GDH, of the three segregating classes of DPD, in B×C2 population, revealed a significant difference of 7 days and 1,434 GDH between classes *dd* and *dp* ($p<0.001$; *Student's T* test), being *dd* genotypes (82.9 days; 7,833 GDH), earlier than *dp* genotypes (90.1 days; 9,267 GDH). No phenotype data for *pp* individuals was available to estimate the phenotypic value of this segregating class.

DISCUSSION

PavDAM characterization and phylogenetic analysis

In this study, six MADS-box proteins, *PavDAM*, were identified in the main BT QTL previously detected in populations derived from the low CR and extra-early BT cultivar 'Cristobalina' (*qP-CD1.1*^{m}/*qP-GDH1.2*^{m}; Chapter 3). This genome region is critical in the genetic control of CR and BT in the species, as QTLs for these traits were also previously reported on the same location, in other sweet cherry populations with different genetic backgrounds (Dirlewanger et al., 2012; Castède et al., 2014). Six tandemly arranged MICK^{c}–type MADS-box, denoted *DAM* genes, have been previously identified in the syntenic region of *qP-CD1.1*^{m}/*qP-GDH1.2*^{m} in the peach and Japanese apricot genomes (Xu et al., 2014; Wells et al., 2015). *DAM* genes have been reported to be the strongest candidate genes for dormancy release and BT in fruit trees species of the *Rosaceae* such as apple, peach, and Japanese apricot based on several evidence (Falavigna et al., 2019). *DAM* genes have been reported to overlap within the main BT and CR QTLs detected in peach and apple (Fan et al., 2010; Zhebentyayeva et al., 2014; Bielenberg et al., 2015; Allard et al., 2016). The quantification of *DAM* transcript levels in peach and Japanese apricot during the season has shown expression patterns that correlate with different dormancy phases (Li et al., 2009; Zhang et al., 2018; Zhao et al., 2018). The *evergrowing* peach mutant, lacking dormancy, has a deletion in the genomic region containing *DAM* genes (Bielenberg et al., 2008). *DAM* genes are phylogenetically close to *SVP* and *AGL24* (Falavigna et al., 2019), which, respectively, are the main repressor and activator genes of flowering in *Arabidopsis* (Jiménez et al., 2009). *SVP* inhibits *FLOWERING LOCUS T* (*FT*) in *Arabidopsis*, and it is believed that in perennial species,

DAM genes may act also as *FT* repressors (Falavigna et al., 2019). Although previous works have reported the relationship of *DAM* genes and dormancy release and BT in sweet cherry (Castède et al. 2015; Rothkegel et al. 2017), this work characterizes for first time the six *PavDAM* genes. Each characterized gene comprises eight exons that include the four characteristic domains of MIKC type II MADS-box, as reported earlier in peach and Japanese apricot (Jiménez et al., 2009; Xu et al., 2014). Furthermore, the genomic structure of the six genes is very similar in the three species; peach, Japanese apricot and sweet cherry (Jiménez et al., 2009; Sasaki et al., 2011; this work). Thus, the six MADS-box (*PavDAM*) genes identified within the BT QTL in this work are solid candidate genes for BT and CR regulation in sweet cherry.

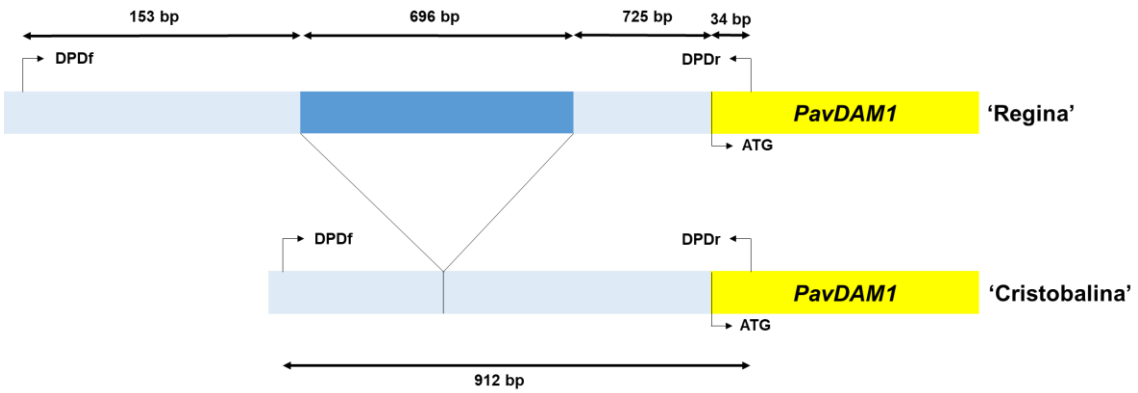

Figure 3.5 Schematic overview of DPD, *PavDAM1* promoter deletion found in 'Cristobalina'.

Phylogenetic analysis revealed that *PavDAM* are orthologs to the peach and Japanese apricot corresponding *DAM* genes. Within each *DAM* gene clade, peach and Japanese apricot genes appeared phylogenetically closer to each other than to sweet cherry genes, reflecting the species phylogeny. Peach and Japanese apricot, belonging respectively to *Amygdalus* and *Prunus* subgenus, are phylogenetically closer to each other than sweet cherry (*Cerasus* subgenus), which is phylogenetically more distant (Potter et al., 2007). The detection of six clades of *DAM* ortholog groups indicates that *DAM* diversification occurred before *Prunus* speciation, additionally the six *DAM* genes may be paralogs (outparalogs), as earlier duplication events may have led to the six tandemly arranged genes (Koonin, 2005). As suggested before (Jiménez et al., 2009; Li et al., 2009),

posterior subfunctionalization and/or neofunctinalization may have resulted in their actual function. The clustering of the *DAM* orthologs in two major clades, namely *DAM1, -2* and *-3* and *DAM4, -5* and *-6,* agrees with previous transcriptomic studies of *DAM* genes in peach and Japanese apricot, in which two different expression patterns have been observed for the two groups of genes. *DAM1, -2* and *-3* have a maximum expression during bud set, while *DAM4, -5* and *-6* show maximum expression when CR are satisfied (Falavigna et al., 2019).

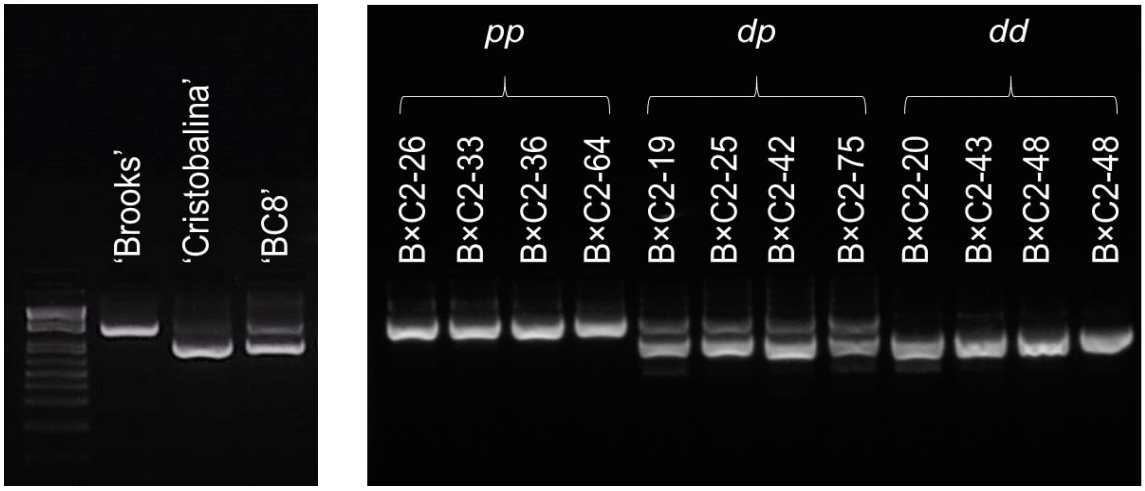

Figure 3.6 DPD analysis in a selected sample (12 individuals) of B×C2 population showing the three segregating classes. DPD analysis in selection 'BC8' and in its parental cultivars ('Brooks' and 'Cristobalina') is also showed.

PavDAM variation in 'Cristobalina'

The re-sequencing, and alignment to the 'Regina' sweet cherry reference genome (Le Dantec et al., 2019), of thirteen sweet cherry cultivars from different genetic backgrounds and showing CRs and BTs variability has allowed the identification of polymorphisms in the *PavDAM* sequences. These polymorphisms could be related with different BT behavior in the different cultivars. 'Cristobalina' *PavDAM* genes showed lowest similarity with the *PavDAM* genes of the rest of cultivars, and accumulated the larger number of unique amino acid substitutions. 'Cristobalina' was the only cultivar that has a unique amino substitution in the M domain of *PavDAM2*, whereas for the rest of cultivars large number of substitutions were observed in its C domain. It has been reported

that M is the most conserved of all MADS-box domains; and C, that is related to protein complex formation and transcriptomical activation, the most variable (Honma and Goto, 2001; Kaufmann et al., 2005). 'Cristobalina' shows low CR and extra-early BT (Tabuenca, 1983; Alburquerque et al., 2008; Chapter 3), and it has been observed that enters endodormancy later, and fulfills its chilling requirements before than medium to late BT cultivars (Fadón et al., 2018). The differences observed in *PavDAM* genes of 'Cristobalina' may be associated to these phenotypic differences in CR and BT with the rest of cultivars. Alternatively, these differences may be due to a different genetic origin and a different evolutionary history of 'Cristobalina' and the rest of cultivars. Analysis of the genetic similarity of sweet cherry cultivars (Wünsch and Hormaza, 2002; Martínez-Royo and Wünsch, 2014) revealed that 'Cristobalina' is more similar to other cultivars from southern Europe like 'Ambrunés' (another Spanish landrace from a different region also analyzed here) than to the other analyzed cultivars. Further research of *PavDAM* genes in these cultivars is needed to confirm either of the two hypothesis.

Additionally, a 696 bp deletion (DPD, *DAM* Promoter Deletion), 725 bp upstream of *PavDAM1* coding sequence, in the putative promoter region, was observed. This deletion was detected in 'Cristobalina' by sequence reads mapping to the 'Regina' reference genome (Le Dantec et al., 2019), and confirmed by sequencing of DPD PCR fragments. Analysis of DPD in the F_2 segregating population B×C2, revealed complete correlation of the segregating classes with BT QTL *qP-CD1.1*^{m}/*qP-GDH1.2*^{m} genotypes (Chapter 3). Additionally, analysis of the phenotype of the DPD segregating classes showed association with early blooming (7 days earlier), for individuals homozygous for the DPD. These evidences indicate that this deletion may be the causal mutation of phenotypic differences associated to main BT QTL (*qP-CD1.1*^{m}/*qP-GDH1.2*^{m}; Chapter 3). The location of DPD mutation in the putative promoter region of the *PavDAM* genes, may affect the regulation of their expression in 'Cristobalina'. Differences in *PavDAM* expression in 'Cristobalina' may, therefore, being the cause of the phenotypic differences observed in 'Cristobalina' CR and BT. Detailed study of the expression pattern of these genes in the period preceding flowering (dormancy) within cultivar of contrasted genotypes and phenotypes would help confirming this hypothesis.

Segregation distortion in DPD resulted in few genotypes of the class *pp*, not allowing investigating the phenotypic value of *pp* genotypes. Large segregation distortion

has been previously observed in this genomic region in this population (Chapter 2), as well as, in homolog regions of other sweet cherry and peach linkage maps (Foulongne et al., 2003; Klagges et al., 2013). Previous studies suggested that BT genes in this region, also possibly involved in seed dormancy, may be the cause of this distortion (Leida et al., 2012; Abbott et al., 2015; Chapter 2). However, the peak of this distortion is about 10 cM away (Chapter 2) from *PavDAM* genes characterized herein, suggesting, therefore, that other genes in this region may be the cause of this distortion.

DPD, a marker for breeding for early blooming and low chilling requirements

'Cristobalina' is a relevant cultivar for breeding, due to self-compatibility, low CRs and extra-early BT. The DPD marker, developed here, is a useful tool for sweet cherry breeding of low CR and early BT from 'Cristobalina' using marker-assisted selection. This marker revealed a complete correlation with the haplotypes of BT QTL (*qP-CD1.1*^{m}/*qP-GDH1.2*^{m}), which accounts for up to 50.1% of the phenotypic variation in 'Cristobalina' derived populations (Chapter 3). The large correlation between QTL and marker genotypes, as well as, the large amount of phenotypic variation explained by this QTL makes DPD marker a useful tool for discriminating individuals with lower CR and earlier blooming, which will be associated to the presence of the deletion DPD in homozygosity or heterozygosity. Earlier blooming is expected to be associated to the presence of the deletion in homozygosity and later blooming and higher CR will be associated to the absence of the deletion.

In the present study, the analysis of candidate genes in the region of a previously detected main BT QTL, has allowed the identification and characterization of *PavDAM* genes, thus confirming *PavDAM* genes as main candidate genes for CR and BT in sweet cherry. Protein sequence polymorphisms in 'Cristobalina' *PavDAM* genes, and a large promoter deletion could be cause of the phenotypic differences exhibited by 'Cristobalina', low CR and extra-early BT. The correlation between DPD genotypes and phenotype value in a segregating population confirmed the association of the deletion mutation with the phenotypic differences, and will allow the use of this marker for selection of low CR and early blooming from 'Cristobalina'.

SUPPLEMENTARY MATERIALS CHAPTER 4

Supplementary Table 3.1 Predicted genes of the 'Regina' sweet cherry genome (Le Dantec et al., 2019) in Chromosome 1: 49,296,241-49,622,837. Sequence description of protein sequences in NCBI database and statistical significance of highest matches from BLAST. Candidate *DAM* genes are shown in bold.

Predicted gene	Description	Max score	Total score	Query cover	E value	Identity
PAV01_g0074801	rho GTPase-activating protein REN1 isoform X1 [*Prunus yedoensis* var. *nudiflora*]	1524	1524	99%	0	91%
PAV01_g0074811	mitochondrial uncoupling protein 5-like [*Prunus avium*]	647	647	99%	0	100%
PAV01_g0074831	probable pectinesterase/pectinesterase inhibitor 7 [*Prunus avium*]	1162	1162	99%	0	100%
PAV01_g0074851	probable pectinesterase/pectinesterase inhibitor 20 [*Prunus avium*]	1162	1162	99%	0	99%
PAV01_g0074861	cytochrome b561 and DOMON domain-containing protein At5g47530-like [*Prunus avium*]	715	715	99%	0	99%
PAV01_g0074871	uncharacterized protein LOC110751910 [*Prunus avium*]	327	327	99%	8.00E-110	100%
PAV01_g0074881	aspartyl protease AED3 [*Prunus avium*]	763	763	99%	0	90%
PAV01_g0074891	universal stress protein PHOS34 [*Prunus avium*]	276	276	99%	1.00E-92	79%
PAV01_g0074901	eukaryotic translation initiation factor 3 subunit C-like isoform X1 [*Prunus avium*]	1941	1941	99%	0	99%
PAV01_g0074911	ubiquitin carboxyl-terminal hydrolase 16-like [*Prunus avium*]	2228	2228	99%	0	98%
PAV01_g0074921	AT-hook motif nuclear-localized protein 17 [*Prunus avium*]	387	387	99%	3.00E-134	100%
PAV01_g0074931	hypothetical protein KK1_049021 [*Cajanus cajan*]	52.4	52.4	57%	3.00E-07	60%
PAV01_g0074941	AP-4 complex subunit mu [*Prunus avium*]	921	921	99%	0	100%
PAV01_g0074951	putative methyltransferase At1g22800 isoform X2 [*Prunus avium*]	705	705	99%	0	100%
PAV01_g0074961	cytochrome b561 and DOMON domain-containing protein At5g47530-like [*Prunus avium*]	715	715	99%	0	99%
PAV01_g0074971	uncharacterized protein LOC110765872 [k]	197	197	71%	4.00E-61	79%
PAV01_g0074981	No significant similarity found	-	-	-	-	-
PAV01_g0074991	hypothetical protein PRUPE_4G104600 [*Prunus persica*]	97.4	97.4	97%	1.00E-24	79%
PAV01_g0075001	small heat shock protein chloroplastic [*Prunus yedoensis* var. *nudiflora*]	314	314	99%	1.00E-106	84%
PAV01_g0075011	putative DNA helicase [*Rosa chinensis*]	102	153	58%	6.00E-23	77%
PAV01_g0075021	beta carbonic anhydrase 5, chloroplastic-like isoform X2 [*Prunus avium*]	648	648	99%	0	99%
PAV01_g0075031	transcription factor bHLH30-like [*Prunus avium*]	491	491	99%	1.00E-175	100%
PAV01_g0075041	uncharacterized protein LOC110751898 [*Prunus avium*]	488	808	99%	1.00E-170	83%
PAV01_g0075051	uncharacterized protein Pyn_34535 [*Prunus yedoensis* var. *nudiflora*]	662	662	99%	0	100%

Supplementary Table 3.1 Continued

PAV01_g0075061	No significant similarity found	-	-	-	-	-
PAV01_g0075071	No significant similarity found	-	-	-	-	-
PAV01_g0075081	**MADS-box protein JOINTLESS-like isoform X5 [*Prunus avium*]**	**472**	**472**	**99%**	**2.00E-168**	**100%**
PAV01_g0075091	**MADS-box protein JOINTLESS-like [*Prunus avium*]**	**424**	**424**	**99%**	**2.00E-149**	**91%**
PAV01_g0075101	**MADS1 [*Prunus avium*]**	**230**	**230**	**99%**	**1.00E-74**	**100%**
PAV01_g0075111	**MADS1 [*Prunus avium*]**	**246**	**246**	**99%**	**1.00E-80**	**99%**
PAV01_g0075121	**MADS-box protein JOINTLESS-like isoform X4 [*Prunus avium*]**	**446**	**717**	**76%**	**1.00E-153**	**99%**
PAV01_g0075131	**MADS-box protein JOINTLESS-like isoform X7 [*Prunus avium*]**	**129**	**129**	**51%**	**2.00E-34**	**86%**
PAV01_g0075141	**MADS-box protein JOINTLESS-like isoform X6 [*Prunus avium*]**	**317**	**317**	**93%**	**4.00E-108**	**100%**
PAV01_g0075151	**MADS-box protein JOINTLESS-like isoform X5 [*Prunus avium*]**	**479**	**479**	**99%**	**9.00E-171**	**100%**
PAV01_g0075161	No significant similarity found	-	-	-	-	-
PAV01_g0075171	O-fucosyltransferase 31 [*Rosa chinensis*]	930	930	99%	0	87%
PAV01_g0075181	mechanosensitive ion channel protein 3, chloroplastic-like isoform X1 [*Prunus avium*]	1457	1457	99%	0	99%
PAV01_g0075191	No significant similarity found	-	-	-	-	-
PAV01_g0075201	kinesin-like protein KIN-4C isoform X1 [*Prunus avium*]	2633	2633	99%	0	100%
PAV01_g0075211	No significant similarity found	-	-	-	-	-
PAV01_g0075231	kinesin-like protein KIN-4C [*Prunus avium*]	1126	1126	99%	0	99%
PAV01_g0075241	argininosuccinate lyase, chloroplastic [*Prunus avium*]	1077	1077	99%	0	100%
PAV01_g0075251	uncharacterized protein LOC110772580 isoform X3 [*Prunus avium*]	344	344	99%	8.00E-120	100%
PAV01_g0075261	protein NETWORKED 2A-like [*Prunus avium*]	2024	2024	99%	0	100%
PAV01_g0075271	pentatricopeptide repeat-containing protein At2g37230 [*Prunus avium*]	1542	1542	96%	0	99%
PAV01_g0075281	uncharacterized protein LOC110772590 isoform X2 [*Prunus avium*]	557	557	99%	0	100%
PAV01_g0075291	uncharacterized protein LOC110772590 isoform X1 [*Prunus avium*]	698	698	95%	0	100%

Supplementary Table 3.2 GFF file of correct annotation of *PavDAM* genes in the 'Regina' sweet cherry genome. Automatic (EuGene) and Manual intro-exon prediction is indicate.

```
###
PAV01_REGINA	EuGene	gene	49457863	49465728	.	+	.	ID=gene:PavDAM1;Name=PavDAM1
PAV01_REGINA	EuGene	mRNA	49457863	49465728	.	+	.	ID=mRNA:PavDAM1;Name=PavDAM1;Parent=gene:PavDAM1
PAV01_REGINA	EuGene	exon	49457863	49457952	.	+	.	ID=exon:PavDAM1.utr0;Parent=mRNA:PavDAM1;Ontology_term=SO:0000204
PAV01_REGINA	EuGene	exon	49458233	49458426	.	+	.	ID=exon:PavDAM1.1;Parent=mRNA:PavDAM1;Ontology_term=SO:0000200
PAV01_REGINA	EuGene	exon	49462000	49462078	.	+	1	ID=exon:PavDAM1.2;Parent=mRNA:PavDAM1;Ontology_term=SO:0000004
PAV01_REGINA	EuGene	exon	49463597	49463658	.	+	0	ID=exon:PavDAM1.3;Parent=mRNA:PavDAM1;Ontology_term=SO:0000004
PAV01_REGINA	EuGene	exon	49463744	49463843	.	+	1	ID=exon:PavDAM1.4;Parent=mRNA:PavDAM1;Ontology_term=SO:0000004
PAV01_REGINA	EuGene	exon	49464102	49464143	.	+	0	ID=exon:PavDAM1.5;Parent=mRNA:PavDAM1;Ontology_term=SO:0000004
PAV01_REGINA	EuGene	exon	49464295	49464336	.	+	0	ID=exon:PavDAM1.6;Parent=mRNA:PavDAM1;Ontology_term=SO:0000004
PAV01_REGINA	EuGene	exon	49464452	49464636	.	+	0	ID=exon:PavDAM1.7;Parent=mRNA:PavDAM1;Ontology_term=SO:0000004
PAV01_REGINA	EuGene	exon	49464942	49465728	.	+	1	ID=exon:PavDAM1.8;Parent=mRNA:PavDAM1;Ontology_term=SO:0000202
PAV01_REGINA	EuGene	five_prime_UTR	49457863	49457952	.	+	.	ID=five_prime_UTR:PavDAM1.0;Parent=mRNA:PavDAM1;Ontology_term=SO:0000204;est_cons=100.0;est_incons=0.0
PAV01_REGINA	EuGene	five_prime_UTR	49458233	49458238	.	+	.	ID=five_prime_UTR:PavDAM1.2;Parent=mRNA:PavDAM1;Ontology_term=SO:0000204;est_cons=100.0;est_incons=0.0
PAV01_REGINA	EuGene	CDS	49458239	49458426	.	+	0	ID=CDS:PavDAM1.1;Parent=mRNA:PavDAM1;Ontology_term=SO:0000196;est_cons=100.0;est_incons=0.0
PAV01_REGINA	EuGene	CDS	49462000	49462078	.	+	1	ID=CDS:PavDAM1.2;Parent=mRNA:PavDAM1;Ontology_term=SO:0000004;est_cons=100.0;est_incons=0.0
PAV01_REGINA	EuGene	CDS	49463597	49463658	.	+	0	ID=CDS:PavDAM1.3;Parent=mRNA:PavDAM1;Ontology_term=SO:0000004;est_cons=100.0;est_incons=0.0
PAV01_REGINA	EuGene	CDS	49463744	49463843	.	+	1	ID=CDS:PavDAM1.4;Parent=mRNA:PavDAM1;Ontology_term=SO:0000004;est_cons=100.0;est_incons=0.0
PAV01_REGINA	EuGene	CDS	49464102	49464143	.	+	0	ID=CDS:PavDAM1.5;Parent=mRNA:PavDAM1;Ontology_term=SO:0000004;est_cons=100.0;est_incons=0.0
PAV01_REGINA	EuGene	CDS	49464295	49464336	.	+	0	ID=CDS:PavDAM1.6;Parent=mRNA:PavDAM1;Ontology_term=SO:0000004;est_cons=100.0;est_incons=0.0
PAV01_REGINA	EuGene	CDS	49464452	49464636	.	+	0	ID=CDS:PavDAM1.7;Parent=mRNA:PavDAM1;Ontology_term=SO:0000004;est_cons=100.0;est_incons=0.0
PAV01_REGINA	EuGene	CDS	49464942	49464951	.	+	1	ID=CDS:PavDAM1.8;Parent=mRNA:PavDAM1;Ontology_term=SO:0000197;est_cons=100.0;est_incons=0.0
PAV01_REGINA	EuGene	three_prime_UTR	49464952	49465728	.	+	.	ID=three_prime_UTR:PavDAM1.18;Parent=mRNA:PavDAM1;Ontology_term=SO:0000205;est_cons=100.0;est_incons=0.0
###
PAV01_REGINA	EuGene	gene	49465730	49475605	.	+	.	ID=gene:PavDAM2;Name=PavDAM2
PAV01_REGINA	EuGene	mRNA	49465730	49475605	.	+	.	ID=mRNA:PavDAM2;Name=PavDAM2;Parent=gene:PavDAM2
```

Supplementary Table 3.2 Continued.

PAV01_REGINA	EuGene	exon	49465730	49466254	.	+	.	ID=exon:PavDAM2.utr0;Parent=mRNA:PavDAM2;Ontology_term=SO:0000204
PAV01_REGINA	EuGene	exon	49466560	49466755	.	+	.	ID=exon:PavDAM2.1;Parent=mRNA:PavDAM2;Ontology_term=SO:0000200
PAV01_REGINA	EuGene	exon	49472342	49472420	.	+	1	ID=exon:PavDAM2.2;Parent=mRNA:PavDAM2;Ontology_term=SO:0000004
PAV01_REGINA	Manual	exon	49473111	49473173	.	+	0	ID=exon:PavDAM2.3;Parent=mRNA:PavDAM2;Ontology_term=SO:0000004
PAV01_REGINA	EuGene	exon	49473262	49473357	.	+	0	ID=exon:PavDAM2.4;Parent=mRNA:PavDAM2;Ontology_term=SO:0000004
PAV01_REGINA	EuGene	exon	49473853	49473894	.	+	0	ID=exon:PavDAM2.5;Parent=mRNA:PavDAM2;Ontology_term=SO:0000004
PAV01_REGINA	EuGene	exon	49474036	49474077	.	+	0	ID=exon:PavDAM2.6;Parent=mRNA:PavDAM2;Ontology_term=SO:0000004
PAV01_REGINA	EuGene	exon	49474161	49474354	.	+	0	ID=exon:PavDAM2.7;Parent=mRNA:PavDAM2;Ontology_term=SO:0000004
PAV01_REGINA	EuGene	exon	49475376	49475605	.	+	1	ID=exon:PavDAM2.8;Parent=mRNA:PavDAM2;Ontology_term=SO:0000202
PAV01_REGINA	EuGene	five_prime_UTR	49465730	49466254	.	+	.	ID=five_prime_UTR:PavDAM2.0;Parent=mRNA:PavDAM2;Ontology_term=SO:0000204;est_cons=100.0;est_incons=0.0
PAV01_REGINA	EuGene	five_prime_UTR	49466560	49466564	.	+	.	ID=five_prime_UTR:PavDAM2.2;Parent=mRNA:PavDAM2;Ontology_term=SO:0000204;est_cons=100.0;est_incons=0.0
PAV01_REGINA	EuGene	CDS	49466565	49466755	.	+	0	ID=CDS:PavDAM2.1;Parent=mRNA:PavDAM2;Ontology_term=SO:0000196;est_cons=100.0;est_incons=0.0
PAV01_REGINA	EuGene	CDS	49472342	49472420	.	+	1	ID=CDS:PavDAM2.2;Parent=mRNA:PavDAM2;Ontology_term=SO:0000004;est_cons=69.6;est_incons=0.0
PAV01_REGINA	EuGene	CDS	49473111	49473171	.	+	0	ID=CDS:PavDAM2.3;Parent=mRNA:PavDAM2;Ontology_term=SO:0000004;est_cons=0.0;est_incons=0.0
PAV01_REGINA	EuGene	CDS	49473262	49473357	.	+	0	ID=CDS:PavDAM2.4;Parent=mRNA:PavDAM2;Ontology_term=SO:0000004;est_cons=0.0;est_incons=0.0
PAV01_REGINA	EuGene	CDS	49473853	49473894	.	+	0	ID=CDS:PavDAM2.5;Parent=mRNA:PavDAM2;Ontology_term=SO:0000004;est_cons=0.0;est_incons=0.0
PAV01_REGINA	EuGene	CDS	49474036	49474077	.	+	0	ID=CDS:PavDAM2.6;Parent=mRNA:PavDAM2;Ontology_term=SO:0000004;est_cons=0.0;est_incons=0.0
PAV01_REGINA	EuGene	CDS	49474161	49474354	.	+	0	ID=CDS:PavDAM2.7;Parent=mRNA:PavDAM2;Ontology_term=SO:0000004;est_cons=80.9;est_incons=0.0
PAV01_REGINA	EuGene	CDS	49475376	49475385	.	+	1	ID=CDS:PavDAM2.8;Parent=mRNA:PavDAM2;Ontology_term=SO:0000197;est_cons=100.0;est_incons=0.0
PAV01_REGINA	EuGene	three_prime_UTR	49475386	49475605	.	+	.	ID=three_prime_UTR:PavDAM2.16;Parent=mRNA:PavDAM2;Ontology_term=SO:0000205;est_cons=100.0;est_incons=0.0
###								
PAV01_REGINA	Manual	gene	49486959	49497738	.	+	.	ID=gene:PavDAM3;Name=PavDAM3
PAV01_REGINA	Manual	mRNA	49486959	49497738	.	+	.	ID=mRNA:PavDAM3;Name=PavDAM3;Parent=gene:PavDAM3
PAV01_REGINA	Manual	exon	49486959	49487610	.	+	.	ID=exon:PavDAM3.1;Parent=mRNA:PavDAM3;Ontology_term=SO:0000200
PAV01_REGINA	Manual	exon	49492939	49493017	.	+	1	ID=exon:PavDAM3.2;Parent=mRNA:PavDAM3;Ontology_term=SO:0000004
PAV01_REGINA	Manual	exon	49495428	49495489	.	+	0	ID=exon:PavDAM3.3;Parent=mRNA:PavDAM3;Ontology_term=SO:0000202
PAV01_REGINA	Manual	five_prime_UTR	49486959	49487419	.	+	.	ID=five_prime_UTR:PavDAM3.0;Parent=mRNA:PavDAM3;Ontology_term=SO:0000204;est_cons=100.0;est_incons=0.0

Supplementary Table 3.2 Continued.

PAV01_REGINA	Manual	CDS	49487420	49487610	.	+	0	ID=CDS:PavDAM3.1;Parent=mRNA:PavDAM3;Ontology_term=SO:0000196;est_cons=100.0;est_incons=0.0
PAV01_REGINA	Manual	CDS	49492939	49493017	.	+	1	ID=CDS:PavDAM3.2;Parent=mRNA:PavDAM3;Ontology_term=SO:0000004;est_cons=100.0;est_incons=0.0
PAV01_REGINA	Manual	CDS	49495428	49495489	.	+	0	ID=CDS:PavDAM3.3;Parent=mRNA:PavDAM3;Ontology_term=SO:0000197;est_cons=100.0;est_incons=0.0
PAV01_REGINA	Manual	exon	49495591	49495690	.	+	1	ID=exon:PavDAM3.4;Parent=mRNA:PavDAM3;Ontology_term=SO:0000200
PAV01_REGINA	Manual	exon	49496003	49496044	.	+	0	ID=exon:PavDAM3.5;Parent=mRNA:PavDAM3;Ontology_term=SO:0000004
PAV01_REGINA	Manual	exon	49496199	49496240	.	+	0	ID=exon:PavDAM3.6;Parent=mRNA:PavDAM3;Ontology_term=SO:0000004
PAV01_REGINA	Manual	exon	49496375	49496559	.	+	0	ID=exon:PavDAM3.7;Parent=mRNA:PavDAM3;Ontology_term=SO:0000004
PAV01_REGINA	Manual	exon	49497205	49497738	.	+	1	ID=exon:PavDAM3.8;Parent=mRNA:PavDAM3;Ontology_term=SO:0000202
PAV01_REGINA	Manual	CDS	49495591	49495690	.	+	1	ID=CDS:PavDAM3.4;Parent=mRNA:PavDAM3;Ontology_term=SO:0000196;est_cons=100.0;est_incons=0.0
PAV01_REGINA	Manual	CDS	49496003	49496044	.	+	0	ID=CDS:PavDAM3.5;Parent=mRNA:PavDAM3;Ontology_term=SO:0000004;est_cons=100.0;est_incons=0.0
PAV01_REGINA	Manual	CDS	49496199	49496240	.	+	0	ID=CDS:PavDAM3.6;Parent=mRNA:PavDAM3;Ontology_term=SO:0000004;est_cons=100.0;est_incons=0.0
PAV01_REGINA	Manual	CDS	49496375	49496559	.	+	0	ID=CDS:PavDAM3.7;Parent=mRNA:PavDAM3;Ontology_term=SO:0000004;est_cons=100.0;est_incons=0.0
PAV01_REGINA	Manual	CDS	49497205	49497214	.	+	1	ID=CDS:PavDAM3.8;Parent=mRNA:PavDAM3;Ontology_term=SO:0000197;est_cons=100.0;est_incons=0.0
PAV01_REGINA	Manual	three_prime_UTR	49497215	49497738	.	+	.	ID=three_prime_UTR:PavDAM3.10;Parent=mRNA:PavDAM3;Ontology_term=SO:0000205;est_cons=100.0;est_incons=0.0
###								
PAV01_REGINA	EuGene	gene	49497742	49507821	.	+	.	ID=gene:PavDAM4;Name=PavDAM4
PAV01_REGINA	EuGene	mRNA	49497742	49507821	.	+	.	ID=mRNA:PavDAM4;Name=PavDAM4;Parent=gene:PavDAM4
PAV01_REGINA	EuGene	exon	49498455	49498645	.	+	0	ID=exon:PavDAM4.1;Parent=mRNA:PavDAM4;Ontology_term=SO:0000004
PAV01_REGINA	EuGene	exon	49502110	49502185	.	+	1	ID=exon:PavDAM4.2;Parent=mRNA:PavDAM4;Ontology_term=SO:0000004
PAV01_REGINA	EuGene	exon	49505693	49505754	.	+	0	ID=exon:PavDAM4.3;Parent=mRNA:PavDAM4;Ontology_term=SO:0000004
PAV01_REGINA	EuGene	exon	49505857	49505956	.	+	1	ID=exon:PavDAM4.4;Parent=mRNA:PavDAM4;Ontology_term=SO:0000004
PAV01_REGINA	EuGene	exon	49506042	49506083	.	+	0	ID=exon:PavDAM4.5;Parent=mRNA:PavDAM4;Ontology_term=SO:0000004
PAV01_REGINA	EuGene	exon	49506193	49506243	.	+	0	ID=exon:PavDAM4.6;Parent=mRNA:PavDAM4;Ontology_term=SO:0000004
PAV01_REGINA	EuGene	exon	49506326	49506468	.	+	0	ID=exon:PavDAM4.7;Parent=mRNA:PavDAM4;Ontology_term=SO:0000004
PAV01_REGINA	EuGene	exon	49506852	49507171	.	+	1	ID=exon:PavDAM4.8;Parent=mRNA:PavDAM4;Ontology_term=SO:0000202
PAV01_REGINA	EuGene	exon	49507315	49507673	.	+	.	ID=exon:PavDAM4.utr22;Parent=mRNA:PavDAM4;Ontology_term=SO:0000205
PAV01_REGINA	EuGene	exon	49507777	49507821	.	+	.	ID=exon:PavDAM4.utr24;Parent=mRNA:PavDAM4;Ontology_term=SO:0000205

Supplementary Table 3.2 Continued.

PAV01_REGINA	EuGene	five_prime_UTR	49497742	49497869	.	+	.	ID=five_prime_UTR:PavDAM4.0;Parent=mRNA:PavDAM4;Ontology_term=SO:0000204;est_cons=100.0;est_incons=0.0
PAV01_REGINA	EuGene	CDS	49498455	49498645	.	+	0	ID=CDS:PavDAM4.1;Parent=mRNA:PavDAM4;Ontology_term=SO:0000004;est_cons=100.0;est_incons=0.0
PAV01_REGINA	EuGene	CDS	49502110	49502185	.	+	1	ID=CDS:PavDAM4.2;Parent=mRNA:PavDAM4;Ontology_term=SO:0000004;est_cons=100.0;est_incons=0.0
PAV01_REGINA	EuGene	CDS	49505693	49505754	.	+	0	ID=CDS:PavDAM4.3;Parent=mRNA:PavDAM4;Ontology_term=SO:0000004;est_cons=100.0;est_incons=0.0
PAV01_REGINA	EuGene	CDS	49505857	49505956	.	+	1	ID=CDS:PavDAM4.4;Parent=mRNA:PavDAM4;Ontology_term=SO:0000004;est_cons=100.0;est_incons=0.0
PAV01_REGINA	EuGene	CDS	49506042	49506083	.	+	0	ID=CDS:PavDAM4.5;Parent=mRNA:PavDAM4;Ontology_term=SO:0000004;est_cons=100.0;est_incons=0.0
PAV01_REGINA	EuGene	CDS	49506193	49506243	.	+	0	ID=CDS:PavDAM4.6;Parent=mRNA:PavDAM4;Ontology_term=SO:0000004;est_cons=100.0;est_incons=0.0
PAV01_REGINA	EuGene	CDS	49506326	49506468	.	+	0	ID=CDS:PavDAM4.7;Parent=mRNA:PavDAM4;Ontology_term=SO:0000004;est_cons=100.0;est_incons=0.0
PAV01_REGINA	EuGene	CDS	49506852	49506861	.	+	1	ID=CDS:PavDAM4.8;Parent=mRNA:PavDAM4;Ontology_term=SO:0000197;est_cons=100.0;est_incons=0.0
PAV01_REGINA	EuGene	three_prime_UTR	49506862	49507171	.	+	.	ID=three_prime_UTR:PavDAM4.20;Parent=mRNA:PavDAM4;Ontology_term=SO:0000205;est_cons=100.0;est_incons=0.0
PAV01_REGINA	EuGene	three_prime_UTR	49507315	49507673	.	+	.	ID=three_prime_UTR:PavDAM4.22;Parent=mRNA:PavDAM4;Ontology_term=SO:0000205;est_cons=100.0;est_incons=0.0
PAV01_REGINA	EuGene	three_prime_UTR	49507777	49507821	.	+	.	ID=three_prime_UTR:PavDAM4.24;Parent=mRNA:PavDAM4;Ontology_term=SO:0000205;est_cons=100.0;est_incons=0.0
###								
PAV01_REGINA	Manual	gene	49507823	49517606	.	+	.	ID=gene:PavDAM5;Name=PavDAM5
PAV01_REGINA	Manual	mRNA	49507823	49517606	.	+	.	ID=mRNA:PavDAM5;Name=PavDAM5;Parent=gene:PavDAM5
PAV01_REGINA	Manual	exon	49507823	49507839	.	+	.	ID=exon:PavDAM5.utr0;Parent=mRNA:PavDAM5;Ontology_term=SO:0000204
PAV01_REGINA	Manual	exon	49508062	49508243	.	+	.	ID=exon:PavDAM5.1;Parent=mRNA:PavDAM5;Ontology_term=SO:0000200
PAV01_REGINA	Manual	five_prime_UTR	49507823	49507839	.	+	.	ID=five_prime_UTR:PavDAM5.0;Parent=mRNA:PavDAM5;Ontology_term=SO:0000204;est_cons=100.0;est_incons=0.0
PAV01_REGINA	Manual	five_prime_UTR	49508062	49508064	.	+	.	ID=five_prime_UTR:PavDAM5.2;Parent=mRNA:PavDAM5;Ontology_term=SO:0000204;est_cons=100.0;est_incons=0.0
PAV01_REGINA	Manual	exon	49513443	49513521	.	+	1	ID=exon:PavDAM5.1;Parent=mRNA:PavDAM5;Ontology_term=SO:0000200
PAV01_REGINA	Manual	exon	49514370	49514431	.	+	0	ID=exon:PavDAM5.2;Parent=mRNA:PavDAM5;Ontology_term=SO:0000004
PAV01_REGINA	Manual	exon	49514524	49514623	.	+	1	ID=exon:PavDAM5.3;Parent=mRNA:PavDAM5;Ontology_term=SO:0000004
PAV01_REGINA	Manual	exon	49515144	49515185	.	+	0	ID=exon:PavDAM5.4;Parent=mRNA:PavDAM5;Ontology_term=SO:0000004
PAV01_REGINA	Manual	exon	49515299	49515340	.	+	0	ID=exon:PavDAM5.5;Parent=mRNA:PavDAM5;Ontology_term=SO:0000004
PAV01_REGINA	Manual	exon	49515475	49515668	.	+	0	ID=exon:PavDAM5.6;Parent=mRNA:PavDAM5;Ontology_term=SO:0000004
PAV01_REGINA	Manual	exon	49516580	49516707	.	+	1	ID=exon:PavDAM5.7;Parent=mRNA:PavDAM5;Ontology_term=SO:0000202
PAV01_REGINA	Manual	exon	49516797	49516858	.	+	.	ID=exon:PavDAM5.utr16;Parent=mRNA:PavDAM5;Ontology_term=SO:0000205

Supplementary Table 3.2 Continued.

PAV01_REGINA	Manual	exon	49517027	49517606	.	+	.	ID=exon:PavDAM5.utr18;Parent=mRNA:PavDAM5;Ontology_term=SO:0000205
PAV01_REGINA	Manual	CDS	49508065	49508243	.	+	0	ID=CDS:PavDAM5.1;Parent=mRNA:PavDAM5;Ontology_term=SO:0000196;est_cons=100.0;est_incons=0.0
PAV01_REGINA	Manual	CDS	49513443	49513521	.	+	1	ID=CDS:PavDAM5.2;Parent=mRNA:PavDAM5;Ontology_term=SO:0000196;est_cons=100.0;est_incons=0.0
PAV01_REGINA	Manual	CDS	49514370	49514431	.	+	0	ID=CDS:PavDAM5.3;Parent=mRNA:PavDAM5;Ontology_term=SO:0000004;est_cons=100.0;est_incons=0.0
PAV01_REGINA	Manual	CDS	49514524	49514623	.	+	1	ID=CDS:PavDAM5.4;Parent=mRNA:PavDAM5;Ontology_term=SO:0000004;est_cons=100.0;est_incons=0.0
PAV01_REGINA	Manual	CDS	49515144	49515185	.	+	0	ID=CDS:PavDAM5.5;Parent=mRNA:PavDAM5;Ontology_term=SO:0000004;est_cons=100.0;est_incons=0.0
PAV01_REGINA	Manual	CDS	49515299	49515340	.	+	0	ID=CDS:PavDAM5.6;Parent=mRNA:PavDAM5;Ontology_term=SO:0000004;est_cons=100.0;est_incons=0.0
PAV01_REGINA	Manual	CDS	49515475	49515668	.	+	0	ID=CDS:PavDAM5.7;Parent=mRNA:PavDAM5;Ontology_term=SO:0000004;est_cons=100.0;est_incons=0.0
PAV01_REGINA	Manual	CDS	49516580	49516619	.	+	1	ID=CDS:PavDAM5.8;Parent=mRNA:PavDAM5;Ontology_term=SO:0000197;est_cons=100.0;est_incons=0.0
PAV01_REGINA	Manual	three_prime_UTR	49516620	49516707	.	+	.	ID=three_prime_UTR:PavDAM5.14;Parent=mRNA:PavDAM5;Ontology_term=SO:0000205;est_cons=100.0;est_incons=0.0
PAV01_REGINA	Manual	three_prime_UTR	49516797	49516858	.	+	.	ID=three_prime_UTR:PavDAM5.16;Parent=mRNA:PavDAM5;Ontology_term=SO:0000205;est_cons=100.0;est_incons=0.0
PAV01_REGINA	Manual	three_prime_UTR	49517027	49517606	.	+	.	ID=three_prime_UTR:PavDAM5.18;Parent=mRNA:PavDAM5;Ontology_term=SO:0000205;est_cons=100.0;est_incons=0.0
###								
PAV01_REGINA	EuGene	gene	49517608	49524699	.	+	.	ID=gene:PavDAM6;Name=PavDAM6
PAV01_REGINA	EuGene	mRNA	49517608	49524699	.	+	.	ID=mRNA:PavDAM6;Name=PavDAM6;Parent=gene:PavDAM6
PAV01_REGINA	EuGene	exon	49517608	49517614	.	+	.	ID=exon:PavDAM6.utr0;Parent=mRNA:PavDAM6;Ontology_term=SO:0000204
PAV01_REGINA	EuGene	exon	49517878	49518072	.	+	.	ID=exon:PavDAM6.1;Parent=mRNA:PavDAM6;Ontology_term=SO:0000200
PAV01_REGINA	EuGene	exon	49521025	49521103	.	+	1	ID=exon:PavDAM6.2;Parent=mRNA:PavDAM6;Ontology_term=SO:0000004
PAV01_REGINA	EuGene	exon	49522143	49522204	.	+	0	ID=exon:PavDAM6.3;Parent=mRNA:PavDAM6;Ontology_term=SO:0000004
PAV01_REGINA	EuGene	exon	49522307	49522406	.	+	1	ID=exon:PavDAM6.4;Parent=mRNA:PavDAM6;Ontology_term=SO:0000004
PAV01_REGINA	EuGene	exon	49523208	49523249	.	+	0	ID=exon:PavDAM6.5;Parent=mRNA:PavDAM6;Ontology_term=SO:0000004
PAV01_REGINA	EuGene	exon	49523384	49523425	.	+	0	ID=exon:PavDAM6.6;Parent=mRNA:PavDAM6;Ontology_term=SO:0000004
PAV01_REGINA	EuGene	exon	49523526	49523722	.	+	0	ID=exon:PavDAM6.7;Parent=mRNA:PavDAM6;Ontology_term=SO:0000004
PAV01_REGINA	EuGene	exon	49524409	49524699	.	+	1	ID=exon:PavDAM6.8;Parent=mRNA:PavDAM6;Ontology_term=SO:0000202
PAV01_REGINA	EuGene	five_prime_UTR	49517608	49517614	.	+	.	ID=five_prime_UTR:PavDAM6.0;Parent=mRNA:PavDAM6;Ontology_term=SO:0000204;est_cons=100.0;est_incons=0.0
PAV01_REGINA	EuGene	five_prime_UTR	49517878	49517881	.	+	.	ID=five_prime_UTR:PavDAM6.2;Parent=mRNA:PavDAM6;Ontology_term=SO:0000204;est_cons=100.0;est_incons=0.0
PAV01_REGINA	EuGene	CDS	49517882	49518072	.	+	0	ID=CDS:PavDAM6.1;Parent=mRNA:PavDAM6;Ontology_term=SO:0000196;est_cons=88.0;est_incons=0.0

Supplementary Table 3.2 Continued.

PAV01_REGINA	EuGene	CDS	49521025	49521103	.	+	1	ID=CDS:PavDAM6.2;Parent=mRNA:PavDAM6;Ontology_term=SO:0000004;est_cons=100.0;est_incons=0.0
PAV01_REGINA	EuGene	CDS	49522143	49522204	.	+	0	ID=CDS:PavDAM6.3;Parent=mRNA:PavDAM6;Ontology_term=SO:0000004;est_cons=100.0;est_incons=0.0
PAV01_REGINA	EuGene	CDS	49522307	49522406	.	+	1	ID=CDS:PavDAM6.4;Parent=mRNA:PavDAM6;Ontology_term=SO:0000004;est_cons=100.0;est_incons=0.0
PAV01_REGINA	EuGene	CDS	49523208	49523249	.	+	0	ID=CDS:PavDAM6.5;Parent=mRNA:PavDAM6;Ontology_term=SO:0000004;est_cons=100.0;est_incons=0.0
PAV01_REGINA	EuGene	CDS	49523384	49523425	.	+	0	ID=CDS:PavDAM6.6;Parent=mRNA:PavDAM6;Ontology_term=SO:0000004;est_cons=100.0;est_incons=0.0
PAV01_REGINA	EuGene	CDS	49523526	49523722	.	+	0	ID=CDS:PavDAM6.7;Parent=mRNA:PavDAM6;Ontology_term=SO:0000004;est_cons=100.0;est_incons=0.0
PAV01_REGINA	EuGene	CDS	49524409	49524418	.	+	1	ID=CDS:PavDAM6.8;Parent=mRNA:PavDAM6;Ontology_term=SO:0000197;est_cons=100.0;est_incons=0.0
PAV01_REGINA	EuGene	three_prime_UTR	49524419	49524699	.	+	.	ID=three_prime_UTR:PavDAM6.18;Parent=mRNA:PavDAM6;Ontology_term=SO:0000205;est_cons=100.0;est_incons=0.0

###

Supplementary Table 3.3 Amino acid substitutions in each *PavDAM* domain in each cultivar (Sup Fig 1). Unique amino acid substitutions are highlighted in bold.

	PavDAM1				***PavDAM2***				***PavDAM3***				***PavDAM4***				***PavDAM5***				***PavDAM6***				**Total**
	M	I	K	C	M	I	K	C	M	I	K	C	M	I	K	C	M	I	K	C	M	I	K	C	**(Unique)**
'Ambrunés'																				1					1
'Brooks'				1									1									1			3
'Cristobalina'		**3**		1	**1**		**1**			**1**	**1**			**2**		**2**	**1**	**1**		**1**					15 (14)
'Ferrovia'			**1**	1																				**1**	3 (2)
'Hedelfinger'				1									1	**1**											3
'Lambert'		**1**											1												2 (1)
'Napoleon'				1																					1
'Rainier'				1									1									1		**1**	4 (1)
'Regina'																									
'Sam'																									0
'Satonishiki'				1									1							**1**					3 (1)
'Sue'																									0
'Summit'																				1					1
'Vic'				1									1									1			3

Sup Table 3.4 Mean bloom time value (2015 to 2019) of B×C2 individuals in calendar days (CD) and growing degree hours (GDH), and *qP-CD1.1*^{m}*/qP-GDH1.2*^{m} (Chapter 3) and DPD genotypes of each individual. Rec= Recombinant.

Individual	**CD**	**GDH**	***qP-CD1.1*^{m}*/qP-GDH1.2*^{m}**	**PDF1/PDR1**
B×C2-01	84.28	8058	*cc*	*dd*
B×C2-04	85.23	8220	*cc*	*dd*
B×C2-05	92.14	9619	*ac*	*dp*
B×C2-06	80.27	7375	*cc*	*dd*
B×C2-08	91.24	9497	*ac*	*dp*
B×C2-09	87.67	8864	*ac*	*dp*
B×C2-11	89.91	9344	*ac*	*dp*
B×C2-12	-	-	*cc*	*dd*
B×C2-15	85.46	8327	*cc*	*dd*
B×C2-16	89.71	9130	*ac*	*dp*
B×C2-17	82.31	7823	*cc*	*dd*
B×C2-18	83.81	7956	*cc*	*dd*
B×C2-19	87.23	8782	*ac*	*dp*
B×C2-20	80.04	7302	*cc*	*dd*
B×C2-21	88.57	9038	*ac*	*dp*
B×C2-22	88.57	9038	*ac*	*dp*
B×C2-23	89.46	9243	*ac*	*dp*

Supplementary Table 3.4 Continued.

B×C2-25	90.35	9354	*ac*	*dp*
B×C2-26	-	-	*aa*	*pp*
B×C2-28	89.94	9210	*ac*	*dp*
B×C2-29	-	-	*Rec*	*dd*
B×C2-30	83.81	7982	*cc*	*dd*
B×C2-31	88.12	8986	*ac*	*dp*
B×C2-32	90.18	9253	*ac*	*dp*
B×C2-33	-	-	*aa*	*pp*
B×C2-34	-	-	*Rec*	*dp*
B×C2-35	85.23	8239	*cc*	*dd*
B×C2-36	-	-	*aa*	*pp*
B×C2-37	89.24	9046	*ac*	*dp*
B×C2-39	79.64	7231	*cc*	*dd*
B×C2-41	-	-	*Rec*	*dp*
B×C2-42	89.46	9243	*ac*	*dp*
B×C2-43	85.46	8290	*cc*	*dd*
B×C2-44	81.45	7485	*cc*	*dd*
B×C2-47	-	-	*Rec*	*dp*
B×C2-48	89.01	9160	*Rec*	*dp*
B×C2-49	80.74	7409	*cc*	*dd*
B×C2-50	82.31	7861	*cc*	*dd*
B×C2-51	89.94	9156	*ac*	*dp*
B×C2-53	85.61	8299	*cc*	*dd*
B×C2-54	92.58	9657	*ac*	*dp*
B×C2-55	93.48	9802	*ac*	*dp*
B×C2-56	-	-	*Rec*	*dp*
B×C2-57	-	-	*Rec*	*dp*
B×C2-59	-	-	*Rec*	*dp*
B×C2-60	-	-	*Rec*	*dp*
B×C2-61	82.4	7653	*cc*	*dd*
B×C2-62	84.05	7968	*cc*	*dd*
B×C2-63	81.22	7532	*cc*	*dd*
B×C2-64	-	-	*aa*	*pp*
B×C2-65	-	-	*Rec*	*dd*
B×C2-66	-	-	*Rec*	*dd*
B×C2-67	84.28	8080	*cc*	*dd*
B×C2-69	89.71	9136	*ac*	*dp*
B×C2-70	91.36	9462	*ac*	*dp*
B×C2-72	93.47	9818	*ac*	*dp*
B×C2-73	-	-	*Rec*	*dd*
B×C2-74	-	-	*Rec*	*dd*
B×C2-75	89.91	9296	*ac*	*dp*
B×C2-76	-	-	*Rec*	*dd*
B×C2-77	-	-	*Rec*	*dp*
B×C2-78	-	-	*Rec*	*dd*
B×C2-80	81.45	7574	*cc*	*dd*
B×C2-82	-	-	*Rec*	*dd*

Supplementary Figure 3.1 Amino acid alignment of deduced amino acid sequences of *PaDAM* genes of 13 sweet cherry cultivars. Discrepancies between sequences are highlight in yellow and marked with an asterisk. MADs-box domains are highlighted in colors (M: green; I: blue; K: pink and C; grey).

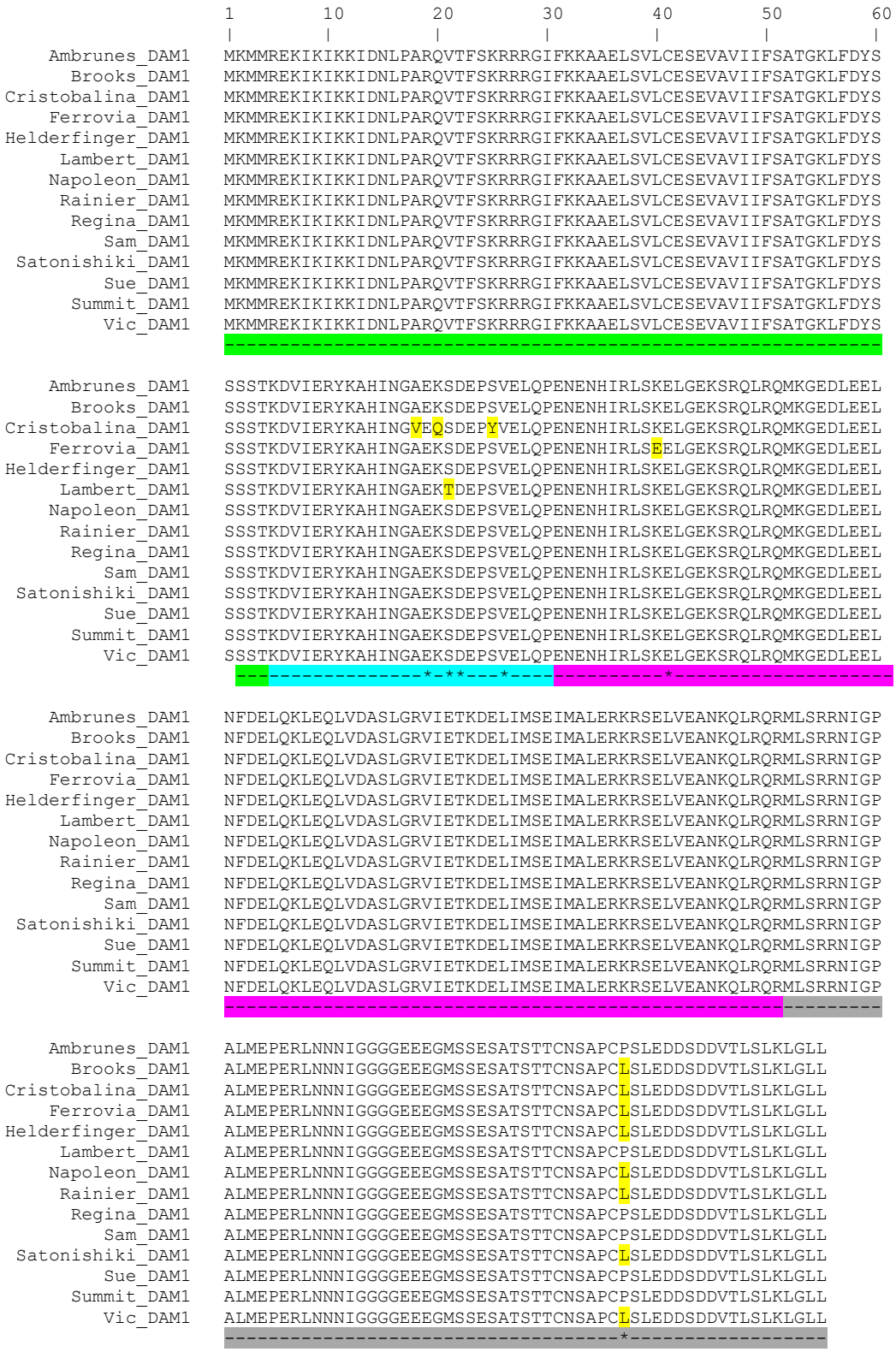

Supplementary Figure 3.1 Continued.

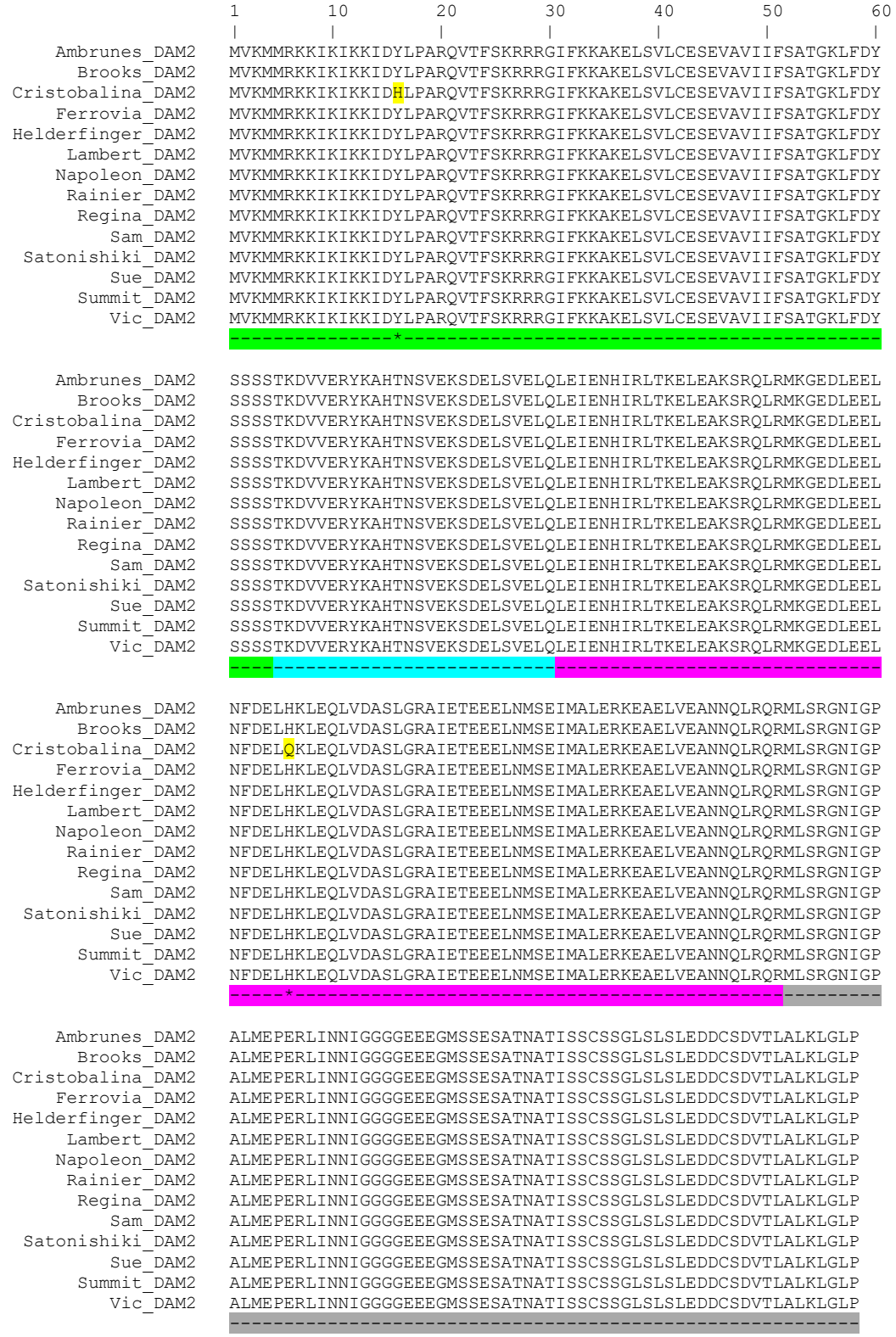

Supplementary Figure 3.1 Continued.

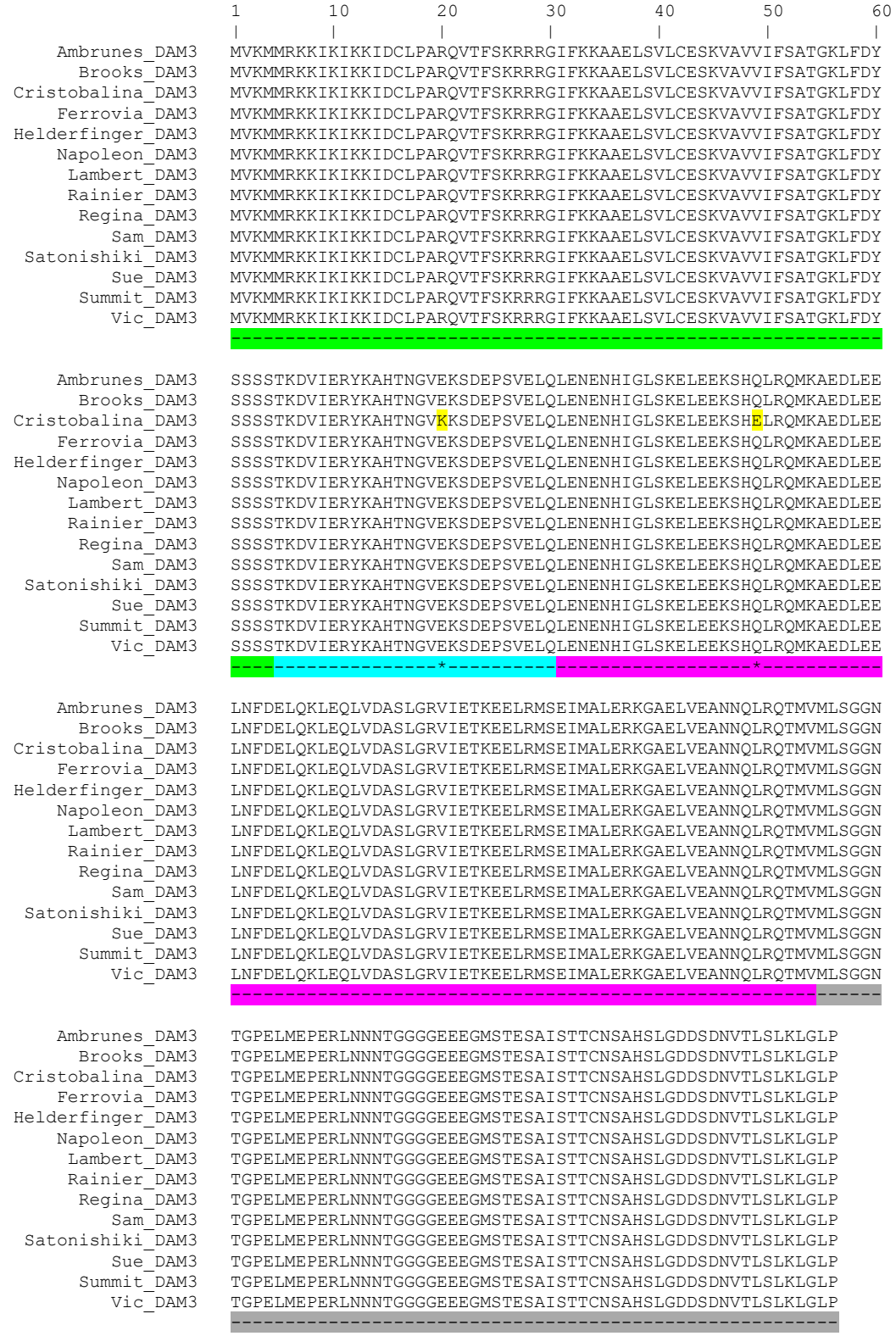

Supplementary Figure 3.1 Continued.

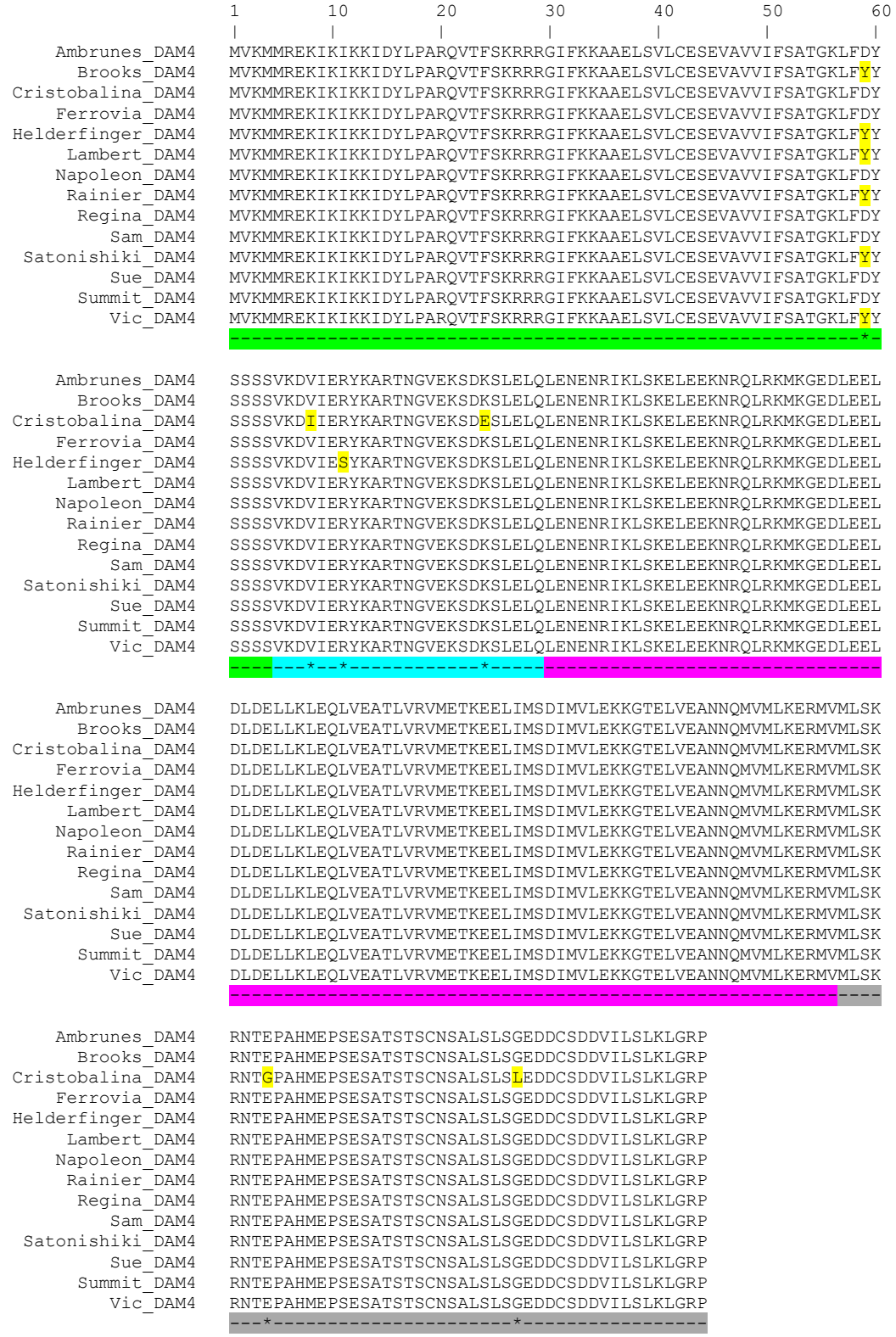

Supplementary Figure 3.1 Continued.

```
                     1         10        20        30        40        50        60
                     |         |         |         |         |         |         |
     Ambrunes_DAM5   MRNKIKIKKIDYLPARQVTFSKRRRGLFKKAAELSVLCESEVAVVIFSATGKLFDYSSSS
       Brooks_DAM5   MRNKIKIKKIDYLPARQVTFSKRRRGLFKKAAELSVLCESEVAVVIFSATGKLFDYSSSS
  Cristobalina_DAM5   MRNKIKIKKIDYLPARQVTFSKRRRGLFKKAAELSVLCESEVAVVIFSATGKLFEYSSSS
      Ferrovia_DAM5   MRNKIKIKKIDYLPARQVTFSKRRRGLFKKAAELSVLCESEVAVVIFSATGKLFDYSSSS
  Helderfinger_DAM5   MRNKIKIKKIDYLPARQVTFSKRRRGLFKKAAELSVLCESEVAVVIFSATGKLFDYSSSS
       Lambert_DAM5   MRNKIKIKKIDYLPARQVTFSKRRRGLFKKAAELSVLCESEVAVVIFSATGKLFDYSSSS
      Napoleon_DAM5   MRNKIKIKKIDYLPARQVTFSKRRRGLFKKAAELSVLCESEVAVVIFSATGKLFDYSSSS
       Rainier_DAM5   MRNKIKIKKIDYLPARQVTFSKRRRGLFKKAAELSVLCESEVAVVIFSATGKLFDYSSSS
        Regina_DAM5   MRNKIKIKKIDYLPARQVTFSKRRRGLFKKAAELSVLCESEVAVVIFSATGKLFDYSSSS
           Sam_DAM5   MRNKIKIKKIDYLPARQVTFSKRRRGLFKKAAELSVLCESEVAVVIFSATGKLFDYSSSS
    Satonishiki_DAM5   MRNKIKIKKIDYLPARQVTFSKRRRGLFKKAAELSVLCESEVAVVIFSATGKLFDYSSSS
           Sue_DAM5   MRNKIKIKKIDYLPARQVTFSKRRRGLFKKAAELSVLCESEVAVVIFSATGKLFDYSSSS
        Summit_DAM5   MRNKIKIKKIDYLPARQVTFSKRRRGLFKKAAELSVLCESEVAVVIFSATGKLFDYSSSS
           Vic_DAM5   MRNKIKIKKIDYLPARQVTFSKRRRGLFKKAAELSVLCESEVAVVIFSATGKLFDYSSSS
                     ------------------------------------------------------*-----

     Ambrunes_DAM5   TKDVIEKYNVHMNGVEKLNDQEIELQLEHENHIKLSKELEEKSRQLRQMKGDDLEGLNLD
       Brooks_DAM5   TKDVIEKYNVHMNGVEKLNDQEIELQLEHENHIKLSKELEEKSRQLRQMKGDDLEGLNLD
  Cristobalina_DAM5   TKDVIEKYNVRMNGVEKLNDQEIELQLEHENHIKLSKELEEKSRQLRQMKGDDLEGLNLD
      Ferrovia_DAM5   TKDVIEKYNVHMNGVEKLNDQEIELQLEHENHIKLSKELEEKSRQLRQMKGDDLEGLNLD
  Helderfinger_DAM5   TKDVIEKYNVHMNGVEKLNDQEIELQLEHENHIKLSKELEEKSRQLRQMKGDDLEGLNLD
       Lambert_DAM5   TKDVIEKYNVHMNGVEKLNDQEIELQLEHENHIKLSKELEEKSRQLRQMKGDDLEGLNLD
      Napoleon_DAM5   TKDVIEKYNVHMNGVEKLNDQEIELQLEHENHIKLSKELEEKSRQLRQMKGDDLEGLNLD
       Rainier_DAM5   TKDVIEKYNVHMNGVEKLNDQEIELQLEHENHIKLSKELEEKSRQLRQMKGDDLEGLNLD
        Regina_DAM5   TKDVIEKYNVHMNGVEKLNDQEIELQLEHENHIKLSKELEEKSRQLRQMKGDDLEGLNLD
           Sam_DAM5   TKDVIEKYNVHMNGVEKLNDQEIELQLEHENHIKLSKELEEKSRQLRQMKGDDLEGLNLD
    Satonishiki_DAM5   TKDVIEKYNVHMNGVEKLNDQEIELQLEHENHIKLSKELEEKSRQLRQMKGDDLEGLNLD
           Sue_DAM5   TKDVIEKYNVHMNGVEKLNDQEIELQLEHENHIKLSKELEEKSRQLRQMKGDDLEGLNLD
        Summit_DAM5   TKDVIEKYNVHMNGVEKLNDQEIELQLEHENHIKLSKELEEKSRQLRQMKGDDLEGLNLD
           Vic_DAM5   TKDVIEKYNVHMNGVEKLNDQEIELQLEHENHIKLSKELEEKSRQLRQMKGDDLEGLNLD
                     ----------*-------------------------------------------------

     Ambrunes_DAM5   ELLKLEQLVEASLGRVMETKEELIKSEIMALERKGAELVEANNQLRQTMVMLSAGNTGPA
       Brooks_DAM5   ELLKLEQLVEASLGRVMETKEELIKSEIMALERKGAELVEANNQLRQTMVMLSAGNTGPA
  Cristobalina_DAM5   ELLKLEQLVEASLGRVMETKEELIKSEIMALERKGAELVEANNQLRQTMVMLSAGNTGPA
      Ferrovia_DAM5   ELLKLEQLVEASLGRVMETKEELIKSEIMALERKGAELVEANNQLRQTMVMLSAGNTGPA
  Helderfinger_DAM5   ELLKLEQLVEASLGRVMETKEELIKSEIMALERKGAELVEANNQLRQTMVMLSAGNTGPA
       Lambert_DAM5   ELLKLEQLVEASLGRVMETKEELIKSEIMALERKGAELVEANNQLRQTMVMLSAGNTGPA
      Napoleon_DAM5   ELLKLEQLVEASLGRVMETKEELIKSEIMALERKGAELVEANNQLRQTMVMLSAGNTGPA
       Rainier_DAM5   ELLKLEQLVEASLGRVMETKEELIKSEIMALERKGAELVEANNQLRQTMVMLSAGNTGPA
        Regina_DAM5   ELLKLEQLVEASLGRVMETKEELIKSEIMALERKGAELVEANNQLRQTMVMLSAGNTGPA
           Sam_DAM5   ELLKLEQLVEASLGRVMETKEELIKSEIMALERKGAELVEANNQLRQTMVMLSAGNTGPA
    Satonishiki_DAM5   ELLKLEQLVEASLGRVMETKEELIKSEIMALERKGAELVEANNQLRQTMVMLSAGNTGPA
           Sue_DAM5   ELLKLEQLVEASLGRVMETKEELIKSEIMALERKGAELVEANNQLRQTMVMLSAGNTGPA
        Summit_DAM5   ELLKLEQLVEASLGRVMETKEELIKSEIMALERKGAELVEANNQLRQTMVMLSAGNTGPA
           Vic_DAM5   ELLKLEQLVEASLGRVMETKEELIKSEIMALERKGAELVEANNQLRQTMVMLSAGNTGPA
                     ------------------------------------------------------------

     Ambrunes_DAM5   LMDPERLNNNIEGGGEEEGMSAESAISTTCNSAVSLSLENDSSDEVTLSLKLGRLQLRNP
       Brooks_DAM5   LMDPERLNNNIEGGGEEEGMSAESAISTTCNSAVSLSLEDDSSDEVTLSLKLGRLQLRNP
  Cristobalina_DAM5   HMDPERLNNNIEGGGEEEGMSAESAISTTCNSAVSLSLEDDSSDEVTLSLKLGRLQLRNP
      Ferrovia_DAM5   LMDPERLNNNIEGGGEEEGMSAESAISTTCNSAVSLSLEDDSSDEVTLSLKLGRLQLRNP
  Helderfinger_DAM5   LMDPERLNNNIEGGGEEEGMSAESAISTTCNSAVSLSLEDDSSDEVTLSLKLGRLQLRNP
       Lambert_DAM5   LMDPERLNNNIEGGGEEEGMSAESAISTTCNSAVSLSLEDDSSDEVTLSLKLGRLQLRNP
      Napoleon_DAM5   LMDPERLNNNIEGGGEEEGMSAESAISTTCNSAVSLSLENDSSDEVTLSLKLGRLQLRNP
       Rainier_DAM5   LMDPERLNNNIEGGGEEEGMSAESAISTTCNSAVSLSLEDDSSDEVTLSLKLGRLQLRNP
        Regina_DAM5   LMDPERLNNNIEGGGEEEGMSAESAISTTCNSAVSLSLEDDSSDEVTLSLKLGRLQLRNP
           Sam_DAM5   LMDPERLNNNIEGGGEEEGMSAESAISTTCNSAVSLSLEDDSSDEVTLSLKLGRLQLRNP
    Satonishiki_DAM5   LMDPERLNNNIEGGGEEEGMSAESAISTTCNSAVSLSLEDDSSDEVTLSLKLGRLQLRDP
           Sue_DAM5   LMDPERLNNNIEGGGEEEGMSAESAISTTCNSAVSLSLEDDSSDEVTLSLKLGRLQLRNP
        Summit_DAM5   LMDPERLNNNIEGGGEEEGMSAESAISTTCNSAVSLSLENDSSDEVTLSLKLGRLQLRNP
           Vic_DAM5   LMDPERLNNNIEGGGEEEGMSAESAISTTCNSAVSLSLEDDSSDEVTLSLKLGRLQLRNP
                     *--------------------------------------*------------------*-
```

Supplementary Figure 3.1 Continued.

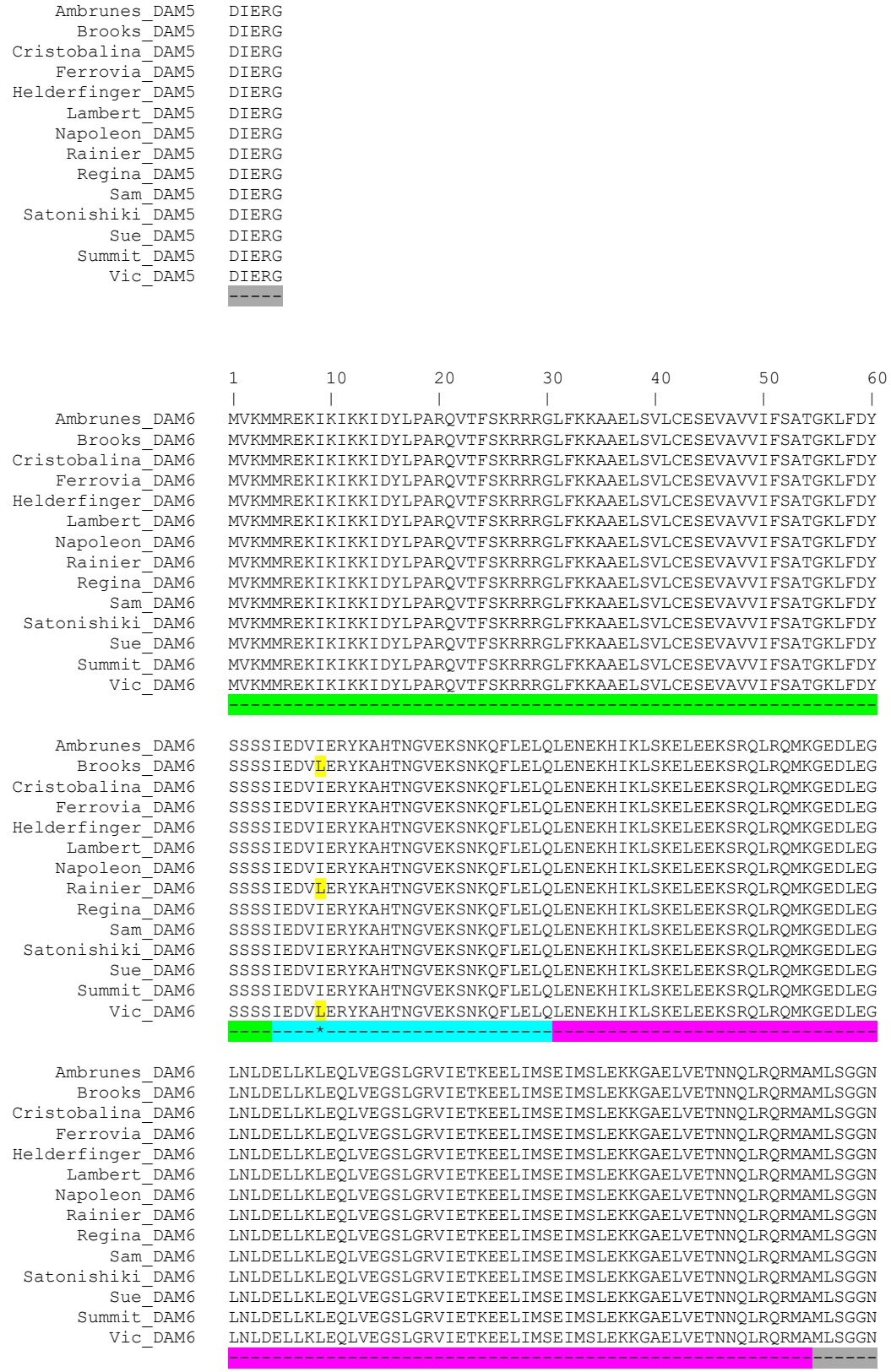

Supplementary Figure 3.1 Continued.

```
     Ambrunes_DAM6   TGPALVEPETLNTNIGGGGEDGMSSESATMATSTSCNSALSLSLEDDCSDVTLSLKLGLP
       Brooks_DAM6   TGPALVEPETLNTNIGGGGEDGMSSESATMATSTSCNSALSLSLEDDCSDVTLSLKLGLP
 Cristobalina_DAM6   TGPALVEPETLNTNIGGGGEDGMSSESATMATSTSCNSALSLSLEDDCSDVTLSLKLGLP
     Ferrovia_DAM6   TGPALVEPETLNTNIGGGGEDGMSSESATMATSTSCNSALSLSLEDDCTDVTLSLKLGLP
 Helderfinger_DAM6   TGPALVEPETLNTNIGGGGEDGMSSESATMATSTSCNSALSLSLEDDCSDVTLSLKLGLP
      Lambert_DAM6   TGPALVEPETLNTNIGGGGEDGMSSESATMATSTSCNSALSLSLEDDCSDVTLSLKLGLP
     Napoleon_DAM6   TGPALVEPETLNTNIGGGGEDGMSSESATMATSTSCNSALSLSLEDDCSDVTLSLKLGLP
      Rainier_DAM6   TGPALVEPGTLNTNIGGGGEDGMSSESATMATSTSCNSALSLSLEDDCSDVTLSLKLGLP
       Regina_DAM6   TGPALVEPETLNTNIGGGGEDGMSSESATMATSTSCNSALSLSLEDDCSDVTLSLKLGLP
          Sam_DAM6   TGPALVEPETLNTNIGGGGEDGMSSESATMATSTSCNSALSLSLEDDCSDVTLSLKLGLP
  Satonishiki_DAM6   TGPALVEPETLNTNIGGGGEDGMSSESATMATSTSCNSALSLSLEDDCSDVTLSLKLGLP
          Sue_DAM6   TGPALVEPETLNTNIGGGGEDGMSSESATMATSTSCNSALSLSLEDDCSDVTLSLKLGLP
       Summit_DAM6   TGPALVEPETLNTNIGGGGEDGMSSESATMATSTSCNSALSLSLEDDCSDVTLSLKLGLP
          Vic_DAM6   TGPALVEPETLNTNIGGGGEDGMSSESATMATSTSCNSALSLSLEDDCSDVTLSLKLGLP
                     --------*-----------------------------------------*-----------
```

Supplementary Figure 3.2 Alignment of 'Cristobalina' PCR products sequences generated from Sanger sequencing with DPDF and DPDR primers. SNPs differentiating two alleles are marked in yellow.

```
                 1         10        20        30        40        50        60
                 |         |         |         |         |         |         |
CristobalinaDPDF ----------------------------------------------TCTTTCTTTCTCTTGG
CristobalinaDPDF ------------------------CTCGTTTCTCTTTC-ATACTCTTTCTTTCTCTTGG
CristobalinaDPDF ---------------------------CGTTTCTCTTTC-ATACTCTTTCTTTCTCTTGG
CristobalinaDPDR ----------ATGGATTCCAATCTCTCGTTTCTCTTTCAATACTCTTTCTTTCTCTTGG
CristobalinaDPDR ------------------------------------------------------------
CristobalinaDPDR TTTTTCTTTTTATGGATTCCAATCTCTCGTTTCTCTTTCAATACTCTTTCTTTCTCTTGG
       Consensus TTTTTCTTTTTATGGATTCCAATCTCTCGTTTCTCTTTCNATACTCTTTCTTTCTCTTGG

CristobalinaDPDF TTGACCAAAAAAAAAACCTCTTTGATGAATTGTTTGTTCCTCAAAGAATATCACAACAAC
CristobalinaDPDF TTGACCAAAAAAAAAACCTCTTTGATGAATTGTTTGTTCCTCAAAGAATATCACAACAAC
CristobalinaDPDF TTGACCAAAAAAAAAACCTCTTTGATGAATTGTTTGTTCCTCAAAGAATATCACAACAAC
CristobalinaDPDR TTGACCAAAAAAAAAACCTCTTTGATGAATTGTTTGTTCCTCAGAGAATATCACAACAAC
CristobalinaDPDR ------AAAAAAAAAACCTCTTTGATGAATTGTTTGTTCCTCAGAGAATATCACAACAAC
CristobalinaDPDR TTGACCAAAAAAAAAACCTCTTTGATGAATTGTTTGTTCCTCAGAGAATATCACAACAAC
       Consensus TTGACCAAAAAAAAAACCTCTTTGATGAATTGTTTGTTCCTCARAGAATATCACAACAAC

CristobalinaDPDF AATAGCAAAACAATGCATGGTAAAAGTGATAAACTACATAGACCAAAAATGATAAAATAG
CristobalinaDPDF AATAGCAAAACAATGCATGGTAAAAGTGATAAACTACATAGACCAAAAATGATAAAATAG
CristobalinaDPDF AATAGCAAAACAATGCATGGTAAAAGTGATAAACTACATAGACCAAAAATGATAAAATAG
CristobalinaDPDR AATAGCAAAACAATGCATGGTAAAAGTGATAAACTACATAGACCAAAAATGATAAAATAG
CristobalinaDPDR AATAGCAAAACAATGCATGGTAAAAGTGATAAACTACATAGACCAAAAATGATAAAATAG
CristobalinaDPDR AATAGCAAAACAATGCATGGTAAAAGTGATAAACTACATAGACCAAAAATGATAAAATAG
       Consensus AATAGCAAAACAATGCATGGTAAAAGTGATAAACTACATAGACCAAAAATGATAAAATAG

CristobalinaDPDF GCACGTGAGAATTGAACCCGGCGTGGACTGTGGGAGCAACAGAAGAAGTGTCGCATGGTG
CristobalinaDPDF GCACGTGAGAATTGAACCCGGCGTGGACTGTGGGAGCAACAGAAGAAGTGTCGCATGGTG
CristobalinaDPDF GCACGTGAGAATTGAACCCGGCGTGGACTGTGGGAGCAACAGAAGAAGTGTCGCATGGTG
CristobalinaDPDR GCACGTGAGAATTGAACCCGGCGTGGACTGTGGGAGCAACAGAAGAAGTGTCGCATGGTG
CristobalinaDPDR GCACGTGAGAATTGAACCCGGCGTGGACTGTGGGAGCAACAGAAGAAGTGTCGCATGGTG
CristobalinaDPDR GCACGTGAGAATTGAACCCGGCGTGGACTGTGGGAGCAACAGAAGAAGTGTCGCATGGTG
       Consensus GCACGTGAGAATTGAACCCGGCGTGGACTGTGGGAGCAACAGAAGAAGTGTCGCATGGTG

CristobalinaDPDF AGTTCAATCAAGTGAGACGACAGCGCATCACCAGTATCAAGGACCATCCTCCTCCACATA
CristobalinaDPDF AGTTCAATCAAGTGAGACGACAGCGCATCACCAGTATCAAGGACCATCCTCCTCCACATA
CristobalinaDPDF AGTTCAATCAAGTGAGACGACAGCGCATCACCAGTATCAAGGACCATCCTCCTCCACATA
CristobalinaDPDR AGTTCAATCAAGTGAGACGACAGCGCATCACCAGTATCAAGGACCATCCTCCTCCACATA
CristobalinaDPDR AGTTCAATCAAGTGAGACGACAGCGCATCACCAGTATCAAGGACCATCCTCCTCCACATA
CristobalinaDPDR AGTTCAATCAAGTGAGACGACAGCGCATCACCAGTATCAAGGACCATCCTCCTCCACATA
       Consensus AGTTCAATCAAGTGAGACGACAGCGCATCACCAGTATCAAGGACCATCCTCCTCCACATA

CristobalinaDPDF AAAGCACAAATTTTATTTATTTATTTTTTATAAAGATATTAAACTTAGATATGGACAAAA
CristobalinaDPDF AAAGCACAAATTTTATTTATTTATTTTTTATAAAGATATTAAACTTAGATATGGACAAAA
CristobalinaDPDF AAAGCACAAATTTTATTTATTTATTTTTTATAAAGATATTAAACTTAGATATGGACAAAA
CristobalinaDPDR AAAGCACAAATTTTATTTATTTATTTTTTATAAAGATATTAAACTTAGATATGGACAAAA
CristobalinaDPDR AAAGCACAAATTTTATTTATTTATTTTTTATAAAGATATTAAACTTAGATATGGACAAAA
CristobalinaDPDR AAAGCACAAATTTTATTTATTTATTTTTTATAAAGATATTAAACTTAGATATGGACAAAA
       Consensus AAAGCACAAATTTTATTTATTTATTTTTTATAAAGATATTAAACTTAGATATGGACAAAA

CristobalinaDPDF CCATTCACAAAAGTAAGATGCCACATTTTCTACTGTCACGTTACAAAATCAACGGTGGAG
CristobalinaDPDF CCATTCACAAAAGTAAGATGCCACATTTTCTACTGTCACGTTACAAAATCAACGGTGGAG
CristobalinaDPDF CCATTCACAAAAGTAAGATGCCACATTTTCTACTGTCACGTTACAAAATCAACGGTGGAG
CristobalinaDPDR CCATTCACAAAAGTAAGATGCCACATTTTCTACTGTCACGTTACAAAATCAACGGTGGAG
CristobalinaDPDR CCATTCACAAAAGTAAGATGCCACATTTTCTACTGTCACGTTACAAAATCAACGGTGGAG
CristobalinaDPDR CCATTCACAAAAGTAAGATGCCACATTTTCTACTGTCACGTTACAAAATCAACGGTGGAG
       Consensus CCATTCACAAAAGTAAGATGCCACATTTTCTACTGTCACGTTACAAAATCAACGGTGGAG
```

Supplementary Figure 3.2 Continued.

```
CristobalinaDPDF   ATCAAATTAATCGAAAAATAGATTTTTTTTTCTTCCATAAAATGGAAAATTGCCTTTGAA
CristobalinaDPDF   ATCAAATTAATCGAAAAATAGATTTTTTTTTCTTCCATAAAATGGAAAATTGCCTTTGAA
CristobalinaDPDF   ATCAAATTAATCGAAAAATAGATTTTTTTTTCTTCCATAAAATGGAAAATTGCCTTTGAA
CristobalinaDPDR   ATCAAATTAATCGAAAAATAGATTTTTTTTTCTTCCATAAAATGGAAAATTGCCTTTGAA
CristobalinaDPDR   ATCAAATTAATCGAAAAATAGATTTTTTTTTCTTCCATAAAATGGAAAATTGCCTTTGAA
CristobalinaDPDR   ATCAAATTAATCGAAAAATAGATTTTTTTTTCTTCCATAAAATGGAAAATTGCCTTTGAA
       Consensus   ATCAAATTAATCGAAAAATAGATTTTTTTTTCTTCCATAAAATGGAAAATTGCCTTTGAA

CristobalinaDPDF   ATCTTCCCTTTCTCGAACAGCTAGCCAGCAGCAGCAGCAGCCAACTCTCCCTCTCTCTCA
CristobalinaDPDF   ATCTTCCCTTTCTCGAACAGCTAGCCAGCAGCAGCAGCAGCCAACTCTCCCTCTCTCTCA
CristobalinaDPDF   ATCTTCCCTTTCTCGAACAGCTAGCCAGCAGCAGCAGCAGCCAACTCTCCCTCTCTCTCA
CristobalinaDPDR   ATCTTCCCTTTCTCGAACAGCTAGCCAGCAGCAGCAGCAGCCAACTCTCCCTCTCTCTCA
CristobalinaDPDR   ATCTTCCCTTTCTCGAACAGCTAGCCAGCAGCAGCAGCAGCCAACTCTCCCTCTCTCTCA
CristobalinaDPDR   ATCTTCCCTTTCTCGAACAGCTAGCCAGCAGCAGCAGCAGCCAACTCTCCCTCTCTCTCA
       Consensus   ATCTTCCCTTTCTCGAACAGCTAGCCAGCAGCAGCAGCAGCCAACTCTCCCTCTCTCTCA

CristobalinaDPDF   TTCTCTTAGGCTTCAAACCCTGAAACCCGACAAAGGTAAACATTAAACAAAGAGAGGAAA
CristobalinaDPDF   TTCTCTTAGGCTTCAAACCCTGAAACCCGACAAAGGTAAACATTAAACAAAGAGAGGAAA
CristobalinaDPDF   TTCTCTTAGGCTTCAAACCCTGAAACCCGACAAAGGTAAACATTAAACAAAGAGAGGAAA
CristobalinaDPDR   TTCTCTTAGGCTTCAGACCCTGAAACCCGACAAAGGTAAACATTAAACAAAGAGAGGAAA
CristobalinaDPDR   TTCTCTTAGGCTTCAGACCCTGAAACCCGACAAAGGTAAACATTAAACAAAGAGAGGAAA
CristobalinaDPDR   TTCTCTTAGGCTTCAGACCCTGAAACCCGACAAAGGTAAACATTAAACAAAGAGAGGAAA
       Consensus   TTCTCTTAGGCTTCARACCCTGAAACCCGACAAAGGTAAACATTAAACAAAGAGAGGAAA

CristobalinaDPDF   CCCAAAATTTAATTAGTTGATTAATTAATGGTTTTCCCTCTTTCTCTTCTTCTTCTTTGT
CristobalinaDPDF   CCCAAAATTTAATTAGTTGATTAATTAATGGTTTTCCCTCTTTCTCTTCTTCTTCTTTGT
CristobalinaDPDF   CCCAAAATTTAATTAGTTGATTAATTAATGGTTTTCCCTCTTTCTCTTCTTCTTCTTTGT
CristobalinaDPDR   CCCAGAATTTAATTAGTTGATTAATTAATGGTTTTCCCTCTTTCTCTTCTTCTTCTTTGT
CristobalinaDPDR   CCCAGAATTTAATTAGTTGATTAATTAATGGTTTTCCCTCTTTCTCTTCTTCTTCTTTGT
CristobalinaDPDR   CCCAGAATTTAATTAGTTGATTAATTAATGGTTTTCCCTCTTTCTCTTCTTCTTCTTTGT
       Consensus   CCCARAATTTAATTAGTTGATTAATTAATGGTTTTCCCTCTTTCTCTTCTTCTTCTTTGT

CristobalinaDPDF   GCTCTGGTACTCTCTAGGCATGTTGTTGTGAACTTGTGACCTATTTTGGTTGGTGGGTTT
CristobalinaDPDF   GCTCTGGTACTCTCTAGGCATGTTGTTGTGAACTTGTGACCTATTTTGGTTGGTGGGTTT
CristobalinaDPDF   GCTCTGGTACTCTCTAGGCATGTTGTTGTGAACTTGTGACCTATTTTGGTTGGTGGGTTT
CristobalinaDPDR   GCTCTGGTACTCTCTAGGCATGTTGTTGTGAACTTGTGACCTATTTTGGTTGGTGGGTTT
CristobalinaDPDR   GCTCTGGTACTCTCTAGGCATGTTGTTGTGAACTTGTGACCTATTTTGGTTGGTGGGTTT
CristobalinaDPDR   GCTCTGGTACTCTCTAGGCATGTTGTTGTGAACTTGTGACCTATTTTGGTTGGTGGGTTT
       Consensus   GCTCTGGTACTCTCTAGGCATGTTGTTGTGAACTTGTGACCTATTTTGGTTGGTGGGTTT

CristobalinaDPDF   TTCTGGGTTTTATTCACTTAGATCTGGGGGCCATTAAATCTTTAAAATTTACAAGAAACC
CristobalinaDPDF   TTCTGGGTTTTATTCACTTAGATCTGGGGGCCATTAAATCTTTAAAATTTACAAGAAACC
CristobalinaDPDF   TTCTGGGTTTTATTCACTTAGATCTGGGGGCCATTAAATCTTTAAAATTTACAAGAAACC
CristobalinaDPDR   TTCTGGGTTTTATTCACTTAGATCTGGGGGCCATTAAATCTTTAAAATTTACAAGAAACC
CristobalinaDPDR   TTCTGGGTTTTATTCACTTAGATCTGGGGGCCATTAAATCTTTAAAATTTACAAGAAACC
CristobalinaDPDR   TTCTGGGTTTTATTCACTTAGATCTGGGGGCCATTAAATCTTTAAAATTTACAAGAAACC
       Consensus   TTCTGGGTTTTATTCACTTAGATCTGGGGGCCATTAAATCTTTAAAATTTACAAGAAACC

CristobalinaDPDF   CAGAAAATCATTTGTAGTTTTTGAGTGTATGAACATAATATATGTGAAAAGTGGTTGGTT
CristobalinaDPDF   CAGAAAATCATTTGTAGTTTTTGAGTGTATGAACATAATATATGTGAAAAGTGGTTGGTT
CristobalinaDPDF   CAGAAAATCATTTGTAGTTTTTGAGTGTATGAACATAATATATGTGAAAAGTGGTTGGTT
CristobalinaDPDR   CAGAAAATCATTTGTAGTTTTTGAGTGTATGAACATAATATA------------------
CristobalinaDPDR   CAGAAAATCATTTGTAGTTTTTGAGTGTATGAACATAATATATGTGAAAAGTGGTTGGTT
CristobalinaDPDR   CAGAAAATCATTTGTAGTTTTTGAGTGTATGAACATAATATATGTGAAAAGTGGTTGGTT
       Consensus   CAGAAAATCATTTGTAGTTTTTGAGTGTATGAACATAATATATGTGAAAAGTGGTTGGTT

CristobalinaDPDF   TGAATTTTTTTGAAGGGGACGATGAAAATGATGAGGGA-----------
CristobalinaDPDF   TGAATTTTTTTGAAGGGGACGATGAAAATGA------------------
CristobalinaDPDF   TGAATTTTTTTGAAGGGGACGATGAAAATGATGAGGGAGAAGATCAGAT
CristobalinaDPDR   --------------------------------------------------
CristobalinaDPDR   TGAA----------------------------------------------
CristobalinaDPDR   TGAATTT-------------------------------------------
       Consensus   TGAATTTTTTTGAAGGGGACGATGAAAATGATGAGGGAGAAGATCAGAT
```

Supplementary Figure 3.3 Alignment of 'Regina' PCR products sequences generated from Sanger sequencing with DPDF and DPDR primers.

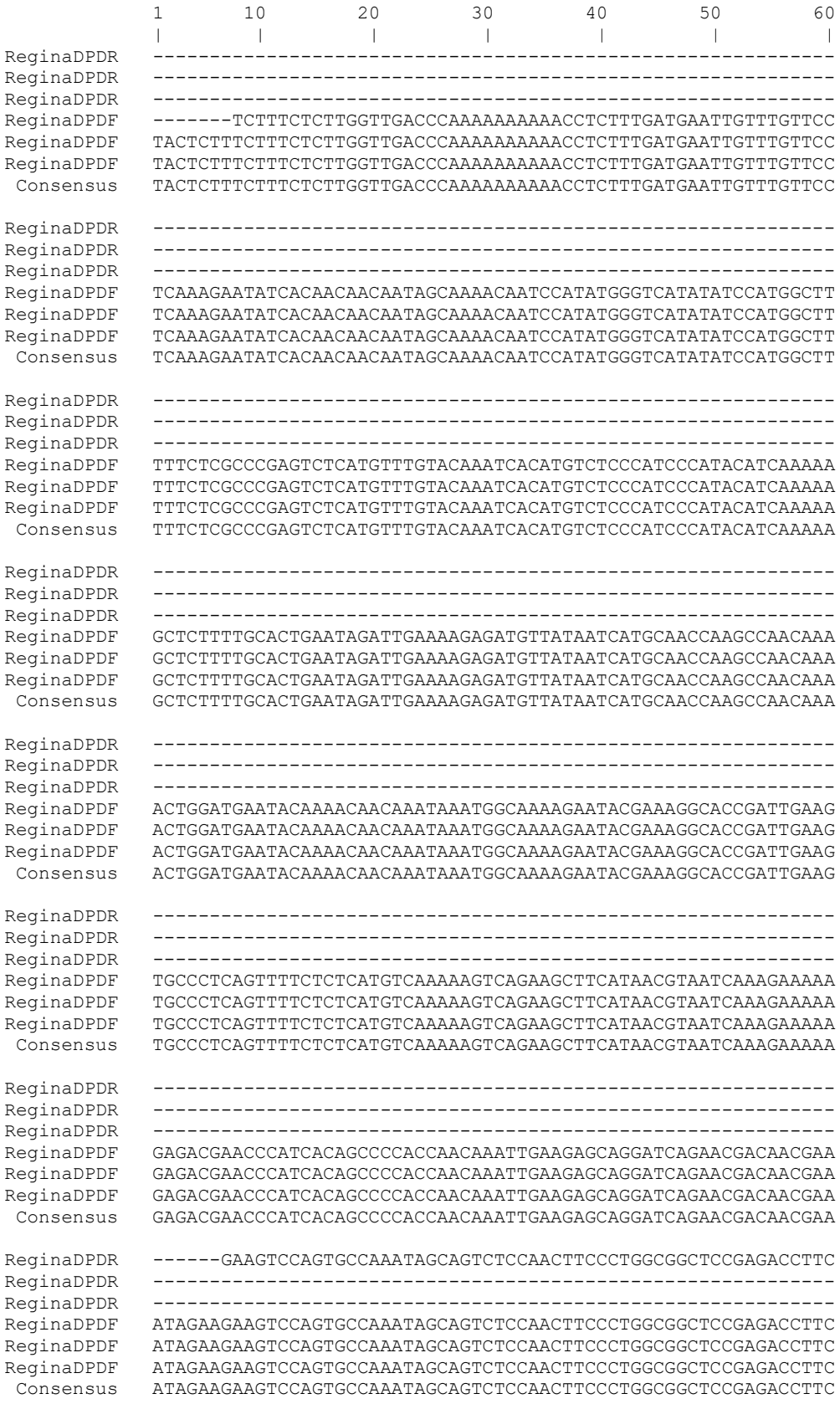

Supplementary Figure 3.3 Continued.

```
ReginaDPDR   GAATAGCAGCCAAGTTCATCAAGATCTAGGTGGTGGAGTTTACTGGGTTGGGGAGATTGG
ReginaDPDR   ------------------------------------------------------------
ReginaDPDR   ------------------------------------------------------------
ReginaDPDF   GAATAGCAGCCAAGTTCATCAAGATCTAGGTGGTGGAGTTTACTGGGTTGGGGAGATTGG
ReginaDPDF   GAATAGCAGCCAAGTTCATCAAGATCTAGGTGGTGGAGTTTACTGGGTTGGGGAGATTGG
ReginaDPDF   GAATAGCAGCCAAGTTCATCAAGATCTAGGTGGTGGAGTTTACTGGGTTGGGGAGATTGG
 Consensus   GAATAGCAGCCAAGTTCATCAAGATCTAGGTGGTGGAGTTTACTGGGTTGGGGAGATTGG

ReginaDPDR   GGTGTGTGTGGTGGTTGGCGGGTGGGCTGGTGAGGGTGGGTTTGGCTGATGGCTTCTCTT
ReginaDPDR   ----------------------------------GGTGGGTTTGGCTGATGGCTTCTCTT
ReginaDPDR   ----------------------------------GTGGGTTTGGCTGATGGCTTCTCTT
ReginaDPDF   GGTGTGTGTGGTGGTTGGCGGGTGGGCTGGTGAGGGTGGGTTTGGCTGATGGCTTCTCTT
ReginaDPDF   GGTGTGTGTGGTGGTTGGCGGGTGGGCTGGTGAGGGTGGGTTTGGCTGATGGCTTCTCTT
ReginaDPDF   GGTGTGTGTGGTGGTTGGCGGGTGGGCTGGTGAGGGTGGGTTTGGC--------------
 Consensus   GGTGTGTGTGGTGGTTGGCGGGTGGGCTGGTGAGGGTGGGTTTGGCTGATGGCTTCTCTT

ReginaDPDR   CCCCTTATATTTTTCTTCTTTTTAGAAAAGAAAAAATCTTTCTTGTTCTTAGATTTAAAT
ReginaDPDR   CCCCTTATATTTTTCTTCTTTTTAGAAAAGAAAAAATCTTTCTTGTTCTTAGATTTAAAT
ReginaDPDR   CCCCTTATATTTTTCTTCTTTTTAGAAAAGAAAAAATCTTTCTTGTTCTTAGATTTAAAT
ReginaDPDF   CCCCTTATATTTTTCTTCTTTTTAGAAAAAAAAAAATCTTTCTTGTTCTTAGATTTAAAT
ReginaDPDF   CCCCTTATATTTTTCTTCTTTTTAGAAAAAAAAAAATCTTTCTTGTTCTTAGATTTAAAT
ReginaDPDF   ------------------------------------------------------------
 Consensus   CCCCTTATATTTTTCTTCTTTTTAGAAAARAAAAAATCTTTCTTGTTCTTAGATTTAAAT

ReginaDPDR   GCCCCTCAACAAGTAACCTCAGTTTAATCTAATTTGATCTAATTTGACAGAAATTGGAGA
ReginaDPDR   GCCCCTCAACAAGTAACCTCAGTTTAATCTAATTTGATCTAATTTGACAGAAATTGGAGA
ReginaDPDR   GCCCCTCAACAAGTAACCTCAGTTTAATCTAATTTGATCTAATTTGACAGAAATTGGAGA
ReginaDPDF   GCCCCTCAACAAGTAACCTCAGTTTAATCTAATTTGATCTAATTTGACAGAAATTGGAGA
ReginaDPDF   GCCCCTCAACAAGTAACCTCAGTTTAATCTAATTTGATCTAATTTGACAGAAATTGGAGA
ReginaDPDF   ------------------------------------------------------------
 Consensus   GCCCCTCAACAAGTAACCTCAGTTTAATCTAATTTGATCTAATTTGACAGAAATTGGAGA

ReginaDPDR   TTGAACTTGAATTGCTTAAATTGAAAATCACAAAGGTAAAAATAATTAAATTGAAAACAC
ReginaDPDR   TTGAACTTGAATTGCTTAAATTGAAAATCACAAAGGTAAAAATAATTAAATTGAAAACAC
ReginaDPDR   TTGAACTTGAATTGCTTAAATTGAAAATCACAAAGGTAAAAATAATTAAATTGAAAACAC
ReginaDPDF   TTGAACTTGAATTGCTTAAATTGAAAATCACAAAGGTAAAAATAATTAAATTGAAAACAC
ReginaDPDF   TTGAACTTGAATTGCTTAAATTGAAAATCACAAAGGTAAAAATAATTAAATTGAAAACAC
ReginaDPDF   ------------------------------------------------------------
 Consensus   TTGAACTTGAATTGCTTAAATTGAAAATCACAAAGGTAAAAATAATTAAATTGAAAACAC

ReginaDPDR   AGAAATTTTAATGGTAAAAGTGATAAACCACATAGACCAAAAATGATAAAATAGGCACGT
ReginaDPDR   AGAAATTTTAATGGTAAAAGTGATAAACCACATAGACCAAAAATGATAAAATAGGCACGT
ReginaDPDR   AGAAATTTTAATGGTAAAAGTGATAAACCACATAGACCAAAAATGATAAAATAGGCACGT
ReginaDPDF   AGAAATTTTAATGGTAAAAGTGATAAACCACATAGACCAAAAATGATAAAATAGGCACGT
ReginaDPDF   AGAAATTTTAATGGTAAAAGTGATAAACCACATAGACCAAAAATGATAAAATAGGCACGT
ReginaDPDF   ------------------------------------------------------------
 Consensus   AGAAATTTTAATGGTAAAAGTGATAAACCACATAGACCAAAAATGATAAAATAGGCACGT

ReginaDPDR   GAGAATTGAACCCGACGTAGACTGTGGGAGCAACCGAAGAAGTGTCGCATGGTGAGTTCA
ReginaDPDR   GAGAATTGAACCCGACGTAGACTGTGGGAGCAACCGAAGAAGTGTCGCATGGTGAGTTCA
ReginaDPDR   GAGAATTGAACCCGACGTAGACTGTGGGAGCAACCGAAGAAGTGTCGCATGGTGAGTTCA
ReginaDPDF   GAGAATTGAACCCGACGTAGACTGTGGGAGCAACCGAAGAAGTGTCGCATGGTGAGTTCA
ReginaDPDF   GAGAATTGAA------------------------------------------------
ReginaDPDF   ------------------------------------------------------------
 Consensus   GAGAATTGAACCCGACGTAGACTGTGGGAGCAACCGAAGAAGTGTCGCATGGTGAGTTCA

ReginaDPDR   ATCAAGTGAGACGACAGCGCATCACCAGTATCAAGGACCATCCTCCTCCACATAAAAGCA
ReginaDPDR   ATCAAGTGAGACGACAGCGCATCACCAGTATCAAGGACCATCCTCCTCCACATAAAAGCA
ReginaDPDR   ATCAAGTGAGACGACAGCGCATCACCAGTATCAAGGACCATCCTCCTCCACATAAAAGCA
ReginaDPDF   ATCAAGTGAGACGACAGCGCATCACCAGTATCAAGGACCATCCTCCTCCACATAAAAGCA
ReginaDPDF   ------------------------------------------------------------
ReginaDPDF   ------------------------------------------------------------
 Consensus   ATCAAGTGAGACGACAGCGCATCACCAGTATCAAGGACCATCCTCCTCCACATAAAAGCA
```

Supplementary Figure 3.3 Continued.

```
ReginaDPDR   CAAATTTTATTTATTTATTTTTTTATAAAGATATTAAACTTAGATATGGACAAAACCATTC
ReginaDPDR   CAAATTTTATTTATTTATTTTTTTATAAAGATATTAAACTTAGATATGGACAAAACCATTC
ReginaDPDR   CAAATTTTATTTATTTATTTTTTTATAAAGATATTAAACTTAGATATGGACAAAACCATTC
ReginaDPDF   CAAATTTTATTTATTTATTT----------------------------------------
ReginaDPDF   ------------------------------------------------------------
ReginaDPDF   ------------------------------------------------------------
 Consensus   CAAATTTTATTTATTTATTTTTTTATAAAGATATTAAACTTAGATATGGACAAAACCATTC

ReginaDPDR   ACAAAAGTAAGATGCCACATTTTCTACTGTCACGTTACAAAATCAACGGTGGAGATCAAA
ReginaDPDR   ACAAAAGTAAGATGCCACATTTTCTACTGTCACGTTACAAAATCAACGGTGGAGATCAAA
ReginaDPDR   ACAAAAGTAAGATGCCACATTTTCTACTGTCACGTTACAAAATCAACGGTGGAGATCAAA
ReginaDPDF   ------------------------------------------------------------
ReginaDPDF   ------------------------------------------------------------
ReginaDPDF   ------------------------------------------------------------
 Consensus   ACAAAAGTAAGATGCCACATTTTCTACTGTCACGTTACAAAATCAACGGTGGAGATCAAA

ReginaDPDR   TTAATCGAAAAATAGATTTTTTTTCTTTCCATAAAATGGAAAATTGCCTTTGAAATCTTC
ReginaDPDR   TTAATCGAAAAATAGATTTTTTTTCTTTCCATAAAATGGAAAATTGCCTTTGAAATCTTC
ReginaDPDR   TTAATCGAAAAATAGATTTTTTTTCTTTCCATAAAATGGAAAATTGCCTTTGAAATCTTC
ReginaDPDF   ------------------------------------------------------------
ReginaDPDF   ------------------------------------------------------------
ReginaDPDF   ------------------------------------------------------------
 Consensus   TTAATCGAAAAATAGATTTTTTTTCTTTCCATAAAATGGAAAATTGCCTTTGAAATCTTC

ReginaDPDR   CCTTTCTCGAACAGCTAGCCAGCAGCAGCAGCCAACTCTCCCTCTCTCTCATTCTCT
ReginaDPDR   CCTTTCTCGAACAGCTAGCCAGCAGCAGCAGCCAACTCTCCCTCTCTCTCATTCTCT
ReginaDPDR   CCTTTCTCGAACAGCTAGCCAGCAGCAGCAGCCAACTCTCCCTCTCTCTCATTCTCT
ReginaDPDF   ------------------------------------------------------------
ReginaDPDF   ------------------------------------------------------------
ReginaDPDF   ------------------------------------------------------------
 Consensus   CCTTTCTCGAACAGCTAGCCAGCAGCAGCAGCCAACTCTCCCTCTCTCTCATTCTCT

ReginaDPDR   TAGGCTTCAGACCCTGAAACCCGACAAAGGTAAACATTAAACAAAGAGAGGAAACCCAGA
ReginaDPDR   TAGGCTTCAGACCCTGAAACCCGACAAAGGTAAACATTAAACAAAGAGAGGAAACCCAGA
ReginaDPDR   TAGGCTTCAGACCCTGAAACCCGACAAAGGTAAACATTAAACAAAGAGAGGAAACCCAGA
ReginaDPDF   ------------------------------------------------------------
ReginaDPDF   ------------------------------------------------------------
ReginaDPDF   ------------------------------------------------------------
 Consensus   TAGGCTTCAGACCCTGAAACCCGACAAAGGTAAACATTAAACAAAGAGAGGAAACCCAGA

ReginaDPDR   ATTTAATTAGTTGATTAATTAATGGTTTTCCCTCTTTCTCTTCTTCTTCTTTGTGCTCTG
ReginaDPDR   ATTTAATTAGTTGATTAATTAATGGTTTTCCCTCTTTCTCTTCTTCTTCTTTGTGCTCTG
ReginaDPDR   ATTTAATTAGTTGATTAATTAATGGTTTTCCCTCTTTCTCTTCTTCTTCTTTGTGCTCTG
ReginaDPDF   ------------------------------------------------------------
ReginaDPDF   ------------------------------------------------------------
ReginaDPDF   ------------------------------------------------------------
 Consensus   ATTTAATTAGTTGATTAATTAATGGTTTTCCCTCTTTCTCTTCTTCTTCTTTGTGCTCTG

ReginaDPDR   GTACTCTCTAGGCATGTTGTTGTGAACTTGTTACCTATTTTGGTTGGTGGGTTTTTCTGG
ReginaDPDR   GTACTCTCTAGGCATGTTGTTGTGAACTTGTTACCTATTTTGGTTGGTGGGTTTTTCTGG
ReginaDPDR   GTACTCTCTAGGCATGTTGTTGTGAACTTGTTACCTATTTTGGTTGGTGGGTTTTTCTGG
ReginaDPDF   ------------------------------------------------------------
ReginaDPDF   ------------------------------------------------------------
ReginaDPDF   ------------------------------------------------------------
 Consensus   GTACTCTCTAGGCATGTTGTTGTGAACTTGTTACCTATTTTGGTTGGTGGGTTTTTCTGG

ReginaDPDR   GTTTTATTCACTTAGATCTGGGGGCCATTAAATCTTTAAAATTTACAAGAAACCCAGAAA
ReginaDPDR   GTTTTATTCACTTAGATCTGGGGGCCATTAAATCTTTAAAATTTACAAGAAACCCAGAAA
ReginaDPDR   GTTTTATTCACTTAGATCTGGGGGCCATTAAATCTTTAAAATTTACAAGAAACCCAGAAA
ReginaDPDF   ------------------------------------------------------------
ReginaDPDF   ------------------------------------------------------------
ReginaDPDF   ------------------------------------------------------------
 Consensus   GTTTTATTCACTTAGATCTGGGGGCCATTAAATCTTTAAAATTTACAAGAAACCCAGAAA
```

Supplementary Figure 3.3 Continued.

```
ReginaDPDR   ATCATTTGTAGTTTTTGAGTGTATGAACATAATATATGTGAAAAGTGGTTGGTTTGAATT
ReginaDPDR   ATCATTTGTAGTTTTTGAGTGTATGAACATAATATATGTGAAAAGTGGTTGGTTTGAA--
ReginaDPDR   ATCATTTGTAGTTTTTGAGTGTATGAACATAATATATGTGAAAAGTGGTTGGTTT-----
ReginaDPDF   ------------------------------------------------------------
ReginaDPDF   ------------------------------------------------------------
ReginaDPDF   ------------------------------------------------------------
 Consensus   ATCATTTGTAGTTTTTGAGTGTATGAACATAATATATGTGAAAAGTGGTTGGTTTGAATT

ReginaDPDR   TTTTGA
ReginaDPDR   ------
ReginaDPDR   ------
ReginaDPDF   ------
ReginaDPDF   ------
ReginaDPDF   ------
 Consensus   TTTT--
```

Supplementary Figure 3.4 Alignment of 'Cristobalina' and 'Regina' consensus sequences generated from DPDf/DPDr PCR fragments sequenced. The base number indicates the base nr upstream of *PavDAM1* start codon. Deleted region in 'Cristobalina' is marked by gaps (-).

```
Cristobalina    671 TACTCTTTCTTTCTCTTGGTTGA-CCAAAAAAAAAACCTCTTTGATGAATTGTTTGTTCC 733
Regina         1515 TACTCTTTCTTTCTCTTGGTTGACCCAAAAAAAAAACCTCTTTGATGAATTGTTTGTTCC 1454

Cristobalina    734 TCARAGAATATCACAACAACAATAGCAAAACAATGC------------------------ 698
Regina         1455 TCAAAGAATATCACAACAACAATAGCAAAACAATCCATATGGGTCATATATCCATGGCTT 1394

Cristobalina    723 ------------------------------------------------------------ 674
Regina         1395 TTTCTCGCCCGAGTCTCATGTTTGTACAAATCACATGTCTCCCATCCCATACATCAAAAA 1334

Cristobalina    723 ------------------------------------------------------------ 674
Regina         1335 GCTCTTTTGCACTGAATAGATTGAAAAGAGATGTTATAATCATGCAACCAAGCCAACAAA 1274

Cristobalina    723 ------------------------------------------------------------ 674
Regina         1275 ACTGGATGAATACAAAACAACAAATAAATGGCAAAAGAATACGAAAGGCACCGATTGAAG 1214

Cristobalina    723 ------------------------------------------------------------ 674
Regina         1215 TGCCCTCAGTTTTCTCTCATGTCAAAAAGTCAGAAGCTTCATAACGTAATCAAAGAAAAA 1154

Cristobalina    723 ------------------------------------------------------------ 674
Regina         1155 GAGACGAACCCATCACAGCCCCACCAACAAATTGAAGAGCAGGATCAGAACGACAACGAA 1094

Cristobalina    723 ------------------------------------------------------------ 674
Regina         1095 ATAGAAGAAGTCCAGTGCCAAATAGCAGTCTCCAACTTCCCTGGCGGCTCCGAGACCTTC 1034

Cristobalina    723 ------------------------------------------------------------ 674
Regina         1035 GAATAGCAGCCAAGTTCATCAAGATCTAGGTGGTGGAGTTTACTGGGTTGGGGAGATTGG 974

Cristobalina    723 ------------------------------------------------------------ 674
Regina          975 GGTGTGTGTGGTGGTTGGCGGGTGGGCTGGTGAGGGTGGGTTTGGCTGATGGCTTCTCTT 914

Cristobalina    723 ------------------------------------------------------------ 674
Regina          915 CCCCTTATATTTTTCTTCTTTTTAGAAAAGAAAAAATCTTTCTTGTTCTTAGATTTAAAT 854

Cristobalina    723 ------------------------------------------------------------  674
Regina          855 GCCCCTCAACAAGTAACCTCAGTTTAATCTAATTTGATCTAATTTGACAGAAATTGGAGA 794

Cristobalina    723 ------------------------------------------------------------ 674
Regina          795 TTGAACTTGAATTGCTTAAATTGAAAATCACAAAGGTAAAAATAATTAAATTGAAAACAC 734

Cristobalina    723 ----------ATGGTAAAAGTGATAAACTACATAGACCAAAAATGATAAAATAGGCACGT 674
Regina          735 AGAAATTTTAATGGTAAAAGTGATAAACCACATAGACCAAAAATGATAAAATAGGCACGT 674

Cristobalina    675 GAGAATTGAACCCGGCGTGGACTGTGGGAGCAACAGAAGAAGTGTCGCATGGTGAGTTCA 614
Regina          675 GAGAATTGAACCCGACGTAGACTGTGGGAGCAACCGAAGAAGTGTCGCATGGTGAGTTCA 614

Cristobalina    615 ATCAAGTGAGACGACAGCGCATCACCAGTATCAAGGACCATCCTCCTCCACATAAAAGCA 554
Regina          615 ATCAAGTGAGACGACAGCGCATCACCAGTATCAAGGACCATCCTCCTCCACATAAAAGCA 554

Cristobalina    555 CAAATTTTATTTATTTATTTTTTATAAAGATATTAAACTTAGATATGGACAAAACCATTC 494
Regina          555 CAAATTTTATTTATTTATTTTTTATAAAGATATTAAACTTAGATATGGACAAAACCATTC 494

Cristobalina    495 ACAAAAGTAAGATGCCACATTTTCTACTGTCACGTTACAAAATCAACGGTGGAGATCAAA 434
Regina          495 ACAAAAGTAAGATGCCACATTTTCTACTGTCACGTTACAAAATCAACGGTGGAGATCAAA 434

Cristobalina    435 TTAATCGAAAAATAGATTTTTTTTTCTTCCATAAAATGGAAAATTGCCTTTGAAATCTTC 374
Regina          435 TTAATCGAAAAATAGATTTTTTTTCTTTCCATAAAATGGAAAATTGCCTTTGAAATCTTC 374

Cristobalina    375 CCTTTCTCGAACAGCTAGCCAGCAGCAGCAGCAGCCAACTCTCCCTCTCTCTCATTCTCT 314
Regina          375 CCTTTCTCGAACAGCTAGCCAGCAGCAGCAGCAGCCAACTCTCCCTCTCTCTCATTCTCT 314

Cristobalina    315 TAGGCTTCARACCCTGAAACCCGACAAAGGTAAACATTAAACAAAGAGAGGAAACCCARA 254
Regina          315 TAGGCTTCAGACCCTGAAACCCGACAAAGGTAAACATTAAACAAAGAGAGGAAACCCAGA 254
```

Supplementary Figure 3.4 Continued.

```
Cristobalina    255 ATTTAATTAGTTGATTAATTAATGGTTTTCCCTCTTTCTCTTCTTCTTCTTTGTGCTCTG 194
Regina          255 ATTTAATTAGTTGATTAATTAATGGTTTTCCCTCTTTCTCTTCTTCTTCTTTGTGCTCTG 194

Cristobalina    195 GTACTCTCTAGGCATGTTGTTGTGAACTTGTGACCTATTTTGGTTGGTGGGTTTTTCTGG 134
Regina          195 GTACTCTCTAGGCATGTTGTTGTGAACTTGTTACCTATTTTGGTTGGTGGGTTTTTCTGG 134

Cristobalina    135 GTTTTATTCACTTAGATCTGGGGGCCATTAAATCTTTAAAATTTACAAGAAACCCAGAAA 74
Regina          135 GTTTTATTCACTTAGATCTGGGGGCCATTAAATCTTTAAAATTTACAAGAAACCCAGAAA 74

Cristobalina     75 ATCATTTGTAGTTTTTGAGTGTATGAACATAATATATGTGAAAAGTGGTTGGTTTGAATT 14
Regina           75 ATCATTTGTAGTTTTTGAGTGTATGAACATAATATATGTGAAAAGTGGTTGGTTTGAATT 14

Cristobalina     15 TTTTTGAAGGGGAC 1
Regina           15 TTTTTGAAGGGGAC 1
```

CHAPTER 5

FRUIT SIZE AND FIRMNESS QTL ANALYSIS IN SWEET CHERRY POPULATION ‘AMBRUNÉS’ × ‘SWEETHEART’

INTRODUCTION

Sweet cherry (*Prunus avium* L.) is mainly cultivated for its edible fruit. Fruit quality depends on biochemical and sensory changes in color, flavour and texture during fruit development and ripening, as well as during the post-harvest storage (Crisosto et al., 2003; Serrano et al., 2005). Consumer survey in diverse geographical regions has demonstrated that large fruit, dark skin and uniformity of color, firmness, sweetness, sourness, flavour intensity, soluble solid concentration and titratable acidity are the main aspects of consumer acceptability (Cliff et al., 1995; Crisosto et al., 2003; Chauving et al., 2009). Moreover, not only consumer preferences, but adequate adjustment to the various processes involved in the food chain should also be considered as fruit quality (Gallardo et al., 2015).

Most fruit quality traits are quantitative (Lamb, 1953; Fogle, 1961) being size and firmness two of these important fruit quality traits in sweet cherry. As sweet cherry is mostly sold as a fresh fruit, grower's profitability directly depends on fruit quality attributes like size and firmness (Whiting et al., 2006). Larger fruit reaches higher prices in production and retail being an essential trait to be consider in every breeding program (Dirlewanger et al., 2009). Fruit diameter and weight are highly correlated, thus larger fruits have more weight (Whiting et al., 2006), and it is usual to find the terms weight, diameter and length used indistinctly in literature regarding sweet cherry fruit size. Several works have studied the genetics of fruit size in sweet cherry. Zhang et al. (2010) identified QTLs related to fruit diameter and weight on linkage groups (LGs) 2 and 6 using 'New York 54' × 'Emperor Francis' population. Rosyara et al. (2013) using four sweet cherry populations ('New York 54' × 'Emperor Francis'; 'Regina' × 'Lapins'; 'Namati' × 'Summit'; 'Namati' × 'Krupnoplodnaya') identified four additional fruit weight QTLs on LGs 1, 2, 3 and 6, and validated the two fruit size QTLs described by Zhang et al. (2010). Furthermore, using two additional progenies ('Regina' × 'Lapins' and 'Regina' × 'Garnet'), Campoy et al. (2015) reported a new major weight QTL located on LG5.

Fruit firmness is an important aspect of organoleptic quality, and it is an important attribute for packing and transport as it contributes to shelf life during postharvest handling and shipping (Zoffoli et al., 2017). Fruit firmness increase is achieved by gibberellic acid treatment or rapid fruit cooling (< 1ºC; Zoffoli et al., 2017). Campoy et al. (2015) reported

the first QTL analysis in sweet cherry ('Regina' × 'Lapins' and 'Regina' × 'Garnet' populations). Firmness QTLs were found on all LGs (except LG7), with a major QTLs found on LG2. More recently, Cai et al. (2019) carried out firmness QTL analyses in three sweet cherry populations ('Fercer' × 'X' F_1 population, the INRA sweet cherry germplasm collection and RosBREED pedigreed population). A major firmness QTL on LG4 (*qP-FF4.1*), explaining 54.0 to 84.6% of phenotypic variation, was found (Cai et al., 2019). Additional minor QTLs on LGs 1, 2, 5, 6 and 8 were also detected (Cai et al., 2019). Haplotype analysis of *qP-FF4.1* revealed a dominant effect of 'soft' alleles over 'firm' ones, being most of bred cultivars homozygous for 'firm' alleles whereas mazzards were homozygous for 'soft' alleles (Cai et al., 2019). *In silico* firmness candidate gene analyses have revealed potential candidate genes related with plant cell wall modification and hormone signalling pathways (Campoy et al., 2015; Cai et al., 2019).

Cultivation and trading of sweet cherry is an important economic activity in different regions of Spain, being of highest relevance in the Jerte Valley (Cáceres). The tradition of cherry production in this area is based on the cultivation of landraces, which are highly adapted to soil and climate conditions. Among these landraces, the cultivar 'Ambrunés' is most extensively cultivated due to its outstanding fruit quality and great post-harvest aptitude (Alique et al., 2005; Serradilla et al., 2012). Additionally, this cultivar is the basis of the Protected Designation of Origin (POD) 'Cereza del Jerte', and is now being used in sweet cherry breeding as a source of high fruit quality. 'Ambrunés' is a vigorous, self-incompatible, early flowering and very late ripening (+31 days after 'Burlat') variety. The fruits are heart-shaped, of medium size, mahogany skin colour and orange flesh, collected without peduncle and show high resistance to cracking due to their firmness (Gella et al., 2001; Quero-García et al., 2017). Also, fruit firmness is well maintained during ripening providing an outstanding post-harvest aptitude (Serradilla et al., 2012). However, 'Ambrunés' has some disadvantages in modern plantations, like the lack of homogeneity among individuals and irregular yields over the years (López-Corrales et al., 2003). Because of its adaptation to the Jerte Valley conditions, its fruit quality and postharvest behaviour, 'Ambrunés' is a very interesting cultivar for sweet cherry breeding, and has been extensively investigated using different approaches like physicochemical and nutritional composition studies (Bernalte et al., 1999; Serradilla et al., 2011a and 2016; Garrido et al., 2014), post-harvest aptitude (Alique et al., 2005; Serradilla et al., 2011b),

and to develop biochemical (Serradilla et al., 2008) and genetic protocols for authentication (Serradilla et al., 2013).

The objective of this work is to investigate the genetic basis of fruit firmness from 'Ambrunés' and to determine if fruit firmness and size are correlated in 'Ambrunés' offspring, with the ultimate goal of enabling marker assisted selection (MAS) of this trait in sweet cherry. Given the relationship observed between fruit firmness and size (Campoy et al., 2015), fruit size was also investigated. To achieve this goal, an F_1 sweet cherry population ('Ambrunés' × 'Sweetheart'), along with parental genotypes that come from two distinct genetic pools (Wünsch and Hormaza, 2002), was used. This population was phenotyped for two years for these quality traits (fruit weight, diameter/size and firmness/texture) and genotyped with RosBREED cherry 6K SNP array v1 to construct a high-density linkage map that allows carrying out QTL mapping of these fruit quality traits**.**

MATERIALS AND METHODS

Plant material

In this work, an F_1 (N=140) sweet cherry population from the cross of 'Ambrunés' (S_3S_6) × 'Sweetheart' ($S_3S_{4'}$) (A×S) was used. This family and the parental cultivars are maintained in the facilities of Centro de Investigaciones Científicas y Tecnológicas de Extremadura (CICYTEX) in the Jerte Valley (Cáceres, Spain). The A×S cross was made in 2009 and offspring individuals were planted in 2010. 'Ambrunés' is a landrace traditionally cultivated in the Jerte Valley and the most cultivated variety in this area. It shows both outstanding organoleptic quality and great post-harvest behaviour, based on its capacity to maintain firmness through time (Alique et al., 2005). 'Sweetheart' is a commercial variety from Pacific Agri-Food Research Centre (PARC) cherry breeding program in Summerland (BC, Canada) that stands out for self-fertility and late ripening (Lane and MacDonald 1996).

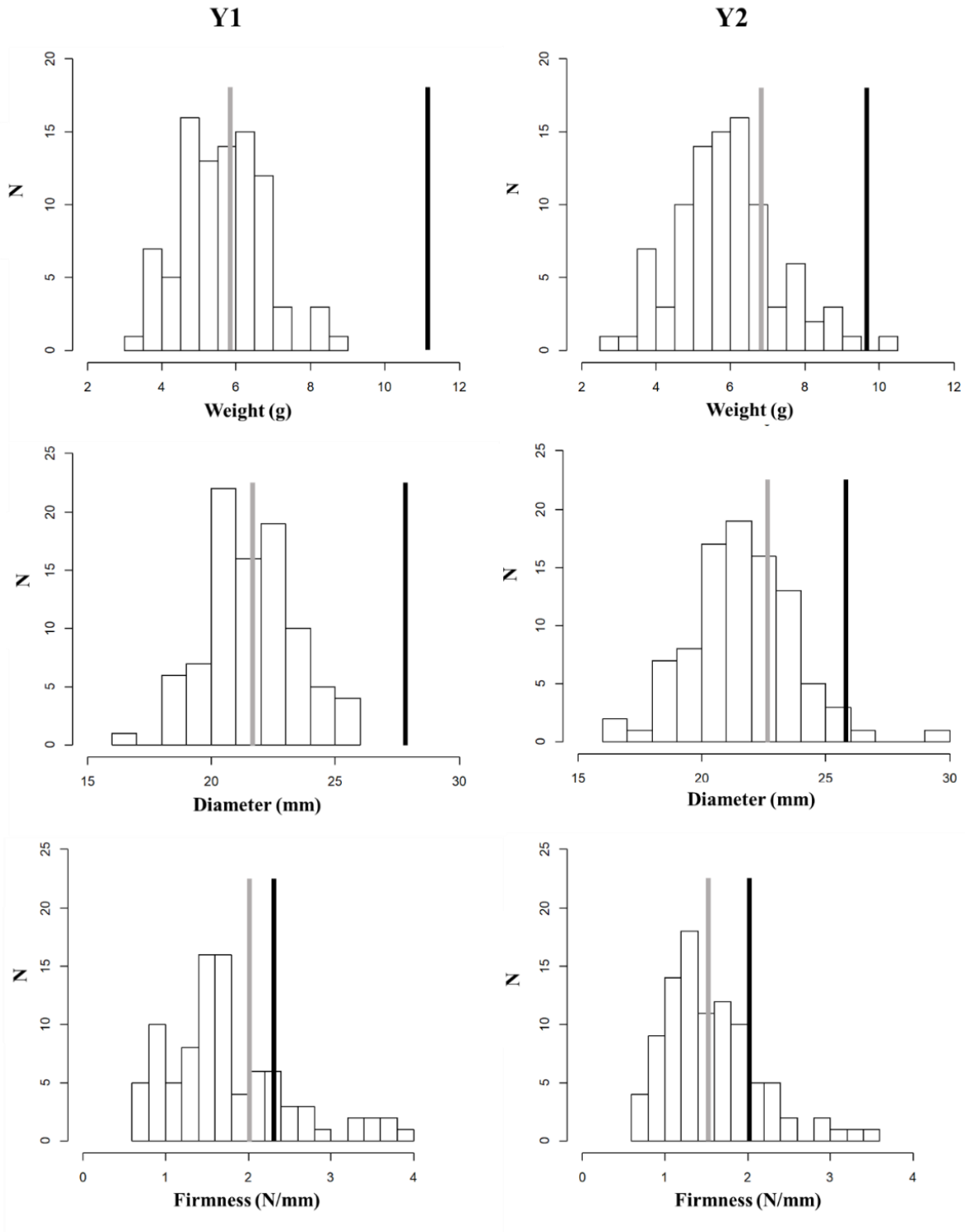

Figure 5.1 Frequency distribution of fruit weight, diameter and firmness for A×S population in two years (Y1 and Y2). Grey and black bars indicate phenotypic values for 'Ambrunés' and 'Sweetheart', respectively.

Fruit size and firmness phenotyping

Phenotyping of weight, diameter and firmness was carried out during two consecutive years (2015 and 2016) for A×S individuals and the parental cultivars at Instituto de Investigaciones Agrarias Finca La Orden – Valdesequera (CICYTEX, Extremadura). In the first year (Y1), 10 fruits per tree were phenotyped, while 25 fruits per tree were phenotyped in the second year (Y2). Fruits of each tree were weighted and measured at its longest axis (perpendicular to suture axis) using a calliper. To evaluate fruit firmness, a texturometer (TA.XT2i Texture Analyser, Stable Microsystems, Godalmimg, UK) was used (Balas et al., 2019). The texturometer was adjusted to measure the force needed to deform a fruit 3% of its diameter (Martínez-Esplá et al., 2014) and provided data of the applied force in Newton (N) and the deformation length in millimetres (mm). The ratio (N/mm) is defined as the firmness in this study (Serradilla et al., 2011b). Firmness measures were performed at two different points of each fruit: on the dorso-ventral axis (traversing the suture) and on the medio-lateral axis (perpendicular to suture). The average of these two measures was used as the firmness value (Balas et al., 2019).

The phenotypic data was analysed to estimate the mean, standard deviation and distribution of each trait in both years. Additionally, analysis of the linear correlation among traits and nonparametric analysis of variance (ANOVA) were carried out. Broad sense heritability (H^2) was estimated using the equation $H^2 = \frac{\sigma_g^2}{\sigma_g^2 + \frac{\sigma_e^2}{n}}$, where σ_g^2 is the genetic variance in the F_1 family, σ_e^2 is the environmental variance and n is the number of years. These statistical analyses were performed using SPSS® statistics v21.0.0 (IBM, Chicago, IL, USA) and R v3.4.1 (R Core Team, 2017).

SNP genotyping and linkage map construction

Genomic DNA from the A×S individuals and the parental cultivars was extracted using DNeasy Plant Mini Kit® (Qiagen N.V., Hilden, Germany). DNA quantification and SNP genotyping of all the individuals and the parental cultivars was carried out at CEGEN-PRB2-ISCIII (Madrid, Spain). SNP genotyping was carried out using the RosBREED cherry 6K SNP array v1 (Peace et al., 2012). The SNP genotypes were clustered, reviewed and filtered using the Genotyping Module of GenomeStudio® software, using the build-in algorithm 'Gentrain2' for all samples with GenCall score above 0.15 (v2011.1, Illumina

Inc., San Diego, CA, USA). The SNP data were clustered using the A×S individuals and a set of 45 sweet cherry accessions, to maximize allelic diversity (Martínez-Royo and Wünsch, 2014). A duplicate individual genotype was included in each 96 plate as control. Identical SNP genotypes were identified for replicated individuals, confirming SNP scan quality and reproducibility. The SNPs incorrectly clustered for the individuals of A×S population were revised and manually edited when possible. Paternity analysis to confirm hybrid identity of all the progeny was performed using the P-P-C (Parent-Parent-Child) module of GenomeStudio. ASSIsT v1.01 software (Di Guardo et al., 2015) was used to filtered SNP markers and assigned input data format prior to linkage mapping.

Linkage map construction was performed using JoinMap® software (v4.1, Kyazma B.V., Wageningen, The Netherlands; van Ooijen, 2006) following the '*Two-step strategy*' described by Tavassolian et al. (2010). Minimum independence of LOD, recombination frequency, maximum likelihood mapping algorithm and Kosambi's mapping function (Kosambi, 1944) were used for map construction following the details described in Chapter 2 for a cross-pollinated population. Markers showing distorted segregation ratios ($p<0.01$) from expected Mendelian segregation were eliminated when they were not surrounded by other markers showing the same distortion. The genetic positions of mapped SNPs were compared with their physical positions in the peach genome v2.0.a1 (Verde et al., 2017).

QTL mapping and haplotype analysis

QTL analysis was performed for the three phenotyped traits (weight, diameter, and firmness) on the parental maps in both years. QTL mapping was carried out using MapQTL® (v.6.0, Kyazma B.V., Wageningen, The Netherlands; van Ooijen, 2009), through the interval mapping method (Lander and Botstein 1989) and MQM mapping (Jansen, 1993 and 1994; Jansen and Stam, 1994). To establish the LOD significance threshold for each QTL in each linkage group (LG), a permutation test was carried out at a significance level of 90% ($p<0.1$) using 10,000 permutations (Lander and Botstein, 1989; van Ooijen, 1992). Graphical representations of LGs and QTLs were obtained using MapChart software (Voorrips, 2002).

QTL haplotypes were constructed for those QTLs detected in both years. SNP markers spanning the QTL regions were selected to determine parental haplotypes.

Progeny showing recombination in these QTL regions were eliminated from the analysis. Mean phenotypic values of each QTL haplotype were estimated in the remaining A×S population individuals. ANOVA calculations and Student's t-test ($p<0.05$) were carried out using SPSS® statistics v21.0.0 software (IBM, Chicago, IL, USA) to compare mean values of the different haplotypes.

RESULTS

Phenotype mean, distribution, heritability and correlation

Phenotyping of fruit weight, diameter and firmness in A×S was carried out for 94 (67%) and 99 (71%) individuals each year (Y1 and Y2, respectively), with a total of 117 trees evaluated in the two years. For both years, 'Sweetheart' fruits were larger, heavier and firmer than 'Ambrunés' fruits (Fig 5.1; Sup Table 5.1). Fruit weight and diameter mean values in the progeny were similar both years (Sup Table 5.1) and no significant differences were observed between years. However, for fruit firmness, a significant difference was observed between Y1 and Y2 (Student's t-test; $p<0.05$), with firmness being higher in Y1 (1.7 N/mm in Y1 and 1.5 N/mm in Y2; Sup Table 5.1). Broad-sense heritability (H^2) ranged from 0.63 to 0.75 for the three traits, being largest (H^2=0.75) for firmness (Sup Table 5.1).

Progeny distributions for the three traits measured revealed that weight (Shapiro Wilk test; Prob<W: 0.345 in Y1; Prob<W: 0.155 in Y2) and diameter (Prob<W: 0.970 in Y1; Prob<W: 0.295 in Y2) fitted normality, whereas firmness showed highly skewed distribution to softer fruits, and therefore did not fit a normal distribution (Y1 Prob<W:<0.0001; Y2 Prob<W: <0.0001). Additionally, positive transgressive segregations for firmness was observed in both years, while for diameter and weight it was only observed in the second year. However, negative transgressive segregation was observed for all the traits both years (Fig 5.1). In fact, the population means were lower than the parental means for the three traits both years.

Pearson's correlation coefficients (r) were calculated amongst the three traits in both years (Fig 5.2). As expected, highly significant positive correlation ($p<0.01$) was observed between diameter and weight in both years (r=0.954 in Y1; r=0.962 in Y2). In

addition, low significant positive correlation was observed between firmness and diameter in the second year (r=0.384, p<0.01 in Y2), indicating that in the second year larger fruits were firmer. No significant correlation (p<0.01) was detected between firmness and weight (Fig 5.2).

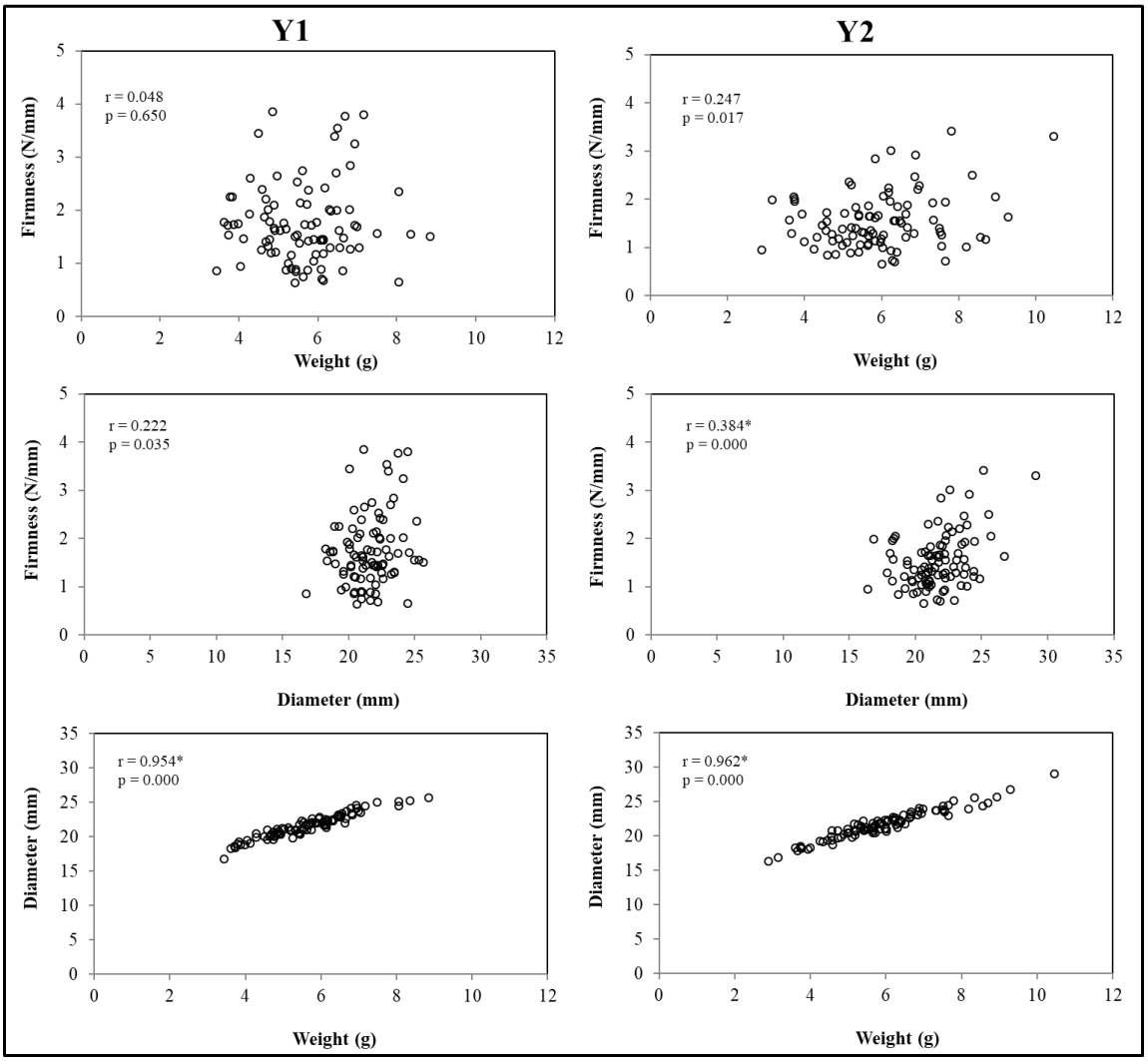

Figure 5.2 Pairwise correlations for fruit weight, diameter and firmness in two years (Y1 and Y2). Pearson coefficient (r) and P value (p) are presented for each plot. Asterisk indicates significant correlation at p<0.01.

SNP genotyping and linkage mapping

From the total of 5,696 SNPs in the array, 5,360 (94%) and 5,377 (94%) SNPs were correctly genotyped in 'Ambrunés' and 'Sweetheart', respectively. 'Ambrunés' showed

higher heterozygosity than ‘Sweetheart’, being 641 heterozygous SNPs in ‘Ambrunés’ and 450 in ‘Sweetheart’. From the genotyped markers in the A×S population, 4,446 (78%) were monomorphic, 355 (6%) were failed to be detected, and the remaining 895 (16%) were polymorphic and informative, and were used for linkage map construction.

Linkage parental maps of ‘Ambrunés’ and ‘Sweetheart’ include 463 and 254 SNPs, respectively. Both maps had 8 LGs, and covered 867.8 and 529.1 cM, respectively (Table 5.1; Sup Table 5.2, Sup Fig 5.1). Being ‘Ambrunés’ highly heterozygous, a larger number of markers could be mapped, showing larger LGs and larger number of markers in most LGs than ‘Sweetheart’ (Table 5.1; Sup Fig 5.1). ‘Sweetheart’ linkage map covered a smaller genetic length and showed smaller LG size for all LGs than ‘Ambrunés’ map. Some ‘Sweetheart’ LGs, like 3, 4 and 7, with 12 to 14 SNPs, had a very low coverage, showing putative large homozygous regions in these chromosomes for this cultivar (Table 5.1; Sup Fig 5.1). Average marker distance was similar in both parental maps (2.1 and 2.4 cM for ‘Ambrunés’ and ‘Sweetheart, respectively), and large gaps were detected in both, ‘Ambrunés’ (33.9 cM on LG2, 28.4 cM on LG2) and ‘Sweetheart’ maps (31.1 cM on LGs 1 and 7) (Table 5.1; Sup Fig 5.1). A group of SNP markers showing distortion from expected Mendelian segregation ratios ($p<0.001$) were observed at bottom region of ‘Sweetheart’ LG6 (Sup Fig 5.1). The A×S consensus map included 820 SNPs, with a total genetic length of 827.6 cM and an average marker distance of 1.0 cM (Table 5.1; Sup Table 5.2; Sup Fig 5.1). Consistent with the parental maps, LG1 was the largest with 185 SNPs and covering 184.7 cM, while LG5 was the shortest with a genetic distance of 76.2 cM (Table 5.1; Sup Fig 5.1).

The SNP order and position in the ‘Ambrunés’, ‘Sweetheart’ and consensus maps were compared with the physical position of the same SNPs in the peach genome v2.0.a1 (Sup Table 5.2). Despite the high degree of collinearity some markers, nine (1.9%) SNPs in ‘Ambrunés’, eight (3.1%) in ‘Sweetheart’ and 59 (7.2%) in the consensus map, were mapped in a different position compared with their physical position in peach genome (Sup Table 5.2). Most noticeable is an inverted region found at top of LG5 that included 8 SNPs in ‘Sweetheart’ and 19 in the consensus map (Sup Table 5.2). In addition, nine makers were mapped in different LG than in peach genome, three of them in ‘Ambrunés’ map and six in ‘Sweetheart’ map (Sup Table 5.3).

QTL analyses

QTL mapping of the three traits (fruit weight, diameter and firmness) in the two years identified 21 significant QTLs distributed on all LGs except LG4 (Sup Table 5.4). Of these, six QTLs, including one for weight, two for diameter and three for firmness, were detected in both years (Table 5.2; Fig 5.3).

For fruit weight, a total of four QTLs were detected on LGs 1, 2, 3 and 5 of 'Ambrunés' and 'Sweetheart' maps (Sup Table 5.4). Of these, the most significant is the QTL detected in both years that maps to 'Ambrunés' LG1 (*qP-Wei1.1*^{m}) at the 97.8 to 119.9 cM, explaining 15.4 to 17.8% of the phenotypic variation (PV) (Table 5.2; Fig 5.3). For fruit diameter, six QTLs were identified on LGs 1, 2, 5, 7 and 8 (Sup Table 5.4) also in both parental cultivars. From these, the two most significant QTLs across both years were also found on 'Ambrunés' LG1, *qP-Dia1.1*^{m} and *qP-Dia1.2*^{m} (Table 5.2; Fig 5.3). *qP-Dia1.1*^{m} was found between 57.2 to 79.2 cM of 'Ambrunés' parental map and explained 11.0 to 12.9% of PV, while *qP-Dia1.2*^{m}, was found from 100.7 to 118.9 cM, and it was associated with a PV of 10.9 and 10.8% in Y1 and Y2, respectively (Table 5.2; Fig 5.3).

Table 5.1 Number of SNP markers, genetic length, average marker distance and maximum gap for the 'Ambrunés' (A), 'Sweetheart' (S) and consensus (A×S) maps. (cM; centiMorgan).

	Genetic map	LG1	LG2	LG3	LG4	LG5	LG6	LG7	LG8	Total
Number of markers	**A**	108	27	63	46	32	41	83	63	**463**
	S	47	53	12	14	42	27	12	47	**254**
	A×S	185	93	85	62	84	91	99	121	**820**
Genetic length (cM)	**A**	196.1	105	117.3	93.2	64	109.5	97.9	84.8	**867.8**
	S	122.2	90.1	25.7	17.9	61.6	84.9	63.9	62.8	**529.1**
	A×S	184.7	98.6	111.1	92.9	76.2	95.7	91.6	76.8	**827.6**
Average marker distance (cM)	**A**	1.8	4	1.9	2.1	2.1	2.7	1.2	1.4	**2.1**
	S	2.2	1.7	2.3	1.5	1.5	3.2	5.7	1.4	**2.4**
	A×S	1	1.1	1.3	1.5	0.9	1.1	0.9	0.6	**1**
Maximum gap (cM)	**A**	23.4	33.9	28.4	31.1	9	17.7	12.7	19.9	**33.9**
	S	31.1	8.1	7.2	7.2	15.6	31.1	28.4	9.9	**31.1**
	A×S	11.9	5.9	12.7	19.9	9.2	7.4	9.9	8.2	**19.9**

For fruit firmness, QTL analysis identified five QTLs on LGs 1, 3 and 6 (Sup Table 5.4). The most significant QTLs across both years were also detected on LG1 (*qP-Fir1.1*^{m} and *qP-Fir1.2*^{m}), in both parental cultivars (Table 5.2; Fig 5.3). *qP-Fir1.1*^{m} explained 12.5 to 18.8% of PV in 'Ambrunés' and *qP-Fir1.2*^{m} from 10.2 to 22.5% in 'Sweetheart' (Table 5.2). It is noticeable that the QTL in 'Sweetheart' (*qP-Fir1.2*^{m}) shows negative values of additive effects (-0.69 and -0.18 N/mm) both years, while these values are positive for 'Ambrunés' (0.20 and 0.33 N/mm for *qP-Fir1.1*^{m}) (Table 5.2). A second relevant firmness QTL was identified on 'Ambrunés' LG6, *qP-Fir6.1*^{m}, explaining 6.7 and 14.3% of PV in Y1 and Y2 respectively (Table 5.2; Fig 5.3).

Some weight, diameter and/or firmness QTLs were found in the same region, this was the case of major stable QTLs, *qP-Wei1.1*^{m} and *qP-Dia1.2*^{m} (Fig 5.3), that cover the same region, and *qP-Dia1.1*^{m} and *qP-Fir1.1*^{m}, all of them found both years on 'Ambrunés' LG1. The same happened with minor and less stable QTLs *qP-Wei3.1, qP-Dia3.1* and *qP-Fir3.1* all detected in 'Sweetheart' LG3 in Y2 (Sup Table 5.4).

Haplotype analysis

Haplotype analysis (Table 5.3, Sup Table 5.5) was carried out for the six most significant QTLs detected in both years (Table 5.2). For fruit weight QTL *qP-Wei1.1*^{m}, the haplotypes analysis in the segregating parent ('Ambrunés') revealed that individuals with *Wei1.1_H2* haplotype had larger fruit weight (0.9 to 1.1 g) in both years than those with *Wei1.1_H1* (Table 5.3). For fruit diameter, 'Ambrunés' haplotypes of both LG1 QTLs, *qP-Dia1.1*^{m} and *qP-Dia1.2*^{m}, showed fruits larger in those trees with haplotypes *Dia1.1_H2* and *Dia1.2_H2*, also both years (1.0 to 1.9 mm larger; Table 5.3). For fruit firmness, haplotypes of 'Ambrunés' and 'Sweetheart' for two QTL region on LG1, *qP-Fir1.1*^{m} and *qP-Fir1.2*^{m}, revealed that individuals with haplotype combination *Fir1.1_H2*/*Fir1.2_H1* were firmer (from 0.5 to 0.8 N/mm) than those with all other haplotype combinations (Table 5.3). For firmness QTL *qP-Fir6.1*^{m}, individuals with haplotype *Fir6.1_H1* also showed higher firmness (0.4 N/mm more) than those with *Fir6.1_H2* (Table 5.3).

Interaction between the two 'Ambrunés' firmness stable QTLs (*qP-Fir1.1*^{m} and *qP-Fir6.1*^{m}) was analyzed (Sup Table 5.6). Individuals with the haplotypes that revealed higher firmness in each QTL, *Fir1.1_H2* and *Fir6.1_H1* (Table 5.3) were the most firm in both years, with firmness values above 2.0 N/mm (Sup Table 5.6), being this firmness

significantly different from that that observed in the other possible genotypes (Sup Table 5.6).

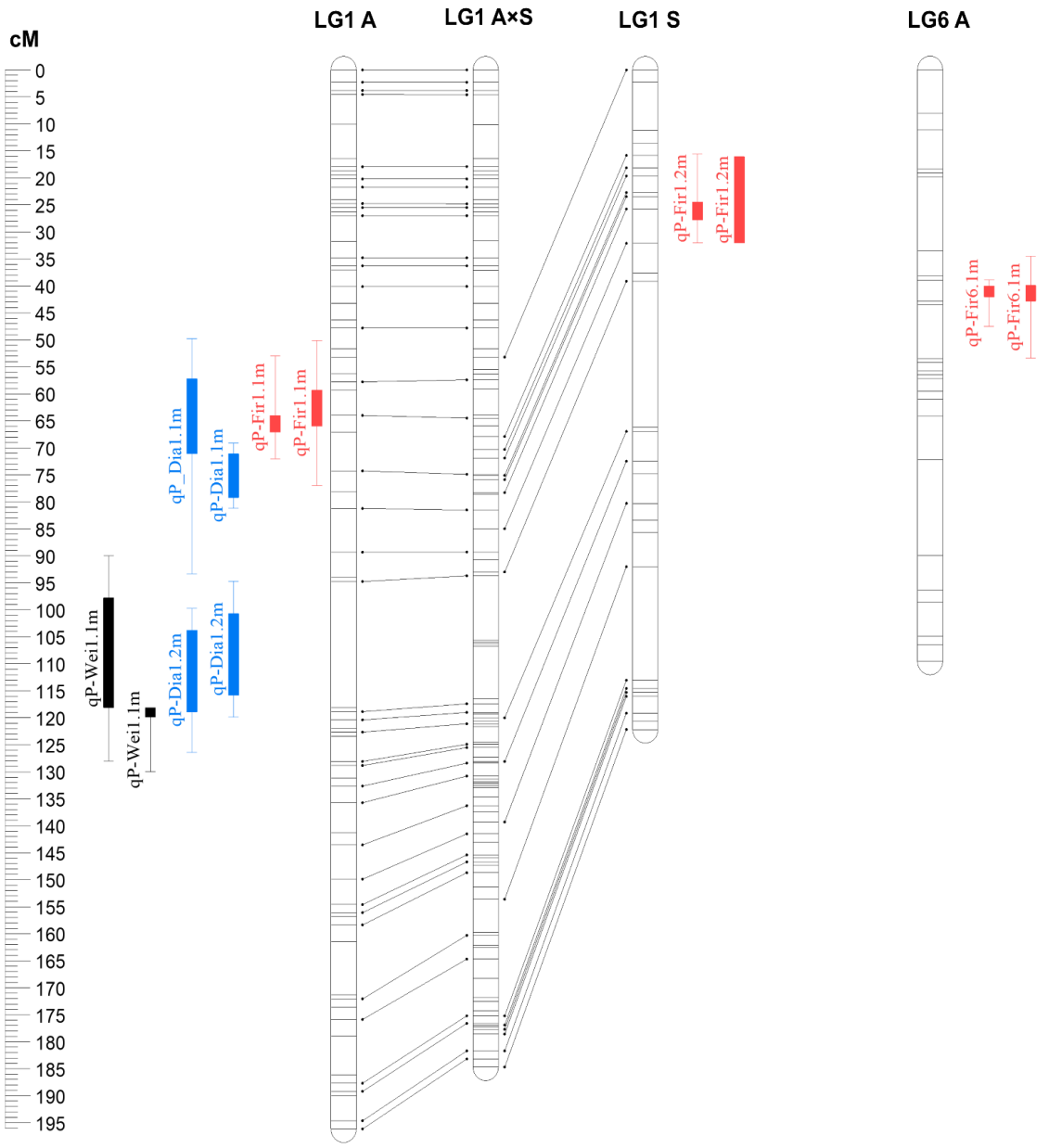

Figure 5.3 Graphical representation of stable (detected in both years) fruit weight (black), diameter (blue) and firmness (red) QTLs identified on 'Ambrunés' and 'Sweetheart' parental maps. All detected QTLs are summarized in Sup Table 5.4.

DISCUSSION

In this work, the use of a unique F_1 population that combines two unrelated sweet cherry genetic pools, to study fruit size and firmness during two years, has allowed identifying relevant QTLs for these traits that will be useful for breeding in the species. QTLs found in this work were previously reported, validating previous findings in other genetic backgrounds and completing the genetic picture of these traits in sweet cherry. Most relevant is the validation of relevant stable QTLs on LG1 for the three evaluated traits, suggesting multiple closely linked genes controlling these traits and/or a single gene with pleiotropic effects. The fact that positive additive effects of these three QTLs are found in 'Ambrunés' and that the favorable alleles are in coupling phase, reveals the potential of this cultivar for breeding for fruit size and firmness.

SNP genotyping and linkage maps

The number of heterozygous markers genotyped in 'Ambrunés' (641) and 'Sweetheart' (450) was in the range (400-700) observed for other sweet cherry cultivars from various origins evaluated (Peace et al., 2012) and genotyped with the same array, like 'Cristobalina' (526), 'Vic' (483), 'Regina' (603), 'Lapins' (515), 'Black Tartarian' (634) or 'Kordia' (526) (Klagges et al., 2013; Chapter 2). A larger number of heterozygous markers were detected in 'Ambrunés' than 'Sweetheart'. 'Ambrunés' is a landrace and is expected to be highly heterozygous, whereas 'Sweetheart' is a commercial cultivar that may have lost some degree of heterozygosity through breeding (Lane and MacDonald, 1996). The large number of heterozygous markers in 'Ambrunés' was evidenced in the total genetic length covered by the genetic map, being the largest of all developed in sweet cherry using SNP markers with the RosBREED cherry 6K SNP array (Klagges et al., 2013; Castède et al., 2014; Chapter 2) and Genotyping by Sequencing (GBS) (Guajardo et al., 2015). On the other side, the presence of large putative homozygous regions in 'Sweetheart' may be a problem for QTLs analyses due to the presences of large genomic regions that were not covered by any segregating marker. This was most noticeable on 'Sweetheart' LGs 3 and 4, where very few markers were heterozygous. Similarly, in

Table 5.2 Significance, genetic interval, QTL peak and physical position of main QTLs identified for both years for weight, diameter and firmness in A×S population. All detected QTLs are shown in Sup Table 5.4.

Trait	Parental cultivar	Year	QTL name	LG	QTL interval (cM)	Physical position*	QTL peak					QTL previously described (Reference)
							SNP	LOD	Variance	PVE (%)	Additive effect	
Weight	'Ambrunés'	Y1	*qP-Wei1.1*^{m}	1	118.1-119.9	30.69-31.94	ss490546431	3.26	1.03	15.4	0.43	*FW_G1* [(1)]
		Y2	*qP-Wei1.1*^{m}	1	97.8-119.9	27.00-31.94	ss490547198	4.27	1.44	17.8	0.63	*fw1.1* [(2)]
Diameter	'Ambrunés'	Y1	*qP-Dia1.1*^{m}	1	69.1-79.2	15.85-23.82	ss490546727	2.69	2.63	12.9	0.62	*fw1.1* [(2)]
		Y2	*qP-Dia1.1*^{m}	1	57.2-71.1	11.55-19.96	ss490546442	2.36	4.01	11.0	0.71	
		Y1	*qP-Dia1.2*^{m}	1	100.7-115.8	28.21-30.34	ss490547003	2.26	2.69	10.9	0.77	*FW_G1* [(1)]
		Y2	*qP-Dia1.2*^{m}	1	103.8-118.9	28.94-30.76	ss490547003	2.32	4.02	10.8	0.82	*fw1.1* [(2)]
Firmness	'Ambrunés'	Y1	*qP-Fir1.1*^{m}	1	64.0-67.1	14.73-15.75	ss490546599	3.25	0.23	12.5	0.20	*ff1.1* [(2)]
		Y2	*qP-Fir1.1*^{m}	1	59.3-66.0	12.62-15.11	ss490546554	4.08	0.45	18.8	0.33	[(3)]
		Y1	*qP-Fir6.1*^{m}	6	38.9-47.5	7.94-9.93	ss490555475	1.64	0.42	6.7	0.20	*ff6.1* [(2)]
		Y2	*qP-Fir6.1*^{m}	6	39.9-42.8	8.01-8.52	ss490555470	3.67	0.23	14.3	0.22	[(3)]
	'Sweetheart'	Y1	*qP-Fir1.2*^{m}	1	16.1-32.1	15.25-24.18	ss490546651	5.00	0.43	22.5	-0.69	*ff1.1* [(2)]
		Y2	*qP-Fir1.2*^{m}	1	24.5-27.8	22.30-23.86	ss490559249	2.43	0.26	10.2	-0.18	[(3)]

* Physical position (Mbps) of SNP markers in peach genome v2.0.a1 (Verde et al., 2017). References: [1] Rosyara et al., 2013, [2] Campoy et al., 2015, [3] Cai et al., 2019.

previous sweet cherry linkage maps developed using same array, large homozygous regions were also detected in some breeding cultivars and inbreed individuals (Chapter 2).

Previous reports have confirmed the collinearity of the cherry and peach genomes with few exceptions (Dirlewanger et al., 2004; Illa et al., 2011; Chapter 2). In this study, this collinearity was also observed. However, the comparison of the SNP map positions and their physical positions in peach genome (Verde et al., 2017) confirmed an inverted region on the top of LG5 in 'Sweetheart' previously reported in other sweet cherry maps (Chapter 2). In addition, as previously observed (Klagges et al., 2013; Chapter 2), three markers (ss490550875, ss490548697 and ss490550875) mapped on a different LG than in peach genome, suggesting the possible translocation of small genome regions between the cherry and peach genomes.

High segregation distortion was observed at the bottom of LG6 in 'Sweetheart' ($p<0.0001$). This distortion overlaps with the *S*-locus, and it is due to gametophytic self-incompatibility in sweet cherry (reviewed in Herrero et al., 2017). Due to the presence of a common *S*-haplotype (S_3) in the two parental cultivars ('Ambrunés', S_3S_6; 'Sweetheart', $S_3S_{4'}$) only 'Sweetheart' $S_{4'}$ pollen can grow down the style, as a result, segregation distortion against S_3 allele and the linked haplotype is observed. A similar segregation distortion, due to cross-incompatibility, in the surroundings of the *S*-locus is common in other sweet cherry and *Prunus* maps (Klagges et al., 2013; Guajardo et al., 2015).

Fruit size

The fruits of 'Sweetheart' had larger diameters and weights than 'Ambrunés' fruits in both years. These values are expected since 'Ambrunés' is a landrace and 'Sweetheart' is a commercial variety from a breeding program. Neither weight nor diameter values of 'Ambrunés' and 'Sweetheart' showed large differences between years, despite the fact that different number of fruits were used for phenotyping between years. These results indicated that phenotyping of larger number of fruits did not result in a significant difference in weight or diameter. In the progeny, normal distribution was observed for weight and diameter, as has also been reported in other sweet and sour cherry studies (Lamb 1953; Fogle 1961; Wang et al., 2000; Zhang et al., 2010; Campoy et al., 2015). In these works, as it happened herein, means of fruit diameter and weight in the population

were lower than parental midpoint, showing an apparent dominance of small fruit alleles. These results suggest that the identification of alleles linked to large sized fruits are extremely helpful for MAS of these traits.

The broad-sense heritability (H^2) values of fruit size traits was moderately high, revealing that a significant portion of the phenotypic variation has a genetic nature, and that some, but not all of the variation observed in these traits can be selected through MAS. Diameter heritability identified herein (0.66) was similar to that estimated by Zhang et al. (2010) for fruit diameter also in two harvest seasons (0.69). However, fruit weight heritability observed in this work (0.63) was lower than that estimated previously in two populations, 'Regina' × 'Garnet' (R×G; H^2=0.76) and 'Regina' × 'Lapins' (R×L; H^2=0.88), evaluated during seven years (Campoy et al., 2015).

Main and stable fruit size (weight and diameter) QTLs identified herein (*qP-Wei1.1*^{m}, *qP-Dia1.1*^{m} and *qP-Dia1.2*^{m}) were found in the middle region of LG1 of 'Ambrunés' map. Since *qP-Wei1.1*^{m} and *qP-Dia1.2*^{m} are overlapping, and both traits are highly correlated, these QTLs are probably the same fruit size determinant phenotyped in two different ways in this work. Fruit weight QTLs, *FW_G1* and *fw1.1*, in the same region, were previously mapped in sweet cherry (Rosyara et al., 2013; Campoy et al., 2015). QTL *fw1.1* spans the three LG1 size QTLs detected in this study (*qP-Wei1.1*^{m}, *qP-Dia1.1*^{m} and *qP-Dia1.2*^{m}), while *FW_G1* detected by Rosyara et al. (2013) overlaps only with *qP-Wei1.1*^{m} and *qP-Dia1.2*^{m}. Thus, the large QTL *fw1.1* (Campoy et al., 2015) is revealed herein as two nearby different QTLs, one of them previously reported by Rosyara et al. (2013), and another in a higher position that is associated to diameter and firmness (see below). Fruit size QTLs in the same LG1 region have been also found in peach (Da Silva Linge et al., 2015; Quilot et al., 2004; Eduardo et al., 2011). In fact, *Cell Number Regulator* (*CNR*) genes have been proposed as strong candidate genes for fruit size on this LG1 region (De Franceschi et al., 2013). This is the case of *PavCNR09*, *PavCNR10* and *PavCNR11*, that were mapped at 30 Mbps in peach chromosome 1 (De Franceschi et al., 2013) corresponding to same interval region spanned by *qP-Wei1.1*^{m} and *qP-Dia1.2*^{m} (27.00 - 31.94 Mbp) in this work.

A larger percentage of the phenotypic variation explained by LG1 size QTLs was observed herein (up to 12.9% of diameter, and up to 17.5% of weight) than in earlier works (8.1 to 9.1%; Rosyara et al., 2013; Campoy et al., 2015), while similar additive effect was

observed (0.4 to 0.8 g ; Rosyara et al., 2013; Campoy et al., 2015). These results indicate that the effect of these LG1 QTLs may vary depending on the genetic background and environmental conditions, and that 'Ambrunés' alleles have a significant positive effect in this trait. In fact, haplotype analysis revealed that 'Ambrunés' haplotypes *Wei1.1_H2*, *Dia1.1_H2* and *Dia1.2_H2* are associated with larger sized fruits and should be selected when breeding for size using 'Ambrunés'.

Other fruit size QTLs previously detected in sweet cherry (Zhang et al., 2010; Rosyara et al., 2013; Campoy et al., 2015), were also validated in this work with minor and less stable effect. This is the case of weight QTLs *qP-Wei2.1*, *qP-Wei3.1* and *qP-Wei5.1* that corresponded to previously detected QTLs for the same trait, *FW_G2c*, *fw3.2* and *fw5.1*, respectively (Rosyara et al., 2013; Campoy et al., 2015). However, the major QTL associated with fruit size previously found on LG2 of cherry (Zhang et al., 2010; Rosyara et al., 2013) was not detected in this study. Fruit size SSR marker BPPCT034, which is located within the QTL region is heterozygous in the parental cultivars ('Ambrunés' 222/229 and 'Sweetheart' 222/332; Cai et al., 2017). Additionally, SNP haplotype analysis of this QTL region confirmed that the parental cultivars 'Ambrunés' and 'Sweetheart' are heterozygous for this genomic region and have one allele in common (data not shown). Therefore, despite this QTL is segregating in this family, no phenotypic differences were observed among the segregating classes (data not shown), explaining why the QTL was not detected.

Firmness

Firmness in 'Ambrunés' and 'Sweetheart' was slightly different between years (Y1 and Y2). This difference may be due to the larger number of phenotyped fruits in Y2, which may have achieved a better accuracy, or else environmental conditions of different harvest years may have influenced this trait. The values of 'Ambrunés' firmness observed in this work, are similar of those described before for the same cultivar at different ripening stages (1.15 N/mm to 2.35 N/mm; Serradilla et al., 2011b and 2012), but 'Sweetheart' firmness values observed here were higher than those described previously at the same ripening stage (1.60 N/mm; Serradilla et al., 2012). Because firmness is highly dependent on the ripening stage (Serradilla et al., 2012) slight differences in the ripening stage during

Table 5.3 Mean phenotypic values of fruit weight, diameter and firmness haplotypes of QTLs detected in two years. Haplotypes highlight in bold are associated with the increase in phenotype values.

Trait	Parent	LG	QTL	Haplotypes	Y1		Y2	
					Mean	N	Mean	N
Weight	'Ambrunés'	1	*qP-Wei1.1*^{m}	*Wei1.1_H1*	5.2 ± 0.9 ^{a}	46	5.5 ± 1.2 ^{a}	56
				Wei1.1_H2	**6.1 ± 1.1** ^{b}	**43**	**6.6 ± 1.5** ^{b}	**33**
Diameter	'Ambrunés'	1	*qP-Dia1.1*^{m}	*Dia1.1_H1*	21.0 ± 1.5 ^{a}	32	20.9 ± 2.1 ^{a}	42
				Dia1.1_H2	**22.2 ± 2.0** ^{b}	**32**	**22.8 ± 2.3** ^{b}	**27**
		1	*qP-Dia1.2*^{m}	*Dia1.2_H1*	21.1 ±1.6 ^{a}	46	21.1 ± 2.0 ^{a}	56
				Dia1.2_H2	**22.1 ± 1.7** ^{b}	**44**	**22.5 ± 2.2** ^{b}	**34**
Firmness	'Ambrunés' / 'Sweetheart'	1	*qP-Fir1.1*^{m} / *qP-Fir1.2*^{m}	*Fir1.1_H1 / Fir1.2_H1*	1.4 ± 0.4 ^{a}	9	1.5 ± 0.33 ^{a}	13
				Fir1.1_H1 / Fir1.2_H2	1.4 ± 0.4 ^{a}	19	1.3 ± 0.42 ^{a}	24
				Fir1.1_H2 / Fir1.2_H1	**2.2 ± 0.8** ^{b}	**22**	**2.0 ± 0.6** ^{b}	**19**
				Fir1.1_H2 / Fir1.2_H2	1.7 ± 0.6 ^{a}	20	1.4 ± 0.4 ^{a}	19
	'Ambrunés'	6	*qP-Fir6.1*^{m}	***Fir6.1_H1***	**2.0 ± 0.8** ^{a}	**34**	**1.8 ± 0.6** ^{a}	**37**
				Fir6.1_H2	1.6 ± 0.7 ^{b}	52	1.4 ± 0.5 ^{b}	52

Different letters indicate significant differences between means at P<0.05

sampling may account for firmness differences. However, most likely the elevate area where the plant material is grown (the Jerte Valley at 800 m above sea level) may have had a relevant effect in fruit firmness in 'Sweetheart', as growing at high altitude has been observed to increase fruit firmness (Chagné et al., 2014). However, 'Ambrunés' fruits are more adequate for post-harvest storage, as firmness in 'Ambrunés' fruits is maintained through post-harvest storage whereas 'Sweetheart' firmness decreases rapidly during conservation (Serradilla et al., 2012).

Previous works on cherry firmness QTLs used a different phenotyping protocol and equipment, and therefore it is not possible to compare the firmness values. In the works by Campoy et al. (2015) and Cai et al. (2019), Durofel® and BioWorks FirmTech 2, respectively, were used for phenotyping, while a texturometer was used in this study. Firmness distribution in the populations studied by Campoy et al. (2015) fitted to normal distribution in all evaluated years, whereas the A×S population shows a skewed segregation to softer fruits in both years, as previously observed in 'Fercer' × 'X' (Cai et al., 2019), probably due to dominance of alleles of softer fruit. Firmness heritability identified in this work (0.75) was within the range previously observed in other sweet cherry populations for this trait (0.73-0.97) (Campoy et al., 2015; Cai et al., 2019).

In this work, a major firmness QTL was also detected on LG1, in this case in both parental cultivars (*qP-Fir1.1*^{m} and *qP-Fir1.2*^{m}). These two QTLs were located nearby and they do not overlap, however, since QTL analysis in each parental map was carried out using different markers, it is highly likely that both QTLs correspond to the same region and it is the same QTL. In fact, a firmness QTL in the same region was previously reported by Campoy et al. (2015) in an F_1 population, and by Cai et al. (2019) in a genome-wide fruit firmness association study of a sweet cherry germplasm collection. Again, as observed for fruit size QTLs on LG1, the PVE of this QTL was lower in earlier works (6.4%; Campoy et al., 2015) than reported in our population (10.2 to 22.5%). It is relevant to notice that for this QTL, a negative additive effect was observed for 'Sweetheart' whereas a positive additive effect was found in 'Ambrunés'. Previously, a negative additive effect was also observed (Campoy et al., 2015). Thus revealing that 'Ambrunés' carries alleles which increase firmness while 'Sweetheart' and other related cultivars may decrease firmness in breeding programs.

The other stable QTL associated to firmness was detected on 'Ambrunés' LG6 (*qP-Fir6.1*^{m}). In prior studies, Campoy et al. (2015) and Cai et al. (2019) reported this same QTL on other plant material. An *endopolygalacturonase* (*endoPG*) homolog gene, implicated in fruit softening by cell wall modifying (Brummell and Harpster, 2001), has been proposed as best candidate to fruit firmness control of this QTL (Campoy et al., 2015). A major firmness QTL reported on LG4 reported in sweet cherry (Cai et al., 2019) was not detected in this work. 'Ambrunés' and 'Sweetheart' are homozygous for same firm allele (*H1H1*) of this QTL (*qP-FF4.1*; Cai et al., 2019), explaining why this QTL was not detected in this study, and why these two cultivars are quite firm.

The haplotype analysis of these QTLs allowed identifying favorable haplotypes (*Fir1.1_H2/Fir1.2_H1* and *Fir6.1_H1*) for firmness breeding using these cultivars. Pyramidal selection of these favorable alleles would lead firmer cultivars. This fact was observed in the 'Ambrunés' haplotypes of *qP-Fir1.1*^{m} and *qP-Fir6.1*^{m}, where individuals with the two firmness haplotypes (*Fir1.1_H2* and *Fir6.1_H2*) were associated with a firmness increase. In addition, 'Ambrunés' haplotypes for QTLs on LG1 associated to fruit size and firmness increase were found on coupling phase, allowing to select a unique 'Ambrunés' LG1 haplotype region to gain fruit size and firmness.

Fruit size and firmness correlation and interaction

The very high (r=0.95-0.96) significant positive correlation observed between weight and diameter in this work indicates that both traits are highly dependent and that either of them could be used indistinctly to measure size. Nevertheless, no correlation between firmness and weigh was observed, but moderate positive correlation between firmness and diameter was observed in Y2, indicating that in certain conditions larger size may also be associated to higher firmness in this plant material.

In fact, in Y2 transgressive positive segregation was observed for the three traits. Campoy et al. (2015) described a significant negative correlation between firmness and weight for two sweet cherry F_1 populations. This negative correlation means that selecting for heavier fruits will result in softer fruits, thus providing a complex scenario for fruit quality breeding in sweet cherry. As herein, Chavoshi et al. (2014) and Piaskowski et al. (2018) observed a moderate positive correlation between fruit firmness and size in the plant

material of the RosBREED sweet cherry crop reference set. These results indicate that distinct genetic backgrounds show different relationship between size and firmness, probably due to the presence of diverse alleles controlling these traits in the different plant materials. The absence of a negative correlation between these traits in this work, and the observation of slight positive correlation between firmness and diameter, indicates that it is possible to select for larger and firmer fruits at the same time in this genetic background (A×S). As an example, offspring L35-60, L35-65, L35-70 and L35-72 showed diameter, weight and firmness values larger than the parental midpoint in both years. These results confirm that 'Ambrunés' could be a useful cultivar for firmness and fruit quality breeding.

The overlapping of main firmness (*qP-Fir1.1*^{m}) and diameter (*qP-Dia1.1*^{m}) QTLs on LG1 of 'Ambrunés' also comes to confirm the correlation between both traits, indicating a possible common genetic determinism. Previous co-localizations of fruit size and firmness QTLs were also reported in sweet cherry and in peach (Campoy et al., 2015; Zeballos et al., 2016).

SUPPLEMENTARY MATERIALS CHAPTER 5

Supplementary Table 5.1 Summary of phenotypic data for fruit weight, diameter and firmness for an A×S population in year 2015 and 2016 (Y1 and Y2).

		Weight (g)		Diameter (mm)		Firmness (N/mm)	
		Y1[a]	**Y2[b]**	**Y1[a]**	**Y2[b]**	**Y1[a]**	**Y2[b]**
'Ambrunés'		5.8	6.8	21.6	22.8	2.0	1.5
'Sweetheart'		11.3	9.5	27.7	25.8	2.2	2.1
A×S	mean	5.6	5.9	21.6	21.6	1.7	1.5
	s.d.	1.1	1.3	1.7	2.1	0.7	0.6
	Min.	3.4	2.9	16.8	16.4	0.6	0.7
	Max.	11.3	13.1	25.7	29.1	3.8	3.4
	H^2	0.63		0.66		0.75	

[a] Measures performed on 10 fruits per individual in year 1; [b] Measures performed on 25 fruits per individual in year 2. s.d.: standard deviation; H^2: Broad-sense heritability.

Supplementary Table 5.2 Genetic position of RosBREED cherry 6K SNP Array v1 SNPs mapped in 'Ambrunés', 'Sweetheart' and consensus map (A×S).

Document available online at http://hdl.handle.net/10532/4737. (Chapter 5 – Supplementary Table 2.xlsx).

Supplementary Table 5.3 SNP markers that were placed on the 'Ambrunés', 'Sweetheart' and A×S genetic maps in different linkage groups compared to their physical map locations on the peach genome v2.0.a1.

	Physical position Peach Genome v2.0.a1		Genetic position (cM)			
SNP	**Chr**	**Position**	**LG**	**'Ambrunés'**	**'Sweetheart'**	**A×S**
ss490545975	1	7885062	8	54.74	-	52.09
ss490549697	2	21123343	1	-	37.64	90.73
ss490547096	2	1599643	8	-	13.66	17.89
ss490551427	3	8158606	6	64.12	-	59.56
ss490550875	3	1870601	8	-	47.18	51.52
ss490548878	4	19842873	7	3.83	-	3.83
ss490548882	4	21492752	8	-	26.29	30.68
ss490555342	6	6504161	1	-	18.13	70.34
ss490557958	8	10717040	2	-	22.77	26.01

Supplementary Table 5.4 Significance, genetic intervals, QTL peaks and physical positions of minor QTLs identified for fruit weight, diameter and firmness in the A×S population.

Trait	Parental	Year	QTL name	LG	QTL interval (cM)	Physical position*	QTL peak					QTL previosly described (Reference)
							SNP	LOD	Variance	PVE	Additive effect	
Weight	'Ambrunés'	Y1	*qP-Wei1.1*^{m}	1	118.1-119.9	30.69-31.94	ss490546431	3.26	1.03	15.4	0.43	[1, 2]
		Y2	*qP-Wei1.1*^{m}	1	97.8-119.9	27.00-31.94	ss490547198	4.27	1.44	17.8	0.63	
		Y2	*qP-Wei5.1*	5	21.2-31.1	8.85-10.23	ss490549133	2.00	1.58	8.7	-0.43	[2]
	'Sweetheart'	Y2	*qP-Wei2.1*	2	67.4-70.2	26.16-26.91	ss490550363	1.31	1.56	5.5	0.36	[1, 2]
		Y2	*qP-Wei3.1*	3	21.1-25.7	23.62-24.41	ss490552023	2.77	1.55	11.9	0.59	[1, 2]
Diameter	'Ambrunés'	Y1	*qP-Dia1.1*^{m}	1	69.1-79.2	15.85-23.82	ss490546727	2.69	2.63	12.9	0.62	[2]
		Y2	*qP-Dia1.1*^{m}	1	57.2-71.1	11.55-19.96	ss490546442	2.36	4.01	11.0	0.71	
		Y1	*qP-Dia1.2*^{m}	1	100.7-115.8	28.21-30.34	ss490547003	2.26	2.69	10.9	0.77	[1, 2]
		Y2	*qP-Dia1.2*^{m}	1	103.8-118.9	28.94-30.76	ss490547003	2.32	4.02	10.8	0.82	
		Y1	*qP-Dia7.1*^{m}	7	78.2-84.8	17.46-19.62	ss490559061	1.87	2.23	7.4	0.49	[2]
		Y2	*qP-Dia7.1*^{m}	7	75.9-78.2	17.34-17.46	ss490557256	1.33	3.42	5.2	0.49	
		Y1	*qP-Dia8.1*	8	82.9-84.8	21.67-22.48	ss490551557	1.63	2.24	6.5	-0.44	[2]
	'Sweetheart'	Y2	*qP-Dia3.1*	3	21.1-25.7	23.62-24.41	ss490552064	1.46	3.97	6.6	0.55	[1, 2]
		Y1	*qP-Dia5.1*	5	50.1-56.7	15.81-16.63	ss490554609	1.60	2.78	7.8	0.49	[2]
Firmness	'Ambrunés'	Y1	*qP-Fir1.1*^{m}	1	64.0-67.1	14.73-15.75	ss490546599	3.25	0.23	12.5	0.20	[2, 3]
		Y2	*qP-Fir1.1*^{m}	1	59.3-66.0	12.62-15.11	ss490546554	4.08	0.45	18.8	0.33	
		Y1	*qP-Fir6.1*^{m}	6	38.9-47.5	7.94-9.93	ss490555475	1.64	0.42	6.7	0.20	[2, 3]
		Y2	*qP-Fir6.1*^{m}	6	39.9-42.8	8.01-8.52	ss490555470	3.67	0.23	14.3	0.22	
	'Sweetheart'	Y1	*qP-Fir1.2*^{m}	1	16.1-32.1	15.25-24.18	ss490546651	5.00	0.43	22.5	-0.69	[2, 3]
		Y2	*qP-Fir1.2*^{m}	1	24.5-27.8	22.30-23.86	ss490559249	2.43	0.26	10.2	-0.18	
		Y2	*qP-Fir3.1*	3	16.4-21.1	21.02-23.62	ss490552038	1.36	0.26	5.6	0.14	[2, 3]

* Physical position (Mbps) of SNP markers in peach genome v2.0.a1 (Verde et al., 2017). References: [1] Rosyara et al., 2013, [2] Campoy et al., 2015, [3] Cai et al., 2019.

Supplementary Table 5.5 Haplotypes for stable fruit weight, diameter and firmness QTLs identified in 'Ambrunés' and 'Sweetheart' cultivars. SNP physical positions (bp) are estimated from the Peach Genome v2.0.a1 (Verde et al., 2017).

qP-Wei1.1^m					
Parent	**SNP**	**Chr**	**bp**	***Wei1.1_H1***	***Wei1.1_H2***
'Ambrunés'	ss490547198	1	30690215	B	A
	ss490546431	1	30764281	A	B

qP-Dia1.1^m					
Parent	**SNP**	**Chr**	**bp**	***Dia1.1_H1***	***Dia1.1_H2***
'Ambrunés'	ss490546442	1	11556023	B	A
	ss490546096	1	12618203	A	B
	ss490546554	1	14735491	B	A
	ss490546591	1	15601111	B	A
	ss490546599	1	15753605	B	A
	ss490546727	1	22976838	B	A
	ss490546746	1	23079385	B	A
	ss490546762	1	23528689	A	B

qP-Dia1.2^m					
Parent	**SNP**	**Chr**	**bp**	***Dia1.2_H1***	***Dia1.2_H2***
'Ambrunés'	ss490547198	1	30690215	B	A
	ss490546431	1	30764281	A	B

qP-Fir1.1^m					
Parent	**SNP**	**Chr**	**bp**	***Fir1.1_H1***	***Fir1.1_H2***
'Ambrunés'	ss490546096	1	12618203	A	B
	ss490546554	1	14735491	B	A
	ss490546591	1	15601111	B	A
	ss490546599	1	15753605	B	A

qP-Fir1.2^m					
Parent	**SNP**	**Chr**	**bp**	***Fir1.2_H1***	***Fir1.2_H2***
'Sweetheart'	ss490546611	1	16036105	A	B
	ss490558902	1	17583149	B	A
	ss490546643	1	17586989	B	A
	ss490546651	1	18545593	B	A
	ss490546675	1	20811017	A	B
	ss490546679	1	20973954	B	A
	ss490559249	1	22747528	B	A
	ss490546811	1	24183767	A	B
	ss490546835	1	24878680	A	B

Supplementary Table 5.5 Continued.

			qP-Fir6.1^m		
Parent	**SNP**	**Chr**	**bp**	***Fir6.1_H1***	***Fir6.1_H2***
'Ambrunés'	ss490555431	6	7943753	A	B
	ss490555470	6	8528220	A	B
	ss490555475	6	8612200	A	B
	ss490555481	6	8706130	A	B

Supplementary Table 5.6 Mean fruit firmness for A×S progeny based on haplotypes for two firmness 'Ambrunés' QTLs (*qP-Fir1.1^m* and *qP-Fir6.1^m*).

qP-Fir1.1^m	***qP-Fir6.1^m***	**Y1**		**Y2**	
		Mean	**N**	**Mean**	**N**
Fir1.1_H1	*Fir6.1_H1*	1.6 ± 0.4 ^{a}	11	1.5 ± 0.3 ^{a}	15
Fir1.1_H1	*Fir6.1_H2*	1.3 ± 0.4 ^{a}	23	1.3 ± 0.4 ^{a}	26
Fir1.1_H2	***Fir6.1_H1***	**2.3 ± 0.9 ^{c}**	**19**	**2.0 ± 0.7 ^{b}**	**16**
Fir1.1_H2	*Fir6.1_H2*	1.8 ± 0.7 ^{ab}	24	1.6 ± 0.5 ^{a}	23

Different letters indicate significant differences between classes (P<0.05)

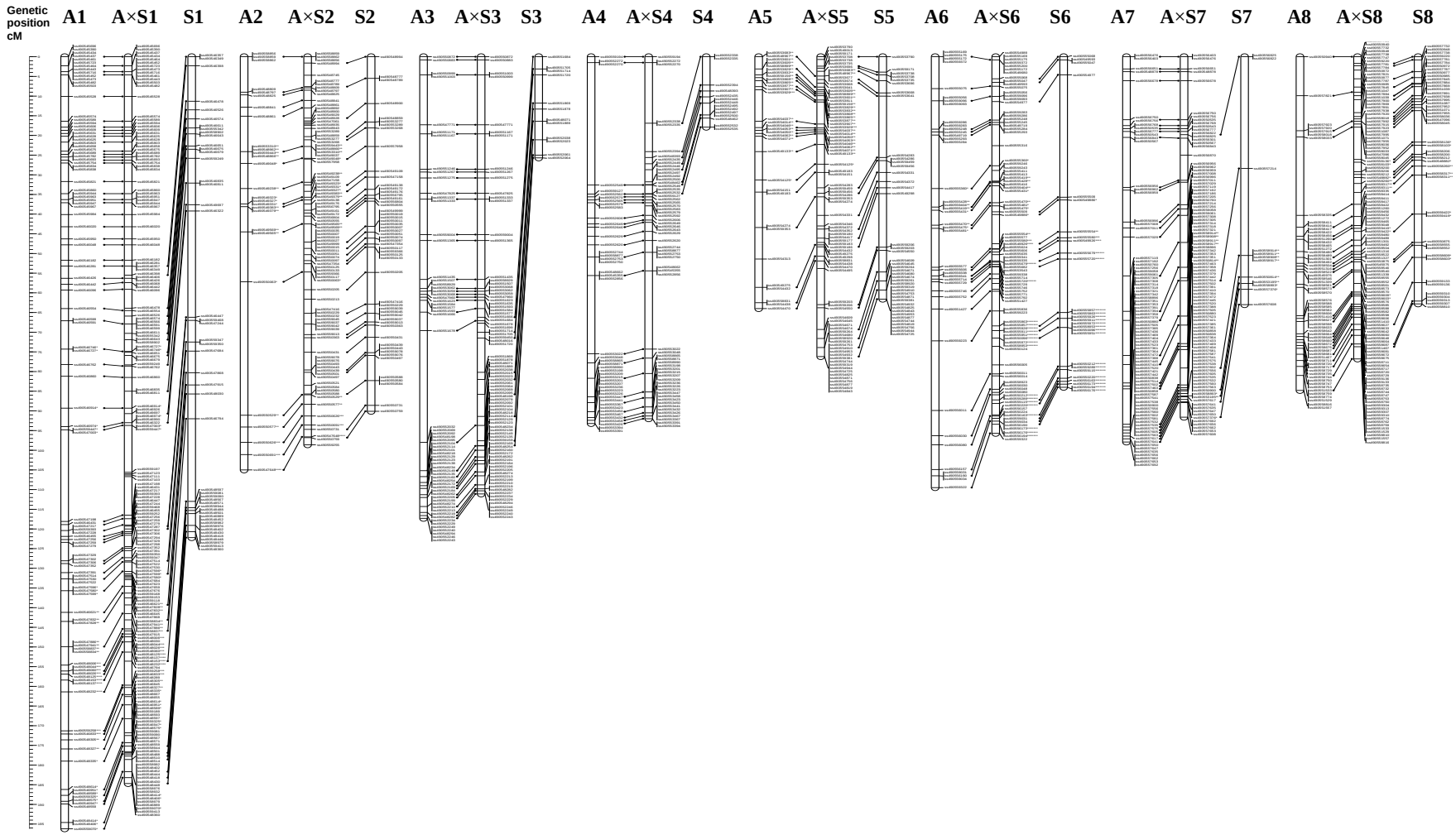

Supplementary Figure 5.1 Alignment of linkage groups for ‘Ambrunés’ (A), ‘Sweetheart’ (S) and the ‘Ambrunés’ × ‘Sweetheart’ (A×S) consensus maps. Asterisks indicate deviation from expected Mendelian segregation (*p<0.1; ** p<0.05; ***p<0.01; **** p<0.005; ***** p<0.001; ****** p<0.0001

CHAPTER 6

QTL MAPPING OF PHENOLOGICAL AND FRUIT QUALITY TRAITS IN MULTIPLE SWEET CHERRY POPULATIONS

INTRODUCTION

Sweet cherry (*Prunus avium* L.), being the earliest ripening stone fruit, and due to its great acceptance, is a highly demanded fruit. Sweet cherries are mainly consumed as fresh fruit, so its market profit is directly related to maturity date and fruit quality (Yue et al., 2014). Maturity date is determinant in sweet cherry price, with early ripening cultivars reaching the highest prices (Zheng et al., 2016). Additionally, due to their narrow ripening period (4 to 5 weeks), extending the harvesting period has become a priority in breeding programs (Dirlewanger et al., 2009). As a result, as well as early ripening cultivars, late maturing cultivars that extend harvest season are sought. Maturity date is related to bloom date and fruit development, with early flowering and short fruit development advancing maturity, although not all late ripening cultivars are late blooming. These traits (bloom date, maturity date and fruit development) display broad inter-annual variability, but a large positive correlation between them has been observed, especially for fruit development and maturity date in apricot and peach (Etienne et al., 2002; Salazar et al., 2016). Although early maturity is a breeding objective, early bloom may not always be a desired trait, as in colder regions early blooming may result in damage due to spring freeze. Thus, the investigation of fruit development time and maturity date, their relationship, and that with bloom time, is of high interest for breeding for early and late maturity in sweet cherry, and for cultivar adaptation to different growing areas.

Quantitative trait locus (QTL) analyses have been conducted in sweet cherry to investigate the genetic control of maturity date (Dirlewanger et al., 2012; Quero-Garcia et al., 2014; Isuzugawa et al., 2019) but not that of fruit development period. Analysis of maturity date in a 'Regina' × 'Lapins' population during three years (Dirlewanger et al., 2012; Quero-García et al., 2014) identified three stable QTLs on linkage groups (LGs) 1, 4 and 5, with a large percentage of variation explained by QTL on LG4 (20.4%), which was associated with advancing maturity 5.4 days (Dirlewanger et al., 2012). This main QTL for maturity day was also identified by Isuzugawa et al. (2019) in the segregating sweet cherry population of 'Beniyutaka' × 'Benikirari' explaining 48.4% of the variation. The same QTL on LG4 has been reported in other *Prunus* species like apricot (*Prunus armeniaca* L.), peach (*Prunus persica* L.) and plum (*Prunus salicina* Lindl.) as the main maturity date QTL (Quilot et al., 2004; Dirlewanger et al., 2012; Nuñez-Lillo et al., 2015;

Salazar et al., 2016 and 2017). Fruit development time has also been investigated in apricot and peach, and a main QTL for this trait was found on the same region detected for maturity date on LG4 in these species (Fresnedo-Ramírez et al., 2015; Salazar et al., 2016; Hernández Mora et al., 2017).

The other main trait of sweet cherry marketability is fruit quality, which depends on various fruit traits, including fruit size, taste, flavor, firmness, sweetness, acidity, skin color and external appearance (Crisosto et al., 2003; Yue et al., 2014; Zheng et al., 2016). Within consumer preferences, fruits with large size, sweet, firm, long shelf life and adequate balance between soluble solids content and titratable acidity have been identified as main attributes to select sweet cherries (Whiting et al., 2006; Chauving et al., 2009). Main QTL analyses regarding sweet cherry fruit quality traits have been conducted on fruit size (Zhang et al., 2010; Rosyara et al., 2013; Campoy et al., 2015; Chapter 5). Zhang et al. (2010) reported fruit size and weight QTLs on LGs 2 and 6 of the population 'New York 54' × 'Emperor Francis'. Alike, Rosyara et al. (2013) detected four novel QTLs associated with fruit weight on LGs 1, 2 and 3; and Campoy et al. (2015) reported a major fruit weight QTL at the bottom region of 'Regina' LG5. More recently, main QTLs controlling fruit size were found on LG1 of Spanish landrace 'Ambrunés', overlapping with a fruit firmness QTL (Chapter 5). For fruit firmness, a large number of minor QTLs controlling this trait were detected in sweet cherry, although two major QTLs showing the largest percentage of variation were found on LGs 2 and 5 (Campoy et al., 2015). However, a recent analysis using a large sample of sweet cherry cultivars and populations revealed a main QTL controlling fruit firmness on LG4 explaining up to 84.6% of phenotype variation (Cai et al., 2019). Additionally, in Chapter 5 using a population derived from the firmness cultivars 'Ambrunés', we identified two main QTLs on LGs 1 and 6 associated with increasing up to 0.33 N/mm in fruit firmness. QTLs analysis of fruit acidity and solid soluble content were reported in apricot, peach and plum (Quilot et al., 2004; Eduardo et al., 2011; Zeballos et al., 2016; Salazar et al., 2013 and 2017) but not in sweet cherry. Main QTLs controlling these traits were located on LGs 1, 2, 4 and 5 for apricot (Salazar et al., 2013), on LGs 4 and 5 for peach (Quilot et al., 2004; Eduardo et al., 2011; Zeballos et al., 2016) and on LGs 1 and 6 for plum (Salazar et al., 2017).

Despite the efforts to understand the genetic control of these traits, the narrow genetic diversity used for QTL analyses and mapping strategies based on single bi-parental

populations, limits QTL detection and difficult marker assisted selection (MAS) implementation in plant material from other genetic backgrounds. Only three major studies on fruit size (Rosyara et al., 2013), fruit firmness (Cai et al., 2019) and bloom time (Chapter 3) have combined a large number of individuals from multiple sweet cherry populations for QTL analysis, resulting in the identification of large stable QTLs for these traits. Thus, larger studies of other relevant traits are necessary to understand maturity and fruit quality genetics in sweet cherry. With this aim, a multi-family approach was used in this work to identify QTLs responsible of maturity date and fruit quality traits in sweet cherry, some of them primarily considered for this species herein, as fruit development time, solid soluble content and titratable acidity. This multi-family approach was carried out using, six F_1 and two F_2 sweet cherry populations, that also descend from local plant material such as 'Ambrunés' or 'Cristobalina'. The landrace cultivar 'Ambrunés' that presents very late ripening, is collected without peduncle, and also has excellent organoleptic quality and great post-harvest aptitude (Serradilla et al., 2012). The landrace 'Cristobalina' is a self-compatible cultivar with low chilling requirements and extra-early maturity date (Wünsch and Hormaza, 2004; Alburquerque et al., 2008; Chapter 3).

MATERIALS AND METHODS

Plant materials

In this work, 411 sweet cherry genotypes from six full-sib populations (N=406), the parental cultivars (N=6) and some ancestors (N=5) were studied (Chapter 3). This material include four cross-pollination populations (F_1), 'Vic' × 'Cristobalina' (V×C; N=158), 'Ambrunés' × 'Cristobalina' (A×C; N=40), 'Brooks' × 'Cristobalina' (B×C; N=29) and 'Lambert' × 'Cristobalina' (L×C; N=14), and two self-pollination populations (F_2.). One F_2 comes from 'Cristobalina' self-pollination (C×C; N=97), and the other from the self-pollination of selection 'BC8' (B×C2; N=68). All the plant material are found at CITA de Aragón orchards (Zaragoza, Spain).

Trait phenotyping

Phenotype data for seven agronomical and fruit quality traits were evaluated during two years (2017 and 2018) in all the plant material. The traits evaluated were: maturity date (MD), fruit development time (FD), fruit size (FS), fruit weight (FW), fruit firmness (FF), fruit titratable acidity (TA) and fruit solid soluble contents (SSC). All fruit traits were evaluated at the estimated optimum ripening stage of each tree. Bloom time (BT) data of this plant material, the same two years, (data previously reported in Chapter 3), was used in correlation tests with traits analyzed in this work.

MD was recorded in calendar days from January 1st as the date when 50% of fruits reached the optimum ripening stage based on visual inspection of fruit color, taste and firmness. FD was the time that the fruit needed to complete development, and it comprised the days between BT and MD. For fruit quality traits, 15 fruits per tree were collected with peduncle at harvest time, and each trait was measured in each individual fruit. FW was measured using a scale, FS was determined on the medio-lateral axis using a calliper and FF was assessed on two opposite medio-lateral axis using DuroColor® texture analyser (Setop Giraud Technologie, Cavaillon, France) and data was expressed in firmness percentage of Durocolor®. TA and SSC data was obtained from juice of the same 15 fruits. TA was determined by titrating 5 g of fruit juice with NaOH 0.1 N to pH 8.1 (AOAC, 1984) using an automatic titrator (Metrohm, Herisau, Swiss). The solid soluble contents (SSC) were determined by dropping a fruit juice into a refractometer (Atago, Tokyo, Japan) and the data were given in ºBrix.

Statistical analysis

Statistical analysis of data were performed to estimate the mean, minimum, maximum and standard deviation in each population per year and trait. Correlation between traits for each year were analyzed using the *Pearson* correlation coefficient. To evaluate whether trait data followed a normal distribution, normality analyses were performed per trait and year using the Shapiro-Wilk test. Broad-sense heritability (H^2) was calculated using the equation: $H^2 = \frac{\sigma_g^2}{\sigma_g^2 + \frac{\sigma_e^2}{n}}$, where σ_g^2 is the variance of genotype effect, σ_e^2 is the variance of the residual term and n is the number of years. All statistical analyses were performed using R v3.4.1 (R Core Team, 2017).

QTL analysis and haplotype construction

The plant material used in this study were previously genotyped with RosBREED cherry 6K SNP array v1 (Chapter 1). For QTL analyses, the Bayesian multiple QTL model implemented in FlexQTL™ (Bink et al., 2008 and 2014) software was used, considering the parameters and linkage map previously described in Chapter 3. Only additive effect with normal prior distribution was considered. Whole-genome QTL analysis was carried out four times for each trait varying prior number of QTLs (1 and 3) and seed numbers to create independence between iterations. For each simulation, Markov chain Monte Carlo (MCMC) simulations with minimum of 500,000 iterations were performed until at least 100 effective chain samples for the overall mean, the residual variance, the number of QTLs and the variance of this number (Bink et al., 2014). Only QTLs with strong and decisive ($2lnBF>5$ and 10, respectively) evidences were reported. The graphical representations of LGs and QTLs were obtained using MapChart software (Voorrips, 2002).

Parental and ancestor haplotypes were constructed for major stable QTL on LG4 (50-54 cM) for FD, MD and FF. Haplotypes were obtained from SNP phase estimated by FlexQTL™. Mean phenotypic values for each segregating class of each population for those individuals without recombination events were considered. Differences between mean phenotypic classes of each population were evaluated using ANOVA calculations, Kruskal-Wallis and two-tailed Student's test ($p<0.01$). Statistical analyses were carried out using IBM SPSS v21 (Chicago, IL, USA).

RESULTS

Phenotyping

Phenotyping of the parental cultivars revealed differences for all evaluated traits in both years (Sup Table 6.1). These differences were most noticeable for FD (differences of 17 and 20 days each year, almost 3 weeks), MD (35 and 41 days each year, 5 to 6 weeks), FW (5 and 6 g), FS (6 and 8 mm) and FF (17.3 and 22.5%; Sup Table 6.1). For these traits, 'Ambrunés', 'Lambert' and 'Vic' showed the largest FD (around 11 weeks) and latest MD (June 2 to 22nd) whereas 'Lambert' and 'Vic' presented the lowest FF (33 to 50%). On the

other side, ‘Cristobalina’ and ‘Brooks’ exhibited shorter FD (8 to 9 weeks) and largest FF (52.1 to 63.4%), with ‘Cristobalina’ showing the earliest MD (May 2nd to 18th; Sup Table 6.1). For FS and FW, largest values were observed for ‘Brooks’ and ‘Vic’ with values

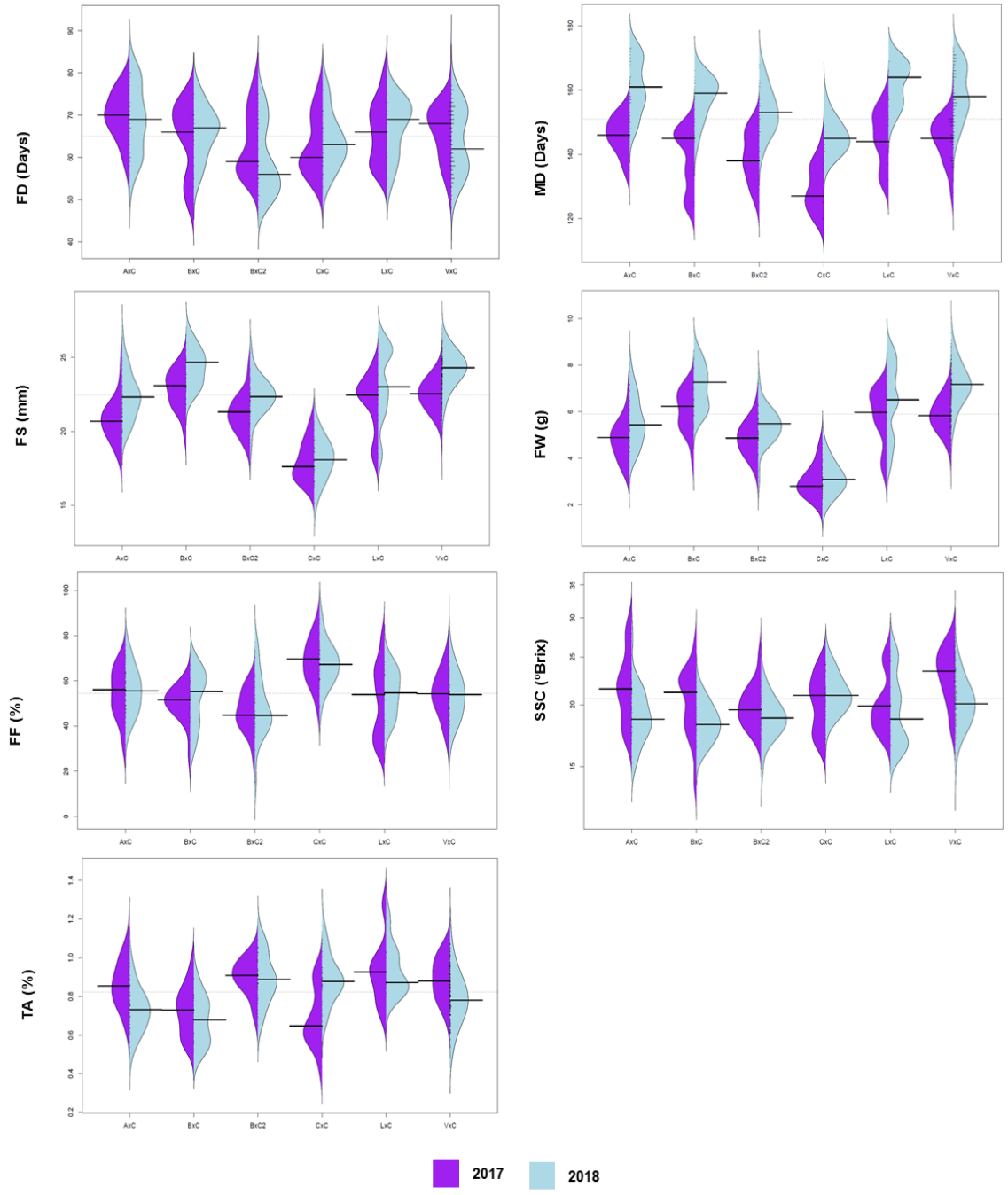

Figure 6.1 Violin plot distribution of phenotyped traits per family in years 2017 (purple) and 2018 (blue). Black lines indicate median values.

around 9 g and 26-27 mm, while ‘Cristobalina’ was by far the smallest with 4 g and 19 mm (Sup Table 6.1). For SSC and TA, parental values showed smaller variation and the results did not reveal any pattern for the same cultivars among years (Sup Table 6.1).

From the six populations analysed, 197 trees (48% of genotyped trees) were phenotyped in 2017 and 257 (63%) in 2018. These data revealed variability in all the populations for all the traits (Fig 6.1). Significant inter-annual variation in the mean phenotype value was observed for all traits except FD and FF (Student’s t test; $p<0.05$), that were the most consistent traits between years (Fig 6.1, Sup Table 6.1). For all the populations, fruits were larger, heavier and matured later in 2018 than in 2017, whereas, except in C×C, sweeter and less acid fruits were harvested in 2017 (Fig 6.1; Sup Table 6.1).

Within populations, large segregation was observed for most traits (Fig 6.1; Sup Table 6.1). For FD, differences larger than a month (36 days, more than 5 weeks) between the shortest (48 days, nearly 7 weeks; trees B×C2-51 and V×C-104; 2018) and largest (84 days, 12 weeks; tree V×C-26; 2017) development period were observed (Fig 6.1; Sup Table 6.1). Between populations, individuals of B×C2 accounted for the shortest FD; and A×C and L×C individuals had the widest periods (Fig 6.1). MD segregation varied within 5 to 6 weeks each year, (120 to 163 days in 2017, and 138 to 173 days in 2018), taking place from early May to late June in both years (Fig 6.1; Sup Table 6.1). C×C population, followed by B×C2 showed the earliest MD, ripening on average 16 days earlier than individuals of other populations (A×C and L×C; Fig 6.1; Sup Table 6.1).

Regarding FS and FW, large variation was also observed within populations, with differences of up to 5.3 g / 7.4 mm, and 8.5 g / 11.4 mm, in the dimension of smaller and larger fruits in 2017 and 2018, respectively (Fig 6.1; Sup Table 6.1). The smallest cherries correspond to C×C individuals, whereas populations derived from bred cultivars (B×C and V×C) had the largest cherries (Fig 6.1). FF displayed broad variation with values ranging from 26.2 to 86.7%, and 15.2 to 87.4%, each year (Sup Table 6.1). Among populations, similar mean FF was observed for A×C, B×C, L×C and V×C ranging from 50.1 to 55.9%. Firmest fruits were, on average, identified in C×C (68.2 and 67.7% in 2017 and 2018, respectively) and the softest in B×C2 (46.5 and 48.2%) (Fig 6.1; Sup Table 6.1). For SSC and TA, large variability was measured, being values of 2018 lower than those observed in 2017 (except for TA in C×C) (Fig 6.1; Sup Table 6.1). Individuals reached values of

SSC of 12.9 to 29.7 ºBrix and 0.43 to 1.28% of TA, being B×C2 and L×C the most acidic populations, and A×C and V×C the sweetest (Fig 6.1; Sup Table 6.1).

Trait distribution were similar both years (Fig 6.2). Only FF, SSC and TA fitted to normal distribution whereas the remaining traits (FD, MD, FW and FS) presented skewed distribution to large phenotype values (Shapiro-Wilk test). A bi-modal distribution for FD was observed both years (Fig 6.2).

Values of broad-sense heritabilities (H^2) varied between traits (0.54 to 0.94) (Table 6.1). Large broad-sense heritability was observed for FD (0.92), MD (0.94), FS (0.93), FW (0.92) and FF (0.84), while lower H^2 were detected for SSC (0.62) and TA (0.54) (Table 6.1).

Trait correlations

Significant correlations between each traits for both years were observed ($p<0.0001$) (Sup Table 6.1). Of these, the largest inter-annual correlations were observed for FD, MD, FW, FS and FF (0.72-0.89), while lower inter-annual correlations were detected for TA and SSC (0.44-0.55) (Sup Table 6.1).

Correlations between pair of traits (Fig 6.2) displayed similar patterns in 2017 and 2018 (Fig 6.2). In both years, high significant positive correlation was observed between FD and MD (0.81 to 0.85), and FW and FS (0.97). These results revealed that fruits that took longer to develop were also the latest to mature, and that largest fruits were also heavier. FD and MD also showed moderate positive correlation with SCC (0.66/0.39 in 2017, and 0.59/0.46 in 2018, respectively), and FD with FF (0.35 in 2017 and 0.56 in 2018) (Fig 6.2). That is, later cherries and those that took longer to develop tended to be firmer and sweeter (Fig 6.2). The analysis of BT data also revealed that in this plant material, BT showed significant moderate positive correlation with MD (0.47 both years), FW (0.52 and 0.58) and FS (0.51 and 0.63 in 2017 and 2018, respectively) (Fig 6.2). In fact, the correlation between these traits was high for early flowering genotypes whereas for medium to late BT genotypes, low or no correlation was observed (Fig 6.2). A negative low-moderate correlation was also observed between FF, and FS and FW (from -0.34 to -0.37) (Fig 6.2), indicating that larger fruits were softer (Fig 6.2).

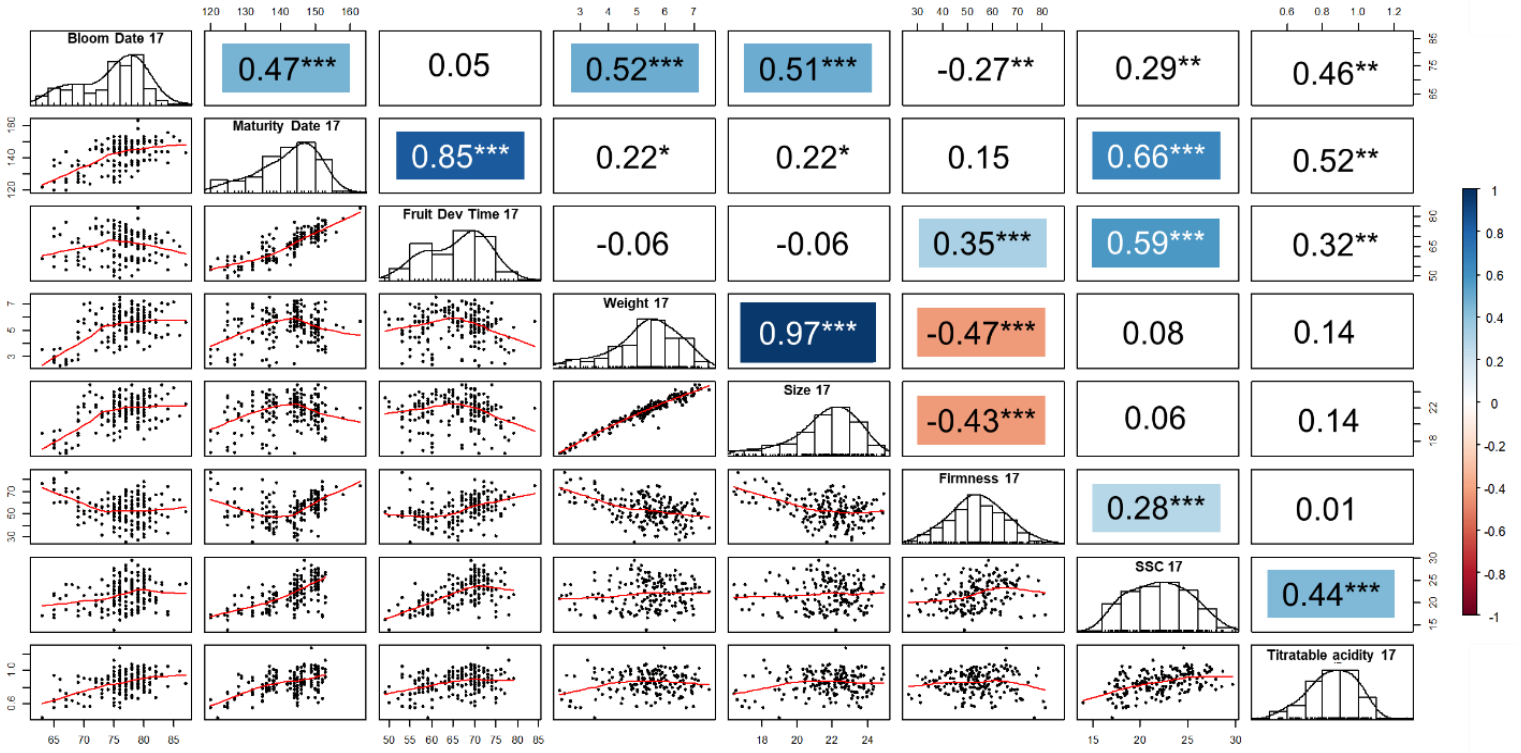

Figure 6.2 *Pearson* correlation coefficient among phenotyped traits, distribution histograms and correlation plots in 2017 and 2018. Asterisks indicate correlation significance level (* p<0.01; ** p<0.001; *** p<0.0001). Positive and negative correlations at p<0.0001 are marked in blue and red respectively, based on *Pearson* correlation coefficient.

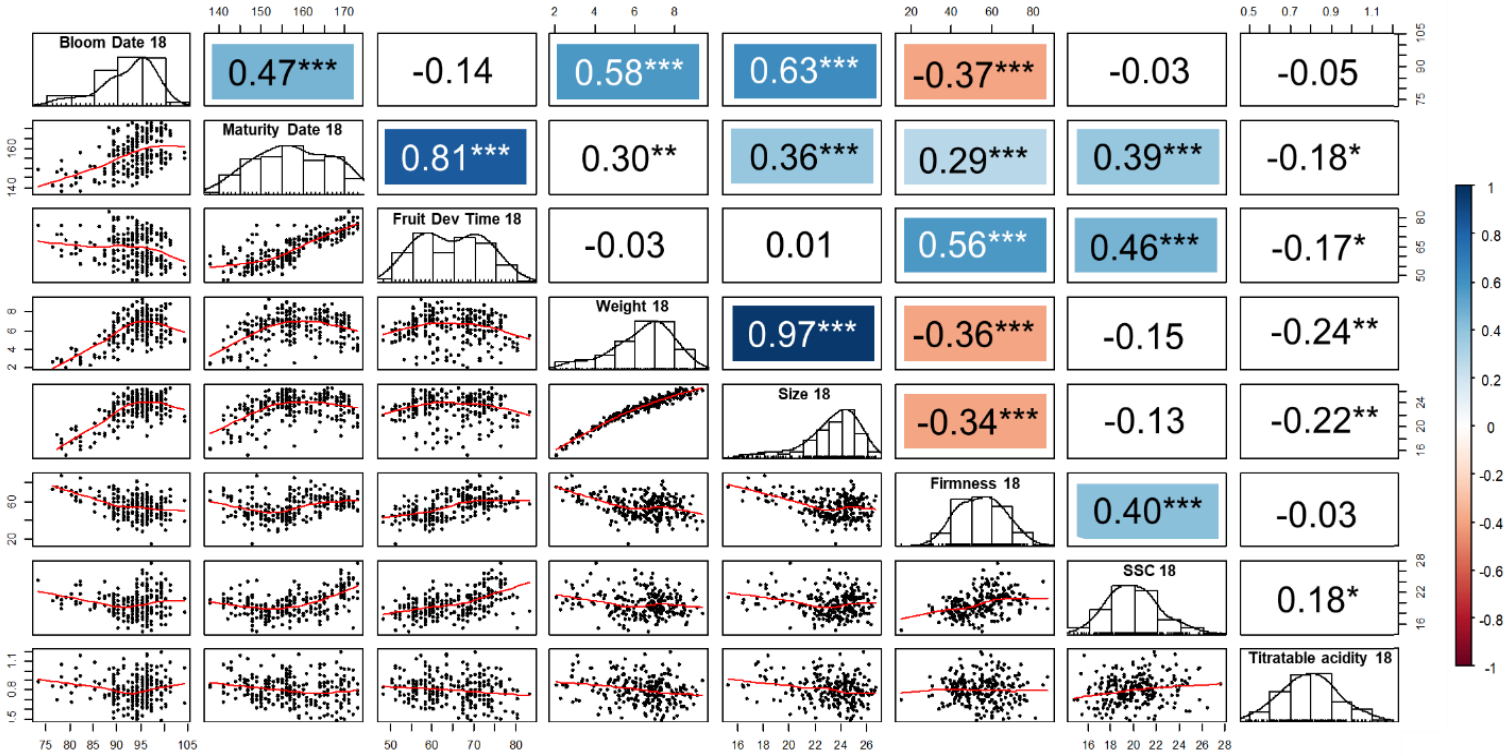

Figure 6.2 Continued

QTL analysis

QTLs were detected for all traits for both phenotyped years (Sup Table 6.2; Sup Fig 6.1). The analyses of both years revealed 48 QTLs for the seven traits (12 for MD, 9 for FW, 8 for FD, 6 for FS, 5 for SSC, 4 for FF and TA; Sup Table 6.2; Sup Fig 6.1). Most of these (33) were identified with strong evidence (2lnBF > 5), while 15 were detected with decisive evidence (2lnBF > 10) (Sup Table 6.2). QTLs detected were found on LGs 1 to 6 (Sup Fig 6.1). The proportion of phenotype variance explained (PVE) by single QTL accounted for 0.4 to 65.3% (Sup Table 6.2). QTLs detected for FD, MD, FW and FF explained more than 60% of total phenotype variation, whereas for SSC and TA, QTLs explained between 20 and 50% (Sup Table 6.2).

Thirty-eight of these QTLs were detected both years for the same trait in identical interval region and corresponded to 18 stable QTLs detected two years (Table 6.1; Fig 6.3). The remaining 13 QTLs, mainly for FW and FS, were detected only one year (Sup Table 6.2; Sup Fig 6.1). Of the QTLs detected both years, 3 of them were for FD, 6 for MD, 3 for FW, 1 for FS, 2 for FF, 2 for SSC and 1 for TA, being 5 of them detected with decisive evidences (Table 6.1; Fig 6.3).

Three stable and significant QTLs for FD were detected on LGs 3 and 4 (Fig 6.3; Table 6.1). Most significant FD QTL, *qP-FD4.2*^{m}, was localized on a highly narrowed region (51-53 cM) of LG4, which explained a large PVE (65.3 and 64.5%) and had an additive effect of 10.8 and 11.7 days each year (Table 6.1; Fig 6.3). For MD, six stable QTLs were reported, two of them detected with decisive evidence. One of them, *qP-MD4.2*^{m}, was in the same region of LG4 as the main FD QTL (*qP-FD4.2*^{m}), revealing the relation of this two traits. This MD QTL showed the largest PVE (46.8 and 52.5%) and the same additive effects as FD, 11.1 and 11.6 days each year respectively (Table 6.1; Fig 6.3). The other QTL with decisive evidence for MD was on LG2 (*qP-MD2.1*^{m}) but explained a lower percentage of variation (10.4 to 11.75%; Table 6.1).

For FW, three stable QTLs (*qP-FW1.1*^{m}, *qP-FW2.1*^{m} and *qP-FW5.1*^{m}) were identified, although none of them presented decisive evidence (Table 6.1; Fig 6.3). The PVE explained by these three QTLs varied largely between years, being the largest effects observed for *qP-FW2.1*^{m} and *qP-FW5.1*^{m} in 2017 and 2018, respectively (Table 6.1). For FS, a stable QTL was identified on LG2 (*qP-FS2.1*^{m}; PVE 21.5 to 23.6) in the same region

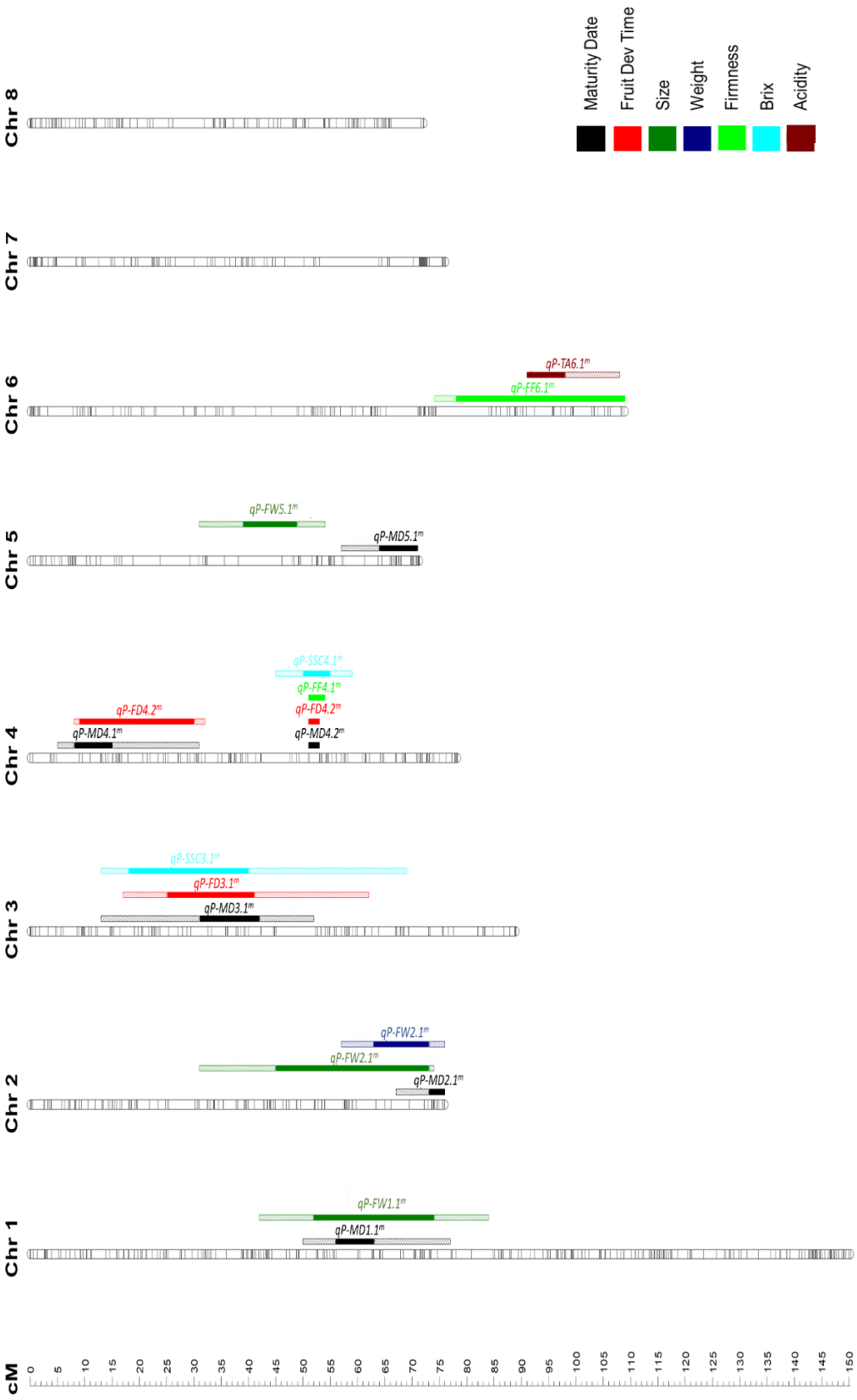

Figure 6.3 Genetic position of stable QTLs (detected both years) in the consensus linkage map. QTLs interval shown covers QTL intervals of both years. QTL interval overlapping both years is shown in bold, intervals detected only one year are shown with diagonal bars. All QTLs detected, including each year interval, are shown in Sup. Fig 6.1

as FW QTL *qP-FW2.1*^{m} (Table 6.1, Fig 6.3), revealing in this case the relation between FW and FS. Regarding FF, a major stable QTL was detected on LG4 (*qP-FF4.1*^{m}) (Table 6.1; Fig 6.3). This QTL also showed decisive evidences both years of analysis and was narrowed to 50-54 cM of LG4 (Table 6.1; Fig 6.3), corresponding to same genomic region where FD and MD major QTLs were detected (Fig 6.3). *qP-FF4.1*^{m} showed large PVE (47.9-64.1%) and additive effects of 14.4 and 15.0% in FF (Table 6.1).

Regarding SSC, a major stable QTL was also found on the same region of LG4, in which main FD, MD and FF QTLs were detected (Table 6.1; Fig 6.3). *qP-SSC4.1*^{m} was located between 50 and 59 cM of LG4 and showed the largest PVE (34.2 - 22.1%), related with variations between 1.7 to 3.0 ºBrix (Table 6.1; Fig 6.3). For TA, a relevant stable QTL, *qP-TA6.1*^{m}, was detected on LG6 explaining from 15.0 to 21.6% of variation (Table 6.1; Fig 6.3).

Haplotype analysis of LG4

Haplotype analysis of the LG4 region between 50 to 54 cM, spanning stable and decisive QTLs for FD (*qP-FD4.2*^{m}), MD (*qP-MD4.2*^{m}) and FF (*qP-FF4.1*^{m}) was carried out for parental cultivars and their ancestors (Fig 6.4; Sup Table 6.3). Four haplotypes (*H4-a* to *–d*) were identified using the six SNPs that span this interval (10.41 to 11.66 Mbp) of LG4 (Sup Table 6.3). Of these, *H4-a* and *H4-b* were the most frequent haplotypes, being present in all parental and ancestor cultivars except in 'Burlat' (Fig 6.4; Sup Table 6.3). The two remaining haplotypes *H4-c* and *H4-d* were only found in 'Burlat' (*H4-c* and *H4-d*), 'Brooks' (that descends from 'Burlat'; *H4-d*); and 'Cristobalina' (*H4-c*) (Fig 6.4; Sup Table 6.3).

The comparison of genotype (diplotypes) effects in the populations revealed that individuals with *H4-c* matured earlier and presented shorter fruit development period than individuals without this haplotype (Fig 6.4; Sup Table 6.4). These individuals (genotypes *c/-*, *-/c* and *cc*) ripened on average 11.7 days earlier than individuals with other haplotype combinations (*a/a, a/b, a/d, d/d*) (Fig 6.4; Sup Table 6.4). In the same manner, *H4-c* induced the shortest FD in all the populations (12.1 days; Fig 6.4; Sup Table 6.4). Smaller differences were observed for the three remaining haplotypes, although individuals with *H4-d* induced MD and FD two days earlier/shorter than individuals with *H4-a* and *–b*

haplotypes (Fig 6.4; Sup Table 6.4). Regarding FF, genotypes effects in the F_1 and F_2 populations revealed that *H4-a*, *H4-b* and *H4-d* were significant firmer than *H4-c* (Fig 6.4; Sup Table 6.4). The firmest individuals corresponded to '*aa*', '*ab*' and '*dd'* genotypes, whereas '-*c*' (or '*c*-') and '*cc*' genotypes were significant softer (Fig 6.4; Sup Table 6.4). The fact that all individuals with *H4-c* presented the lowest phenotype value for MD, FD and FF (early ripening and soft), suggests this haplotype is dominant over the others.

DISCUSSION

Bloom time, fruit development and maturity date

Understanding and identifying trait correlations provides knowledge for a more efficient phenotyping and breeding selection. Low positive correlation or no correlation at all has been previously reported in sweet cherry for BT and MD (Dirlewanger et al., 2012; Chavoshi et al., 2014; Piaskowski et al., 2018). In this study, also moderate positive correlation between these two traits was observed for this plant material. This correlation was most evident in the earlier flowering and ripening cultivars. The inclusion in this work of C×C, which shows extra-early blooming (Chapter 3) and maturity dates compared to the rest of material, may have biased the correlation of these two traits when analyzing all the plant material. The results, therefore suggests that blooming time and maturity are not completely correlated, and as observed in many cultivars not all early blooming genotypes are early maturing and vice versa.

This work analyzes FD in sweet cherry for first time. The high positive correlation between MD and FD observed herein, has been previously observed in peach and apricot (Etienne et al., 2002, Salazar et al., 2013 and 2016). Results herein confirm the same relationship between these traits observed in other *Prunus* species. This result indicates that MD is mostly dependent on FD period; therefore, the date of maturity essentially depends on the time the fruit takes to mature. However, the low positive correlation also observed between BT and MD, also indicates, that sometimes, or to a certain degree, MD also depends on BT. If blooming takes place earlier, as it happened in 2017, then maturity also takes place earlier, or vice versa, independently of the FD time. However, since, BT

Table 6.1 Summary of QTLs detected both years. Genetic and physical position spanned for both years, and maximum Bayes Factor (2lnBF), mean additive effect, and PVE for both years. In bold, QTLs with 2lnBF>10 (decisive evidence). Full list of all detected QTLs and single year details are found in Supplementary Table 6.2.

	H^2	QTL name	LG	Genetic position (cM)	Physical position* (Mbp)	Average 2lnBF	Additive effect	PVE (%)
Fruit Development Time (FD)	0.92	*qP-FD3.1*^{m}	3	17-62	4.16-19.65	3.4 / 6.2	2.8 / 3.1	2.7 / 6.9
		qP-FD4.1^m	4	8-32	1.98-6.82	3.9 / 5.9	5.1 / 5.7	5.8 / 18.2
		***qP-FD4.2*^{m}**	**4**	**51-53**	**10.88-11.66**	**11.7 / 11.8**	**10.8 / 11.7**	**65.3 / 64.5**
Maturity Date (MD)	0.94	*qP-MD1.1*^{m}	1	50-77	14.33-28.94	3.8 / 7.6	3.4 / 4.1	5.4 / 8.6
		qP-MD2.1^m	2	68-76	25.24-29.94	6.1 / 11.7	3.9 / 4.9	11.7 / 10.4
		qP-MD3.1^m	3	13-52	3.70-15.84	3.5 / 8.1	5.4 / 3.8	19.5 / 6.7
		qP-MD4.1^m	4	5-33	1.98-6.82	2.7 / 7.7	3.9 / 6.1	4.2 / 11.0
		***qP-MD4.2*^{m}**	**4**	**51-53**	**10.88-11.66**	**9.5 / 11.8**	**11.1 / 11.6**	**46.8 / 52.5**
		qP-MD5.1^m	5	57-71	13.62-18.41	4.7 / 8.1	2.2 / 2.3	2.1 / 2.8
Fruit Weight (FW)	0.92	*qP-FW1.1*^{m}	1	42-84	11.08-30.61	5.2 / 4.5	0.8 / 1.1	6.1 / 15.7
		qP-FW2.1^m	2	31-74	17.86-28.60	4.9 / 5.9	1.0 / 1.7	23.9 / 53.9
		qP-FW5.1^m	5	31-54	8.42-13.18	6.5 / 4.4	1.5 / 1.3	45.4 / 6.9
Fruit Size (FS)	0.93	*qP-FS2.1*^{m}	2	57-76	23.74-29.94	6.7 / 7.2	1.4 / 1.1	23.6 / 21.5
Fruit Firmness (FF)	0.84	***qP-FF4.1*^{m}**	**4**	**50-54**	10.41-12.57	**11.7 / 9.5**	**14.4 / 15.0**	**47.9 / 64.1**
		qP-FF6.1^m	6	74-109	22.65-30.45	4.8 / 2.3	3.7 / 2.9	2.5 / 1.3
Soluble Solid Content (SSC)	0.62	*qP-SSC3.1*^{m}	3	18-69	4.50-21.85	4.8 / 4.2	1.5 / 0.9	10.4 / 7.4
		***qP-SSC4.1*^{m}**	**4**	**50-59**	**10.41-13.10**	**11.7 / 6.8**	**3.0 / 1.7**	**34.2 / 22.1**
Titratable Acidity (TA)	0.54	*qP-TA6.1*^{m}	6	91-108	26.77-30.45	9.6 / 6.3	0.09 / 0.07	21.6 / 15.0

and FD are independent of each other, results indicate that MD depends on both traits (BT and FD period), but on FD to a larger extent. In terms of breeding, this result translates in the possibility of combining BT and FD to achieve specific breeding goals in terms of maturity date. To either advance or delay maturity date using short or long FD period, and at the same time try to adapt to environmental conditions by introducing late (avoidance of late frosts) or early blooming (low chilling).

High H^2 was estimated for most traits analyzed, but as previously described in other *Prunus* species (reviewed in Aranzana et al., 2019), broad-sense heritability was highest in the phenology traits. The H^2 estimated for FD (0.92) and MD (0.94) was very high, and similar to that estimated previously in sweet cherry for MD (0.76 to 0.83; Dirlewanger et al., 2012; Piaskowski et al., 2018) and in peach for FD (0.88 and 0.92; Fresnedo-Ramírez et al., 2015; Hernández Mora et al., 2017). As FD has not been evaluated previously in sweet cherry, results herein confirmed previous works in *Prunus*, in which this this trait showed very high heritability (Fresnedo-Ramírez et al., 2015; Hernández Mora et al., 2017). Despite the large heritability, FD showed small variability between years, while for MD large differences were observed, as in average maturity was reached 20 days earlier in 2017 than in 2018. The same year effect was observed in the BT of the same plant material the same years (Chapter 3), with blooming being 20 days earlier in 2017 than in 2018. Thus, as discussed above, revealing that in this work, MD inter-annual variation was due to inter-annual blooming variation.

Traits showing normal (MD) and bimodal (FD) distribution were observed in this study, implying different behavior of these traits. As reported here, normal distribution was previously observed for MD in sweet cherry (Quero-García et al., 2014) and apricot (Salazar et al., 2013 and 2016). However, in most peach populations, bimodal distributions for MD were reported (Quilot et al., 2004; Eduardo et al., 2011; Nuñez-Lillo et al., 2015), corresponding to individuals of early and late ripening and suggesting the presence of a major locus governing the trait. The same type of bi-modal distribution was observed here for FD, but not for MD. This different behavior between cherries and peach can be explained by the different length of FD between species. In cherries, FD is narrower than in peach and therefore BD has a larger effect on MD than in peach. In peach, FD is much larger and therefore the influence of BD in MD is much smaller. This situation may explain why bimodal distribution was observed for MD in peach, and only for FD in sweet cherry.

This different effect of BT and FD in MD was also translated to QTLs effects. The major QTLs detected for MD in this work are the same as those detected for FD (*qP-MD3.1*^{m}, *4.1*^{m} and *4.2*^{m}). Also, the rest of MD QTLs detected in this work (*qP-MD1.1*^{m}, *5.1*^{m}) are in the same position as QTLs previously detected for BT in the same plant material (Chapter 3). These results confirm the correlation between these traits discussed above, and indicate that in our sweet cherry plant material MD depends on the genetic control of BT and FD. Thus, FD QTLs on LGs 4 and 3 (*qP-FD4.2*^{m} and *qP-FD 3.1*^{m}) are the main drivers of MD, followed by BT QTL *qP-BT2.1*^{m} (Chapter 3) that coincides with MD QTL *qP-MD2.1*^{m}. Previously, MD QTLs have also been mapped on LGs 1, 4 and 5 of sweet cherry (Dirlewanger et al., 2012; Isuzugawa et al., 2019) but not on LGs 2 and 3 as herein. In other *Prunus* species, MD QTLs have been previously reported in LGs 1 to 7 in peach (Quilot et al., 2004; Eduardo et al., 2011; Fresnedo-Ramírez et al., 2015; Nuñez-Lillo et al., 2015; Serra et al., 2017; Hernández-Mora et al., 2017), and in apricot (Salazar et al., 2016), and on LG4 of plum (Salazar et al., 2017). In these works, as detected herein, the main QTL controlling MD and FD was mapped on the central region of LG4, where a NAC transcription factor has been reported as the strongest candidate gene for this trait (Pirona et al., 2013).

Fruit size and firmness

Heritability of fruit quality was highest for FS (0.93) and FW (0.92), which is higher than previously reported in other sweet cherry studies (0.63 to 0.88) (Zhang et al., 2010; Campoy et al., 2015; Piaskowski et al., 2018; Chapter 3). However, inter-annual variation with significant smaller fruits in 2017 than 2018 was observed, indicating that environmental factors affecting fruit development and size varied between years. Both years, skewed distribution to large fruits was observed in all the plant material, opposing semi-dominance of small fruit size previously reported in the species (Zhang et al., 2010; Campoy et al., 2015; Chapter 5). This segregation could be explained by C×C large amount of homozygosity (Chapter 1). As C×C individuals have very small fruit size, when compared with the individuals of the other populations, the FW and FS were skewed towards larger fruits. Firmness H^2 (0.84) was in the same range as earlier reported (0.73 to 0.97; Campoy et al., 2015; Cai et al., 2019; Chapter 3), but mean inter-annual differences

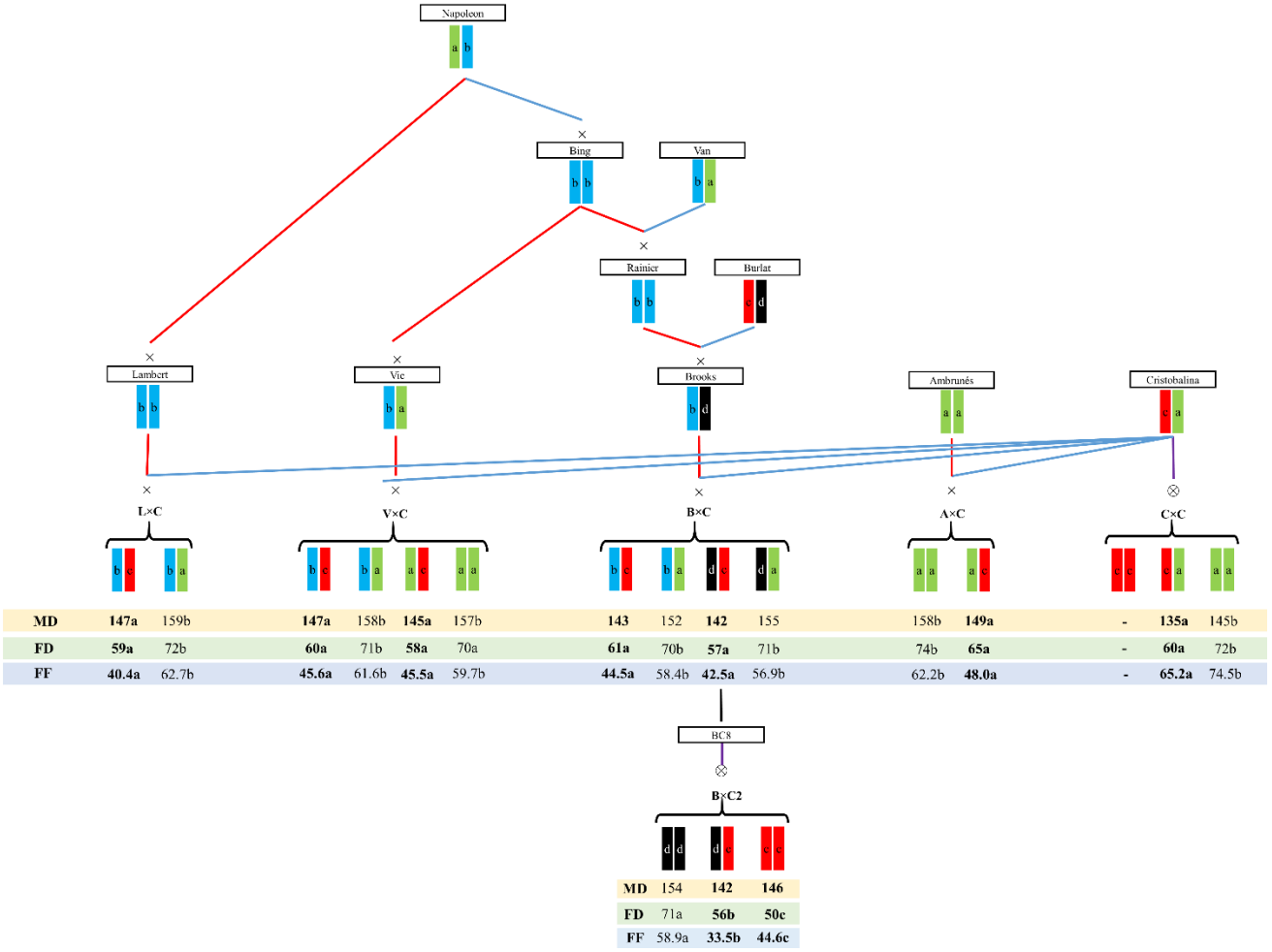

Figure 6.4 Diagram of inheritance of LG4 fruit development period, maturity date and firmness QTLs (*qP-FD4.2*^{m} / *qP-MD4.2*^{m} / *qP-FF4.1*^{m}; LG4: 50-54 cM) haplotypes in the families, parental and ancestor cultivars. Mean phenotype value of both years (2017 and 2018) of each segregating class in each family are shown. Means significant differences between segregating classes are identified by different letters ($p<0.05$).

were not observed, revealing this trait is more stable than size. Normal distribution, as described previously for FF in sweet cherry, was observed in this study (Campoy et al., 2015).

The negative correlation observed between fruit size (FS and FW) and FF is relevant as these traits are considered main drivers of cherry acceptability (Cliff et al., 1995). The same negative correlation has been observed before (Campoy et al., 2015), however in other genetic backgrounds a positive correlation between these traits has also been observed (Chavoshi et al., 2014; Piaskowski et al., 2018; Chapter 5). The results indicate the presence of different alleles in the different plant material analyzed.

The influence of environmental conditions in fruit size and the diverse plant materials used in previous studies for QTL analyses of these traits has resulted in the report of different size QTLs with highly variable PVE. Main size QTLs on sweet cherry were mapped on LGs 2 and 6 (Zhang et al., 2010; Rosyara et al., 2013), LG5 (Campoy et al., 2015) and LG1 (Chapter 5). Herein, we identified four stable QTLs for FS and FW on LG1, 2 and 5 (*qP-FW1.1*^{m}, *qP-FW2.1*^{m}, *qP-FS2.1*^{m} and *qP-FW5.1*^{m}) in regions previously reported for fruit size QTLs (Zhang et al., 2010; Rosyara et al., 2013; Campoy et al., 2015; Chapter 5). The main stable QTLs for FS and FW (*qP-FW2.1*^{m} and *qP-FS2.1*^{m}) in this work, overlapped on LG2 and spanned same physical region previously reported (Zhang et al., 2010; Rosyara et al., 2013), thus validating this LG2 region as a main determinant of fruit size in sweet cherry. Other stable size QTLs for fruit size detected also overlapped with QTL regions earlier reported. The physical position spanned by *qP-FW1.1*^{m} (11.08 to 30.61 Mbp) corresponds to same region where a cluster of fruit size and firmness QTLs were found on 'Ambrunés' cultivar (Chapter 5). Similarly, the region between 8.34-13.18 Mbp with presence of significant fruit size QTLs on LG5 (*qP-FW5.1*^{m} and *qP-FS5.1*) also overlapped with FW QTLs detected by Campoy et al. (2015) and in Chapter 5. The validation in this work of the main fruit size QTLs detected previously in sweet cherry highlights the potential of the multi-family QTL approach used in this work to investigate the genetics of quantitative traits, as all main fruit size QTLs found previously using single populations were detected in this work.

Main FF QTL, stable among years and showing large effects, was found on LG4 (*qP-FF4.1*^{m}). This major QTL was previously reported by Cai et al. (2019) (*qP-FF4.1*) but not in other sweet cherry firmness studies using single mapping populations (Campoy et

al., 2015; Chapter 5). The haplotype analysis of *qP-FF4.1* (Cai et al., 2019) revealed that the majority of bred cultivars carried firm alleles for this QTL, whereas only mazzards were homozygous for soft alleles (Cai et al., 2019). These results revealed selection of firm alleles at this QTL during cherry domestication and explained why it had not been detected in other works that considered bred and firm cultivars (Campoy et al., 2015; Chapter 5). However, in this study, we used 'Cristobalina', a landrace with a firm/soft genotype at this QTL (*qP-FF4.1*^{m}) as parental cultivar of all populations. This QTL was segregating in the populations analyzed and was therefore detected in this work. Another firmness QTL detected here with minor effects on LG6 (*qP-FF6.1*^{m}) has also been previously detected in sweet cherry (Campoy et al., 2015; Cai et al., 2019; Chapter 5) also at lower PVE, revealing presence of other genes having minor effects on fruit firmness.

Soluble solids contents and Titrable Acidity

In this work, as earlier reported in cherry (Piaskowski et al., 2018) and peach (Bassi et al., 1996; Dirlewanger et al., 1999; Hernández Mora et al., 2017), moderate H^2 was observed for SSC (0.62) and TA (0.54). In fact, not a common pattern in sugars or acid content was observed in the parental cultivars and years, confirming the large dependence of environmental conditions on acids and sugar content (Morandi et al., 2008). In addition, the normal distribution showed for SSC and TA herein, as previously observed in other peach populations for the same traits (Quilot et al., 2004; Eduardo et al., 2011) reveals the quantitative nature of these traits.

QTLs for SSC and TA are firstly reported for sweet cherry in this study. Previous QTL analyses in apricot, peach and plum of these traits reported large number of QTLs demonstrating the polygenic nature of these traits in the genus (Etienne et al., 2002; Quilot et al., 2004; Eduardo et al., 2011; Zeballos et al., 2016; Salazar et al., 2013 and 2017). In peach, TA QTLs were reported on LGs 2, 3, 4, 5 and 6 (Etienne et al., 2002; Quilot et al., 2004; Eduardo et al., 2011; Zeballos et al., 2016), and a major locus (*D*) mapped on LG5 has been reported as the major determinant of acid and subacid fruit taste in peach (Boudehri et al., 2009; Eduardo et al., 2014). This major QTL was not detected herein, although *qP-TA6.1*^{m}, found in this work as the main QTL controlling acidity, was reported in homologous region of peach (*qTA6.2*; Hernández Mora et al., 2017). For SSC, the main QTL found in this work on LG4 (*qP-SSC4.1*^{m}) also overlapped with a region of LG4 where

main QTLs for this trait were found in peach (Etienne et al., 2002; Eduardo et al., 2011; Zeballos et al., 2016; Hernández Mora et al., 2017), confirming a common path regulating this trait in both species.

Correlation between phenology and fruit quality traits were observed in this work. The correlation observed between MD and FD with FF and SSC confirms previous results in other sweet cherry genetic backgrounds in which higher firmness and sugar content was observed in those genotypes with later maturity (Chavoshi et al., 2014; Piaskowski et al., 2018). In fact, traditional varieties, such as 'Ambrunés', with late ripening date and large FD period presented higher SSC and FF than varieties of early ripening (Serradilla et al., 2012). These results also confirmed previous studies that indicate that SSC is related to photoassimilate, in which cultivars of large FD period are expected to accumulate larger SSC than those with shorter periods (Genard et al., 2003).

Phenology and fruit quality hotspot on LG4

In this study, stable and major QTLs for MD, FD, FF and SSC were identified overlapping in a narrow region of LG4 (50 to 59 cM; 10.41 to 12.57 Mbp). Additionally, correlation between some of these traits was observed in this work. In other sweet cherry populations, as well as in this plant material, BT QTLs were also mapped in this region (Dirlewanger et al., 2012; Castède et al., 2014; Chapter 3). Similarly, a cluster of QTLs was reported on the homologous regions of peach (Quilot et al., 2004; Eduardo et al., 2011; Zeballos et al., 2016), apricot (Salazar et al., 2013) and plum (Salazar et al., 2017) for related traits. In apple, Kenis et al. (2008) mapped a large number of QTLs for these traits on LG10, a syntenic region to LG4 of *Prunus* species (Illa et al., 2011). Therefore, a conserved region within the *Rosaceae* determines some main phenology and fruit quality traits. Two different explanations have been postulated related to this cluster: multiple linked genes or a major gene for MD with pleiotropic effect on fruit quality traits (Eduardo et al., 2011). This major MD gene could be associated with SSC and FF variations, as consequence of different FD between genotypes. During ripening, fruits accumulate sugars, acids and other volatile compounds, and cultivars with shorter FD period may not complete their physiological maturation as much as cultivars with long FD, which have more time to assimilate and synthetize these compounds.

Therefore, investigation of this region is of interest for breeding, as selection of certain haplotypes of this hotspot will allow selection of various phenology and quality traits at the same time. In the plant material analyzed in this work, 'Cristobalina' and 'Burlat', both original from Southern Europe (Wünsch and Hormaza, 2002) have an allele associated with early MD and short FD (*H4-c*). Both are cultivars of early maturity, and the presence of this haplotype may explain this phenotype. However, the same haplotype *H4-c* is also associated with softer fruits. As we have seen that early maturity is associated with short FD, it may be that soft fruits is a result of a short FD period. In any case, breeding for early fruit will result in soft fruits from this plant material, revealing a complex scenario for breeding of firm and early fruits from these materials. However, as in this plant material BT and MD are mainly determined by different loci, BT on LGs 1 and 2 (Chapter 3) and MD on LG4 (this work), trying to combine early flowering and large FD could lead to relatively early MD cultivars and higher firmness.

The use of multiple sweet cherry populations with parental cultivars of different genetic backgrounds that show large phenotypic variability has provided valuable information about the genetic control of relevant phenology and fruit quality traits that will be useful for breeding and for broadening the understanding of the genetics of these traits. The trait correlations observed were confirmed by QTL mapping, as various correlated traits were mapped on same region. Results have revealed that MD is dependent in FD and BT, being FD the main cause of MD. Most relevant is a region on LG4 with presence of most significant and stable QTLs for MD, FD, FF and SSC, which represent a target region for MAS.

SUPPLEMENTARY MATERIALS CHAPTER 6

Supplementary Table 6.1 Minimum (Min), Maximum (Max), means and standard deviation (SD) for populations (a) and parental (b) in phenotype years.

a)

		FD (Days)		MD (Days)		FW (g)		FS (mm)		FF (%)		SSC (ºBrix)		TA (%)	
		2017	**2018**	**2017**	**2018**	**2017**	**2018**	**2017**	**2018**	**2017**	**2018**	**2017**	**2018**	**2017**	**2018**
A×C	**Min**	58	53	135	148	3.3	3.9	18.1	20	31.2	38.2	16.7	15.2	0.61	0.51
	Max	78	83	153	173	7.2	8.1	24.9	26.3	71.2	75.6	29.7	27.5	1.12	0.97
	Mean	69.8	68.7	146	161.2	4.8	5.6	20.8	22.3	54.3	55.9	21.9	19.1	0.86	0.73
	SD	5.5	8.0	5.4	8.2	0.9	1.1	1.4	1.6	11	9.9	3.7	2.4	0.12	0.11
B×C	**Min**	49	55	124	144	4.03	5.83	20	22.7	27.6	31.1	14	16.4	0.55	0.51
	Max	75	75	150	166	7.24	8.62	24.8	26.5	59.8	67.4	26.1	21.2	0.97	0.89
	Mean	64.5	66	138.6	157.8	6	7	22.9	24.4	50.1	52.5	20.4	18.5	0.72	0.67
	SD	8.7	5.9	9.5	6.4	0.9	0.9	1.3	1.2	7.3	12.4	3.1	1.5	0.12	0.12
B×C2	**Min**	53	48	125	141	3.44	3.19	19	19.2	26.2	15.2	17.1	14.9	0.71	0.65
	Max	79	75	151	168	6.33	7.21	24.3	25.3	59	77	25.1	22.4	1.01	1.13
	Mean	63.4	59.2	139.3	153.7	4.8	5.4	21.2	22.4	46.5	48.2	19.9	18.9	0.9	0.89
	SD	7.9	8.3	7.7	7.2	0.7	0.7	1.2	1.2	8.7	13.7	2	1.6	0.09	0.13
C×C	**Min**	53	53	120	138	2.27	2.03	16.4	15.2	48	49	16.6	18.7	0.43	0.67
	Max	77	76	144	158	4.45	4.61	20.5	20.6	86.7	87.4	24.1	24.4	0.95	1.17
	Mean	62.8	63.8	129.5	145.6	3	3.1	18	18.1	68.2	67.7	20.3	21.2	0.69	0.89
	SD	7.1	6.3	7.2	4.9	0.6	0.6	1.3	1.3	10	8.8	2.6	1.7	0.15	0.12
L×C	**Min**	57	55	132	151	3.52	3.77	18.2	18.5	29.9	40.1	17.3	15.9	0.7	0.8
	Max	79	75	158	169	7.12	8.57	24.5	26.2	78.4	68.3	25.1	25.7	1.28	1.2
	Mean	65.9	67.2	145.3	162.1	5.8	6.5	22	23.3	50.6	54.7	20.2	19.6	0.92	0.93
	SD	7.4	6.6	8.8	6.6	1.2	1.6	2	2.6	16.6	9.9	2.8	3.5	0.17	0.13
V×C	**Min**	50	48	127	142	4.08	5.07	19	20.9	33	28.7	17.3	14.6	0.62	0.49
	Max	84	77	163	173	7.54	9.38	24.9	26.6	74.7	81.2	28.5	26.3	1.07	1.17
	Mean	66	63.8	144.5	159.3	5.8	7.2	22.5	24.3	54	53.3	23.1	20.2	0.89	0.79
	SD	6.4	7.6	6.7	8	0.7	0.8	1	1.1	9.8	10.4	2.8	2.2	0.11	0.13
Pearson Correlation Coeff (2017-2018)		0.84		0.89		0.87		0.88		0.72		0.55		0.44	

Supplementary Table 6.1 Continued.

b)

	FD (Days)		MD (Days)		FW (g)		FS (mm)		FF (%)		SSC (ºBrix)		TA (%)	
	2017	**2018**	**2017**	**2018**	**2017**	**2018**	**2017**	**2018**	**2017**	**2018**	**2017**	**2018**	**2017**	**2018**
'Ambrunés'	77	77	153	171	7.63	8.99	24.69	26.12	54.9	48.6	18.7	18.8	0.81	0.57
'Brooks'	64	57	142	155	7.97	9.07	26.07	27.59	52.1	55.6	19.8	19.1	0.75	0.78
'Cristobalina'	58	60	122	138	4.01	4.15	19.5	19.69	63.4	52.9	17	21	0.6	0.71
'Lambert'	78	72	163	173	9.24	8.65	25.41	25.46	47.3	33.1	-	18.8	-	0.76
'Vic'	71	68	153	169	9.42	9.23	26.28	26.31	46.1	50.3	20.6	21.3	0.88	0.71

Supplementary Table 6.2 QTLs identified both years.

	Year	Identified both years?	QTL name	QTL Evidences	LG	Interval (cM)	QTL peak (cM)	Physical poisiton* (Mbp)	Max 2lnBF	Average 2lnBF	Mean Additive effect	PVE (%)	Total Phenotype Variance Explained by QTLs
Maturity Day (MD)	2017	Yes	*qP-MD1.1*^{m}	Strong	1	56-77	67	18.54-28.94	6.31	3.83	3.35	5.39	89.65
	2017	Yes	*qP-MD2.1*^{m}	Decisive	2	68-76	75	25.24-29.94	11.67	6.08	3.88	11.71	
	2017	Yes	*qP-MD3.1*^{m}	Strong	3	13-52	43	3.70-15.84	5.17	3.49	5.37	19.51	
	2017	Yes	*qP-MD4.1*^{m}	Strong	4	5-33	15	1.98-6.82	4.06	2.71	3.87	4.18	
	2017	Yes	*qP-MD4.2*^{m}	Decisive	4	51-53	53	10.88-11.66	12.07	9.53	11.14	46.78	
	2017	Yes	*qP-MD5.1*^{m}	Strong	5	57-71	69	13.62-18.41	6.16	4.73	2.18	2.1	
	2018	Yes	*qP-MD1.1*^{m}	Strong	1	50-63	57	14.33-23.45	8.92	7.59	4.06	8.62	92.06
	2018	Yes	*qP-MD2.1*^{m}	Decisive	2	73-76	75	26.96-29.94	15.15	11.67	4.93	10.4	
	2018	Yes	*qP-MD3.1*^{m}	Strong	3	31-42	33	7.50-10.88	9.72	8.1	3.8	6.68	
	2018	Yes	*qP-MD4.1*^{m}	Strong	4	8-15	11	1.93-4.19	9.29	7.72	6.13	11.03	
	2018	Yes	*qP-MD4.2*^{m}	Decisive	4	51-53	53	10.88-11.66	14.89	11.76	11.6	52.53	
	2018	Yes	*qP-MD5.1*^{m}	Decisive	5	64-71	67	15.81-18.41	11.18	8.15	2.32	2.81	
Fruit Development Time (FD)	2017	Yes	*qP-FT3.1*^{m}	Strong	3	17-62	45	4.16-19.65	5.08	3.44	2.77	2.66	73.83
	2017	Yes	*qP-FT4.1*^{m}	Strong	4	9-32	21	2.15-6.82	5.31	3.93	5.07	5.85	
	2017	Yes	*qP-FT4.2*^{m}	Decisive	4	51-53	53	10.88-11.66	14.04	11.69	10.77	65.32	
	2018	No	*qP-FT1.1*	Strong	1	44-65	59	11.78-23.59	8.59	5.72	2.51	3.67	93.65
	2018	Yes	*qP-FT3.1*^{m}	Decisive	3	25-41	35	6.02-10.88	10.93	6.24	3.12	6.91	
	2018	Yes	*qP-FT4.1*^{m}	Decisive	4	8-30	17	1.98-6.58	10.16	5.93	5.74	18.16	
	2018	Yes	*qP-FT4.2*^{m}	Decisive	4	51-53	53	10.88-11.66	14.02	11.77	11.66	64.53	
	2018	No	*qP-FT5.1*	Strong	5	59-67	61	13.70-16.87	6.08	5.22	1.83	0.38	
Weight (FW)	2017	Yes	*qP-FW1.1*^{m}	Strong	1	52-74	63	14.89-27.67	6.27	5.16	0.81	6.07	83.73
	2017	Yes	*qP-FW2.1*^{m}	Strong	2	31-74	39	17.86-28.60	7.53	4.87	0.98	23.95	
	2017	No	*qP-FW4.1*	Strong	4	43-61	51	9.15-13.61	9.06	5.31	0.4	3.39	
	2017	Yes	*qP-FW5.1*^{m}	Strong	5	31-49	35	8.42-12.39	9.34	6.51	1.45	45.42	
	2017	No	*qP-FW6.1*	Strong	6	13-33	23	4.17-7.26	9.18	6.01	0.39	4.89	

Supplementary Table 6.2 Continued.

	2018	Yes	*qP-FW1.1*^{m}	Strong	1	42-84	71	11.08-30.61	5.52	4.49	1.14	15.73	78.84
	2018	Yes	*qP-FW2.1*^{m}	Strong	2	45-73	67	21.72-27.46	8.96	5.93	1.73	53.9	
	2018	No	*qP-FW3.1*	Strong	3	19-52	29	4.45-15.84	7.33	4.84	0.43	2.27	
	2018	Yes	*qP-FW5.1*^{m}	Strong	5	39-54	49	11.20-13.18	5.46	4.37	1.28	6.94	
Size (FS)	2017	Yes	*qP-FS2.1*^{m}	Strong	2	57-76	65	23.74-29.94	8.99	6.75	1.43	23.59	75.06
	2017	No	*qP-FS5.1*	Strong	5	30-50	35	8.34-12.39	9.2	4.93	2.18	44.56	
	2017	No	*qP-FS6.1*	Strong	6	15-31	25	4.63-7.06	9.94	6.88	0.73	6.92	
	2018	No	*qP-FS1.1*	Strong	1	45-71	55	12.30-26.89	7.31	5.31	1.76	22.21	48.07
	2018	Yes	*qP-FS2.1*^{m}	Decisive	2	63-73	71	24.83-27.46	10.96	7.21	1.06	21.49	
	2018	No	*qP-FS4.1*	Strong	4	10-46	21	2.55-10.08	6.83	5.11	0.78	4.37	
Firmness (FF)	2017	Yes	*qP-FF4.1*^{m}	Decisive	4	50-54	51	10.41-12.57	12.15	11.75	14.4	47.95	63.68
	2017	Yes	*qP-FF6.1*^{m}	Strong	6	78-109	99	23.80-30.45	6.86	4.83	3.66	2.54	
	2018	Yes	*qP-FF4.1*^{m}	Decisive	4	51-53	51	10.88-11.66	11.03	9.51	15	64.05	86.02
	2018	Yes	*qP-FF6.1*^{m}	Strong	6	74-109	87	22.65-30.45	3.36	2.27	2.86	1.31	
Soluble solid content (SSC)	2017	Yes	*qP-SSC3.1*^{m}	Strong	3	13-40	27	3.94-10.77	9.32	4.76	1.5	10.42	44.58
	2017	Yes	*qP-SSC4.1*^{m}	Decisive	4	50-55	53	10.41-12.72	14.09	11.7	3.04	34.16	
	2018	No	*qP-SSC1.1*	Strong	1	37-74	63	9.77-27.67	9.01	4.82	1.26	15.26	44.78
	2018	Yes	*qP-SSC3.1*^{m}	Strong	3	18-69	59	4.50-21.85	8.29	4.19	0.89	7.41	
	2018	Yes	*qP-SSC4.1*^{m}	Strong	4	45-59	53	10.08-13.10	9.6	6.82	1.69	22.11	
Titratable acidity (TA)	2017	No	*qP-TA4.1*	Strong	4	34-64	51	7.06-14.83	7.31	4.14	0.0561	5.39	26.97
	2017	Yes	*qP-TA6.1*^{m}	Decisive	6	91-98	95	26.68-27.49	11.83	9.65	0.0941	21.57	
	2018	No	*qP-TA3.1*	Strong	3	72-89	87	22.74-26.99	9.94	6.17	0.0588	5.01	20.02
	2018	Yes	*qP-TA6.1*^{m}	Decisive	6	91-108	97	26.77-30.45	10.29	6.33	0.0694	15.02	

Supplementary Table 6.3 Parental and ancestor haplotypes for FD (*qP-FD4.2*^{m}), MD (*qP-MD4.2*^{m}) and FF (*qP-FF4.1*^{m}) QTLs spanning LG4 50-54 cM.

SNP	Genetic position (cM)	Physical position (bp)	Haplotype																			
			'Ambrunes'		'BC8'		'Bing'		'Brooks'		'Burlat'		'Cristobalina'		'Lambert'		'Napoleon'		'Rainier'		'Van'		'Vic'	
			H4-a	*H4-a*	*H4-d*	*H4-c*	*H4-b*	*H4-b*	*H4-b*	*H4-d*	*H4-c*	*H4-d*	*H4-c*	*H4-a*	*H4-b*	*H4-b*	*H4-a*	*H4-b*	*H4-b*	*H4-b*	*H4-b*	*H4-a*	*H4-b*	*H4-a*
ss490559054	50.96	10414884	B	B	B	B	A	A	A	B	B	B	B	B	A	A	B	A	A	A	A	B	A	B
ss490552906	51.09	10880163	A	A	A	B	A	A	A	A	B	A	B	A	A	A	A	A	A	A	A	A	A	A
ss490552928	53.03	11472398	B	B	A	A	B	B	B	A	A	A	A	B	B	B	B	B	B	B	B	B	B	B
ss490552931	53.12	11520743	A	A	A	B	A	A	A	A	B	A	B	A	A	A	A	A	A	A	A	A	A	A
ss490548726	53.41	11661240	A	A	B	A	A	A	A	B	A	B	A	A	A	A	A	A	A	A	A	A	A	A
ss490552936	53.41	11661765	A	A	B	A	A	A	A	B	A	B	A	A	A	A	A	A	A	A	A	A	A	A

Supplementary Table 6.4 Phenotypic values and number of individuals (N) in each segregating class of each family for MD (*qP-MD4.2*^{m}), FD (*qP-FD4.2*^{m}) and FF (*qP-FF4.1*^{m}) QTLs in LG4. Statistical differences ($p<0.05$) within classes for families are indicated.

Population	Haplotype combination	N	MD		FD		FF	
			2017 (Mean ± SD)	2018 (Mean ± SD)	2017 (Mean ± SD)	2018 (Mean ± SD)	2017 (Mean ± SD)	2018 (Mean ± SD)
A×C	*a / a*	18	148.9 ± 4.0 a	167.1 ± 6.2 a	72.4 ± 4.2 a	74.7 ± 5.6 a	62.3 ± 6.3 a	62.1 ± 9.6 a
	a / c	20	142.5 ± 4.7 b	155.9 ± 5.9 b	66.4 ± 5.2 b	63.3 ± 5.8 b	45.3 ± 7.8 b	50.8 ± 6.8 b
B×C	*a / b*	9	143.0 ± 5.8 a	160.3 ± 3.0 a	69.7 ± 4.5 ab	69.3 ± 3.9 a	55.0 ± 3.4	61.7 ± 5.7 a
	b / c	8	133.5 ± 10.5 b	152.0 ± 8.0 b	60.0 ± 8.4 ab	61.5 ± 6.6 b	44.9 ± 9.1	44.1 ± 8.7 b
	a / d	6	147.0 ± 1.7 a	163.3 ± 2.3 b	71.3 ± 2.3 b	70.3 ± 3.2 a	51.5 ± 4.6	62.3 ± 4.1 a
	c / d	5	128.5 ± 4.9 b	156.0 ± 2.8 ab	52.5 ± 4.9 a	62.0 ± 2.8 b	48.6 ± 4.9	36.3 ± 7.3 b
B×C2	*c / c*	11	-	146.5 ± 7.8 a	-	50.0 ± 2.8 a	-	33.5 ± 5.8 a
	c / d	32	134.4 ± 5.4 a	150.3 ± 4.3 a	57.9 ± 6.2 a	55.1 ± 3.6 a	45.1 ± 4.2 a	44.1 ± 5.0 b
	d / d	18	145.9 ± 4.1 b	162.1 ± 4.1 b	71.9 ± 4.8 b	70.6 ± 3.1 b	53.0 ± 7.0 b	64.8 ± 7.9 c
C×C	*a / a*	11	138.4 ± 3.4 b	150.7 ± 4.0 b	72.6 ± 2.9 b	70.9 ± 3.9 b	71.2 ± 7.8 a	77.7 ± 7.1 a
	a / c	56	126.2 ± 5.3 a	144.4 ± 3.5 a	59.2 ± 4.3 a	60.9 ± 3.6 a	66.7 ± 11.1 b	63.7 ± 6.6 b
	c / c	17	-	-	-	-	-	-
L×C	*a / b*	7	153.0 ± 3.2 a	165.4 ± 4.4 a	72.6 ± 4.0 a	70.9 ± 3.1 a	65.6 ± 8.7 a	59.9 ± 6.2 a
	b / c	6	138.8 ± 5.9 b	154.3 ± 3.1 b	60.3 ± 3.8 b	58.7 ± 3.2 b	38.2 ± 8.9 b	42.5 ± 2.5 b
V×C	*a / a*	30	148.8 ± 3.2 a	165.4 ± 4.7 a	70.6 ± 3.0 a	69.9 ± 3.6 a	58.6 ± 6.6 a	60.8 ± 7.0 a
	a / c	41	137.4 ± 4.5 b	152.1 ± 4.6 b	58.6 ± 3.8 b	56.9 ± 4.0 b	44.8 ± 6.6 b	46.3 ± 7.7 b
	a / b	41	149.2 ± 3.4 a	167.3 ± 3.5 a	70.5 ± 3.0 a	71.6 ± 3.2 a	61.0 ± 6.3 a	62.3 ± 5.7 a
	b / c	40	139.6 ± 6.0 b	154.3 ± 4.9 b	61.4 ± 4.8 b	58.7 ± 4.1 b	45.7 ± 6.8 b	45.4 ± 4.8 b

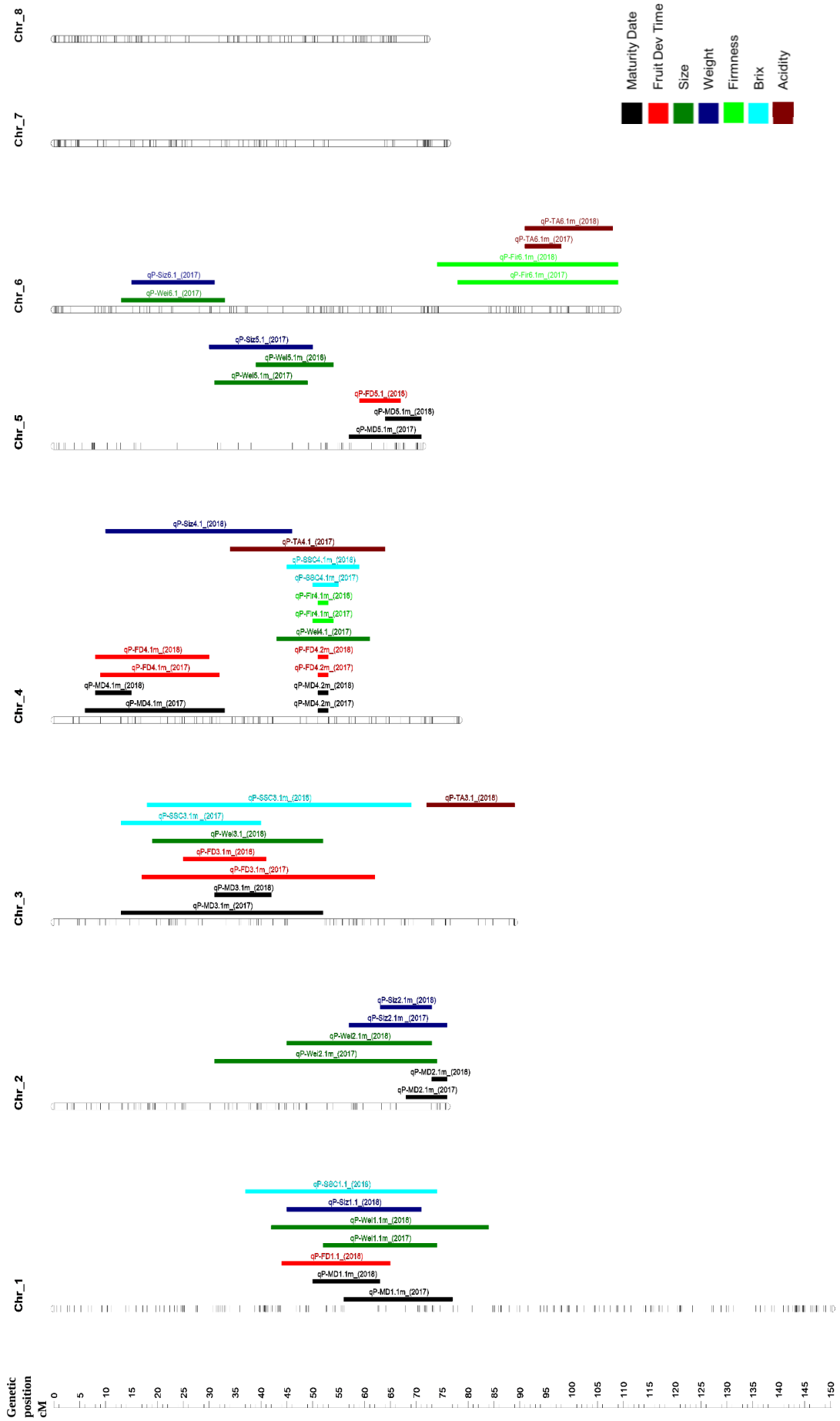

Supplementary Fig 6.1 Genetic position of all QTLs detected both years in the consensus linkage map.

CHAPTER 7

GENETIC ANALYSIS OF FRUIT COLOR AND POLYPHENOL CONTENT IN SWEET CHERRY

INTRODUCTION

Sweet cherries are an excellent source of numerous phytochemical compounds with health-promoting properties (Ballistreri et al., 2013). Many epidemiological studies have demonstrated a strong correlation between regular sweet cherry consumption and potential human health benefits such as the reduction of cancer susceptibility (Kang et al., 2003) and risk of suffer a heart attack (Ma and Kinneer, 2002), inflammation (Jacob et al., 2003), or protection against neurodegenerative diseases (Kim et al., 2005). Within these, polyphenols or phenolic compounds were reported as the main phytochemical compounds in sweet cherry (Serra et al., 2011; Ballistreri et al., 2013; Serradilla et al., 2017). Cherry polyphenols, in addition to their health-promoting properties, also play relevant roles in some sensory fruit characteristics such as color, flavor, taste or astringency (Lee, 2000; Tomás-Barberán et al., 2001). Polyphenols present in sweet cherry derive from shikimate acid, and can be divided into two different classes based on their chemical structure and biosynthesis pathway: phenolic acids (hydroxycinnamic and hydroxybenzoic acids) that derived from cinnamic acid, and flavonoids (anthocyanins, flavonolds and flavan-3-ols) that derived from phenylpropanoid (Serradilla et al., 2017; Cheynier et al., 2013).

Phenolic acids correspond to a type of aromatic acid compound that mainly contribute to sweet cherry quality characteristics, preservation of organoleptic properties, and fruit color through the process of co-pigmentation which favors anthocyanin stability (Eiro and Heinonen, 2002; Ballistreri et al., 2013). They are classified into two subgroups, the hydroxybenzoic acids that have been found in small amounts in sweet cherry (Mattila et al., 2006) and hydroxycinnamic acids that are the prominent and more important phenolic acids in sweet cherry (Martínez-Esplá et al., 2014). Within hydroxycinnamic acids, neochlorogenic, *p*-coumaroylquinic and chlorogenic are the main compounds found in sweet cherry (Serradilla et al., 2016). The ratio of these acids is specific of each cultivar and large differences amongst them have been observed (Mozetic et al., 2006; Ballistreri et al., 2013).

The other major group of polyphenols correspond to flavonoids. Flavonoids include flavanols, flavan-3-ols and anthocyanins, with this latter present in much larger amounts than the other in sweet cherry. Anthocyanins are a water-soluble pigment located in the vacuole and are involved in red, blue and purple color variations in many plant organs

(flowers, fruits, leaves, seeds and roots) (Field et al., 2001; Regan et al., 2001; García-Alonso et al., 2004). Apart from color, anthocyanins are also involved in other process as fruit flavor, bitterness, astringency, seed dispersal, protection against UV light damage and pathogen attack (Schaefer et al., 2004). As expected, cherry anthocyanins have also shown potent antioxidant and anti-inflammatory activities (Chaovanalikit and Wrolstad, 2004; Serra et al., 2011). Four main anthocyanins have been identified in sweet cherry: cyanidin-3-O-rutinoside (cy3-rut), cyanidin-3-O-glucoside (cy3-glu), peonidin-3-O-rutinoside (peon3-rut) and peonidin-3-O-glucoside (peon3-glu) (Serradilla et al., 2017). Cy-3-rut, mainly associated with red-purple coloration (Gonçalves et al., 2007), represents almost 80% of total anthocyanins concentration, whereas the other three that are related to orange-red color, are presented in lower amounts in sweet cherry fruits (Gonçalves et al., 2007; Serradilla et al., 2016). Anthocyanins are distributed in the whole fruit with larger amount in skin rather than flesh tissues.

Despite the significant importance of polyphenols, most studies in sweet cherry, have focused on the evaluation of phenolic compounds content at cultivar level, as well as, its changes during postharvest storage (Serra et al., 2011; Ballistreri et al., 2013; Serradilla et al., 2017). However, there is little information about the genetic control of these compounds content. In the Rosaceae, genetic studies of polyphenols content based on QTL analysis have been reported in apple (*Malus* × *domestica* Borkh.; Chagné et al., 2012b; Khan et al., 2012; Verdu et al., 2014) and peach (Zeballos et al., 2016). In apple, QTLs identified were clustered on different linkage groups (LGs) based on compound structure, with a region at top of LG16 mainly controlling flavonol content variation. In peach (*Prunus persica* L.), polyphenol content QTLs were found on various LGs, but none of them was stable during the years of study (Zeballos et al., 2016).

Within polyphenols, the molecular basis of anthocyanin content has been most studied due to its relationship with red fruit coloration. Studies in apple identified an R2R3 MYB transcription factor (*MdMYB10*), which is considered the main regulator of red coloration in fruits and leaves, by regulation of the anthocyanin pathway (Chagné et al., 2007; Allan et al., 2008). In sweet cherry, and other *Prunus* species, a homologous gene, *MYB10*, has been characterized and associated with the regulation of the anthocyanin biosynthetic pathway (Lin-Wang et al., 2010). This candidate gene in located on the LG3 region where a main skin and flesh color QTL was detected in sweet cherry

(Sooriyapathirana et al., 2010). This gene was shown by transcription analysis to be associated with anthocyanin content and to be absent in yellow cherries (Wünsch et al., 2014; Jin et al., 2016). An SSR marker that correlates with mahogany and blush haplotypes in this QTL has been proposed for the identification of fruit color in sweet cherry (Sanderful et al., 2016). For phenolic acids, QTLs have only been reported in apple (Khan et al., 2012; Chagné et al., 2012b; Verdu et al., 2014), in which main genomic regions associated to these compounds content were reported on LGs 14 and 15. For these QTLs, *shikimate/quinate O-hydroxycinnamoyl transferase* (*HCT/HQT*) were proposed as main candidate gene (Verdu et al., 2014).

This work aims to investigate the main genomic regions associated to polyphenol content in sweet cherry, and their relationship with fruit color, by using a QTL mapping approach. To achieve this goal, accurate phenotyping of polyphenol content by high-performance liquid chromatography (HPLC), in a color segregating sweet cherry F_1 population ('Vic' × 'Cristobalina'), and saturated linkage mapping with RosBREED 15K SNP array were used.

MATERIALS AND METHODS

Plant material

In this work, a cross-pollinated sweet cherry population (N=161) from 'Vic' × 'Cristobalina' (V×C) was used. The V×C population cross was made in 2010 and planted in 2013, and has been observed to segregate for skin and flesh color. 'Vic' and 'Cristobalina' cultivars, both belonging to the CITA de Aragón sweet cherry collection, were also used. All plant material is found at the orchard of CITA de Aragón (Zaragoza, Spain).

Cherry polyphenol and color phenotyping

Phenotyping of sweet cherries skin and flesh color and polyphenols were carried out one year (2017) from sample fruits of V×C population and the parental cultivars. Skin and flesh color were evaluated in fifteen fruits per tree at the optimum ripening stage based

on visual inspection of color, firmness and taste. Skin color was measured on the two opposite sides of each fruit medio-lateral axis using a DuroColor colorimeter (Setop Giraud Technologie, Cavaillon, France), in which data is recorded in CTIFL Index (1 to 7). Flesh color was visually defined according to UPOV color chart for flesh (1 to 5).

Table 7.1 Number of makers, genetic length, average marker distance and maximum gaps for 'Vic' (V), 'Cristobalina' (C) and consensus (V×C) SNP maps.

	Genetic map	LG1	LG2	LG3	LG4	LG5	LG6	LG7	LG8	Total
Number of markers	**V**	302	32	49	73	142	96	118	98	**910**
	C	104	173	120	75	63	152	29	73	**789**
	V×C	440	225	213	219	242	293	161	207	**2000**
Genetic length (cM)	**V**	142.9	84.1	53.4	68.9	61.5	95.5	58.3	72.1	**636.7**
	C	66.5	84.5	92.9	88.6	76.9	117.4	70.5	68.7	**666.0**
	V×C	177.2	89.1	89.6	84.9	71.0	113.6	70.7	98.2	**794.3**
Average marker distance (cM)	**V**	2.5	5.4	2.9	2.9	2.1	2.6	1.8	3.5	**3.0**
	C	2.8	2.0	2.4	3.4	3.8	2.8	6.3	3.1	**3.3**
	V×C	1.6	1.3	1.2	1.2	0.9	1.0	1.4	11.6	**2.5**
Maximum gap (cM)	**V**	9.0	22.9	8.2	12.1	6.0	11.3	3.9	19.0	**11.6**
	C	10.5	7.5	8.2	11.9	12.1	9.0	19.0	10.5	**11.1**
	V×C	8.7	9.8	4.7	6.7	3.7	3.0	5.7	10.8	**6.6**

For analyses of polyphenols, fruit samples were frozen and stored at -20 ºC. Individual phenolic compounds were extracted as described by Serradilla et al. (2011a). For each tree, 10 g of homogenate obtained from 15 fruits, partially defrosted and pitted, was transferred to a volumetric flask and 50 mL of methanol solution containing 0.1% hydrochrolic acid was added. Subsequently, samples were incubated for 24h at -20ºC in darkness. Chromatographic analysis was carried out employing an Agilent 1100 model LC system (Hewlett-Packard, Waldbronn, Germany) equipped with an UV-Vis diode-array detector and with a rapid scan fluorescence spectrophotometer detector. Separation and quantification was performed according to Cabrera-Bañegil et al. (2017). Individual hydroxycinnamic acids [neochlorogenic acid (NA), *p*-coumaroylquinic acid (CQA) and *p*-coumaric acid (CA)] and anthocyanins [cyanidin-3-*O*-glucoside (cy3-glu), cyanidin-3-*O*-rutinoside (cy3-rut), peonidin-3-*O*-glucoside (peo3-glu) and peonidin-3-*O*-rutinoside

(peo3-rut)] were quantified against external standards (Sigma-Aldrich, Spain). Results are expressed as mg 100 g^{-1} FW.

SNP genotyping, linkage mapping and QTL analysis

Genomic DNA from the population and parental cultivars was obtained from young leave samples extracted using DNeasy® Plant Mini Kit (Qiagen, MD, USA). Genome-wide SNP genotyping of the population and the parental cultivars was carried out using RosBREED Cherry 15K Illumina Infinium® SNP array. DNA quantification by Quant-iT™ PicoGreen® (Invitrogen Ltd., Paisley, UK) and SNP genotyping was carried out at CEGEN-PRB2-ISCIII (Madrid, Spain).

SNP filtering and clustering, as well as linkage map development were conducted as described previously for cross-pollinated populations (Chapter 2). QTL analysis in the parental maps was carried out using MapQTL® v.6.0 (Kyazma BV, Wageningen, The Netherlands, van Ooijen, 2009). Interval mapping and MQM mapping strategies was used for QTL discovery in both parental cultivars (Lander and Bostein, 1989; Jansen, 1993 and 1994; Jansen and Stam, 1994). Significant threshold to considered a QTL in a given linkage group was calculated using Permutation Test at a significance level of 90% ($p<0.1$) using 10,000 permutations (van Ooijen, 1992). MapChart software were used for graphical representation of linkage groups (LGs) and QTLs.

Statistical analysis

Mean, minimum, maximum and standard deviation of V×C population was evaluated for each trait. Analysis of correlation among traits was carried out using *Pearson* correlation coefficient. All statistical analysis were conducted using SPSS statistics v21.0.0 software (IBM, IL, USA) and R v3.4.1 (R Core Team, 2017).

RESULTS AND DISCUSSION

Genotyping and linkage mapping

Genotyping of 'Vic' and 'Cristobalina' with RosBREED cherry 15K SNP array (Vanderzande et al., 2019) allowed scoring 11,566 (85.3%) and 11,616 (85.6%) SNPs in each cultivar, respectively. From the total of scored SNPs, 1,256 SNPs were heterozygous in 'Vic' and 1,136 were heterozygous in 'Cristobalina'. Within these, 335 SNPS were heterozygous in both cultivars. From the rest of scored markers, 8,317 and 8,537 SNPs were homozygous in 'Vic' and 'Cristobalina' respectively. The 15K array used in this work includes the markers available in the RosBREED cherry 6K SNP array (Peace et al., 2012) plus a selection of 9,000 additional SNPs, resulting in a significant increase of SNPs available for whole genome genotyping. The number of heterozygous markers detected in this work is larger (1.5 to 1.9 times larger) than the number reported for the same parental cultivars (483 in 'Vic', and 526 in 'Cristobalina'), and for other cultivars (450 to 641 SNPs; Klagges et al., 2014; Chapters 2 and 5) using the RosBREED cherry 6K SNP array.

The 2,057 heterozygous informative SNPs in the parental cultivars were used for V×C linkage mapping. Only those markers heterozygous in one parental cultivar and homozygous in the other were considered for parental linkage mapping. The remaining 11,502 SNPs (84.8%) of the array were discarded for further analysis due to various reasons; failed to be detected (2,305; 17.0%), were monomorphic (9,043; 66.7%) or resulted in unexpected segregations (154; 1.1%). Linkage mapping grouped the selected SNPs into the eight expected linkage groups (LGs) in each parental cultivar map. 'Vic' linkage map includes 910 SNPs spanning a total length of 636.7 cM, and the 'Cristobalina' linkage map has 789 SNPs and covers 666.0 cM (Table 7.1). Like in the maps developed using the RosBREED 6K SNP array (Chapter 2), LG1 in 'Vic' and, LG2 in 'Cristobalina' were the groups with the largest number of SNPs, while 'Vic' LG2 and 'Cristobalina' LG7 were the groups with the lowest number of markers (Table 7.1). Large gaps of ~20 cM were observed in 'Vic' LGs 2 and 6, and in 'Cristobalina' LG7, in same region as detected in the 6K SNP array (Chapter 2; Table 7), confirming that these regions are probably homozygous in these cultivars (Chapter 2). The V×C consensus map included 2,000 SNPs and covered a genetic distance of 794.3 cM, with an average distance between markers of 2.5 cM (Table 7.1). LGs 1 and 7, with 440 and 161 SNPs, were the LGs with largest and

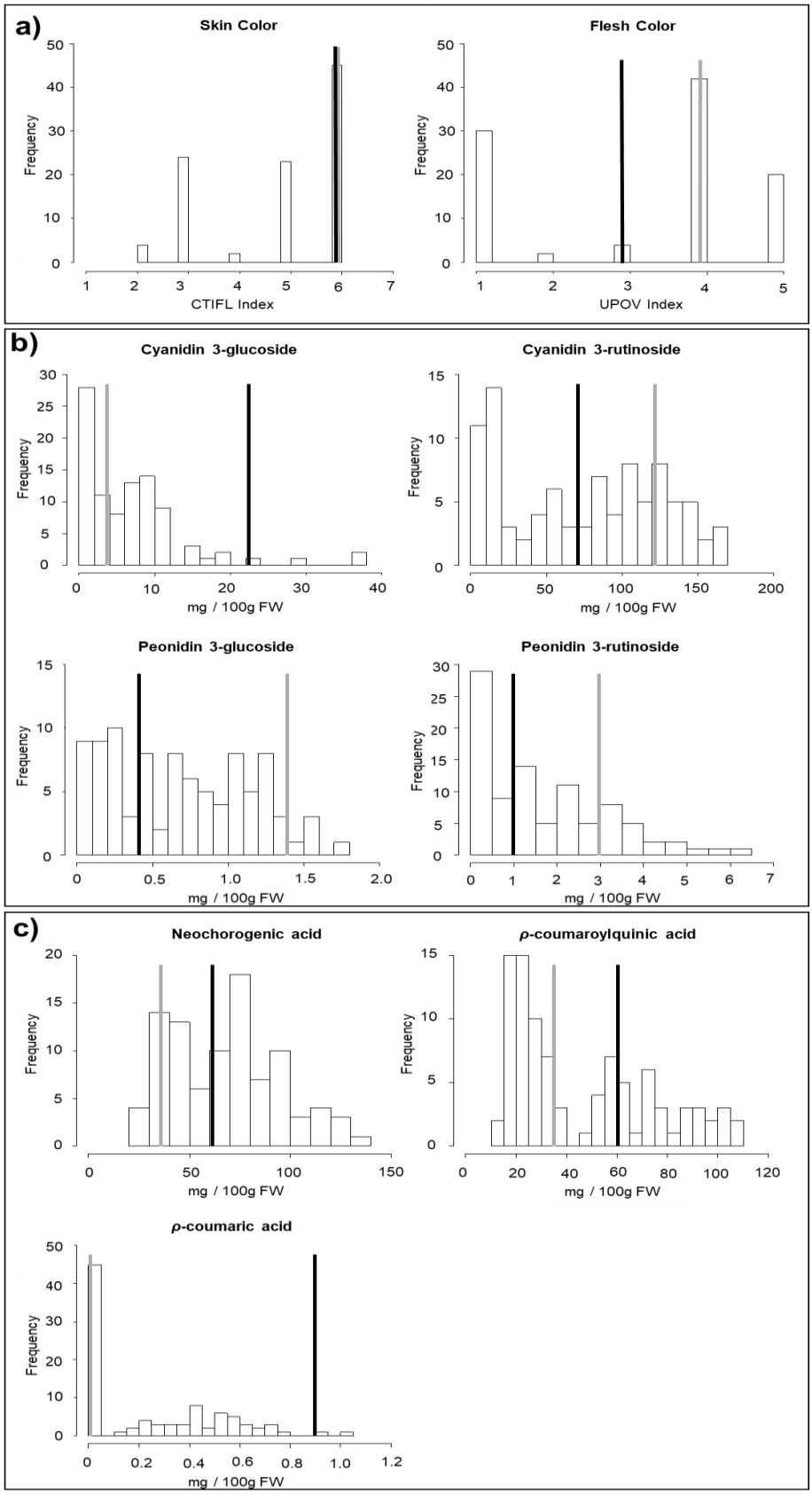

Figure 7.1 Distribution of phenotyped traits in V×C population. a) Skin and flesh color, b) anthocyanins, and c) phenolic acids. Mean parental values are indicated in grey ('Vic') and black ('Cristobalina').

least number of mapped markers respectively. A reduction in the average marker distance (2.5 cM) and gap size was observed in the consensus map compared with both parental maps (3.0 and 3.3 cM in 'Vic' and 'Cristobalina', respectively) (Table 7.1).

The use of the RosBREED 15K SNP array improved the linkage maps developed using the RosBREED 6K SNP array (Klagges et al., 2014; Chapters 2 and 5), as a larger number of markers could be mapped and a reduction in the average distance between these SNPs was observed. Additionally, the presence of additional markers in 15K SNP array allowed filling some gaps previously detected in the 6K SNP array derived maps (Sup Fig 1, Chapter 2). Despite the number of mapped markers is significantly larger than those mapped using the 6K SNP array, the relative low number of segregating individuals (161) limited the possibility of recombination and resulted in a large number of markers mapped at the same genetic position (64.7%, 66.3 and 60.7% in 'Vic', 'Cristobalina' and V×C, respectively). Alternatively, this may be due to SNPs found in regions with low recombination, which are inherited as blocks.

Color and anthocyanin content segregation and correlation

Skin and flesh color in sweet cherry are quantitative traits that exhibit a range of coloration from yellow to dark mahogany (Schmidt, 1998; Sooriyapathirana et al., 2010). In this work, skin and flesh color were evaluated in V×C, a population whose parental cultivars have similar mahogany fruit skin color (CTIFL code 6, Sup Fig 1), and pink and medium-red flesh (UPOV codes: 3 for 'Cristobalina' and 4 for 'Vic). Despite both parental cultivars have dark fruits, segregation was observed for both traits in the 98 phenotyped individuals, with value codes ranging from 2 to 6 for skin color, and from 1 to 5 for flesh color (Fig 7.1; Table 7.2; Sup Fig 1). The distribution of these traits in the segregating population was similar to that observed previously in cherry fruit color studies, in which a skewed distribution towards darker skin fruits was reported (Schmidt, 1998; Sooriyapathirana et al., 2010; Jin et al., 2016). Sixty-nine trees with fruit red to mahogany, or dark skin color (skin card >4) and 29 bicolor (yellow with orange overcolor) or light colored (skin card <4) were observed (Sup Fig 2). This segregation adjusts to a 3:1 (dark:light) ratio (χ^2=0.039), confirming that fruit color may be determined by a major gene with minor genes showing epistasis effects (Fogle, 1958; Schimidt, 1998). In this population, both parental cultivars 'Vic' and 'Cristobalina' would be heterozygous for this

major gene, with the dark allele being dominant and the light color allele being recessive. This recessive allele for light color will only have a phenotypic expression in determined crosses, when it is found in homozygosis. Jin et al. (2016), in a population also derived from another two dark cultivars, like the population analyzed herein, also reported a segregation of 3:1 (dark:light). Sooriyapathirana et al. (2010) observed a 9:7 (dark:light) segregation in a population whose parental cultivars were light and dark, fitting a 1:1 (dark:light) segregation (χ^2=0.028), and therefore adjusting to the described genetic model.

Table 7.2 Minimum (Min), maximum (Max) and mean values for evaluated traits in 'Vic', 'Cristobalina' and V×C population.

Trait	Units	'Vic'	'Cristobalina'	V×C population		
				Min	Max	Mean ± SD
Skin color	CTIFL Index	6	6	2	6	4.7 ± 1.4
Flesh color	UPOV Index	4	3	1	5	3.2 ± 1.6
Cy3-glu	mg / 100g FW	4.5	23.1	0	37.2	6.7 ± 7.2
Cy3-rut	mg / 100g FW	122.5	69.2	4.1	165.5	74.6 ± 50.6
Peo3-glu	mg / 100g FW	1.5	0.5	0	1.7	0.7 ± 0.5
Peo3-rut	mg / 100g FW	2.9	0.9	0	6.1	1.7 ± 1.5
NA	mg / 100g FW	89.3	43.0	24.5	136.5	68.1 ± 28.3
CQA	mg / 100g FW	35.9	61.5	13.9	105.4	45.9 ± 28.4
CA	mg / 100g FW	0	0.9	0	1.03	0.2 ± 0.3

Four anthocyanins were identified in 'Vic' and 'Cristobalina' fruits: cy3-glu, cy3-rut, peo3-glu and peo3-rut (Table 7.2). In both parental cultivars, the most abundant anthocyanins were cy3-rut (122.5 and 69.2 mg/100g FW in 'Vic' and 'Cristobalina' respectively), followed by cy3-glu (4.5 and 23.1 mg/100g FW in 'Vic' and 'Cristobalina' respectively), while peo3-glu and peo3-rut content was very low in both cultivars (0.9 to 2.9 mg/100g FW; Fig 7.1; Table 7.2). The same anthocyanins were reported by other authors in sweet cherry, with cy3-rut also accounting for 77 to 96% of total anthocyanin content (Serradilla et al., 2016). In V×C, only cy3-rut was detected in all the seedlings with concentrations ranging from 4.1 to 165.5 mg/100g FW (Fig 7.1; Table 7.2). This compound is the main pigment related to the sweet cherry color, and have been observed in light-colored cultivars as 'Rainier' or 'Gold' that the concentration was not higher than 1 mg/100g FW, it is absent in white cherries (Wünsch et al., 2014), whereas in dark cherries like 'Bing', cy3-rut can reach up to 297 mg/100g FW (Gao and Mazza, 1995; Serradilla et

al., 2016). The other anthocyanins ranged from being absent in most light-colored seedlings to 1.7 (peo3-glu), 6.1 (peo3-rut) and 37.2 (cy3-glu) mg/100g FW in red-black individuals (Fig 7.1; Table 7.2). All anthocyanins detected showed positive and negative transgressive segregation.

Trait correlation analyses revealed large positive correlation for skin and flesh color, and the four anthocyanins detected (Table 7.3). But the highest correlation was observed for cy3-rut and skin color (0.907; Table 7.3), confirming that anthocyanin content, most specifically cy3-rut, is the major component of sweet cherry fruit color (Gao and Mazza, 1995).

Table 7.3 Correlation between phenotyped traits.

	FC	**Cy3-glu**	**Cy3-rut**	**Peo3-glu**	**Peo3-rut**	**NA**	**CQA**	**CA**
SC	0.922*	0.632*	0.907*	0.834*	0.755*	-0.057	-0.148	-0.149
FC		0.603*	0.870*	0.821*	0.744*	-0.088	-0.124	-0.145
Cy3-glu			0.660*	0.581*	0.397*	-0.022	-0.165	-0.170
Cy3-rut				0.908*	0.870*	-0.006	-0.100	-0.116
Peo3-glu					0.763*	-0.054	-0.020	-0.010
Peo3-rut						0.038	-0.063	-0.071
NA							-0.533*	-0.570*
CQA								0.836*

***** Correlation is significant at the 0.001 level.

Color and anthocyanins QTL analyses

Previous QTL analysis for fruit color in sweet cherry (Sooriyapathirana et al., 2010) revealed a main QTL governing this trait on LG3. In this work, QTL analysis of color and anthocyanin content were conducted, being the analysis of anthocyanin content carried out for first time in sweet cherry. Most significant and stable QTLs of fruit color and all anthocyanins detected (cy3-glu, cy3-rut, peo3-glu and peo3-rut) were found on the same region of LG3 of both parental maps (Fig 7.2; Table 7.4). This region spans from 19.38 to 32.84 cM in 'Vic' map and from 35.95 to 59.45 cM in 'Cristobalina' map, which corresponds to same region of chromosome 3 in the sweet cherry genome (6.72 to 10.41Mbp in 'Vic' and 8.52 to 13.56 Mbp in 'Cristobalina'), where *PavMYB10* is located, and where the main fruit color QTL was detected (Sooriyapathirana et al., 2010).

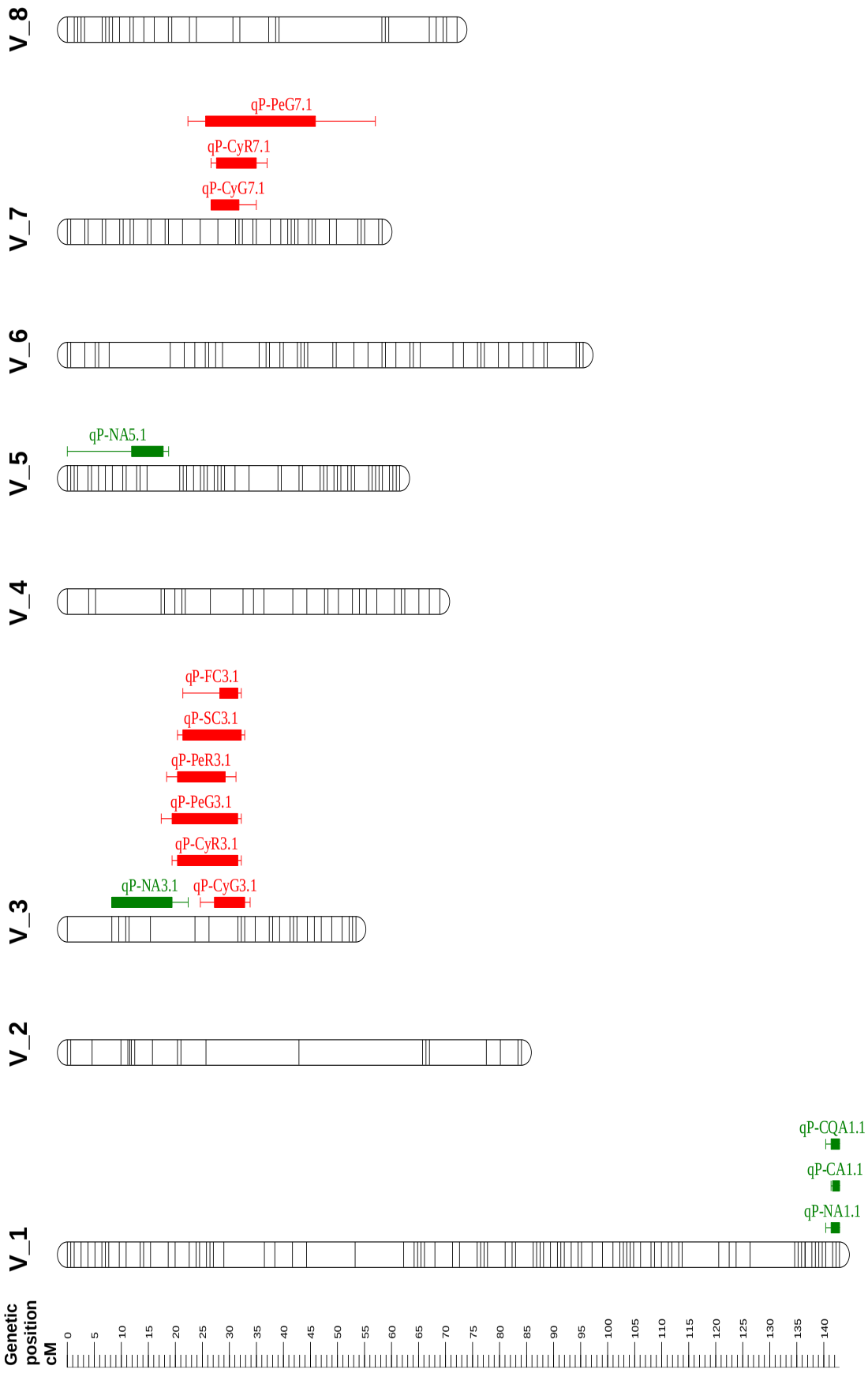

Figures 7.2 'Vic' linkage map and detected QTLs.

For skin and flesh colors, only this major QTL was identified in both parental cultivars explaining from 23.8 (*qP-SC3.2*) to 30.1% (*qP-SC3.1*) of phenotypic variation (Fig 7.2; Table 7.4). For anthocyanins, QTLs detected on this region of LG3 showed variable percentages of phenotypic variation, ranging from 13.6 to 22.7% in 'Vic' (*qP-CyG3.1, qP-CyR3.1; qP-PeG3.1* and *qP-PeR3.1*) and from 11.9 to 21.8 in 'Cristobalina' (*qP-CyG3.2; qP-CyR3.2; qP-PeG3.2* and *qP-PeR3.2*) (Table 7.4). The overlapping of the major QTLs for these traits, color and anthocyanins content, on a narrow region of LG3 confirms the correlation reported for these traits and the same genetic control (Sooriyapathirana et al., 2010). The transcription factor *PavMYB10* located in this region is the candidate gene of major determinant of sweet cherry color due to anthocyanin content, by regulating the anthocyanin biosynthesis pathway (Jin et al., 2016).

Minor QTLs for anthocyanin content were mapped on LG7 of 'Vic' (*qP-CyG7.1; qP-CyR7.1* and *qP-PeG7.1*) and on 'Cristobalina' LG4 (*qP-PeR4.1*; Fig 7.2; Table 7.4). These QTLs are firstly reported in this study and may also be associated with fruit color. The use of a low precision phenotyping methodology for fruit color in this work may have limit the QTL detection possibilities, indicating that should be necessary to complete this work with a more precise phenotyping of skin and flesh color in order to identify other color QTLs segregating in this population, and/or to confirm the correlation of the minor anthocyanin content QTLs detected with fruit color.

Additive effects were calculated for the detected QTLs to identify the effect of alleles associated with fruit color and anthocyanins content (Table 7.4). Positive values were observed for 'Vic' QTLs on LG3 for fruit color and all anthocyanins detected (*qP-CyG3.1, qP-CyR3.1; qP-PeG3.1, qP-PeR3.1, qP-SC3.1* and *qP-FC3.1*), suggesting that alleles from 'Vic' are associated with an increase in anthocyanin content and darker coloration. On the other side, 'Cristobalina' QTLs on LG3 and 'Vic' QTLs on LG7 were associated with negative additive effects. The largest additive positive and negative effect observed for cy3-rut QTLs on LG3 confirm the large effect of this QTL on fruit color and anthocyanin content.

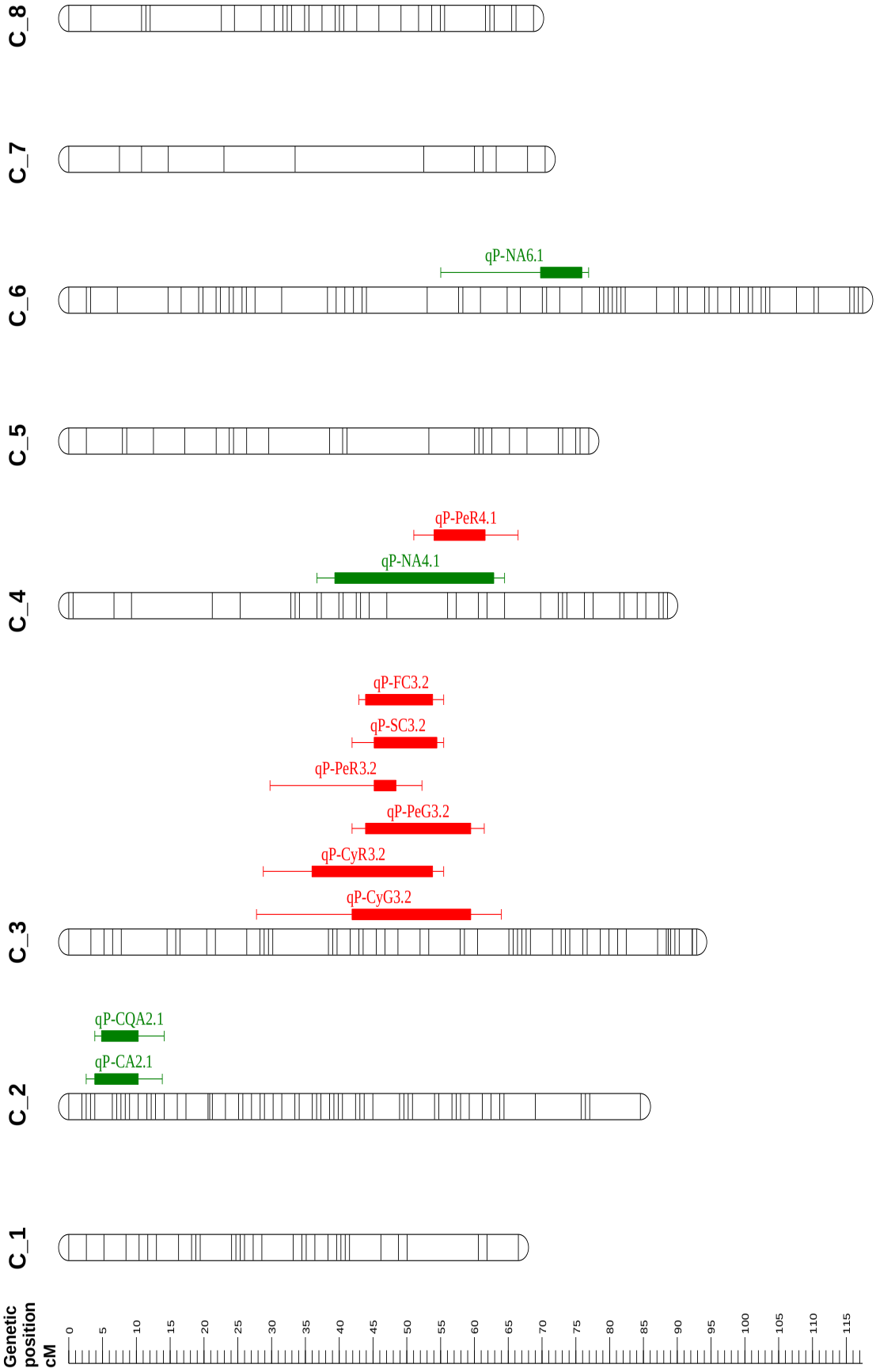

Figures 7.3 'Cristobalina' linkage map and detected QTLs.

Phenolic acids content and QTL analysis

Three phenolic acids, NA, CQA and CA, which derive from the hydroxycinnamic acid (Cheynier et al., 2013), were identified in the population and the parental cultivars (Fig 7.1; Table 7.2). The highest concentrations in the parental cultivars were observed for NA in 'Vic' (89.3 mg/100 FW) and CQA in 'Cristobalina' (61.5 mg/100 FW), while CA was only detected in 'Cristobalina' at very low concentration (0.9 mg/100 FW; Table 7.2). In the population, a large mean value (68.1 mg/100g FW) was observed for NA, which ranged from 24.5 to 136.5 mg/100g FW, followed by CQA with a mean of 45.9 mg/100g FW (13.9 to 105.4 mg/100g FW). As in the parental cultivars, CA was only detected in some individuals of V×C, with maximum concentrations of 1.03 mg/100g FW (Fig 7.1; Table 7.2). Similar results have been observed in other sweet cherry cultivars, in which a larger amount of NA than CQA has been reported (Usenik et al., 2008; Serrano et al., 2009). However, we observed in 'Cristobalina', as well as has been previously observed in 'Burlat' (Gonçalves et al., 2004), a larger amount of CQA than NA, indicating that the ratio of these compounds is specific of each cultivar and might be related to fruit development, as both are very early ripening cultivars, or to genetic similarity, as both are original from southern Europe (Wünsch and Hormaza, 2002).

A significant negative correlation was observed between NA and the others two phenolic acids, CQA (-0.533) and CA (-0.570) that were highly positively correlated (0.836). As expected, no correlation was observed between anthocyanins and phenolic acids, as both types of compounds derive from different biosynthesis pathways, the anthocyanins that derive from phenylpropanoid, and the phenolic acids, which derived from hydroxycinnamic acid (Cheynier et al., 2013).

This lack of correlation between the two groups of compounds was also observed in the QTL analysis, as different QTLs were detected for the phenolic acids content, confirming their different genetic control. A major QTL for the phenolic acids (NA, CQA and CA), was found on a narrow region at the bottom of 'Vic' LG1 at great LOD values (19.9 to 32.5; Fig 7.2; Table 7.4), and explaining a large proportion of the variation (60.3 to 77.9). These QTLs were associated with additive effects of 21.40, 24.90 and 0.23 mg/100g FW for NA, CQA and CA, respectively (Fig 7.2; Table 7.4). This QTL is probably associated with a major gene determinant of the phenolic acids content, therefore

Table 7.4 QTLs identified for evaluated traits in 'Vic' and 'Cristobalina' cultivars.

Trait	Parental	QTL name	LG	QTL interval (cM)	Physical position*	QTL peak				
						Cofactor SNP	LOD	Variance	PVE	Additive effect
Skin color	Vic	*qP-SC3.1*	3	21.39-32.20	7.50-10.00	PAV3_13025963	7.7	1.20	30.1	0.74
	Cristobalina	*qP-SC3.2*	3	45.17-54.45	12.11-13.56	PAV3_12987920	5.8	1.31	23.8	-0.67
Flesh Color	Vic	*qP-FC3.1*	3	21.39-28.22	7.50-9.05	PAV3_13025963	6.1	1.83	24.8	0.79
	Cristobalina	*qP-FC3.2*	3	43.90-53.82	11.68-13.37	PAV3_12987920	7.3	1.73	28.8	-0.87
Cy3-glu	Vic	*qP-CyG3.1*	3	27.22-32.84	8.91-10.41	PAV3_13025963	3.5	43.84	13.7	2.68
	Vic	*qP-CyG7.1*	7	26.60-31.77	13.94-15.73	PAV7_13940978	1.3	47.78	5.9	-1.74
	Cristobalina	*qP-CyG3.2*	3	41.90-59.45	9.21-13.56	PAV3_12987920	3.1	44.74	11.9	-2.60
Cy3-rut	Vic	*qP-CyR3.1*	3	20.39-31.56	6.72-9.05	PAV1_30710911	5.5	1935	22.7	24.29
	Vic	*qP-CyR7.1*	7	27.60-34.98	13.94-16.86	PAV7_16310608	1.9	2294	8.3	-14.48
	Cristobalina	*qP-CyR3.2*	3	35.95-53.82	8.52-12.98	PAV3_15373201	4.8	2030	18.9	-22.95
Peo3-glu	Vic	*qP-PeG3.1*	3	19.39-31.53	6.72-10.41	PAV1_30710911	3.6	0.18	16.4	0.19
	Vic	*qP-PeG7.1*	7	25.60-45.92	12.92-18.28	PAV7_16310608	1.8	0.20	8.4	-0.13
	Cristobalina	*qP-PeG3.2*	3	43.90-59.45	10.91-13.56	PAV3_12987920	3.0	0.19	13.6	-0.18
Peo3-rut	Vic	*qP-PeR3.1*	3	20.39-29.22	6.72-9.05	PAV1_30710911	4.3	1.89	17.8	0.65
	Cristobalina	*qP-PeR3.2*	3	45.17-48.39	10.47-16.21	PAV3_15373201	5.3	1.80	21.8	-0.75
	Cristobalina	*qP-PeR4.1*	4	54.04-61.58	10.18-11.94	PAV4_10981932	4.1	1.92	16.7	-0.63
NA	Vic	*qP-NA1.1*	1	141.34-142.90	43.21-47.58	PAV1_47015014	19.9	297	60.3	-21.40
	Vic	*qP-NA3.1*	3	8.24-19.39	9.35-16.60	PAV4_16184822	4.0	233	6.2	-7.02
	Vic	*qP-NA5.1*	5	11.90-17.76	4.30-8.19	PAV5_4897952	2.9	203	3.6	-5.26
	Cristobalina	*qP-NA4.1*	4	39.35-62.68	7.14-12.01	PAV4_10184036	2.4	679	9.3	-8.51
	Cristobalina	*qP-NA6.1*	6	69.78-75.89	19.16-20.91	PAV6_19476076	2.0	615	7.1	7.28
CQA	Vic	*qP-CQA1.1*	1	141.34-142.90	43.21-47.58	PAV1_47015014	32.5	174	77.9	24.90
	Cristobalina	*qP-CQA2.1*	2	4.85-10.27	0.52-4.23	PAV2_2274343	3.0	688	12.4	9.90
CA	Vic	*qP-CA1.1*	1	141.34-141.63	43.21-47.01	PAV1_47472494	23.6	0.02	67.9	0.23
	Cristobalina	*qP-CA2.1*	2	3.85-10.27	0.50-4.23	PAV2_2274343	2.0	0.07	7.4	0.07

*Physical position on sweet cherry genome v1 (Shirasawa et al., 2017)

candidate gene analysis in this region will allow to identify potential genes for the regulation of phenolic acid content in sweet cherry.

This is the first genetic analysis of phenolic acids in a *Prunus* species, but QTL analyses of phenolic acids have been previously carried out in other *Rosaceae* species like apple (Khan et al., 2012; Chagné et al., 2012b; Verdu et al., 2014). Comparison of QTLs from this study and those detected in apple, revealed that the main region on LG1, in which most significant QTLs for phenolic acids were found in this study is syntenic to LGs 14 and 15 in apple (Illa et al., 2011), where the main QTLs for phenolic acids have also been reported (Chagné et al., 2012b; Verdu et al., 2014). Within these QTL intervals, candidate genes for phenolic acid content were reported in apple (Chagné et al., 2012b; Verdu et al., 2014). These are, genes homologous to *shikimate/quinate O-hydroxycinnamoyl transferase* (*HCT/HQT*) that has been shown to contribute to hydroxycinnamic acid synthesis in other plant species (Lepelley et al., 2007; Sonnante et al., 2010), and other genes such as *flavonoid 3'-hydrolase* and *MYB* genes (*MYB110a* and *MYB110b*; Verdu et al., 2014). Being syntenic the regions that control phenolic acids in *Malus* and *Prunus*, the candidate genes reported in apple may also be candidate genes in sweet cherry and *Prunus* species for phenolic acids content regulation, suggesting a conserved regulation mechanism of phenolic acids content within *Rosaceae*. Further studies should be carried out to confirm this hypothesis.

Conclusion

This study is the first report in sweet cherry of QTLs for polyphenols, anthocyanins and phenolic acids, traits that are associated with fruit quality, color and health-promoting properties. The use of the recently developed RosBREED cherry 15K SNP array allowed the saturation of previously generated SNP maps in the species, revealing a powerful tool for QTL and genetic analysis. Segregation of the studied phenolic compounds in the V×C population allowed identifying two main cluster of QTLs, on LGs 1 and 3, associated with the phenotype variation of these traits. A major QTL on LG3 regulates anthocyanin content and therefore fruit color, most likely due to the presence of the previously reported transcription factor *PavMYB10*. In the bottom region of LG1, another major QTL regulates phenolic acid compounds content, in a syntenic region in which QTLs for same compounds were reported in apple, suggesting candidate genes might be the same as those reported in

Malus. In addition, this study allowed identifying additional QTLs of anthocyanin content that may also be associated to fruit color.

SUPPLEMENTARY MATERIALS CHAPTER 7

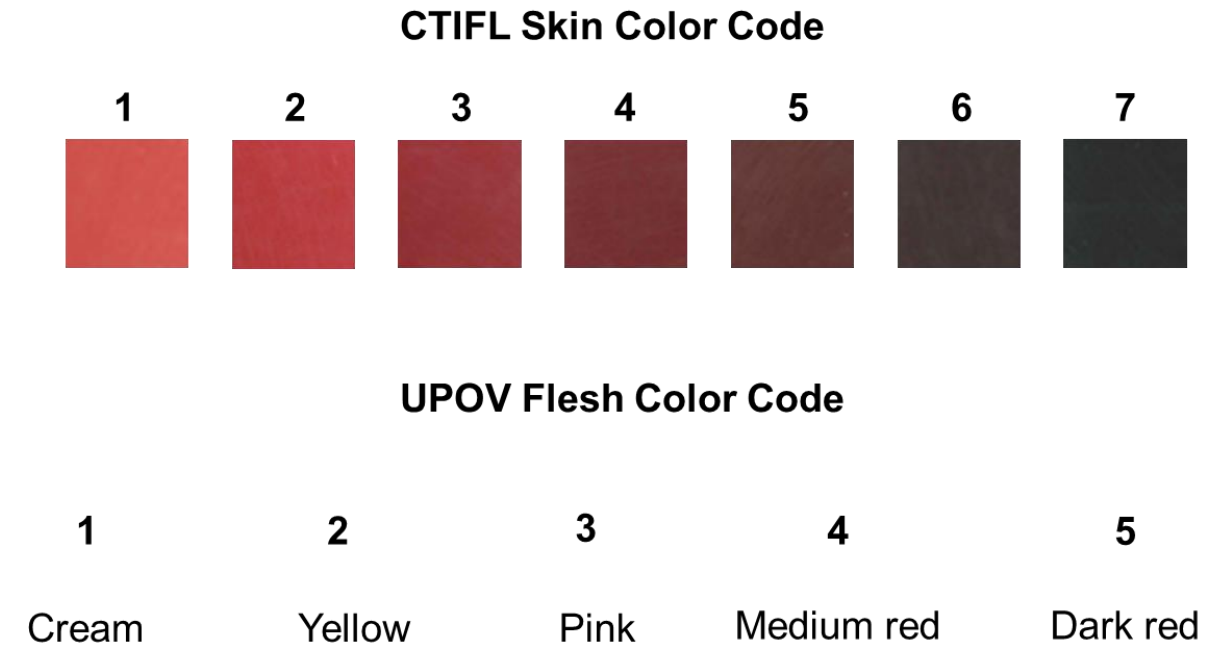

Supplementary Fig 1 CTIFL and UPOV color codes.

Supplementary Fig 2 Example of bicolor/light and mahogany/dark colored fruit of V×C population.

8. DISCUSSION

SNP genotyping and linkage maps

Sweet cherry cultivars from different genetic backgrounds, including landraces like 'Cristobalina' and 'Ambrunés', and bred cultivars, have been genotyped in this study using the whole genome Illumina RosBREED cherry 6K and 15K SNP arrays (Peace et al., 2013; Vanderzande et al., 2019). These arrays have allowed identifying heterozygous markers in the same range as previously reported for other cultivars, 400-700 for the 6K (Peace et al., 2012; Klagges et al., 2013), and near 2,300 in the 15K array (Vanderzande et al., 2019). Within cultivars, those that derived from breeding programs, and descend from a few ancestors, had lower number of heterozygous markers than the landrace 'Ambrunés', confirming a loss of heterozygosity in bred cultivars as a result of inbreeding (Choi and Kappel, 2004). But, surprisingly, a low number of heterozygous markers were found in the landrace 'Cristobalina' compared with other cultivars. This low heterozygosity and the large homozygous regions observed in most of the LGs, detected with both 6K and 15K arrays, suggests that 'Cristobalina' may derive from self-pollination, and this fact could be the cause of some of its characteristics, like low vigor and small fruit size.

Four sweet cherry populations were used for linkage map development using the 6K array (Chapters 2 and 5). Additionally, one of these populations (V×C) was also used for map construction using the 15K array (Chapter 7), being the first report of a linkage map using this array. In general, the 6K maps were similar in terms of number of SNPs, genetic length, average distances between markers and gaps sizes than observed for other maps developed using the same array (Klagges et al., 2013), adding this study new high-density linkage maps to the previously developed in the species (Klagges et al., 2013; Guajardo et al., 2015; Wang et al., 2015; Shirasawa et al., 2017). These maps (Chapter 2, 5 and 7) are a useful tool for the investigation of sweet cherry genetics, and are the basis of other studies carried out in this work, as they gave an insight in the study of inbreeding depression in the species (Chapter 2), allowed performing QTL analysis and discovery for several relevant quantitative breeding traits, and were used for haplotype analysis for the identification of relevant QTL alleles of sweet cherry breeding (Chapters 3, 5, 6 and 7). In addition, all developed maps derive from local plant material ('Cristobalina' and

'Ambrunés'), which are highly interesting cultivars for breeding purposes due to their relevant characters, and as a source of genetic variability in the narrow genetic diversity of many commercial sweet cherry cultivars (Wünsch, 2019). Results revealed that the inclusion of this plant material was useful to investigate the genetics of traits of breeding interest like low chilling requirements and early bloom date from 'Cristobalina' (Chapters 3 and 4) for example, or the high fruit firmness and late maturity date from 'Ambrunés' (Chapters 5 and 6).

Despite various linkage maps have been constructed in sweet cherry from intraspecific and interspecific crosses with other related species (reviewed in Salazar et al., 2014; Iezzoni et al., 2017), this work reports the first time linkage maps of self-pollinated populations, adding a useful tool for sweet cherry genetic analyses. The natural self-compatibility of 'Cristobalina' (Wünsch and Hormaza, 2004; Ono et al., 2018) made possible to develop F_2 populations in the species. These F_2 populations (C×C and B×C2) were used in this work for linkage mapping and allowed carrying out genetic analyses that could not be investigate in cross-pollination populations. For example, B×C2 population resulted highly useful to investigate the BT, FD and MD QTL effects (Chapters 3 and 6). In addition, these F_2 populations led to take a first look at genome-wide effect of self-pollination in an obligate outcrossing species as sweet cherry. Self-pollination lead to an increase in homozygosity that was associated with a reduction in fitness by inbreeding depression (Chapter 2).

QTL analyses

In this work, a QTL mapping approach using multi-families and multi-years data was used when possible (i.e. phenotype data from various years was available or could be generated within the research period, or plant material was available). This approach was used for the study of BT, FD, MD, FS, FW, FF, TA and SSC. The use of this approach has proven very useful for QTL detection and the identification of allele variation of these traits. Only two previous studies have used a similar approach for QTL analysis in sweet cherry (Rosyara et al., 2013; Cai et al., 2019), in which FS and FF were investigated. This strategy, combined with the use of F_2 populations and local germplasm, has resulted in a highly efficient tool for genetic analyses of relevant traits in the species and the identification of relevant alleles for breeding purposes. An example of translating this QTL

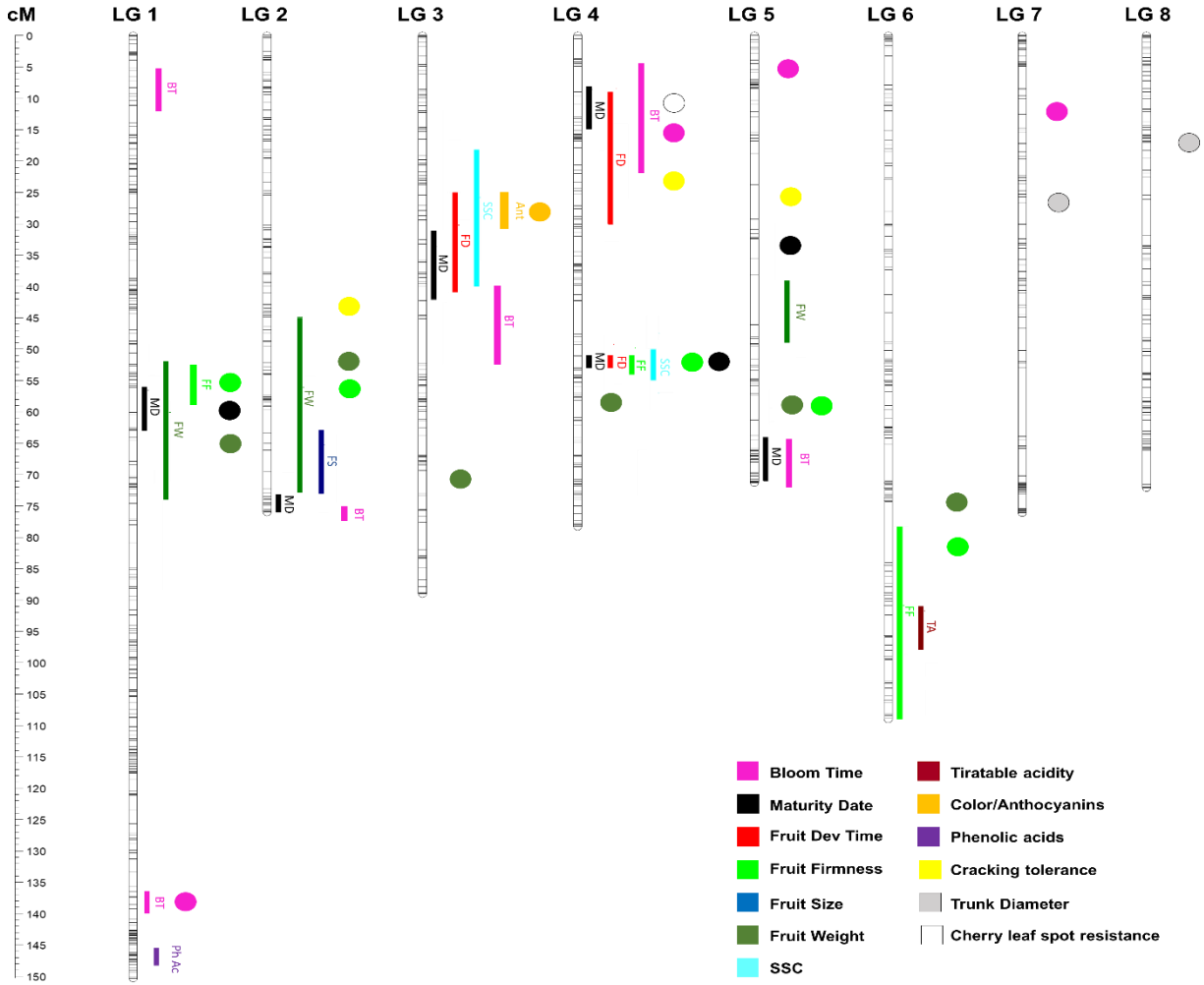

Figure 8.1 Genetic position of most relevant QTLs identified in this study (colored bars). Only QTLs detected ≥ 2 years are shown, except for polyphenols content, for which QTLs detected one year with LOD>3.0 are shown. Colored circles indicate approximate genetic position of main QTLs for the same traits reported previously (Iezzoni et al., 2017; Quero-García, 2019).

analysis into breeding efficiency is shown in results derived from QTL studies from Chapter 3 that resulted in a breeding marker for early blooming (Chapter 4). A similar approach could be applied to the other traits investigated.

New major QTLs

In general, QTL analyses of several phenology and fruit traits in this work allowed, either the detection of new QTLs, or the validation of previously detected QTLs in the species for the same traits, and the identification of new alleles. As some investigated traits [FD, TA, SSC and polyphenolic compounds (anthocyanins and phenolic acids)] have been considered for QTL analyses by first time in this work, new QTLs were reported for them in the species. For all them, major QTLs were found, suggesting the presence of major genes associated with the genetic control of these traits (Fig 8.1). Major QTLs for these traits were found on LG1 for phenolic acids, on LG3 for anthocyanin content, on LG4 for FD and SSC, and on LG6 for TA (Fig 8.1). Some of these were very stable, as multiple year data allowed their detection in various years such is the case of FD, TA or SSC. Other traits were only studied one year (polyphenolic compounds) but the large significance and variation explained suggest they are also probably stable QTLs. Nevertheless, additional data (more years) should be analyzed to confirm the results.

Some of these sweet cherry newly detected major QTLs (FD and polyphenolics content), are found in syntenic regions to QTLs previously described for the same traits in other *Prunus* and *Malus* species (Chagné et al., 2012; Verdu et al., 2014; Fresnedo-Ramírez et al., 2015; Hernández Mora et al., 2017), and therefore candidate genes for these traits may be the same as previously reported for these species (Table 8.1). Also, some of these major new QTLs, are found in the same region of QTLs of correlated traits. This was the case of main FD and SSC or FF QTLs that overlap with the region of main MD QTL (Chapter 6; Dirlewanger et al., 2012; Isuzugawa et al., 2019), suggesting that these traits may be determined by linked genes, or a by major FD gene with pleiotropic effect over SSC and FF. As a larger fruit development period, and hence later maturity, is associated with sugar accumulation, SSC and FF may be result from a longer development period, and hence both traits may be determined by the same gene/s. Another example is anthocyanin content and fruit color, with QTLs overlapping on same region of LG3 (Chapter 7; Sooriyapathirana et al., 2010), thus confirming that both traits are determined

by the same regulatory gene (*MYB10*), and anthocyanins (most specifically cy3-rut) are the main determinant of sweet cherry coloration (Lin-Wang et al., 2010; Jin et al., 2016). On the other side, QTL and correlation analyses revealed that for the two types of polyphenolic compounds studied their genetic control is not related. Phenolic acids and anthocyanins content are not correlated and are associated to different QTLs on LGs 1 and 3, respectively, revealing different regulatory genes of the corresponding biosynthesis pathways.

QTL validation and new alleles

Other traits investigated herein (BT, MD, FF, FS and FW) have been previously studied using QTL analysis in sweet cherry (Zhang et al., 2010; Dirlewanger et al., 2012; Rosyara et al., 2013; Quero-García et al., 2014; Campoy et al., 2015; Cai et al., 2019; Isuzugawa et al., 2019). This study validated most of previously reported QTLs for these traits in a different genetic background, and revealed new minor QTLs, thus completing the genetic picture of these traits. Additionally, and most relevant, for some of these major validated QTLs, a different effect and/or new alleles were identified in this work. This is the case of BT QTL analysis, in which main QTLs on LGs 1 and 2 were associated a much larger proportion of the variation in this work (Chapter 3) than previously reported (Castède et al., 2014). Additionally, the main QTL previously reported for this trait, on LG4 (Dirlewanger et al., 2012; Castède et al., 2014), did not have a large effect in this plant material. The inclusion in the analysis of populations derived from 'Cristobalina', with low CR and extra-early BTs, allowed identifying that the effect of these QTLs (LGs 1 and 2) is larger in this plant material, and hence these major QTLs are associated with low CR and early bloom. Similarly, for MD, the major QTL previously described on LG4 in sweet cherry and other *Prunus* species (Dirlewanger et al., 2012; Isuzugawa et al., 2019; Quilot et al., 2004; Dirlewanger et al., 2012; Nuñez-Lillo et al., 2015; Salazar et al., 2016 and 2017) was validated in this work, but again, in this work new alleles were identified, in cultivars of early MD as 'Cristobalina' and 'Burlat', mainly associated with short FD period and early MD.

For FF, also new QTL effects and alleles were identified in this work in the major QTLs identified on LG1 (Chapter 5; Campoy et al., 2015; Cai et al., 2019) and LG4 (Chapter 6; Cai et al., 2019). On LG1, a relevant QTL was identified in 'Ambrunés' ×

‘Sweetheart’, in which ‘Ambrunés’ contributes for larger fruit size and firmness (Chapter 5). The use of ‘Cristobalina’ in the multi-family approach also allowed detecting the recently reported main FF QTL on LG4 (Chapter 6; Cai et al., 2019). Bred cultivars evaluated in this study were homozygous for firm alleles on FF QTL of LG4 (Cai et al., 2019), which suggest this locus was objective of selection during domestication and cherry breeding, and only in some landraces, like ‘Cristobalina’, soft alleles were segregating for this QTL (Chapter 6). Similar regions under selection in sweet cherry breeding have been observed on LG2 for FS (Cai et al., 2017), in which main FS QTL was found in this study only when parental cultivars of low fruit size as ‘Cristobalina’ was considered (Chapter 6).

Candidate genes

The description of major QTLs for evaluated traits in this work will allow the description and study of candidate genes that can be associated to the observed phenotypic variation, and that will permit MAS and/or optimization of the breeding process. This strategy was successfully carried out in this work for major BT QTL on LG1 (Chapters 3 and 4). A similar approach could be attempt for other relevant QTLs detected in this work as candidate genes in these QTL regions have been previously described in sweet cherry and other related species (Table 8.1; reviewed in Aranzana et al., 2019). Furthermore, the availability of sweet cherry genome sequences (Shirasawa et al., 2017; Le Dantec et al., 2019) will allow the analysis of these genome regions to identify additional candidate genes for these traits.

In this study, using the sweet cherry genome sequence available (Le Dantec et al., 2019), CR and BT candidate *DAM* genes (Bielenberg et al., 2008; Jiménez et al., 2009; Sasaki et al., 2011) were identified and characterized (*PavDAM*) in major BT QTL on LG1 (Chapters 3 and 4). Cultivar sequence comparison allowed identifying cultivar specific polymorphisms that may be associated to phenotypic variation, and a deletion (DPD) in the promoter region of ‘Cristobalina’ *PavDAM* associated with early BT (Chapter 4). This mutation may help explaining low CR and extra-early flowering of this cultivar (Chapter 3; Tabuenca, 1983; Alburquerque et al., 2008) but additional experiments are needed to confirm this hypothesis. Nevertheless, the polymorphism detected (DPD) will be useful for MAS of early BT.

Table 8.1 Candidate genes in main QTLs detected in this work, reported in sweet cherry and other *Rosaceae* species (Aranzana et al., 2019).

Trait	Ch	QTL	Candidate gene	*P. avium*	Other species
BT	1	*qP-GDH1.2^{m}*	*DAM1-6*	Chapter 4 Castède et al. (2015)	*P. persica* (Bielenberg et al., 2008) *P. mume* (Sasaki et al., 2011)
	2	*qP-GDH2.1^{m}*	*SOC1*	Castède et al. (2015)	*P. armeniaca* (Trainin et al., 2013)
			FAR1	Castède et al. (2015)	
MD	4	*qP-MD4.2^{m}*	*NAC*	Isuzugawa et al. (2019)	*P. persica* (Pirona et al., 2013)
FF	4	*qP-FF4.1^{m}*	*Expansin-A12* *endoPG*	Cai et al. (2019)	 *P. persica* (Peace et al., 2005)
FS	1	*qP-Dia1.2^{m}*	*PavCNR09* *PavCNR10* *PavCNR11*	De Franceschi et al. (2013) De Franceschi et al. (2013) De Franceschi et al. (2013)	
	2	*qP-FS2.1^{m}*	*PavCNR12*	De Franceschi et al. (2013)	
Color/ Anthoc.	3	*qP-SC3.1* *qP-CyR3.1*	*MYB10*	Sooriyapathirana et al. (2010) Lin-Wang et al. (2010) Chapter 7	Apple (Espley et al., 2007)
Pheno. acids	1	*qP-NA1.1* *qP-CQA1.1* *qP-CA1.1*	*HCT/HQT*	Chapter 7	Apple (Chagné et al., 2012) Verdu et al. (2014)

For the other relevant QTLs identified (Figure 8.1), for BT and other analyzed traits, candidate genes which have been previously reported (Table 8.1) could be also investigated. This is the case of MADS-box genes, *SOC1* and *FAR1* in main BT QTL of LG2 (Chapter 3; Trainin et al., 2013; Castède et al., 2015), or NAC transcription factor for MD on LG4 (Chapter 6; Pirona et al., 2013; Isuzugawa et al., 2019). Other relevant candidate genes proposed for fruit quality traits in the QTLs described and/or validated herein are *expansin-A12* and *endopolygalacturonase* for fruit firmness on LG4 (Chapter 6; Peace et al., 2005; Cai et al., 2019), *CNR* on fruit size LGs 1 (*PavCNR09*, *PavCNR10* and *PavCNR11*) and 2 (*PavCNR12*) (Chapter 4 and 5; De Franceschi et al., 2013), *PavMYB10* for fruit color and anthocyanin content (Chapter 7; Sooriyapathirana et al., Lin-Wang et al., 2010; Wünsch et al., 2014; Jin et al., 2016) or *shikimate/quinate O-hydroxycinnamoyl transferase* genes for phenolic acids on LG1 (Chapter 7; Verdu et al., 2014).

Applications in sweet cherry breeding

Trait correlations studied in this work will be useful for cherry breeding as evidence was obtained that in the plant material analysed some traits are significantly highly correlated, and therefore selecting for one of them implies selecting for another. These

correlations were observed within phenology (e.g. FD and MD; Chapter 6) and fruit quality traits (e.g. FW and FS, or FF and SSC) studied, but also amongst both types of traits (e.g. FD/MD and SSC/FF). These correlations may be the result of one trait being the cause of another (e.g. FD and SSC), or because both traits have the same genetic control (e.g. FD and MD). The later was confirmed in this work for some traits by identifying the same associated QTLs (e.g. FD and MD; fruit color and anthocyanin content).

For the phenology traits studied, FD showed a high positive correlation with MD confirming the same previously reported correlation in other *Prunus* species (Chapter 6; Etienne et al., 2002, Salazar et al., 2013 and 2016). In addition, the overlapping of main MD QTLs, in the syntenic regions of BT and FD QTLs, revealed that MD genetic control can be dissected into BT and FD QTLs, which are independent of each other (Chapters 3 and 6). These results indicated that to breed for early or late MD, in order to adapt to different climatic conditions and chilling areas, to obtain early cherries, or to extend the growing season in order to reduce seasonality; short or long FD and early or late BT could be selected.

Other highly correlated traits in this study were mapped on clusters of stable and major QTLs (Chapters 5, 6 and 7) as observed in other fruit species (Quilot et al., 2004; Kenis et al., 2008; Eduardo et al., 2011; Zeballos et al., 2016; Salazar et al., 2013 and 2017). This was the case of MD, FD, FF and SSC on LG4; FS, FS and FF on LG1; anthocyanin compounds and fruit color on LG3; and phenolic acids on LG1 (Fig 8.1). These clusters of QTLs are of high interest for breeding, as selection of certain haplotypes will allow selection various traits at the same time. Additionally, the haplotype analysis of these QTL regions in various parental cultivars, including local landraces, allowed the identification of QTL haplotypes or alleles of breeding interest, like the ‘Cristobalina’ haplotypes on LGs 1 and 2 (*H1-c* and *H2-f* ; Chapter 3) that are associated to early flowering and low CR; the ‘Cristobalina’ and ‘Burlat’ haplotype on LG4 (*H4-c*; Chapter 6) that is associated with short FD and early MD but also to low FF; or the ‘Ambrunés’ haplotypes on LG1 (*Wei1.1_H2*; *Dia1.1_H2*; *Fir1.1_H2*; Chapter 5) that could be used for increasing fruit size and firmness at the same time. The identification of these new QTLs haplotypes/alleles will be useful for sweet cherry breeding, as MAS for these traits can be done by selecting the appropriate haplotypes in segregating populations from these

parental cultivars, either by using the SNP haplotypes defined in these works or by designing PCR markers from SNP markers at these haplotypes.

Most direct application for sweet cherry breeding was developed in this work in Chapter 4 for BT as described above. By characterising the candidate genes of this trait at the main BT QTL (*PavDAM*), identifying a mutation associated to the phenotypic variation (early blooming), and developing a PCR marker (DPD) associated to this polymorphism, early BT, and most likely low CR material, can be selected from 'Cristobalina' derived individuals using this PCR marker.

Due to the narrow genetic diversity of sweet cherry, especially for bred cultivars, local landraces like 'Cristobalina' and 'Ambrunés', are an opportunity for the genetic improvement of relevant breeding traits. In this work, genetic analysis and genomic tools were successfully used to study phenology and fruit quality traits derived from this plant material, facilitating the selection of this local phenotypic variability in breeding programs. This work will be useful to release new cultivars adapted to the growers, market intermediaries and consumer demands, to improve adaptation and hence allow a more sustainable production, and to confront the challenge of global threats like climate change and global warming.

9. CONCLUSIONS

1. Genotyping of intra-specific sweet cherry populations with genome-wide 6K and 15K SNP arrays allowed constructing high-density linkage maps from cross- and self-pollinated populations, providing a useful tool to enable genetic analysis. The genetic maps from the F_2 populations, being the first in the species, revealed a high degree of homozygosity, providing an opportunity to investigate inbreeding depression in this naturally outbreeding species.

2. Sweet cherry linkage maps comparison with peach genome allowed confirming a high degree of synteny between both species genomes, although specific differences like small translocated and inverted regions, with the most noticeable inversion at top of LG5, were detected.

3. The multi-family QTL mapping approach implemented by FlexQTL™ software, combined with the use of F_1 and F_2 populations derived from local germplasm, proved to be a useful approach for detecting QTLs for the phenology and fruit quality traits studied and for identifying new QTL variants of breeding interest.

4. The multi-year bloom time QTL analysis using populations derived from the low chilling and early blooming cultivar 'Cristobalina', allowed validating two main QTLs on linkage groups 1 and 2 accounting for nearly 63% of the phenotypic variation, and revealed that in these plant material phenotypic variation is not determined by the major bloom time QTL previously reported on LG4 in other populations with medium to late bloom time. These QTLs are, therefore, major determinants of bloom time in this low chilling plant material.

5. 'Cristobalina' early bloom haplotypes for major bloom time QTLs on LGs 1 and 2 can be selected for breeding for low chilling and early blooming, as this was the only evaluated cultivar that contributed with alleles for early blooming in these QTLs.

6. Characterization in the ‘Regina’ sweet cherry genome of six MADS-box proteins (*PavDAM*), orthologues to *P. mume* and *P. persica DAM* genes, on major bloom time QTL on LG1 confirmed that these genes are main candidates of low chilling requirements and bloom time regulation in sweet cherry.

7. Alignment of the genome sequences of 13 sweet cherry cultivars with different chilling requirements and bloom times allowed detecting polymorphisms in the *PavDAM* sequences that may be associated to these phenotypic differences. Additionally, a 696 bp deletion in ‘Cristobalina’ *PavDAM* promoter, that correlates with early blooming, was also identified. A marker developed to detect this mutation will be useful for marker-assisted selection of low chilling requirements and early blooming from ‘Cristobalina’.

8. The multi-year and multi-family analysis of fruit development period and maturity date revealed that both traits are highly correlated, and that both are associated to a major QTL region on LG4, indicating that maturity date is most likely mainly dependent on genetic control of fruit development period. Additionally, minor QTLs for maturity date were the same of those reported for bloom time, revealing that, to a minor extent in sweet cherry, maturity date also depends on the genetic control of bloom time.

9. The use of an F_1 population from two unrelated cultivars, ‘Ambrunés’ and ‘Sweetheart’, allowed validating previously reported QTLs in the species for diameter, weight and firmness. Additionally, QTLs for the three traits, in the same region of LG1, have alleles of breeding interest in coupling phase in ‘Ambrunés’, revealing that selection of this haplotype from ‘Ambrunés’ will provide larger and firmer fruits.

10. The genetic analysis of fruit quality traits (size, firmness, solid soluble content and titratable acidity) allowed validating main QTLs previously detected for these traits in other genetics backgrounds, and identifying new major QTLs for sugar content and acidity on LGs 4 and 6 respectively.

11. Major QTLs for fruit development period, fruit firmness and sugar content, traits which are also correlated, were mapped on the same narrow region of LG4. These results indicate that these traits may have the same genetic regulation or that a major gene regulating fruit development time may have a pleiotropic effect in the other fruit quality traits, as a larger development period may result in the accumulation of sugars and in fruit firmness increase.

12. The identification of a cluster of major phenology and fruit quality traits QTLs on LG4 will be useful for breeding purposes as specific haplotypes of this QTL region will allow selecting for short or long developing period and hence early or late maturity date, and sugar content or firmness at the same time. 'Cristobalina' and 'Burlat' haplotypes of this region associated to short fruit development time may be of interest for breeding for early maturity, but these haplotypes are also associated to low firmness.

13. The identification of major anthocyanins content QTLs on LG3, overlapping with skin and flesh color QTLs also validated in this work, confirmed that anthocyanins content, and cyanidin 3-rutinoside in largest amount, is the main determinant of color variation most likely due to the previously proposed candidate gene, the transcription factor *PavMYB10*, which regulates the anthocyanin biosynthesis pathway.

14. First report of a phenolic acids content QTL analysis in sweet cherry and *Prunus* species, has allowed identifying a major QTL on LG1, explaining up to 78% of the variation. This QTL is located in a syntenic region to the QTL region regulating the same traits in apple and therefore, candidate genes *HCT/HQT* for this trait in apple may be also regulating phenolic acid content in sweet cherry and *Prunus* species.

9. CONCLUSIONES

1. El genotipado de poblaciones intra-específicas de cerezo con los arrays de SNPs 6K y 15K permitió la construcción de mapas de ligamiento de alta densidad de familias de cruzamientos y de autopolinzaciones, proporcionando una herramienta de utilidad para el desarrollo de análisis genéticos. Los mapas genéticos de las poblaciones F_2 son los primeros en la especie y revelaron un alto grado de homocigosidad, proporcionando una oportunidad para investigar la depresión por consanguinidad en esta especie de polinización cruzada.

2. La comparación de los mapas de ligamiento de cerezo con el genoma del melocotonero permitió confirmar el alto grado de sintenia entre los genomas de ambas especies, aunque diferencias específicas como pequeñas regiones translocadas e invertidas fueron detectadas, siendo una inversión en la parte superior del GL5 la más destacable.

3. El mapeo de QTLs utilizando varias familias, implementado con el software FlexQTL™, combinado con el uso de poblaciones F_1 y F_2 derivadas de material local, fue una estrategia útil para detectar QTLs de los caracteres fenológicos y de calidad de fruto estudiados y para identificar nuevas variantes de QTLs de interés para la mejora.

4. El análisis multianual de QTLs para fecha de floración usando poblaciones derivadas del cultivar de bajos requerimientos de frio y floración temprana ‘Cristobalina’, permitió validar dos QTLs principales en los grupos de ligamientos 1 y 2, que explicaron casi el 63% de la variación fenotípica; revelando que en este material la variación fenotípica no está determinada por el QTL principal de floración previamente identificado en el GL4 en familias de floración media a tardía. Por lo tanto, estos QTLs son los principales determinantes de la fecha de floración en este material de bajos requerimientos de frio.

5. Los haplotipos de floración temprana de ‘Cristobalina’, en los QTLs principales de floración identificados en los grupos de ligamiento 1 y 2, pueden ser seleccionados para la mejora genética de bajos requerimientos de frío y floración temprana, ya que éste fue el único cultivar evaluado que presentó alelos de floración temprana en estos QTLs.

6. La caracterización de seis proteínas MADS-box (*PavDAM*) en el genoma del cultivar de cerezo ‘Regina’ en la región del QTL principal de floración en el GL1, y que son ortólogos a los genes *DAM* identificados en *P. mume* y *P. persica*,, confirmó que estos son los principales genes candidatos al control de bajos requerimientos de frio y fecha de floración en cerezo.

7. El alineamiento de la secuencia genómica de 13 cultivares de cerezo con diferentes requerimientos de frío y fechas de floración permitió detectar polimorfismos en las secuencias de los genes *PavDAM* que podrían estar asociadas a estas diferencias fenotípicas. Además, también se identificó una deleción de 696 pb en el promotor de los *PavDAM* en ‘Cristobalina’, que esta correlacionada con floración temprana. El marcador desarrollado para detectar esta mutación será de utilidad para la selección asistida por marcadores de bajos requerimientos térmicos y floración temprana de ‘Cristobalina’.

8. El análisis plurianual y multifamiliar del período de desarrollo de fruto y la fecha de maduración reveló que ambos caracteres están muy correlacionados, y que ambos están asociados a un QTL principal en la misma región del GL4, lo que indica que probablemente la fecha de maduración depende principalmente del control genético de período de desarrollo del fruto. Además, QTLs menores para la fecha de maduración fueron los mismos que los identificados para fecha de floración, revelando que la fecha de maduración también depende del control genético de la fecha de floración, aunque en menor medida.

9. El uso de una población F_1 de dos cultivares no relacionados, ‘Ambrunés’ y ‘Sweetheart’, permitió validar QTLs previamente identificados en la especie para diámetro, peso y firmeza. Además, QTLs para los tres caracteres localizados en la misma región de GL1, tienen alelos de interés en fase de acoplamiento en ‘Ambrunés’, lo que indica que la selección de este haplotipo de ‘Ambrunés’ permitirá seleccionar frutos más grandes y más firmes.

10. El análisis genético de los caracteres de calidad de fruto (tamaño, firmeza, contenido en sólidos solubles y acidez titulable) permitió validar los QTLs principales detectados previamente para estos caracteres en otros fondos genéticos e identificar nuevos QTLs mayores para el contenido en azúcares y acidez en los GL 4 y 6 respectivamente.

11. QTLs mayores para período de desarrollo de fruto, firmeza y contenido en azúcares, que son caracteres que además están correlacionados entre si, se mapearon en la misma estrecha región del GL4. Estos resultados indican que estos caracteres pueden tener el mismo control genético o que un gen mayor que regule el periodo de desarrollo de fruto pueda tener un efecto pleiotrópico sobre los otros caracteres, ya que un período de desarrollo más largo puede resultar en un aumento de la acumulación de azúcares y en una mayor firmeza del fruto.

12. La identificación de un grupo de QTLs mayores en el GL4 para caracteres fenológicos y de calidad de fruto será de utilidad para la mejora ya que los haplotipos específicos de esta región permitirán seleccionar para un período de desarrollo corto o largo y, por lo tanto, una fecha de maduración temprana o tardía, así como para contenido de azúcares o firmeza al mismo tiempo. Los haplotipos de ‘Cristobalina’ y ‘Burlat’ de esta región asociados con un desarrollo de fruto corto pueden ser de interés para la mejora para maduración temprana, pero estos holotipos también están asociados a una menor firmeza.

13. La identificación de QTLs principales para el contenido de antocianinas en el grupo de ligamiento 3, en la misma región que los QTLs para color de piel y pulpa que también fueron validados en este trabajo, confirmó que el contenido de antocianinas, y en particular la cianidina 3-rutinósido, es el principal determinante de la variación de color, probablemente debido al gen candidato previamente propuesto, el factor de transcripción *PavMYB10*, que regula la ruta de biosíntesis de antocianinas.

14. El primer trabajo de análisis de QTLs para el contenido de ácidos fenólicos en cerezo y especies del genero *Prunus* ha permitido identificar un QTL principal en el grupo de ligamiento 1 que explica hasta el 78% de la variación. Este QTL está ubicado en una región sinténica a la región del QTL que regula este mismo carácter en manzano, y por tanto los genes candidatos *HCT/HQT* para este carácter en manzano puede que también regulen el contenido en ácido fenólicos en cerezo y otras especies del genero *Prunus*.

10. BIBLIOGRAPHY

Abbott AG, Zhebentyayeva T, Barakat A, Liu Z.A (2015) The genetic control of bud-break in trees. Advances in Botanical Research 74: 201-228.

Afgan E, Baker D, Batut B, Van Den Beek M, Bouvier D, Cech M, Chilton J, Clements D, Coraor N, Grüning BA, Gueler A, Hillman-Jackson J, Hiltmann S, Jalili V, Rasche H, Soranzo N, Goecks J, Taylor J, Nekrutenko A, Blankenberg D (2018) The Galaxy platform for accessible, reproducible and collaborative biomedical analyses: 2018 update. Nucleic Acids Research 46: 537-544.

Alburquerque N, García-Montiel F, Carrillo A, Burgos L (2008) Chilling and heat requirements of sweet cherry cultivars and the relationship between altitude and the probability of satisfying the chill requirements. Environmental and Experimental Botany 64(2): 162-170.

Alique R, Zamorano JP, Martínez MA, Alonso J (2005) Effect of heat and cold treatments on respiratory metabolism and shelf-life of sweet cherry, type picota cv 'Ambrunés'. Postharvest Biology and Technology 35(2): 153–165.

Allan AC, Hellens RP, Laing WA (2008) MYB transcription factors that colour our fruits. Trends in Plant Sciences 13: 99-102.

Allard A, Bink MCAM, Martinez S, Kelner JJ, Legave JM, di Guardo M, Laurens F, van de Weg EW, Costes E (2016) Detecting QTLs and putative candidate genes involved in budbreak and flowering time in apple multiparental population. Journal of Experimental Botany 67(9): 2875-2888.

Anciro A, Mangandi J, Verma S, Peres N, Whitaker VM, Lee S (2018) *FaRCg1*: a quantitative trait locus conferring resistance to *Colletotrichum* crown rot caused by *Colletotrichum gloeosporioides* in octoploid strawberry. Theoretical and Applied Genetics 131: 2167-2177.

Anderson JL, Seeley SD (1993) Bloom delay in deciduous fruits. Horticultural Reviews 15: 97-144.

AOAC (1984) Official Methods of Analysis. Association of Official Analytical Chemists. 14th Edition, AOAC, Arlington.

Aranzana MJ, Decroocq V, Dirlewanger E, Eduardo I, Gao ZS, Gasic J, Iezzoni A, Jung S, Peace C, Prieto H, Tao R, Verde I, Abbott AG, Arús P (2019) *Prunus* genetics and applications after de novo genome sequencing: achievements and prospects. Horticulture Research 6: 58.

Arumuganathan K, Earle ED (1991) Nuclear DNA content of some important plant species. Plant Molecular Biology Reporter 9(3): 208-218.

Atkinson CJ, Brennan RM, Jones HG (2013) Declining chilling and its impact on temperate perennial crops. Environmental and Experimental Botany 91: 48–62.

Badenes ML, Zuriaga E (2016) "Frutales de hueso" in Las variedades locales en la mejora genética de plantas eds. Ruiz de Galarreta JI, Prohens J, Tierno R (Servicio central de publicaciones del Gobierno Vasco) 239-258.

Baggiolini M (1980) Stades repères du cerisier - Stades repères du prunier. Stades repères de l'abricotier. Stades repères du pêcher. ACTA. Guide Pratique de Défense des Cultures, Paris.

Balas F, López-Corrales M, Serradilla MJ, Cai L, Iezzoni A, Wünsch A (2019) Firmness QTL mapping using an 'Ambrunés' × 'Sweetheart' sweet cherry population. Acta Horticulturae: 1235.

Ballester J, Socias i Company R, Arús P, Vicente MC (2001) Genetic mapping of a major gene delaying blooming time in almond. Plant Breeding 120: 268-270.

Ballistreri G, Continella A, Gentile A, Amenta M, Fabroni S, Rapisarda P (2013) Fruit quality and bioactive compounds relevant to human health of sweet cherry (Prunus avium L.) cultivars growth in Italy. Food Chemistry 140: 630-638.

Bargioni G (1996) "Sweet cherry scions. Characteristics of the principal commercial cultivars, breeding objectives and methods" in Cherries: Crop physiology, production and uses eds. Webster AD, Looney NE (CAB International): 73-112.

Bassi D, Bartolozzi F, Muzzi E (1996) Patterns and heritability of carboxylic acids and soluble sugar in fruits of apricot (Prunus armeniaca L.). Plant Breeding 118: 97-100.

Bassil NV, Davis TM, Zhang H, Ficklin S, Mittmann M, Webster T, Mahonet L, Wood D, Alperin ES, Rosyara UR, Putten HK, Monfort A, Sargent DJ, Amaya I, Denoyes B, Bianco L, van Dijk T, Pirani A, Iezzoni A, Main D, Peace C, Yang Y, Whitaker V, Verma S, Bellon L, Brew F, Herrera R, van de Weng E (2015) Development and preliminary evaluation of a 90K Axiom® SNP array for the allo-octoploid cultivated strawberry *Fragaria* × *ananassa*. BMC Genomics 16:1.

Bates D, Maechler M, Bolker B, Walker S (2015) Fitting Linear Mixed-Effects Models Using lme4. Journal of Statistical Software. 67(1): 1-48.

Becker A, Theißen G (2003) The major clades of MADS-box genes and their role in the development and evolution of flowering plants. Molecular Phylogenetics and Evolution 29: 464–489.

Bernalte MJ, Hernández MT, Vidal-Aragón MC, Sabio E (1999) Physical, chemical, flavor and sensory characteristics of two sweet cherry varieties grown in 'Valle del Jerte' (Spain). Journal of Food Quality 22(4): 403–416.

Bianco L, Cestaro A, Linsmith G, Muranty H, Denancé C, Théron A, Poncet C, Micheletti D, Kerschbamer E, Di Pierro EA, Larger S, Pindo M, Van de Weg E, Davassi A, Laurens F, Velasco R, Durel CE, Troggio M (2016) Development and validation of the Axiom® apple 480K SNP genotyping array. Plant Journal 86: 62–74.

Bianco L, Cestaro A, Sargent DJ, Banchi E, Derdak S, Di Guardo M, Salvi S, Jansen J, Viola R, Gut I, Laurens F, Chagné D, Velasco R, van de Weg E, Troggio M (2014) Development and validation of a 20K single nucleotide polymorphism (SNP) whole genome genotyping array for apple (*Malus* × *domestica* Borkh). PLoS ONE 9(10): e110377.

Bielenberg DG, Rauh B, Fan S, Gasic K, Abbott AG, Reighard GL, Okie WR, Wells CE (2015) Genotyping by sequencing for SNP-based linkage map construction and QTL analysis of chilling requirement and bloom date in peach [*Prunus persica* (L.) Batsch] PLoS ONE. 10(10): e0139406.

Bielenberg DG, Wang Y, Li ZG, Zhetentyayeva T, Fan SH, Reighard GL, Scorza R, Abbott AG (2008) Sequencing and annotation of the evergrowing locus in peach *Prunus persica* (L.) Batsch reveals a cluster of six MADS-box transcription factors as candidate genes for regulation of terminal bud formation. Tree Genetics and Genomes 4: 495-507.

Bink MCAM, Boer MP, ter Braak CJF, Jansen J, Voorrips RE, van de Weg WE (2008) Bayesian analysis of complex traits in pedigreed plant populations. Euphytica 161: 85–96.

Bink MCAM, Jansen J, Madduri M, Voorrips RE, Durel CE, Kouassi AB, Laurens F, Mathis F, Gessler C, Gobbin D, Rezzonico F, Patocchi A, Kellerhals M, Boudichevskaia A, Dunemann F, Peil, Nowicka A, Lata B, Stankiewicz-Kosyl M, Jeziorek K, Pitera E, Soska A, Tomala K, Evans KM, Fernández-Fernández F, Guerra W, Korbin M, Keller S, Lewandowski M, Plocharski W, Rutkowski K, Zurawicz E,Costa F, Sansavini S, Tartarini S, Komjanc M, Mott D, Antofie A, Lateur M, Rondia A, Gianfranceschi L, van de Weg WE (2014) Bayesian QTL analyses using pedigreed families of an outcrossing species, with application to fruit firmness in apple. Theoretical and Applied Genetics 127: 1073–1090.

Bodénès C, Chancerel E, Ehrenmann F, Kremer A, Plomion C (2016) High-density linkage mapping and distribution of segregation distortion regions in the oak genome. DNA Research 23:115–124.

Bolger AM, Lohse M, Usadel B (2014) Trimmomatic: A flexible trimmer for Illumina sequence data. Bioinformatics 30: 2114–2120.

Boškovic R, Tobutt KR (1998) Inheritance and linkage relationships of isoenzymes in two interspecific cherry progenies. Euphytica 103: 273–286.

Boudehri K, Bendahmane A, Cardinet G, Troadec C, Moing A, Dirlewanger E (2009) Phenotypic and fine genetic characterization of the *D* locus controlling fruit acidity in peach. BMC Plant Biology 9: 59.

Brown SK, Iezzoni AF, Fogle HW (1996) "Cherries" in Fruit Breeding. Tree and tropical fruits, eds. Janick J and Moore JN (John Wiley and Sons) vol 1: 213-255.

Brummell D, Harpster M (2001) Cell wall metabolism in fruit softening and quality and its manipulation in transgenic plants. Plant Molecular Biology 47: 311-340.

Cabrera A, Rosyara UR, De Franceschi P, Sebolt A, Sooriyapathirana SS, Dirlewanger E, Quero-García J, Schuster M, Iezzoni A, van der Knaap E (2012) Rosaceae conserved orthologous sequences marker polymorphism in sweet cherry germplasm and construction of a SNP-based map. Tree Genetics and Genomes 8: 237–247.

Cabrera-Bañegil M, Schaide T, Manzano R, Delgado-Adámez J, Durán-Merás I, Martín-Vertedor D (2017) Optimization and validation of a rapid liquid chromatography method for determination of the main polyphenolic compounds in table olives and in olive paste. Food Chemistry 233: 164-173.

Cáceres-Molina J, Rothkegel K, Sánchez E, Carrasco-Valenzuela T, Meneses C, Prieto H, Almeida AM (2019) A draft genome of *Prunus avium* 'Karina' as a tool for genomic studies. Acta Horticulturae 1235: 85-91.

Cachi AM, Wünsch A (2011) Characterization and mapping of non-S gametophytic self-compatibility in sweet cherry (*Prunus avium* L.). Journal of Experimental Botany 62: 1847–1856.

Cachi AM, Wünsch A (2014) Characterization of self-compatibility in sweet cherry varieties by crossing experiments and molecular genetic analysis. Tree Genetics and Genomes 10: 1205–1222.

Cai L, Quero-García J, Barreneche T, Dirlewanger E, Saski C, Iezzoni A (2019). A fruit firmness QTL identified on linkage group 4 in sweet cherry (*Prunus avium* L.) is associated with domesticated and bred germplasm. Scientific Reports 9: 5008.

Cai L, Stegmeir T, Sebolt A, Zheng C, Bink MCAM, Iezzoni A (2018) Identification of bloom date QTLs and haplotype analysis in tetraploid sour cherry (*Prunus cerasus*). Tree Genetics and Genomes 14: 22.

Cai L, Voorrips RE, van de Weg E, Peace C, Iezzoni A (2017) Genetic structure of a QTL hotspot on chromosome 2 in sweet cherry indicates positive selection for favorable haplotypes. Molecular Breeding 37: 85.

Campoy JA, Darbyshire R, Dirlewanger E, Quero-García J, Wenden B (2019) Yield potential definition of the chilling requirement reveals likely underestimation of the risk of climate change on winter chill accumulation. International Journal of Biometeorology 63(2): 183-192.

Campoy JA, Le Dantec L, Barreneche T, Dirlewanger E, Quero-García J (2015) New insights into fruit firmness and weight control in sweet cherry. Plant Molecular Biology Reporter 33(4): 783–796.

Campoy JA, Lerigoleur-Balsemin E, Christmann H, Beauvieux R, Girollet N, Quero-García J, Dirlewanger E, Barreneche T (2016) Genetic diversity, linkage disequilibrium, population structure and construction of a core collection of *Prunus avium* L. landraces and bred cultivars. BMC Plant Biology 16: 49.

Campoy JA, Ruiz D, Allderman L, Cook N, Egea J (2011) The fulfilment of chilling requirements and the adaptation of apricot (*Prunus armeniaca* L) in warm winter climates: An approach in Murcia (Spain) and the Western Cape (South Africa). European Journal of Agronomy 37(1): 43-55.

Castède S, Campoy JA, Le Dantec L, Quero-García J, Barreneche T, Weden B, Dirlewanger E (2015) Mapping of candidate genes involved in bud dormancy and flowering time in sweet cherry (*Prunus avium*). PLoS ONE 10(11): e0143250.

Castède S, Campoy JA, Quero-García J, Le Dantec L, Lafargue M, Barreneche T, Wenden B, Dirlewanger E (2014). Genetic determinism of phenological traits highly affected by climate change in *Prunus avium*: flowering date dissection into chilling and heat requirements. New Phytologist 202: 703-715.

Chagné D, Carlise CM, Blond C, Volz RK, Whitworth CJ, Oraguzie NC, Crowhurst RN, Allan AC, Espley RV, Hellen RP, Gardiner SE (2007) Mapping a candidate gene (*MdMYB10*) for red flesh and foliage colour in apple. BMC Genomics 8: 212.

Chagné D, Crowhurst RN, Troggio M, Davey MW, Gilmore B, Lawley C, Vanderzande S, Hellens RP, Kumar S, Cestaro A, Velasco R, Main D, Rees JD, Iezzoni A, Mockler T, Wilhelm L, Van de Weg E, Gardiner SE, Bassil N, Peace C (2012a) Genome-wide

SNP detection, validation, and development of an 8K SNP array for apple. PLoS ONE 7(2): e31745.

Chagné D, Dayatilake D, Diack R, Oliver M, Ireland H, Watson A, Gardiner SE, Johnston JW, Schaffer R, Tustin S (2014) Genetic and environmental control of fruit maturation, dry matter and firmness in apple (*Malus* × *domestica* Borkh.). Horticulture Research 1: 14046.

Chagné D, Krieger C, Rassam M, Sullivan M, Fraser J, André C, Pindo M, Troggio M, Gardiner SE, Henry RA, Allan AC, McGhie TK, Laing WA (2012b) QTL and candidate gene mapping for polyphenolic composition in apple fruit. BMC Plant Biology 12: 12.

Chaovanalikit A, Wrolstad RE (2004) Total anthocyanins and total phenolic of flesh and processed cherries and their antioxidant properties. Journal of Food Science 69: 67-72.

Charlesworth B, Charlesworth D (1999) The genetic basis of inbreeding depression. Genetics Research 74(3): 329–340.

Chauving M, Withing M, Ross CF (2009) The influence of harvest time on sensory properties and consumer acceptance of sweet cherries. Horticulture Technology 19: 748–754.

Chavoshi M, Watkins C, Oraguzie B, Zhao Y, Iezzoni A, Oraguzie N (2014) Phenotyping protocol for sweet cherry (*Prunus avium* L.) to facilitate an understanding of trait inheritance. Journal of American Pomology Society 68(3): 125-134.

Cheynier V, Comte G, Davies KM, Lattanzio V, Martens S (2013) Plant phenolics: recent advances on their biosynthesis, genetics and ecophysiology. Plant Physiology and Biochemistry 72: 1-20.

Choi C, Kappel F (2004) Inbreeding, coancestry, and founding clones of sweet cherries from North America. Journal of the American Society for Horticultural Science 129(4): 535-543.

Christensen JV (1972) Cracking in cherries III. Determination of cracking susceptibility. Acta Agriculturae Scandinavica 22: 128-136.

Clarke JB, Sargent DJ, Boškovic RI, Belaj A, Tobutt KR (2009) A cherry map from the inter-specific cross *Prunus avium* 'Napoleon' × *P. nipponica* based on microsatellite, gene-specific and isoenzyme markers. Tree Genetics and Genomes 5: 41–51

Cliff MA, Dever MC, Hall JW, Girard B (1995) Development and evaluation of multiple regression methods for prediction of sweet cherry liking. Food Research International 28: 583–589.

Cooke JEK, Eriksson ME, Junttila O (2012) The dynamic nature of bud dormancy in trees: Environmental control and molecular mechanisms. Plant, Cell and Environment 35: 1707–1728.

Crisosto CH, Crisosto GM, Metheney P (2003) Consumer acceptance of 'Brooks' and 'Bing' cherries is mainly dependent on fruit SSC and visual skin color. Postharvest Biology and Technology 28: 159–167.

Da Silva Linge C, Bassi D, Bianco L, Pacheco I, Pirona R, Rossini L (2015) Genetic dissection of fruit weight and size in an F_2 peach (*Prunus persica* (L.) Batsch) progeny. Molecular Breeding 35: 71.

De Franceschi P, Stegmeir T, Cabrera A, van der Knapp E, Rosyara UR, Sebolt AM, Dondini L, Dirlewanger E, Quero-García J, Campoy JA, Iezzoni AF (2013) Cell number regulator genes in *Prunus* provide candidate genes for the control of fruit size in sweet and sour cherry. Molecular Breeding 32: 311-326.

Di Guardo M, Micheletti D, Bianco L, Koehorst-Van Putten HJJ, Longhi S, Costa F, Aranzana MJ, Velasco R, Arús P, Troggio M, van deWeg EW (2015) ASSIsT: an automatic SNP scoring tool for in- and outbreeding species. Bioinformatics 31: 3873–3874

Di Guardo M, Bink MCAM, Guerra W, Letschka T, Lozano L, Busatto N, Poles L, Tadiello A, Bianco L, Visser RGF, van de Weg E, Costa E (2017) Deciphering the genetic control of fruit texture in apple by multiple family-based analysis and genome-wide association. Journal of Experimental Botany 68: 1451-1466.

Di Pierro EA, Gianfranceschi L, Di Guardo M, Koehorst-van Putten HJJ, Kruisselbrink JW, Longhi S, Troggio M, Bianco L, Muranty H, Pagliarani G, Tartarini S, Letschka T, Lozano Luis L, Garkava-Gustavsson L, Micheletti D, Bink MCAM, Voorrips RE, Aziz E, Velasco R, Laurens F, van deWegWE (2016) A high-density, multiparental SNP genetic map on apple validates a new mapping approach for outcrossing species. Horticulture Research 3: 16057.

Dickson GH (1959) Vista, Venus and Vic sweet cherries. In: Ontario Hort. Expt. Sta. and Prod. Lab. Rpt. for 1957–58. Vineland Station, Ont: 43–44.

Dirlewanger E, Claverie J, Iezzoni A, Wünsch A (2009) "Sweet and sour cherries: Linkage maps, QTL detection and marker assisted selection" in Genetics and Genomics of Rosaceae, Plant Genetics and Genomic: Crops and Model 6 eds. Folta KM and Gardiner SE (Springer Science): 291-313.

Dirlewanger E, Graziano E, Joobeur T, Garriga-Calderé F, Cosson P, Howad W, Arús P (2004) Comparative mapping and marker assisted selection in Rosaceae fruit crops. PNAS 101: 9891–9896.

Dirlewanger E, Quero-García J, Le Dantec L, Lambert P, Ruiz D, Dondini L, Illa E, Quilot-Turion B, Audergon JM, Tartarini S, Letourmy P, Arús P (2012) Comparison of the genetic determinism of two key phenological traits, flowering and maturity dates, in three *Prunus* species: peach, apricot and sweet cherry. Heredity 109: 280–292.

Dondini L, Lugli S, Sansavini S (2018) "Cherry breeding: sweet cherry (*Prunus avium* L.) and sour cherry (*Prunus cerasus* L.)" in Advances in plant breeding strategies: fruits eds. Al-Khayri JM, Jain SM, Hohnsin DV (Springer): 31-88.

Edgar RC (2004) MUSCLE: Multiple sequence alignment with high accuracy and high throughput. Nucleic Acids Research 32: 1792–1797.

Eduardo I, Pacheco I, Chietera G, Bassi D, Pozzi C, Vecchietti A, Rossini L (2011) QTL analysis of fruit quality in two peach intraspecific populations and importance of maturity date pleiotropic effect. Tree Genetics and Genomes 7: 323-335.

Eiro MJ, Heinonen M (2002) Anthocyanin colour behavior and stability during storage: effect of intermolecular copigmentation. Journal Agricultural and Food Chemistry 50: 7461e7466.

Espley RV, Hellens RP, Puterill J, Kutty-Amma S, Allan AC (2007) Red colouration in apple fruit it due to the activity of a *MYB* transcription factor, *MdMYB10*. Plant Journal 49: 414-427.

Etienne C, Rothan C, Moing A, Plomion C, Bodénès C, Svanella-Dumas L, Cosson P, Pronier V, Monet R, Dirlewanger E (2002) Candidate genes and QTLs for sugar and organic acid content in peach [*Prunus persica* (L.) Batsch]. Theoretical and Applied Genetics 105: 145-159.

Fadón E, Rodrigo J (2018) Unveiling winter dormancy through empirical experiments. Environmental and Experimental Botany 152: 28-36.

Fadón E, Rodrigo J, Herrero M (2018) Is there a specific stage to rest? Morphological changes in flower primordia in relation to endodormancy in sweet cherry (*Prunus avium* L.). Trees 32(6): 1583-1594.

Falavigna V, Guitton B, Costes E, Andrés F (2019) I want to (bud) break free: the potential role of *DAM* and *SVP*-like genes in regulating dormancy cycle in temperate fruit trees. Frontier in Plant Science 9: 1–17.

Fan S, Bielenberg DG, Zhebentyayeva TN, Reighard GL, Okie WR, Holland D, Abbott AG (2010) Mapping quantitative trait loci associated with chilling requirement, heat requirement and bloom date in peach (*Prunus persica*). New Phytologist 185: 917–930.

FAOSTAT (2018) Food and Agriculture Organization of the United Nations database http://www.fao.org/faostat.

FAOSTAT (2019) Food and Agriculture Organization of the United Nations database http://www.fao.org/faostat.

Faust M, Surányi D (1997) "Origin and dissemination of cherry" in Horticultural Reviews eds. Janick J, Wiley J and Sons Inc. Vol 19.

Field TS, Lee DW, Holbrook NM (2001) Why leaves turn red in autumn. The role of anthocyanins in senescing leaves of red-osier dogwood. Plant Physiology 127(2): 566-574.

Fogle HW (1958) Inheritance of fruit color in sweet cherries (*Prunus avium* L.). Journal of heredity 49: 294-298.

Fogle HW (1961) Inheritance of some fruit and tree characteristics in sweet cherry crosses. Proceedings of the American Society for Horticultural Science 78: 76–85.

Fogle HW (1975) "Cherries" in Advances in Fruit Breeding, eds. Janick J and Moore JN (Purdue University Press): 348-366.

Foulongne M, Pascal T, Arús P, Kervella J (2003) The potential of *Prunus davidiana* for introgression into peach (*Prunus persica* (L.) Batsch) assessed by comparative mapping. Theoretical and Applied Genetics 107: 227–238.

Fresnedo-Ramírez J, Bink MCAM, van de Weg E, Famula T, Crisosto C, Frett T, Gasic K, Peace C, Gradziel T (2015) QTL mapping of pomological traits in peach and related species breeding germplasm. Molecular Breeding 35: 166.

Fresnedo-Ramírez J, Frett TJ, Sandefur PJ, Salgado-Rojas A, Clark JR, Gasic K, Peace CP, Anderson N, Hartmann TP, Byrne DH, Bink MCAM, van de Weg E, Crisosto CH, Gradziel TM (2016) QTL mapping and breeding value estimation through pedigree-based analysis of fruit size and weight in four diverse peach breeding programs. Tree Genetics and Genomes 12: 25.

Fresnedo-Ramírez J, Martínez-García PJ, Parfitt DE, Crisosto CH, Gradziel TM (2013) Heterogeneity in the entire genome for three genotypes of peach [*Prunus persica* (L.) Batsch] as distinguished from sequence analysis of genomic variants. BMC Genomics 14: 750–750.

Gallardo RK, Li H, McCracken V, Yue C, Luby J, McFerson JR (2015) Market intermediaries' willingness to pay for apple, peach, cherry and strawberry quality attributes. Agribusiness 31: 259-280.

Gao L, Mazza G (1995) Characterization, quantification and distribution of anthocyanins and colorless phenolic in sweet cherries. Journal of Agricultural and Food Chemistry 43: 343-346.

García-Alonso A, de Pascual-Teresa S, Santos-Buelga C, Rivas-Gonzalo JC (2004) Evaluation of the antioxidant properties of fruits. Food Chemistry 84: 13-18.

Garrido M, Rodríguez AB, Lozano M, Hernández MT, González-Gómez D (2014) Formulation and characterization of a new nutraceutical product based on sweet cherries (*Prunus avium* L.) grown in the Jerte Valley of Spain. Acta Horticulturae 1020: 149-152.

Gella R, Fustero R, Rodrigo J (2001) Variedades de cerezo. Servicio de Investigación Agroalimentaria. Diputación General de Aragón.

Gelman A, Rubin DB (1992) Inference from iterative simulation using multiple sequences. Statistical Science 7(4): 472–475.

Genard M, Lescourret F, Gomez L, Habib R (2003) Changes in fruit sugar concentrations in response to assimilate supply, metabolism and dilution: a modeling approach applied to peach fruit (*Prunus persica*). Tree Physiology 23(6): 373-385.

Gonçalves B, Landbo AK, Let M, Silva AP, Rosa E, Meyer AS (2004) Storage affects the phenolic profiles and antioxidant activities of cherries (*Prunus avium* L.) on human low-density lipoproteins. Journal of the Science of Food and Agriculture 84: 1013-1020.

Gonçalves B, Silva AP, Moutinho-Pereira J, Bacelar E, Rosa E, Meyer AS (2007) Effects of ripeness and postharvest storage on the evolution of colour and anthocyanins in cherries (*Prunus avium* L.). Food Chemistry 103: 976-984.

Gramzow L, Theissen G (2010) A hitchhiker's guide to the MADS world of plants. Genome Biology 11(6): 214

Guajardo V, Solís S, Sagredo B, Gainza F, Muñoz C, Gasic K, Hinrichsen P (2015) Construction of high density sweet cherry (*Prunus avium* L.) linkage maps using

microsatellite markers and SNPs detected by genotyping-by-sequencing (GBS). PLoS ONE 10:1–17.

Guan Y, Peace C, Rudell D, Verma S, Evans K (2015) QTLs detected for individual sugars and soluble solids content in apple. Molecular Breeding 35: 135.

Hansche PE, Beres W, Doyle J, Micke WC (1988) 'Brooks' sweet cherry. Hortscience 23: 664.

Hedrick UP, Howe GH, Taylor OM, Tubergen CB, Wellington R (1915) The cherries of New York. Report of the New York Agricultural Experiment Station for the Year 1914 II. Lyon, Albany.

Hernández Mora JR, Micheletti D, Bink M, van de Weg E, Cantín C, Nazzicari N, Caprera A, Dettori MT, Micali S, Banchi E, Campoy JA, Dirlewanger E, Lambert P, Pascal T, Troggio M, Bassi D, Rossini L, Verde I, Quilot-Turion B, Laurens F, Arús P, Aranzana MJ (2017) Integrated QTL detection for key breeding traits in multiple peach progenies. BMC Genomics 18: 404.

Herrero J (1964) Cartografía de las variedades frutales de hueso y pepita. CSIC, Aula Dei, Zaragoza.

Herrero M, Rodrigo J, Wünsch A (2017) "Flowering, fruit set and development", in Cherries: Botany, production and uses, eds. Quero-García J, Iezzoni A, Pulawska J and Lang G (CAB International): 14-35.

Honma T, Goto K (2001) Complexes of MADS-box proteins are sufficient to convert leaves into floral organs. Nature 409: 525–529.

Howard NP, van de Weg E, Tillman J, Tong CBS, Silverstein KAT, Luby JJ (2018) Two QTL characterized for solf scald and soggy breakdown in apple (*Malus* × *domestica*) though pedigree-based analysis of large population of interconnected families. Tree Genetics and Genomes 14: 2.

Iezzoni A, Wünsch A, Höfer M, Giovannini D, Jensen M, Quero-García J, Campoy JA, Vokurka A, Barreneche T (2017) "Biodiversity, germplasm resources and breeding methods" in Cherries: botany, production and uses eds. Quero-García J, Iezzoni A, Paławska LG (CAB International): 36–57.

Iezzoni A., Schmidt H, Albertini A (1990) "Cherries (*Prunus*)" in Genetic resources of temperate fruits and nuts crops eds. Moore J and Ballington J (International Society of Horticultural Science): 110–173.

Iezzoni AF (2008) "Cherries" in Temperate fruit crop breeding: Germplasm to genomics ed. Hancock J (Springer): 151-175.

Iglesias I, Peris M, Ruiz S, Rodrigo J, Malagón F, García F, López P, Bañuls MA, Manzano MA, López-Corrales M, Rubio JA (2016) Produzione, mercato e consumi della cerasicoltura spagnola. Froticoltura 4: 20–27.

Ikeda K, Watari A, Ushijima K, Yamane H, Hauck NR, Iezzoni AF, Tao R (2004) Molecular markers for the self-compatible S_4'-haplotype, a pollen-part mutant in sweet cherry (*Prunus avium* L.). Forestry Ideas 18: 28-36.

Illa E, Sargent DJ, Lopez Girona E, Bushakra J, Cestaro A, Crowhurst R, Pindo M, Cabrera A, var der Knaap E, Iezzoni A, Gardiner S, Velasco R, Arús P, Chagné D, Troggio M

(2011) Comparative analysis of rosaceous genomes and the reconstruction of a putative ancestral genome for the family. BMC Evolutionary Biology 11: 9.

Isuzugawa K, Shirasawa K, Kurosaka S, Takahashi Y, Saito Y, Adachi E, Ikenaga M, Yamamoto T (2019) QTL analysis and candidate gene SNP for harvest day in sweet cherry (*Prunus avium* L.). Acta Horticulturae 1235: 33-40.

Jacob RA, Spinozzi GM, Simon VA, Kelley DS, Prior RL, Hess-Pierce B, Karder AA (2003) Consumption of cherries lowers plasma urate in healthy women. Journal of Nutrition 133: 1826–1829.

Jansen RC (1993) Interval mapping of multiple quantitative trait loci. Genetics 135: 205-211.

Jansen RC (1994) Controlling the type I and type II errors in mapping quantitative trait loci. Genetics 138: 871-881.

Jansen RC, Stam P (1994) High resolution of quantitative traits into multiple loci via interval mapping. Genetics 136: 1447-1455.

Jiménez S, Lawton-Rauh AL, Reighard GL, Abbott AG, Bielenberd DG (2009) Phylogenetic analysis and molecular evolution of the dormancy associated MADS-box genes from peach. BMC Plant Biology 9: 81.

Jiménez S, Reighard GL, Bielenberg DG (2010) Gene expression of DAM5 and DAM6 is suppressed by chilling temperatures and inversely correlated with bud break rate. Plant Molecular Biology 73: 157-167.

Jin W, Wang H, Li M, Wang J, Yang Ym Zhang X, Yan G, Zhang H, Liu J, Zhang K (2016) The R2R3 MYB transcription factor *PavMYB10.1* involves in anthocyanin biosynthesis and determines fruit color skin colour in sweet cherry (*Prunus avium* L.). Plant Biotechnology Journal 14(11): 2120-2133.

Jung S, Lee T, Cheng CH, Buble K, Zheng P, Yu J, Humann J, Ficklin SP, Gasic K, Scott J, Frank M, Ru S, Hough H, Evans K, Peace C, Olmstead M, De Vetter LW, McFerson J, Coe M, Wegrzun JL, Staton ME, Abbott AG, Main D (2019) 15 years of GDR: New data and functionality in the Genome Database for Rosaceae. Nucleic Acids Research 47: 1137-1145.

Jung S, Staton M, Lee T, Blenda A, Svancara R, Abbott A, Main D (2008) GDR (genome database for Rosaceae): integrated web database for Rosaceae genomics and genetics data. Nucleic Acids Research 36: 1034–1040.

Kang SY, Seeram N P, Nair MG, Bourquin L D (2003) Tart cherry anthocyanins inhibit tumor development in Apc^{Min} mice and reduce proliferation of human colon cancer cells. Cancer Letters 194: 13–19.

Kappel F, Granger A, Hrotkó K, Schuster M (2012) “Cherry” in Fruit breeding, handbook of plant and breeding eds. Badanes ML, Byme DH (Springer and Business Media): 459-504.

Kass RE, Raftery AE (1995) Bayes factors. Journal of the American Statistical Association 90: 773–795.

Kaufmann K, Melzer R, Theißen G (2005) MIKC-type MADS-domain proteins: Structural modularity, protein interactions and network evolution in land plants. Gene 347: 183–198.

Kenis K, Keulemans J, Davey MW (2008) Identification and stability of QTLs for fruit quality traits in apple. Tree Genetics and Genomes 4: 647-661.

Khan SA, Chibon P-Y, de Vos RCH, Schipper BA, Walraven E, Beekwilder J, van Dijk T, Finkers R, Visser RGF, van de Weg EW, Bovy A, Cestaro A, Velasco R, Jacobsen E, Schouten HJ (2012) Genetic analysis of metabolites in apple fruits indicates an mQTL hotspot for phenolic compounds on linkage group 16. Journal of Experimental Botany 63: 2895–2908.

Kim DO, Heo HJ, Kim YJ, Yang HS, Lee CY (2005) Sweet and sour cherry phenolic and their protective effects on neuronal cells. Journal of Agricultural and Food Chemistry 53: 9921–9927.

Kitamura Y, Habu T, Yamane H, Nishiyama S, Kajita K, Soube T, Kawai T, Numaguchi K, Nakazaki T, Kitajima A, Tao R (2018) Identification of QTLs controlling chilling and heat requirements for dormancy release and bud break in Japanese apricot (*Prunus mume*). Tree Genetics and Genomes 14: 33.

Klagges C, Campoy JA, Quero-García J, Guzmán A, Mansur L, Gratacós E, Silva H, Rosyara UR, Iezzoni A, Meisel LA, Dirlewanger E (2013) Construction and comparative analyses of highly dense linkage maps of two sweet cherry intra-specific progenies of commercial cultivars. PLoS ONE 8(1): e54743.

Koonin EV (2005) Orthologs, paralogs, and evolutionary genomics. Annual Review of Genetics 39: 309-338.

Kosambi DD (1944) The estimation of map distances from recombination values. Annuals Eugenics 12: 172–175.

Kumar S, Stecher G, Li M, Knyaz C, Tamura K (2018) MEGA X: Molecular evolutionary genetics analysis across computing platforms. Molecular Biology and Evolution 35: 1547–1549.

Lamb RC (1953) Notes on the inheritance of some characters in sweet cherry (*Prunus avium*). Proceedings of the American Society for Horticultural Science 61: 293–298.

Lambert P, Campoy JA, Pacheco I, Mauroux JB, Da Silva LC, Micheletti D, Bassi D, Rossini L, Dirlewanger E, Pascal T, Troggio M, Aranzana MJ, Patocchi A, Arús P (2016) Identifying SNP markers tightly associated with six major genes in peach [*Prunus persica* (L.) Batsch] using a high-density SNP array with an objective of marker assisted selection (MAS). Tree Genetics and Genomes 12: 121.

Lander ES, Botstein D (1989) Mapping Mendelian factors underlying quantitative traits using RFLP linkage maps. Genetics 121: 185–199.

Lane WD, MacDonald RA (1996) Sweetheart sweet cherry. Canadian Journal of Plant Science 76(1): 161-163.

Lang GA, Early JD, Martin GC, Darrel RL (1987) Endo-, para-, and endodormancy: physiological terminology and classification for dormancy research. Hortscience 22: 37-377.

Langmead Ben, Steven S (2013) Fast gapped-read alignment with Bowtie 2. Nature Methods 9: 357–359.

Le Dantec L, Girollet N, Gouzy J, Sallet E, Fouché M, Quero-Garcia J, Dirlewanger E (2019) An Improved Assembly of the Diploid 'Regina' Sweet Cherry Genome.

International Plant & Animal Genome XXVII / January 12-16, 2019 - San Diego, CA, USA.

Lee HS (2000) “HPLC analysis of phenolic compounds” in: Food Analysis by HPLC ed. Nollet ML (Marcel Dekker, Inc.): 775–823.

Leida C, Conejero A, Arbona V, Gómez-Cadenas A, Llácer G, Badenes ML, Rios G (2012) Chilling-dependent release of seed and bud dormancy in peach associates to common changes in gene expression. PLoS ONE 7: e35777.

Lepelley M, Cheminade G, Tremillon N, Simkin A, Caillet V, McCarthy J (2007) Chlorogenic acid synthesis in coffee: An analysis of CGA content and real-time RT-PCR expression of *HTC*, *HQT*, *C3H1* and *CCoAOMT1* genes during grain development in *C. canephora*. Plant Science 172(2): 978-996.

Lewis D (1949) Structure of the incompatibility gene. II. Induced mutation rate. Heredity 3: 339–355.

Li H, Kilian A, Zhou M, Wenzl P, Huttner E, Mendham N, McIntyre L, Vaillancourt RE (2010) Construction of a high-density composite map and comparative mapping of segregation distortion regions in barley. Molecular Genetics and Genomics 284: 319–331.

Li Z, Reighard GL, Abbott AG, Bielenberg DG (2009) Dormancy-associated MADS genes from the EVG locus of peach [*Prunus persica* (L.) Batsch] have distinct seasonal and photoperiodic expression patterns. Journal of Experimental Botany 60: 3521-3530.

Lin-Wang K, Bolitho J, Grafton K, Kortstee A, Karunairetnam S, McGhie TK, Espley RV, Hellens RP, Allan AC (2010) An R2R3 MYB transcription factor associated with regulation of the anthocyanin biosynthetic pathway in Rosaceae. BMC Plant Biology 10: 50.

López-Corrales M, Gragera J, Manzano M (2003) Selección de las variedades de cerezo ‘Ambrunés’, ‘Pico Negro’ y ‘Pico Colorado’ tradicionalmente cultivadas en el Valle del Jerte. Actas de Horticultura 39: 297–299.

Lu H, Romero-Severson J, Bernardo R (2002) Chromosomal regions associated with segregation distortion in maize. Theoretical and Applied Genetics 105: 622–628.

Luedeling E (2012) Climate change impacts on winter chill for temperate fruit and nut production: a review. Sciencia Horticulturae 144: 218–229.

Ma Q, Kinneer K (2002) Chemoprotection by phenolic antioxidants. Inhibition of tumor necrosis factor alpha induction in macrophages. Journal of Biology and Chemistry 277: 2477e2484.

Mahmood K, Carew JG, Hadley P, Battey NH (2000) The effect of chilling and post-chilling temperature on growth and flowering of sweet cherry (*Prunus avium* L.). The Journal of Horticultural Science and Biotechnology 75(5): 598-601.

Mahoney LL, Sargent DJ, Abebe-Akele F, Wood DJ, Ward JA, Bassil NV, Hancock JF, Folta KM, Davis TM (2016) A high-density linkage map of the ancestral diploid strawberry, *Fragaria iinumae*, constructed with single nucleotide polymorphism markers from the IStraw90 array and genotyping by sequencing. Plant Genome 9(2): 1–14.

Mangandi J, Verma S, Osorio L, Peres NA, van de Weg E, Whitaker VM (2017) Pedigree-based analysis in multiparental population of octoploid strawberry reveals QTL alleles conferring resistance to *Phytopthora cactorum*. G3-Genes Genomics and Genetics 7(6): 1707-1719.

Manzano MA, Bañuls P, Serradilla MJ, Pérez-Gragera F, López-Corrales M (2014) Programa de mejora genética de cerezo en el Instituto de Investigaciones Científicas y Tecnológicas de Extremadura (CICYTEX-La Orden). Fruticultura 38: 42-55.

MAPA (2019) Anuario de estadística Agroalimentaria 2017. Ministerio de Agricultura, Pesca y Alimentación.

Marchese A, Boškovic R, Caruso T, Raimondo A, Cutuli M, Tobutt K (2007) A new self-compatibility haplotype in the sweet cherry 'Kronio', $S_{5'}$, attributable to a pollen-part mutation in the SFB gene. Journal of Experimental Botany 58: 4347–4356.

Martínez-Esplá A, Zapata PJ, Valero D, García-Viguera C, Castillo S, Serrano M (2014) Preharvest application of oxalic acid increased fruit size, bioactive compounds and antioxidant capacity in sweet cherry cultivars (*Prunus avium* L.). Journal of Agricultural and Food Chemistry 62: 3432-3437.

Martínez-Royo A, Wünsch A (2014) Genetic structure of sweet cherry with the 6K SNP Array v1. 7th International Rosaceae Genomics Conference. Seattle, USA.

Mattila P, Hellström J, Törrönen R (2016) Phenolic acids in berries, fruits, and beverages. Journal of Agriculture and Food Chemistry 54(19): 7193-7199.

Meland M, Kaise C, Christensen MJ (2014) Physical and chemical methods to avoid fruit cracking in cherry. AgroLife Scientific Journal 3: 177-183.

Messenguy F, Dubois E (2003) Role of MADS-box proteins and their cofactors in combinatorial control of gene expression and cell development. Gene 316: 1–21.

Mimida N, Saito T, Moriguchi T, Suzuki A, Komori S, Wada M (2015) Expression of DORMANCY-ASSOCIATED MADS-BOX (DAM)-like genes in apple. Biologia Plantarum 59: 237–244.

Morandi B, Grappadellu LC, Rieger M, Lo Bieanco R (2008) Carbohydrate availability affects growth and metabolism in peach fruit. Physiologia Plantarum 133(2): 229-241.

Mozetic B, Simcic M, Trebse P (2006) Anthocyanins and hydroxycinnamic acids of Lambert compact cherries (*Prunus avium* L.) after cold storage and 1-methylcyclopropene treatment. Food Chemistry 97: 302–309.

Myburg AA, Vogl C, Griffin AR, Sederoff RR, Whetten RW (2004) Genetics of postzygotic isolation in *Eucalyptus*: whole-genome analysis of barriers to introgression in a wide interspecific cross of *Eucalyptus grandis* and E. *globulus*. Genetics 166: 1405–1418.

Negueroles J (2005) Cherry cultivation in Spain. Acta Horticulturae 667: 293-302.

Nuñez-Lillo G, Cifuentes-Esquivel A, Troggio M, Micheletti D, Infante R, Campos-Vargas R, Orellana A, Blanco-Herrera F, Meneses C (2015) Identification of candidate genes associated with mealiness and maturity date in peach [*Prunus persica* (L.) Batsch] using QTL analysis and deep sequencing. Tree Genetics and Genomes 11: 86.

Okie WR, Blackburn B (2011) Increasing chilling reduces heat requirement for floral budbreak in peach. HortScience 46: 245-252.

Olmstead JW, Sebolt AM, Cabrera A, Sooriyapathirana SS, Hammar S, Iriarte G, Wang D, Chen CY, van der Knaap E, Iezzoni A (2008) Construction of an intra-specific sweet cherry (*Prunus avium* L.) genetic linkage map and synteny analysis with the Prunus reference map. Tree Genetics and Genomes 4: 897–910.

Olukolu BA, Trainin T, Fan S, Kole C, Bielenberg DG, Reighard GL, Holland D (2009). Genetic linkage mapping for molecular dissection of chilling requirement and budbreak in apricot (*Prunus armeniaca* L.). Genome 52(10): 819-828.

Ono K, Akagi T, Morimoto T, Wünsch A, Tao R (2018) Genome resequencing of diverse sweet cherry (*Prunus avium*) individuals reveals a modifier gene mutation conferring pollen-part self-compatibility. Plant Cell Physiology: pcy068.

Pauly L, Flajoulot S, Garon J, Julier B, Béguier V, Barre P (2012) Detection of favorable alleles for plant height and crown rust tolerate in three connected populations of perennial ryegrass (*Lolium perenne* L.). Theoretical and Applied Genetics 124: 1139-1153.

Peace C, Bassil N, Main D, Ficklin S, Rosyara UR, Stegmeir T, Sebolt A, Gilmore B, Lawley C, Mockler TC, Bryant DW, Wilhelm L, Iezzoni A (2012) Development and evaluation of a genome-wide 6K SNP array for diploid sweet cherry and tetraploid sour cherry. PLoS ONE 7(12): e48305.

Peace C, Crisosto CH, Gradziel TM (2005) Endopolygalacturonase: a candidate gene for freestone and melting fleshin peach. Molecular Breeding 16: 21-31.

Piaskowski J, Hardner C, Cai L, Zhao Y, Iezzoni A, Peace C (2018) Genomic heritability estimates in sweet cherry reveal non-additive genetic variance is relevant for industry-prioritized traits. BMC Genetics 19(1): 23.

Pirona R, Eduardo I, Pacheco I, Da Silva Linge C, Miculan M, Verde I, Tartarini S, Dondini L, Pea G, Bassi D, Rossini L (2013) Fine mapping and identification of a candidate gene for a major locus controlling maturity date in peach. BMC Plant Biology 13: 166.

Potter D, Eriksson T, Evans RC, Oh S, Smedmark JEE, Morgan DR, Kerr M, Robertsonv KR, Arsenault M, Dickinson TA, Campbell CS (2007) Phylogeny and classification of Rosaceae. Plant Systematics and Evolution 266: 5–43.

Quero-García J (2019) Cherry breeding in the world: current analysis and future perspectives. Italus Hortus 26 (1): 9-20.

Quero-García J, Fodor A, Reignier A, Capdeville G, Joly J, Tauzin Y, Fouilhaux L, Dirlewanger E (2014) QTL detection of important agronomic traits for sweet cherry breeding. Acta Horticulturae 1020: 57-64.

Quero-García J, Shuster M, López-Ortega G, Charlot G (2017) “Sweet cherry varieties and improvement” in Cherries: Botany, Production and Uses eds. Quero-García J, Iezzoni A, Pulawska J, Lang G (CAB International): 60-94.

Quilot B, Wu BH, Kervella J, Génard M, Foulongne M, Moreau K (2004) QTL analysis of quality traits in an advanced backcross between *Prunus persica* cultivars and the wild relative species *P. davidiana*. Theoretical and Applied Genetics 109: 884-897.

R Core Team (2017) R: a language and environment for statistical computing. R Foundation for Statistical Computing, Vienna. http://www.R-project.org/.

Regan BC, Julliot C, Simmen B, Vienot F, Charles-Dominique P, Mollon JD (2001) Fruits, foliage and the evolution of primate colour vision. Philosophical Transactions of the Royal Society B: Biological Sciences 356(1407): 229-283.

Richardson EA, Seeley SD, Walter DR (1974) A model for estimating the completion of rest for 'Redhaven' and 'Elberta' peach trees. HortScience 9(4): 331-332.

Ritter A, Iñigo S, Fernández-Calvo P, Heyndrickx KS, Dhondt S, Shi H, De Milde L, Bossche V, De Clercq R, Eeckhout D, Ron M, Somers DE, Inzé D, Gevaert K, De Jaeger G, Vandepoele K, Pauwels L, Goossens A (2018) The transcriptional repressor complex *FRS7-FRS12* regulates flowering time and growth in *Arabidopsis*. Nature Communications 8: 15235.

Roach JA, Verma S, Peres NA, Jamieson AR, van de Weg WE, Bink MCAM, Bassil NV, Lee S, Whitake VM (2016) *FaRXf1*: a locus conferring resistance to angular leaf spot caused by *Xanthomonas fragariae* in octoploid strawberry. Theoretical and Applied Genetics 129: 1191–1201.

Rodriguez AJ, Sherman WB, Scorza R, Wisniewski M, Okie WR (1994) 'Evergreen' peach, its inheritance and dormant behavior. Journal of American Society of Horticultural Science 119: 789–792.

Rohde A, Bhalerao RP (2007) Plant dormancy in the perennial context. Trends in Plant Science 12: 217–223.

Romeu JF, Monforte AJ, Sanchez G, Granell A, Garcia-Brunton J, Badenes ML, Rios G (2014) Quantitative trait loci affecting reproductive phenology in peach. BMC Plant Biology 14: 52.

Rosyara UR, Bink MCAM, van de Weg E, Zhang G, Wang D, Sebolt A, Dirlewanger E, Quero-García J, Shuster M, Iezzoni AF (2013) Fruit size QTL identification and the prediction of parental QTL genotypes and breeding values in multiple pedigreed populations in sweet cherry. Molecular Breeding 32: 875-887.

Rothkegel K, Sánchez E, Montes C, Greve M, Tapia S, Bravo S, Prieto H, Almeida AM (2017) DNA methylation and small interference RNAs participate in the regulation of MADS-box genes involved in dormancy in sweet cherry (*Prunus avium* L.). Tree Physiology 37: 1739–1751.

Saito T, Bai S, Ito A, Sakamoto D, Saito T, Ubi BE, Imai T, Moriguchi T (2013) Expression and genomic structure of the dormancy-associated MADS-box genes MADS13 in Japanese pears (*Pyrus pyrifolia* Nakai) that differ in their chilling requirement for endodormancy release. Tree Physiology 33: 654–667.

Salazar J, Ruiz D, Campoy JA, Sánchez-Pérez R, Crisosto C, Martínez-García P, Blenda A, Jung S, Main D, Martínez-Gómez P, Rubio M (2014) Quantitative trait loci (QTL) and Mendelian trait loci (MTL) analysis in Prunus: a breeding perspective and beyond. Plant Molecular Biology Report 32: 1–18.

Salazar JA, Pacheco I, Shinya P, Zapata P, Silva C, Aradhya M, Velasco D, Ruiz D, Martínez-Gómez P, Infante R (2017) Genotyping by sequencing for SNP-based

linkage analysis and identification of QTLs linked to fruit quality traits in Japanese plum (*Prunus salicina* Lindl.) Frontiers in Plant Science 8: 476.

Salazar JA, Ruiz D, Campoy JA, Tartarini S, Dondini L, Martínez-Gómez P (2016) Inheritance of reproductive phenology traits and relates QTL identification in apricot. Tree Genetics and Genomes 12:71.

Salazar JA, Ruiz D, Egea J, Martínez-Gómez P (2013) Transmission of fruit quality traits in apricot (*Prunus armeniaca* L.) and analysis of linked quantitative trait loci (QTLs) using simple sequence repeat (SSR) markers. Plant Molecular Biology Report 31(6): 1506-1517.

Sánchez-Pérez R, Dicenta F, Martinez-Gomez P (2012) Inheritance of chilling and heat requirements for flowering in almond and QTL analysis. Tree Genetics and Genomes 8(2): 379–389.

Sanderful P, Oraguzie M, Peace C (2016) A DNA test for routine prediction in breeding of sweet cherry fruit color, *Pav-Rf-SSR*. Molecular Breeding 36: 33.

Sansavini S, Lugli S (2008) Sweet cherry breeding programs in Europe and Asia. Acta Horticulturae 795: 41-58.

Sasaki R, Yamane H, Ooka T, Jotatsu H, Kitamura Y, Akagi T, Tao R (2011) Functional and expressional analyses of *PmDAM* genes associated with endodormancy in Japanese apricot. Plant Physiology 157: 485–497.

Schaefer HM, Schaefer V, Levey DJ (2004) How plant-animal interactions signals new insights in communications. Trends in Ecology and Evolution 19(11): 577.

Schmidt H (1998) On the genetics of fruit colour in sweet cherries. Acta Horticulturae 468: 77-81.

Serra AT, Duarte RO, Bronze MR, Duarte CMM (2011) Identification of bioactive response in traditional cherries from Portugal. Food Chemistry 125(2): 318–325

Serra O, Giné-Bordonaba J, Eduardo I, Bonany J, Echeverria G, Larrigaudière C, Arús P (2017) Genetic analysis of the slow-melting flesh character in peach. Tree Genetics and Genomes 13: 77.

Serradilla M, Hernández A, Ruíz-Moyano S, Benito MJ, López-Corrales M, Córdoba MDG (2013) Authentication of 'Cereza del Jerte' cherry cultivars using real time PCR. Food Control 30(2): 679–685.

Serradilla MJ, Aksic MF, Manganaris GA, Ercisli S, González-Gómez D, Valero D (2017) "Fruit chemistry, nutritional benefits and social aspects of cherries", in Cherries: Botany, production and uses, eds. Quero-García J, Iezzoni A, Pulawska J and Lang G (CAB International): 420-441.

Serradilla MJ, Hernández A, López-Corrales M, Ruíz-Moyano S, Córdoba MG, Martín A (2016) "Composition of the Cherry (*Prunus avium* L. and k L.; Rosaceae)" in Nutritional Compositions of Fruit Cultivars, eds. Simmonds MSJ and Preedy VR (Academic Press): 127–147.

Serradilla MJ, Lozano M, Bernalte MJ, Ayuso MC, López-Corrales M, González-Gómez D (2011b) Physicochemical and bioactive properties evolution during ripening of 'Ambrunés' sweet cherry cultivar. LWT-Food Science and Technology 44: 199-205.

Serradilla MJ, Martín A, Aranda E, Hernández A, Benito MJ, López-Corrales M, Cordoba MG (2008) Authentication of 'Cereza del Jerte' sweet cherry varieties by free zone capillaray electrophoresis (FZCE). Food Chemistry 111 (2): 457-461.

Serradilla MJ, Martín A, Hernández A, López-Corrales M, Lozano M, Córdoba MG (2011a) Effect of the commercial ripening stage and postharvest storage on microbial and aroma changes of 'Ambrunés' sweet cherries. Journal of Agricultural and Food Chemistry 58: 9157-9163.

Serradilla MJ, Martín A, Ruíz-Moyano S, Hernández A, López-Corrales M, Córdoba MDG (2012) Physicochemical and sensorial characterization of four sweet cherry cultivars grown in Jerte Valley (Spain). Food Chemistry 133(4): 1551–1559.

Serrano M, Díaz-Mula HM, Zapata PJ, Castillo S, Guillén F, Martínez-Romero D, Valverde JM, Valero D (2009) Maturity stage at harvest determines the fruit quality and antioxidant potential after storage of sweet cherry cultivars. Journal of Agricultural and Food Chemistry 57(8): 3240-3324.

Serrano M, Guillén F, Martínez-Romero D, Castillo S, Valero, D (2005) Chemical constituents and antioxidant of sweet cherry at different ripening stages. Journal Agricultural and Food Chemistry 53: 2741-2745.

Shirasawa K, Isuzugawa K, Ikenaga M, Saito Y, Yamamoto T, Hirakawa H, Isobe S (2017) The genome sequence of sweet cherry (*Prunus avium*) for use in genomics-assisted breeding. DNA Research 24(5): 499– 508.

Smaczniak C, Immink RGH, Angenent GC, Kaufmann K (2012) Developmental and evolutionary diversity of plant MADS-domain factors: insights from recent studies. Development 139: 3081–3098.

Sonnante D, D'Amore R, Blanco E, Pierri CL, De Palma M, Luo J, Tucci M, Martin C (2010) Novel hydroxycinnamoyl-coenzyme A quinate transferase genes from artichoke are involved in the synthesis of chorogenic acid. Plant Physiology 153(3): 1224-1238.

Sooriyapathirana SS, Khan A, Sebolt A, Wang D, Bushakra JM, Lin-Wang K, Allan AC, Gardiner SE, Chagné D, Iezzoni A (2010) QTL analysis and candidate gene mapping for skin and flesh color in sweet cherry fruit (*Prunus avium* L.). Tree Genetics and Genomes 6: 821-832.

Sorensen D, Gianola D (2002) Likelihood, Bayesian, and MCMC methods in quantitative genetics. New York: Springer-Verlag.

Soriano JM, Vera-Ruiz EM, Vilanova S, Martínez-Calvo J, Llácer G, Badenes ML, Romero C (2008) Identification and mapping of a locus conferring plum pox virus resistance in two apricot improved linkage maps. Tree Genetics and Genomes 4: 391–402.

Stegmeir T, Cai L, Basundati RA, Sebolt A, Iezzoni A (2015) A DNA test for fruit flesh color in tetraploid sour cherry (Prunus cerasus L.). Molecular Breeding 35: 149.

Stegmeir T, Schuster M, Sebolt A, Rosyara U, Sundin GW, Iezzoni A (2014) Cherry leaf spot resistance in cherry (*Prunus*) is associated with a quantitative trait locus on linkage group 4 inherited from *P. canescens*. Molecular Breeding 34(3): 927-935.

Stockinger EJ, Mullnix CA, Long CM, Brettin TS, Iezzoni AF (1996) A linkage map of sweet cherry based on RAPD analysis of a microspore-derived callus culture population. Journal of Heredity 87(3): 214–218.

Tabuenca MC (1983) Winter chilling requirements of cherry varieties. I Congreso Nacional de la Sociedad Española de Ciencias Hortícolas (Valencia). Comunicaciones, SECH: 661–667.

Tamura K, Nei M (1993) Estimation of the number of nucleotide substitutions in the control region of mitochondrial DNA in humans and chimpanzees. Molecular Biology and Evolution 10: 512-526.

Tao R, Iezzoni AF (2010) The S-RNase-based gametophytic self-incompatibility system in *Prunus* exhibits distinct genetic and molecular features. Scientia Horticulturae 124: 423–433.

Tavassolian I, Rabiei G, Gregory D, Mnejja M, Wirthensohn MG, Hunt PW, Gibson JP, Ford CM, Sedgley M, Wu SB (2010) Construction of an almond linkage map in an Australian population Nonpareil × Lauranne. BMC Genomics 11: 551.

Thorvaldsdóttir H, Robinson JT, Mesirov JP (2013) Integrative Genomics Viewer (IGV): High-performance genomics data visualization and exploration. Briefings Bioinformatics 14: 178–192.

Tomás-Barberán FA, Gil MI, Cremin P, Waterhouse AL, Hess-Pierce B, Kader AA (2001) HPLC-DAD-ESIMS analysis of phenolic compounds in nectarines, peaches, and plums. Journal of Agricultural and Food Chemistry 49: 4748–4760.

Trainin T, Bar-Ya'akov I, Holland D (2013) *ParSOC1*, a MADS-box gene closely related to *Arabidopsis AGL20/SOC1*, is expressed in apricot leaves in a diurnal manner and is linked with chilling requirements for dormancy break. Tree Genetics and Genomes 9(3): 753-766.

Usenik V, Fabĉiĉ J, Stampar F (2008) Sugars, organic acids, phenolic composition and antioxidant activity of sweet cherry (*Prunus avium* L.). Food Chemistry 107: 185-192.

van Ooijen JW (1992) Accuracy of mapping quantitative trait loci in autogamous species. Theoretical and Applied Genetics 84: 803–811.

van Ooijen JW (2006).JoinMap® 4, Software for the calculation of genetic linkage maps in experimental populations, Wageningen, Netherlands: Kyazma B.V.

van Ooijen JW (2009). MapQTL® 6, software for mapping of quantitative trait in experimental populations of diploid species. Wageningen, Netherlands: Kyazma B.V.

Vanderzande S, Zheng P, Cai L, Iezzoni A, Main D, Peace C (2019) Development and initial assessment of the 9K SNP addition to the sweet and sour cherry genome wide SNP array. International Plant & Animal Genome XXVII / January 12-16, 2019 - San Diego, CA, USA.

Verde I, Abbott AG, Scalabrin S, Jung S, Shu S, Marroni F, Zhebentyayeva T, Dettori MT, Grimwood J, Cattonaro F, Zuccolo A, Rossini L, Jenkins J, Vendramin E, Meisel LA, Decroocq V, Sosinski B, Prochnik S, Mitros T, Policriti A, Cipriani G, Dondini L, Ficklin S, Goodstein D, Xuan P, Del Fabbro C, Aramini V, Copetti D, Gonzalez S, Horner D, Falchi R, Lucas S, Mica E, Maldonado J, Lazzari B, Bielenberg D, Pirona R, Miculan M, Barakat A, Testolin R, Stella A, Tartarini S, Tonutti P, Arús P, Orellana

A, Wells C, Main D, Vizzotto G, Silva H, Salamini F, Schmutz J, Morgante M, Rokhsar DS (2013) The high-quality draft genome of peach (*Prunus persica*) identifies unique patterns of genetic diversity, domestication and genome evolution. Nature Genetics 45(5): 487–496.

Verde I, Bassil N, Scalabrin S, Gilmore B, Lawley CT, Gasic K, Micheletti D, Rosyara UR, Cattonaro F, Vendramin E, Main D, Aramini V, Blas AL, Mockler TC, Bryant DW, Wilhelm L, Troggio M, Sosinski B, Aranzana MJ, Arús P, Iezzoni A, Morgante M, Peace C (2012) Development and evaluation of a 9K SNP array for peach by internationally coordinated SNP detection and validation in breeding germplasm. PLoS ONE 7(4): e35668.

Verde I, Jenkins J, Dondini L, Micali S, Pagliarani G, Vendramin E, Paris R, Aramini V, Gazza L, Rossini L, Bassi D, Troggio M, Shu S, Grimwood J, Tartarini S, Dettori MT, Schmutz J (2017) The Peach v2.0 release: high-resolution linkage mapping and deep resequencing improve chromosome-scale assembly and contiguity. BMC Genomics 18: 1–18.

Verdu CF, Guyot S, Childerbrand N, Bahut M, Celton JM, Gaillard S, Lasserre-Zuber P, Troggio M, Guilet D, Laurens F (2014) QTL analysis and candidate gene mapping for the polyphenol content in cider apple. PloS ONE 9(10): e107103.

Vilanova S, Romero C, Abbott AG, Llácer G, Badenes ML (2003) An apricot (*Prunus armeniaca* L.) F_2 progeny linkage map based on SSR and AFLP markers, mapping plum pox virus resistance and self-incompatibility traits. Theoretical and Applied Genetics 107: 239–247.

Voorrips RE (2002) MapChart: Software for the graphical presentation of linkage maps and QTLs. The Journal of Heredity 93(1): 77-78.

Voorrips RE (2007) Pedimap: Software for visualization of genetic and phenotypic data in pedigrees. Plant Research International, Wagenigen, The Netherlands.

Wang D, Gao Z, Du P, Xiao W, Tan Q, Chen X, Li L, Gao D (2016) Expression of ABA metabolism-related genes suggests similarities and differences between seed dormancy and bud dormancy of peach (*Prunus persica*). Front in Plant Science 6: 1248.

Wang D, Karle R, Iezzoni, AF (2000) QTL analysis of flower and fruit traits in sour cherry. Theoretical and Applied Genetics, 100(3–4): 535–544.

Wang J, Zhang K, Zhang X,Yan G, Zhou Y, Feng L, NiY, DuanX (2015) Construction of commercial sweet cherry linkage maps and QTL analysis for trunk diameter. PLoS ONE 10(10): e0141261.

Ward JA, Bhangoo J, Fernández-Fernández F, Moore P, Swanson JD, Viola R, Velasco R, Bassil N, Weber CA, Sargent DJ (2013) Saturated linkage map construction in *Rubus idaeus* using genotyping by sequencing and genome-independent imputation. BMC Genomics 14(2): 1–14.

Watkins R (1976) “Cherry, plum, peach, apricot and almond” in Evolution of crop plants, ed. Simmonds NW (Longman): 242-247.

Webster AD (1996) “The taxonomic classification of sweet and sour cherries and a brief history of their cultivation” in Cherries: Crop physiology, production and uses, eds. Webster AD and Looney NE (CAB International): 3-25.

Wells CE, Vendramin E, Jimenez Tarodo S, Verde I, Bielenberg DG (2015) A genome-wide analysis of MADS-box genes in peach [*Prunus persica* (L.) Batsch]. BMC Plant Biology 15: 1–15.

Whiting MD, Ophardt D, McFerson JR (2006) Chemical blossom thinners vary in their effect on sweet cherry fruit set, yield, fruit quality, and crop value. Horticulture Technology 16: 66–70.

Wünsch A (2017) Mejora genética de cerezo: del pasado al presente. Opiniones y Experiencias RICA. Red de Intercambio Agroalimentario. http://opiniones-y-experiencias.chil.me/post/mejora-genetica-de-cerezo-del-pasado-al-presente-177751

Wünsch A (2019) El acervo genético del cerezo en España y su potencial para la mejora del cultivo. Opiniones y Experiencias RICA. Red de Intercambio Agroalimentario. http://rica.chil.me/post/el-acervo-genetico-del-cerezo-en-espana-y-su-interes-para-la-mejora-del-cultivo-267171

Wünsch A, Hormaza JI (2002) Molecular characterization of sweet cherry (*Prunus avium* L.) cultivars using peach (*Prunus persica* L. Batsch.) SSR sequences. Heredity 89(1): 56-63.

Wünsch A, Hormaza JI (2004) Genetic and molecular analysis in Cristobalina sweet cherry, a spontaneous self-compatible mutant. Sexual Plant Reproduction 17: 203–210.

Wünsch A, Lin-Wang K, Allan AC (2014) Differential expression of cherry *MYB10* in white and red varieties is responsible for anthocyanin levels. 7th International Rosaceae Genomics Conference. Seattle, Washington (USA).

Xu Y, Zhu L, Xiao J, Huang N, McCouch SR (1997) Chromosomal regions associated with segregation distortion of molecular markers in F_2, backcross, double haploid, and recombinant inbred populations in rice (*Oryza sativa* L.). Molecular Genetics and Genomics 253: 535–545.

Xu Z, Zhang Q, Sun L, Du D, Cheng T, Pan H, Yang W, Wang (2014) Genome-wide identification, characterization and expression analysis of the MADS-box gene family in *Prunus mume*. Molecular Genetics and Genomics 289: 903–920.

Yamane H (2014) Regulation of bud dormancy and bud break in Japanese apricot (*Prunus mume* Siebold & Zucc.) and peach [*Prunus persica* (L.) Batsch]: a summary of recent studies. Journal of Japanese Society for Horticultural Science 83: 187–202.

Yamane H, Ooka T, Jotatsu H, Hosaka Y, Sasaki R, Tao R (2011) Expressional regulation of *PpDAM5* and *PpDAM6* peach (*Prunus persica*) dormancy-associated MADS-box genes, by low temperature and dormancy-breaking reagent treatment. Journal of Experimental Botany 62: 3481-3488.

Yue C, Gallardo RK, Luby JJ, Rihn AL, McFerson JR, McCracken V, Oraguzie N, Weebadde C, Sebolt A, Iezzoni A (2014) An evaluation of U.S. tart and sweet cherry producers trait prioritization: evidence from audience surveys. Hortscience 49: 931–937.

Zeballos JL, Abidi W, Giménez R, Monforte AJ, Moreno MA, Gogorcena Y (2016) Mapping QTLs associated with fruit quality traits in peach [*Prunus persica* (L.) Batsch] using SNP maps. Tree Genetics and Genomes 12: 37.

Zhang G, Sebolt AM, Sooriyapathirana SS, Wang D, Bink MCAM, Olmstead JW, Iezzoni A (2010) Fruit size QTL analysis of an F_1 population derived from a cross between a domesticated sweet cherry cultivar and a wild forest sweet cherry. Tree Genetics and Genomes 6(1): 25–36.

Zhang YM (2012) F2 designs for QTL analysis. Methods in Molecular Biology 871: 17–29.

Zhang Z, Zhuo X, Zhao K, Zheng T, Han Y, Yuan C, Zhang Q (2018) Transcriptome profiles reveal the crucial roles of hormone and sugar in the bud dormancy of *Prunus mume*. Science Reports 8: 1–15.

Zhao K, Zhou Y, Ahmad S, Xu Z, Li Y, Yang W, Cheng T, Wang J, Zhang Q (2018). Comprehensive cloning of *Prunus mume* dormancy associated MADS-box genes and their response in flower bud development and dormancy. Front in Plant Science 9: 1–12.

Zhebentyayeva TN, Fan S, Chandra A, Bielenberg DG, Reighard GL, Okie WR, Abbott AG (2014) Dissection of chilling requirement and bloom date QTLs in peach using a whole genome sequencing of sibling trees from an F_2 mapping population. Tree Genet Genomes 10: 35–51.

Zheng X, Yue C, Gallardo K, McCracken V, Luby J, McFerson J (2016) What attributes are consumers looking for in sweet cherries? Evidence from choice experiments. Journal of Agricultural and Resource Economics 45: 124–142.

Zoffoli JP, Toivonen P, Wang Y (2017) "Postharvest Biology and Handling for Fresh Markets" in Cherries: Botany, Production and Uses eds. Quero-García J, Iezzoni A, Pulawska J, Lang G (CAB International): 460-484.

APPENDIX I

High-density linkage maps constructed in sweet cherry (*Prunus avium* L.) using cross- and self-pollination reveal chromosomal homozygosity in inbred families and non-syntenic regions with the peach genome

Tree Genetics & Genomes (2018) 14: 37.

Tree Genetics & Genomes (2018) 14:37
https://doi.org/10.1007/s11295-018-1252-2

ORIGINAL ARTICLE

High-density linkage maps constructed in sweet cherry (*Prunus avium* L.) using cross- and self-pollination populations reveal chromosomal homozygosity in inbred families and non-syntenic regions with the peach genome

Alejandro Calle[1] · Lichun Cai[2] · Amy Iezzoni[2] · Ana Wünsch[1]

Received: 27 February 2018 / Revised: 10 April 2018 / Accepted: 3 May 2018

Abstract

The landrace sweet cherry (*Prunus avium* L.) cultivar 'Cristobalina' is a useful resource for sweet cherry breeding due to several important traits, including low chilling requirement, early maturity date, and self-compatibility. In this work, three families (N = 325), derived from 'Cristobalina', were used to develop high-density genetic maps using the RosBREED 6K Illumina Infinium® cherry SNP array. Two of the families were derived from self-pollination, which allowed construction of the first F_2 genetic maps in the species. The other map developed was from an interspecific cross of cultivars 'Vic' × 'Cristobalina'. The maps developed include 511 to 816 mapped SNPs covering 622.4 to 726.0 cM. Mapped SNP marker order and position were compared to the sweet cherry and peach genome sequences, and a high degree of synteny was observed. However, inverted and small translocated regions between peach and sweet cherry genomes were observed with the most noticeable inversion at the top of LG5. The progeny resulting from self-pollination also revealed a high level of homozygosity, as large presumably homozygous regions as well as entire homozygous LGs were observed. These maps will be used for genetic analysis of relevant traits in sweet cherry breeding by QTL analysis, and self-pollination populations will be useful for investigating inbreeding depression in a naturally outbreeding species.

Keywords Sweet cherry 6K SNP array · Genetic map · 'Cristobalina' · Homozygosity · Self-compatibility

Introduction

Sweet cherry (*Prunus avium* L.), a diploid species ($2n = 2x = 16$) in the *Rosaceae*, is mainly cultivated for its fruit. World sweet cherry production has increased over 30% during the last two decades, reaching 2.2 M tons in 2014 (FAOSTAT 2018). The increase in sweet cherry consumption, combined with challenges posed by climate change, and grower and consumer demands require breeding and production improvements. New genomic technologies and physical and genetic linkage maps generated contribute to an increase in knowledge that can lead to an improvement in breeding efficiency. In the *Rosaceae* family, various genome sequences have been published in recent years [Genome Database for *Rosaceae* (GDR); Jung et al. 2008]. Verde et al. (2013) sequenced the peach genome, the first *Prunus* genome sequenced, and, just recently, a sweet cherry genome was published (Shirasawa et al. 2017). Next generation sequencing (NGS) technologies have also allowed the identification of single nucleotide polymorphisms (SNPs) along the genome and the development of SNP array platforms for *Rosaceae* crops. This is the case for peach (Verde et al. 2012), sweet and sour cherry (Peace et al. 2012), strawberry (Bassil et al. 2015),

Communicated by E. Dirlewanger

Electronic supplementary material The online version of this article (https://doi.org/10.1007/s11295-018-1252-2) contains supplementary material, which is available to authorized users.

✉ Ana Wünsch
awunsch@aragon.es

[1] Unidad de Hortofruticultura, Centro de Investigación y Tecnología Agroalimentaria de Aragón (CITA), Instituto Agroalimentario de Aragón-IA2 (CITA-Universidad de Zaragoza), Avenida de Montañana 930, 50059 Zaragoza, Spain

[2] Department of Horticulture, Michigan State University, 1066 Bogue St, East Lansing, MI 48824-1325, USA

Published online: 15 May 2018

and apple (Chagné et al. 2012; Bianco et al. 2014, 2016). These arrays have enabled the development of highly saturated linkage maps in the different species (Klagges et al. 2013; Di Pierro et al. 2016; Mahoney et al. 2016; Lambert et al. 2016). Linkage maps are a useful tool for the identification of quantitative trait loci (QTL), genomic regions associated with variation for quantitative traits. QTL for traits of breeding and production interest can be further used for marker-assisted selection or to identify candidate genes responsible for these traits.

Numerous linkage maps have been constructed in sweet cherry (reviewed in Salazar et al. 2014; Iezzoni et al. 2017). The first sweet cherry linkage maps were constructed using RAPDs (Stockinger et al. 1996) and isoenzymes (Boškovi and Tobutt 1998). Later, maps were developed using SSR markers (Dirlewanger et al. 2004; Olmstead et al. 2008; Clarke et al. 2009) and SNP markers (Cabrera et al. 2012). High-density maps have been developed more recently (Klagges et al. 2013; Balas et al. in press) using the RosBREED cherry 6K Illumina Infinium® SNP array v1 (Peace et al. 2012), Genotyping By Sequencing (GBS; Guajardo et al. 2015), and Specific-Locus Amplified Fragment (SLAF; Wang et al. 2015). Most recently, an integrated consensus linkage map containing 2317 SNPs and 65 SSRs spanning 1165 cM, from three cross-pollination populations (Shirasawa et al. 2017), was constructed using double-digest restriction site-associated DNA sequencing (ddRAD-Seq).

All linkage maps developed in sweet cherry to date have been constructed from F_1 populations from interspecific or intraspecific crosses. Sweet cherry is a natural outcrossing species that exhibits a gametophytic self-incompatibility system controlled by the *S* locus. Pollen tube growth expressing an *S* allele that matches one of the two *S* alleles expressed in the diploid style is inhibited (Tao and Iezzoni 2010). As a result of gametophytic self-incompatibility, self-fertilization is not possible in this species. F_1 mapping populations developed in sweet cherry have been made between cross-compatible parents. However, self-compatible mutants do exist in sweet cherry. The self-compatible mutant most widely used in breeding is a mutation that was induced using irradiation that renders S_4 pollen compatible in an S_4containing style (Lewis 1949). Therefore, any sweet cherry that carries this S_4 mutant, termed $S_{4'}$, is self-compatible. However, natural self-compatible mutants have been found in local germplasm, including the landrace cultivars 'Cristobalina' (Wünsch and Hormaza 2004), 'Talegal Ahim', 'Son Miro' (Cachi and Wünsch 2014), and 'Kronio' (Marchese et al. 2007).

These cultivars, and any cultivar with $S_{4'}$, can be used to develop populations from self-pollination. Self-pollinated populations are useful for the genetic dissection of quantitative traits, especially in species with a low level of heterozygosity, because genetic effects (additive and dominant) can be estimated, and therefore, these population types are frequently used in fine mapping of QTLs (Zhang 2012). In the genus *Prunus*, linkage maps have been developed using F_1 and F_2 populations, and these maps have been used for QTL analyses for traits of interest. In peach, most linkage maps come from F_2 populations [Genome Database for *Rosaceae* (GDR); Jung et al. 2008], but in other *Prunus* species that are self-incompatible, like almond or sweet cherry, all genetic maps have been developed in F_1 populations. In apricot, in which some cultivars are self-compatible, F_2 linkage maps have also been developed (Soriano et al. 2008; Vilanova et al. 2003). In breeding of sweet cherry, use of these self-compatible mutants makes it possible for the breeder to do self-pollinations or sib-matings that were previously not possible, raising the question of whether an associated increase in homozygosity in this naturally cross-pollinated crop could lead to inbreeding depression.

'Cristobalina', a landrace cultivar from Eastern Spain, specifically, a mountain area (Sierra de Espadán, Castellón) near the Mediterranean coast, offers many opportunities for sweet cherry breeding. This cultivar has a very low chilling requirement (< 800 h), compared with other sweet cherry cultivars, such as 'Van' or 'Napoleon' (> 1100 h), that have large chilling requirements (Tabuenca 1983). This trait makes 'Cristobalina' an important cultivar for breeding for low chilling, looking to extend the area of production to areas with warmer winters. This cultivar also has a very early maturity date, which makes it of interest for breeding early maturing cultivars. In addition, 'Cristobalina' has compact growth and medium to small size fruit (4–5 g) with dark red skin. Another relevant aspect is that 'Cristobalina' is self-compatible (Wünsch and Hormaza 2004) due to a mutation located on linkage group (LG) 3 and therefore unlinked to the *S* locus that is on LG6 (Cachi and Wünsch 2011). Thus, it is an alternative source for breeding for self-compatibility. Being self-compatible, 'Cristobalina' also offers the possibility to use F_2 populations for genetic analysis of these important production traits and to investigate the possibility of inbreeding depression in this naturally cross-pollinated species.

In this work, we used three sweet cherry families that have 'Cristobalina' as a parental cultivar, two of which are self-pollinations, to develop genetic maps using the RosBREED Cherry 6K SNP array v1. These maps were compared with previous sweet cherry linkage maps and with sweet cherry and peach physical maps (Shirasawa et al. 2017; Verde et al. 2017) to estimate the degree of similarity and synteny. The two self-pollinated populations derived from 'Cristobalina' were further used to investigate extent of homozygosity exhibited by the self-pollinated progeny.

Materials and methods

Plant material

Three sweet cherry families were used for linkage map construction that all include 'Cristobalina' (S_3S_6, *Mm*) in the parentage or ancestry. 'Cristobalina' has the *S* locus genotype S_3S_6; however, it is self-compatible because it is heterozygous for a self-incompatibility modifier locus (*Mm*) on LG3 (Cachi and Wünsch 2011; Ono et al. 2018). All self-compatible 'Cristobalina' pollen has the *m* allele and either S_3 or S_6 (Cachi and Wünsch 2011; Ono et al. 2018). These three families were an F_1 family from the cross of cultivars 'Vic' (S_2S_4, *MM*) × 'Cristobalina' (V × C; $N = 161$), an F_2 family from the self-pollination of 'Cristobalina' (C × C, $N = 97$), and an F_2 family derived from the self-pollination of a progeny (S_6S_9, *Mm*) of the cross of 'Brooks' (S_1S_9, *MM*) × 'Cristobalina' (B × C2, $N = 67$). These trees come from crosses and self-pollinations made from 2008 to 2010 and are grown at the experimental orchards of CITA de Aragón in Zaragoza (Spain). All the parental cultivars belong to the CITA de Aragón sweet cherry cultivar collection. 'Vic' (Dickson 1959) is a cultivar, derived from the cross of 'Bing' × 'Schmidt', with late blooming and maturity dates and dark large fruits. 'Brooks' is a cultivar from the cross of 'Rainier' and 'Burlat', which shows early blooming and maturity dates and dark red and firm fruits (Hansche et al. 1988). Progeny from three additional sweet cherry populations from the crosses 'Lambert' (S_3S_4, *MM*) × 'Cristobalina' (L × C, $N = 14$), 'Ambrunés' (S_3S_6, *MM*) × 'Cristobalina' (A × C, $N = 40$), and 'Brooks' (S_1S_9, MM) × 'Cristobalina' (B × C, $N = 33$) were genotyped using the 6K RosBREED cherry array and used to perform SNP clustering.

SNP genotyping

Genomic DNA was obtained from lyophilized leaves using DNeasy® Plant Mini Kit (Qiagen, MD, USA). Genomic DNA was extracted from the parental cultivars and all the progeny individuals. A duplicate genotype was included in each 96-plate as a quality control to evaluate reproducibility. Initial genomic DNA quantification was carried out using Nanodrop® (Thermo Fisher Scientific, Waltham, MA, USA). Genome-wide SNP genotyping of the three families and the parental cultivars was done using the RosBREED Cherry 6K Illumina Infinium® SNP Array v1 (Peace et al. 2012). Information about the SNP array, including the name, SNP type, position on the peach genome, Gbrowse link, and flanking sequence for the SNPs, can be downloaded from the Genome Database for *Rosaceae* (https://www.rosaceae.org/species/prunus/cherry) (Jung et al. 2008). Genotyping was carried out at CEGEN-PRB2-ISCIII (Madrid, Spain) by quantification with Quant-iT™ PicoGreen® (Invitrogen Ltd., Paisley, UK) and array scanning with Illumina iSCAN System® (Illumina Inc., San Diego, CA, USA).

SNP genotypes were analyzed using the Genotyping Module (v1.9.4) of GenomeStudio™ (v2011.1; Illumina Inc., San Diego, CA, USA) software. Manifest file providing a description of the SNP and probe content on the array was used for the SNP genotype calling. In order to maximize allelic diversity, SNP clustering was performed by GenomeStudio™ using 480 sweet cherry genotypes. This sample included 325 genotypes corresponding to the three mapping progenies, 45 cultivars from the CITA sweet cherry cultivar collection previously genotyped with the same array (Martínez-Royo and Wünsch 2014), 87 individuals from the remaining three families described previously, and 23 genotypes including the parents and technical duplicates. Only samples that had GenCall scores above 0.15 were initially clustered using the GenomeStudio™ build-in algorithm "Gentrain2". Clustering for all the SNPs was also visually checked and adjusted manually if needed. Duplicated genotypes in each plate were tested for reproducibility using the Genome Studio "Replicate" analysis function. Genome Studio "parent–parent–child" (P-P-C) analysis function was used to test progenies and marker heritability in all the progenies. Further SNP quality filtering and data formatting for input in JoinMap were carried out using ASSIsT 1.0 (Di Guardo et al. 2015) with default parameters for each of these three populations.

To confirm homozygous LGs, a selected sample of eight individuals from C × C that collectively exhibited homozygosity for all LGs with the RosBREED Cherry 6K Illumina Infinium® SNP Array v1, was also genotyped with the recently developed RosBREED Cherry 15K Illumina Infinium® SNP array. Genotyping and SNP analysis was carried out as described previously, but SNP clustering was performed using a smaller sample (183 individuals) of sweet cherry populations and cultivars from CITA orchards. As the additional SNPs on the 15K array had not yet been placed on the linkage map generated from the C × C family, the SNP positions used were the physical positions of each SNP indicated in the array Manifest file.

Linkage map construction

Linkage map construction was performed using JoinMap 4.1® (Kyazma B.V., Netherlands; van Ooijen 2006). All individuals with more than 5% missing data and all SNPs with more than 10% missing data were excluded from map construction.

For V × C, a cross-pollination, a "*Two-step method*" (Klagges et al. 2013; Tavassolian et al. 2010), was used. In the first mapping step, only heterozygous markers in each parent were used to develop parental linkage maps. Minimum independence of LOD (= 10.0) was used for marker

grouping. All informative markers were included in the parental map construction in the first mapping round. In the second round, markers showing segregation distortion ($p < 0.01$) were excluded if they were not surrounded by other segregation distorted markers. A recombination frequency threshold of 0.6 was selected to prevent suspect linkages. False double recombination events were checked using "*Genotype Probabilities*" option with a threshold of 2.0 [− Log 10 (P)]. The Maximum Likelihood mapping algorithm with default parameters was used for LG construction (van Ooijen 2006), and recombination frequency was converted into genetic distance (centiMorgan, cM) using Kosambi's mapping function (Kosambi 1944). In the second mapping step, heterozygous markers for both parents as well as all the markers previously mapped in each parental map were used to create the V × C consensus map. SNP markers with identical segregation were included in the linkage maps using the function "*Assign identical loci to their groups*."

For the construction of the C × C and B × C2 linkage maps, in both segregating as F_2 populations, a "*One-step method*" was carried out using JoinMap 4.1. This method consisted of a single mapping step using all heterozygous markers of the parental tree. Minimum independence of LOD (= 10), a recombination frequency of 0.6, and maximum likelihood mapping algorithm were used for linkage map construction. As described for V × C mapping, markers showing segregation distortion ($p < 0.01$) were excluded when not surrounded by other markers exhibiting segregation distortion. MapChart v2.2 was used to draw linkage maps (Voorrips 2002). Deviation from expected Mendelian segregation was evaluated in the three families by Chi-square goodness-of-fit at $p < 0.001$ to avoid false positives, using JoinMap 4.1. In addition, for each progeny individual, marker data was evaluated to identify chromosomes with just monomorphic markers, and these chromosomes were presumed to be homozygous.

Comparative mapping

The genetic positions of the SNPs placed on the genetic maps constructed were compared with their physical positions in the cherry genome PAV_r1.0 (Shirasawa et al. 2017). SNP flanking sequences were searched against the cherry genome PAV_r1.0 using the BLAST function at the Genome Database for Rosaceae (GDR, www.rosaceae.org; Jung et al. 2008), and only the best matching sequence was included as a result (Online Resource 1).

The SNPs mapped in the three maps were also aligned with their physical position in the peach genome v2.0.a1 (Verde et al. 2017), and the peach physical and cherry linkage map positions were compared. When discrepancies between genetic and physical order occurred, the genetic marker order was used, and physical positions for the new marker locations were extrapolated using the physical positions of flanking markers in the peach genome v2.0.a1 (Campoy et al. 2016). Using this method, the chromosomes of C × C, B × C2, 'Vic' (V), and 'Cristobalina' (C) maps (this work) and those of 'Regina' (R), 'Lapins' (L), 'Black Tartarian' (BT), and 'Kordia' (K) (Klagges et al. 2013) were drawn using MapChart v2.2 (Voorrips 2002).

Results

SNP genotyping and linkage map construction

SNP genotyping of V × C revealed 842 SNPs (14.8%) that were polymorphic in the parental cultivars and segregating in the family. The remaining SNPs were either monomorphic (4201 SNPs, 73.7%), showed unexpected segregation (11 SNPs, 0.2%), or failed detection (642 SNPs, 11.3%) and were, therefore, discarded. From the 842 segregating SNPs, 483 (8.5%) were heterozygous in 'Vic' and 526 (9.2%) were heterozygous in 'Cristobalina' with 167 SNPs heterozygous in both cultivars. Using these markers, parental linkage maps of 'Vic' and 'Cristobalina' were constructed that each had the expected eight LGs (Table 1; Fig. 1; Online Resource 1). The 'Vic' map has 313 SNPs covering 707.2 cM, with an average distance between markers of 3.1 cM. For 'Cristobalina', 370 SNPs were mapped, spanning 659.6 cM, with an average distance between markers of 4.0 cM. The largest numbers of markers were mapped to 'Vic' LG1 (100 SNPs) and 'Cristobalina' LG2 (95 SNPs), while 'Vic' LG2 (10 SNPs) and 'Cristobalina' LG7 (5 SNPs) were the LGs with least numbers of markers. The V × C consensus linkage map has 816 markers distributed along 726.0 cM and an average distance between markers of 0.9 cM (Table 1; Fig. 1; Online Resource 1).

In the C × C family, of 526 SNPs heterozygous in 'Cristobalina', 511 were mapped to the eight LGs. This map covered 634.1 cM with an average distance between markers of 1.7 cM (Table 1; Fig. 2; Online Resource 1). Like in the 'Cristobalina' parental map, the largest and lowest numbers of markers were mapped to LG2 (105) and LG7 (9 SNPs), respectively. As expected, the 'Cristobalina' linkage map generated from the two populations (V × C and C × C) was highly similar and mostly collinear (Fig. 2); however, more SNPs were placed on the C × C map than the 'Cristobalina' V × C parental map. This difference occurred due to different criteria used for including markers in map construction. For C × C, all heterozygous markers in 'Cristobalina' could potentially be used for linkage map construction. However, the 'Cristobalina' parental map from V × C was constructed using only markers heterozygous for 'Cristobalina' and not with those that were heterozygous in both parental cultivars ('Cristobalina' and 'Vic'), as these were only used in the construction of the consensus V × C map. This effect is evident in

Table 1 Number of SNP markers, genetic length, average distance between markers, maximum gap size, and number of markers with expected Mendelian segregation distortion (SD) ($p < 0.001$) per linkage group (LG) in 'Vic' (V), 'Cristobalina' (C), V × C, C × C, and B × C2 maps

		LG1	LG2	LG3	LG4	LG5	LG6	LG7	LG8	Total
Number of markers	V	100	10	23	28	44	29	54	25	313
	C	67	95	54	34	32	49	5	34	370
	V × C	185	111	89	100	92	95	68	76	816
	C × C	85	105	66	75	51	71	9	49	511
	B × C2	133	75	70	56	48	66	51	53	552
Genetic length (cM)	V	169.8	65.3	64.2	75.7	79.2	106.7	68.7	77.6	707.2
	C	63.4	75.2	91.1	91.1	72.5	120.5	75.9	70.2	659.9
	V × C	150.3	79.8	89	78.5	71.3	108.9	76.1	72.1	726.0
	C × C	58.9	94.9	100.2	80.9	72.2	111.5	42.9	72.6	634.1
	B × C2	124.7	73.1	52.6	71.8	68.5	86.8	70.4	74.5	622.4
Average marker distance (cM)	V	1.7	7.2	2.9	2.8	1.8	3.8	1.3	3.2	3.1
	C	0.9	0.7	1.7	2.8	2.3	2.5	18.9	2.1	4.0
	V × C	0.8	1.2	1.0	0.8	0.8	1.1	1.1	0.9	0.9
	C × C	0.7	0.9	1.5	1.0	1.4	1.6	5.3	1.5	1.7
	B × C2	0.9	0.9	0.7	1.3	1.4	1.3	1.4	1.4	1.2
Largest gap size (cM)	V	18.7	50.7	15.2	8.1	16.9	23.5	7.4	29.9	50.7
	C	10.3	6.6	9.5	16.8	11.9	17.7	43.3	18.6	43.3
	V × C	6.8	5.4	6.1	6.7	7.9	7.6	10.9	5.9	10.9
	C × C	7.8	13.4	10.4	8.6	6.7	11.1	26.4	9.7	26.4
	B × C2	7.5	16.2	3.8	11.8	6.4	9.1	12.7	12.4	16.2
Number of markers with SD ($p < 0.001$)	V	–	–	–	–	–	–	–	–	0
	C	–	36	–	–	–	–	–	–	36
	V × C	–	32	–	–	–	–	–	–	32
	C × C	–	4	32	–	12	1	1	6	56
	B × C2	15	–	30	–	–	1	–	1	47

the different size observed at the top of LGs 5 and 7 and bottom of LGs 2 and 3, where heterozygous SNPs in 'Cristobalina' were only used in C × C map construction but not in the 'Cristobalina' parental map. Other differences are also observed between both maps. For example, the last SNP (ss490557364) mapped at the bottom of LG7 of 'Cristobalina' was not present in the C × C map since this marker exhibited a high level of segregation distortion and was therefore excluded from the C × C map. Therefore, a big gap spanning 26.4 cM at the bottom of LG7 in the 'Cristobalina' parental map was not detected in the C × C map (Fig. 2). Both maps have similar genetic length in total, and thus, the larger number of SNPs mapped in the C × C family resulted in a denser map although the average marker distances vary between LGs (Table 1).

SNP genotyping of the parent that was self-pollinated to generate the B × C2 family identified 589 (10.3%) heterozygous SNPs, 4725 (82.9%) homozygous SNPs, and 382 (6.7%) that failed detection. From genotyping the B × C2 family, a linkage map was constructed from 552 SNPs. The resulting map covered a total genetic length of 622.4 cM, with a marker density of 1.2 cM (Table 1; Fig. 3; Online Resource 1). Like in 'Vic', the largest number of markers and larger genetic length was observed for LG1 (133 SNPs, 124.7 cM), and like in the other two maps, LG7 had the lowest number of markers (51).

Large gaps (> 10 cM) were identified on the 'Vic' parental map for all LGs, except in LG4 and LG7 (Table 1, Fig. 1). The maximum gap on the 'Vic' map spanned 50.7 cM and was located on LG2. For 'Cristobalina', large gaps were detected on six of the eight linkage groups (LG1, 4–8), with the largest gap of 43.3 cM found on LG7. Fewer large gaps were observed on the V × C, C × C, and B × C2 maps compared to the 'Vic' and 'Cristobalina' maps. Additionally, the largest gaps were smaller in these maps than in the parental maps, revealing the generation of denser maps from consensus and the F_2 populations compared to the F_1 parental maps.

SNP markers showing distortion from the expected Mendelian segregation ratios ($p < 0.001$) were identified in all the maps constructed except in the 'Vic' parental map. The number of skewed markers ranged from 32 in the V × C consensus map to 56 in C × C, being most frequent on LG2 and LG3 (Table 1). These markers were grouped in

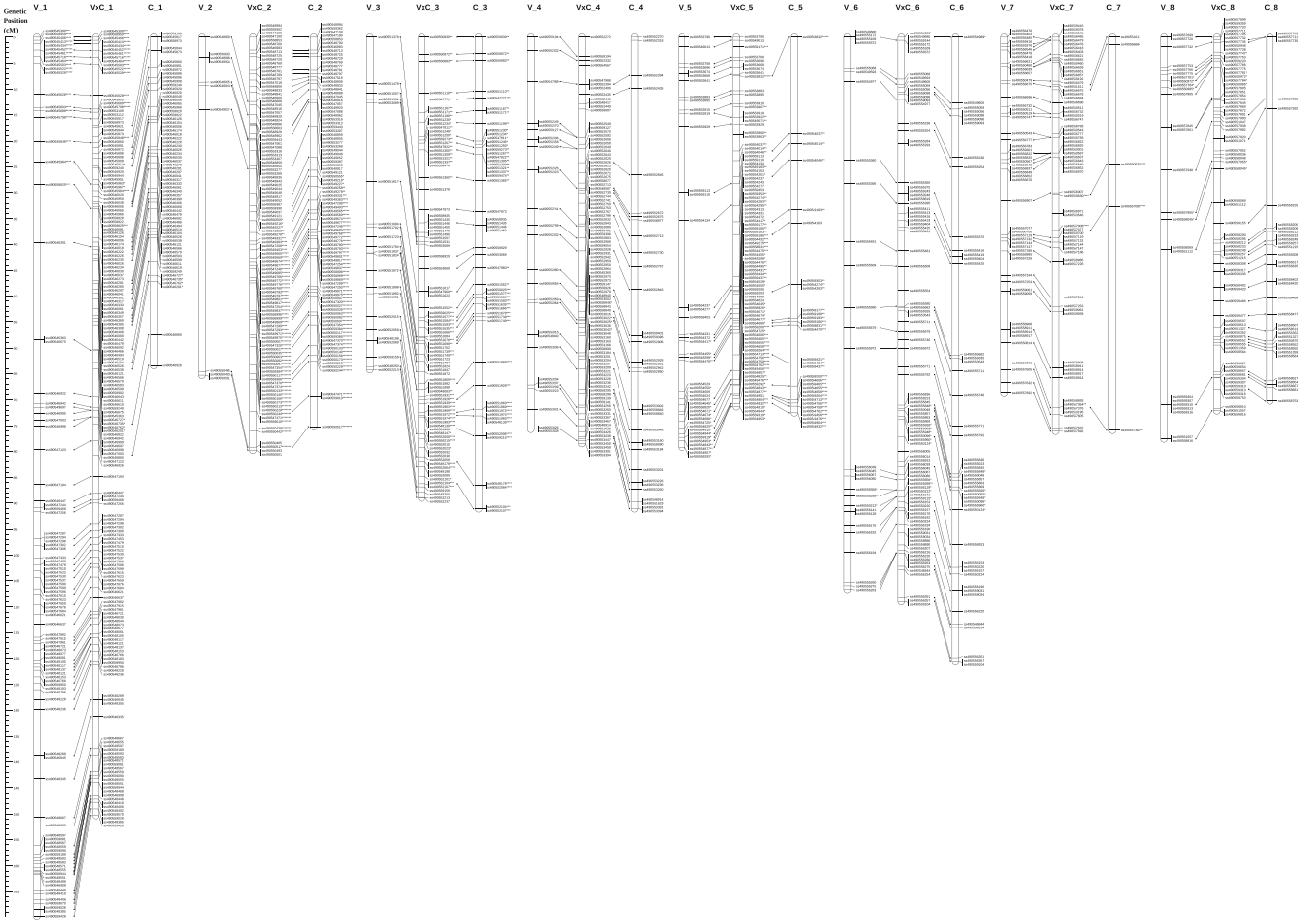

Fig. 1 'Vic' (V), 'Cristobalina' (C), and V × C consensus (V × C) linkage maps. Asterisks indicate deviation from expected Mendelian segregation (*$p < 0.1$; **$p < 0.05$; ***$p < 0.01$; ****$p < 0.005$; *****$p < 0.001$; ******$p < 0.0005$)

segregation distortion regions (SDRs; Fig. 4), such as the bottom of LG2 (26.96–27.58 Mbp) for 'Cristobalina' and C × C maps and the bottom of LG3 (16.41–25.38 Mbp) for the C × C and B × C2 maps, where the 'Cristobalina' self-compatibility locus is located (Cachi and Wünsch 2011). Segregation distortion also occurred in the C × C map, but not in the other maps, at the lower region of LGs 5 and 8 and in B × C2 at the lower part of LG1. Segregation distortion in SDRs showed distortion against one homozygous class.

Comparative mapping

Comparison of the SNPs placed on the three linkage maps with their physical position in the sweet cherry genome PAV_r1.0 (Shirasawa et al. 2017) revealed agreement in LG assignment and marker order for most of the SNPs (82%; Online Resource 1). Within each LG, only a few markers were mapped to orders that differed from that of the sweet cherry genome. However, some inverted regions were observed. These regions were located at the bottom of chromosome 1 and top of chromosomes 5, 6, and 7 (Online Resource 1). Additionally, 5% of the SNPs were mapped to different LGs than predicted by the sweet cherry genome sequence (Online Resource 2). Specifically, regions of chromosomes 2, 3, and 4 were mapped to different LGs for all maps (Online Resource 2).

Comparison of the genetic positions of the sweet cherry genetically mapped SNPs and their physical location in the peach genome v2.a.01 (Verde et al. 2017) revealed high co-linearity (Online Resource 3). However, SNPs mapped in different orders within a LG or to different LGs compared to the peach genome v2.0.a1 were observed. SNPs mapped in different orders within LGs were observed in all maps at different positions, but the number of inconsistencies was highest at the top of LG5, where an inverted region was observed for the 'Vic', V × C, and B × C2 maps compared to the peach physical map (671,433–2,722,392 bp; Online Resource 3). Some SNPs were also mapped to different LGs compared to the peach genome; some of these occurred in more than one map (Online Resource 4).

The physical positions of the RosBREED cherry 6K SNPs in the peach genome v2.a.01 were compared to the genetic

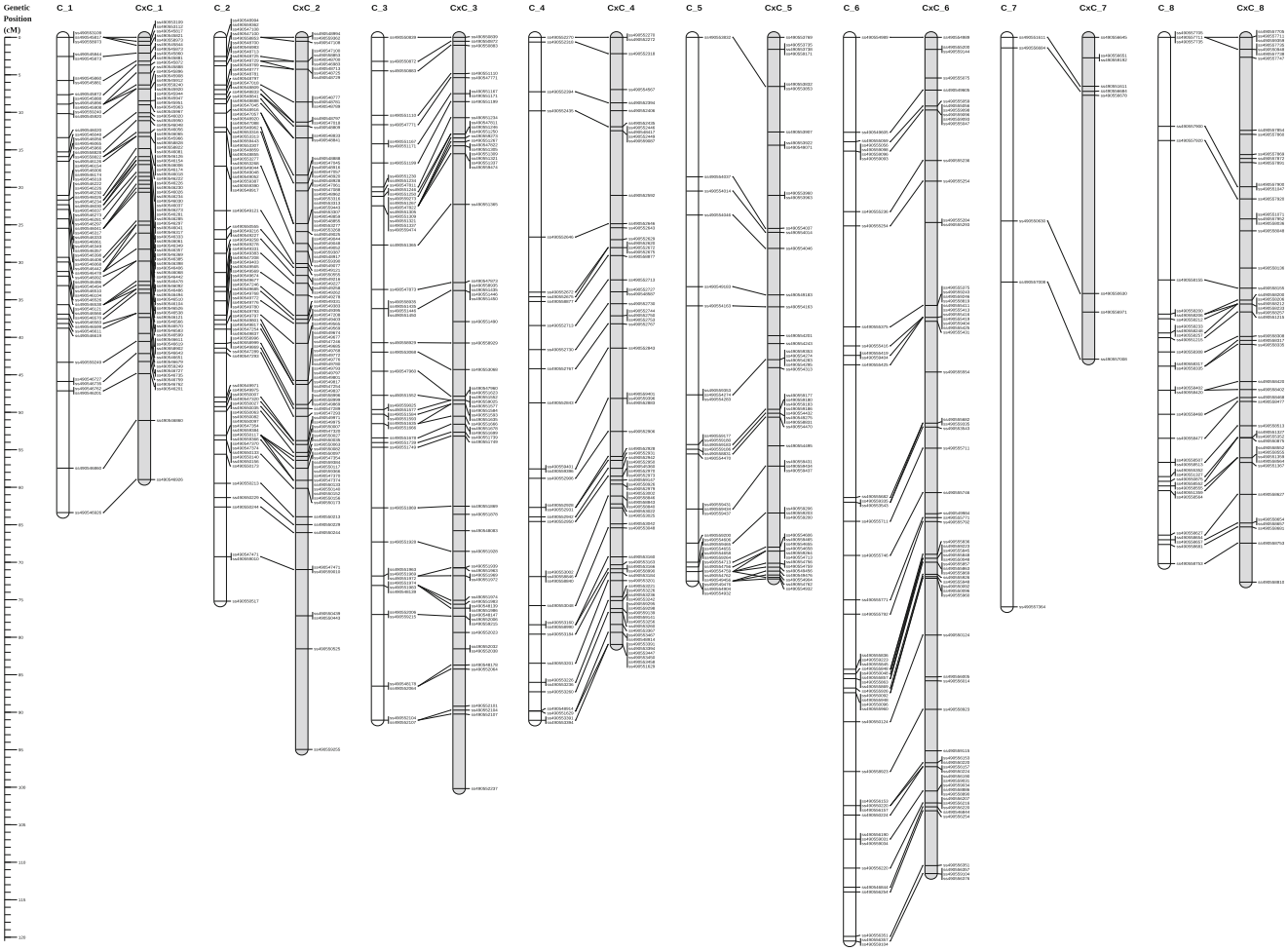

Fig. 2 'Cristobalina' parental map (white) and C × C linkage map (gray)

positions from the maps in this work and previous linkage maps using other cultivars (Klagges et al. 2013). This analysis allowed the visualization of the chromosomal regions covered by the mapped SNPs in the different sweet cherry maps (Online Resource 5). For the 'Cristobalina' and C × C maps, large regions of chromosomes 1 and 7 did not have any segregating markers. These regions could be homozygous as no heterozygous markers were detected. Thus, large presumably homozygous regions were observed in these maps for these regions. Similarly, 'Vic' was predicted to be homozygous at the top of chromosomes 2 and 3. The other cultivars also showed various regions of suspected homozygosity. This was most noticeable at the top and/or bottom of LG2 in 'Vic', 'Black Tartarian', 'Kordia', and 'Lapins'; in LG4 for 'Black Tartarian' and 'Kordia'; the top of LG5 in 'Cristobalina' and 'Kordia'; and the top of LG7 in 'Kordia'.

Homozygosity

Progeny individuals with presumably homozygous LGs based on the absence of any heterozygous SNPs on these LGs were identified in the two populations derived from self-pollination, C × C and B × C2 (Online Resource 6). For C × C, 38 individuals (38%) had one homozygous LG, 13 (13%) had two homozygous LGs, and three (3%) had three homozygous LGs. Overall, more than half of the progeny (54 individuals, 54%) had at least one homozygous LG. For C × C, LG7 was the LG most often homozygous (28 individuals), followed by LG1 and LG5 being homozygous in 12 individuals. This is consistent with 'Cristobalina' being homozygous for the majority of LGs 1 and 7 and a portion of LG 5 (Online Resource 5). In B × C2, a similar proportion, nearly half of the family (32 individuals; 48%), had trees with homozygous LGs. Of these, 23 had one homozygous LG, eight had two homozygous LGs, and one individual had four homozygous LGs. The LG most frequently homozygous was LG3, occurring for 12 individuals, while the least frequent homozygous LG was LG6 in both families.

To confirm the homozygosity of these LGs, eight individuals of C × C (Table 2) that collectively exhibited homozygosity for all LGs with SNPs from the RosBREED Cherry 6K array were also genotyped with the 15K RosBREED Cherry Illumina Infinium® SNP array. A larger number of

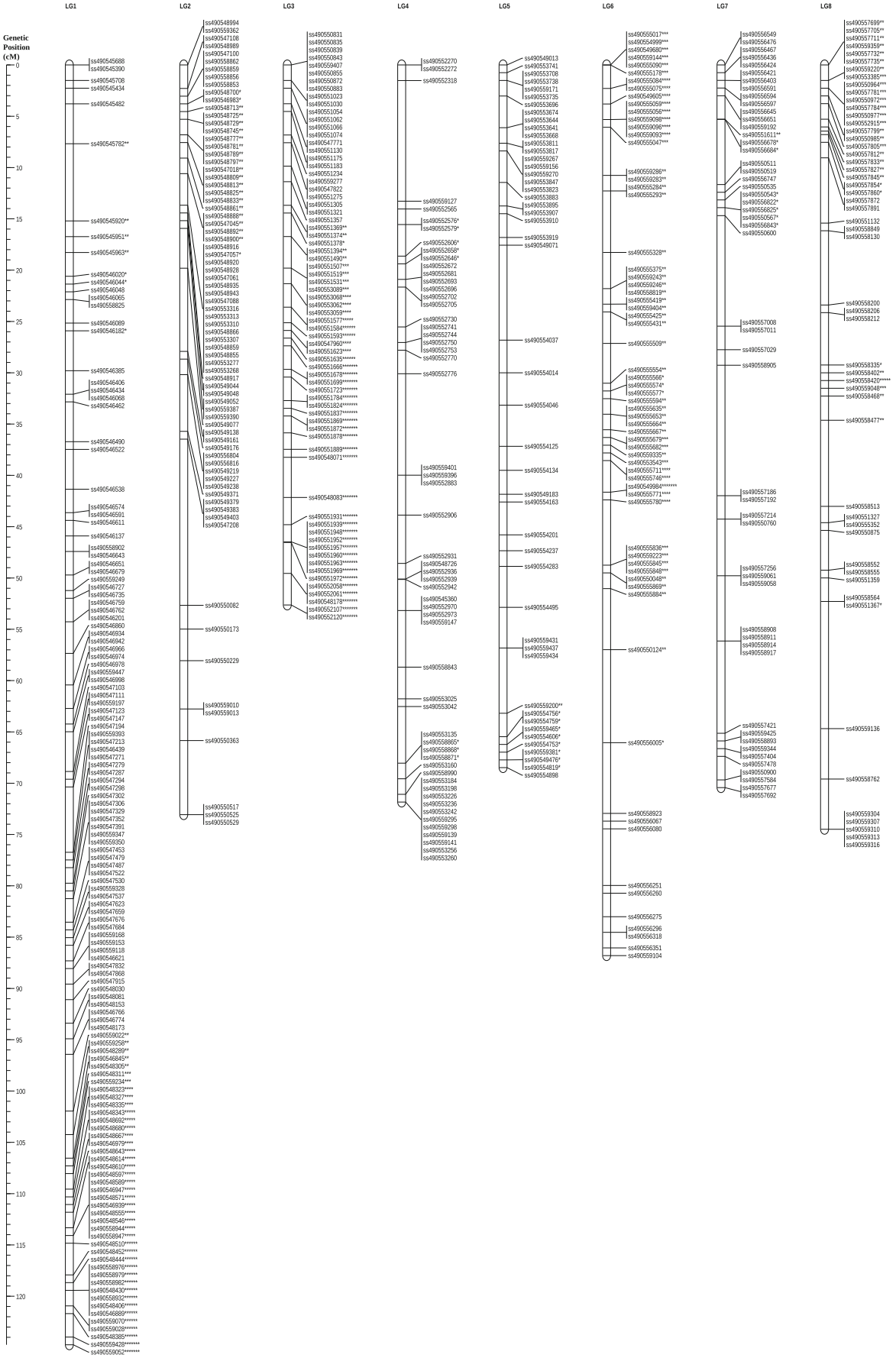
Genetic Position (cM)
LG1
LG2
LG3
LG4
LG5
LG6
LG7
LG8

◀**Fig. 3** B × C2 linkage map. Asterisk indicates deviation from expected Mendelian segregation (*$p < 0.1$; **$p < 0.05$; ***$p < 0.01$; ****$p < 0.005$; *****$p < 0.001$; ******$p < 0.0005$)

heterozygous SNPs could be scored with the 15K array in each LG (Table 2). The assay revealed that of the 16 presumably homozygous LGs in the eight trees, seven are likely homozygous after the analysis with the 15K array, as no heterozygous markers were assigned to these LGs. Furthermore, presumably homozygous linkage groups were confirmed in all LGs, except 3, 6, and 7 (Table 2). The results show that increasing the number of genotyped SNPs reduced the number of homozygous LGs, but that homozygosity was confirmed in about half of them. In the LGs that were homozygous with the 6K array and not with the 15K array, few heterozygous markers were detected indicating that large regions of homozygosity are present for these LGs. In LG7, a large number of presumably homozygous LGs were detected in the RosBREED cherry 6K array; however, this seems to be due to the low number of markers mapped to this LG with this array, as this was not the case after the analysis with the 15K array.

Discussion

Linkage maps

The three populations and linkage maps constructed in this work will be used for future QTL analysis for chilling requirement, bloom and maturity time, and fruit size. The understanding of the map coverage and regions of segregation distortion and low marker density gained from the maps generated will be critical for interpreting the forthcoming QTL results. In general, the maps developed in this work and those previously constructed using the same SNP array revealed similar numbers of markers, genetic lengths, average distances between markers, and gap sizes (Klagges et al. 2013). However, for LG7 from 'Cristobalina' and C × C and LG2 from 'Vic', very few markers were heterozygous and met the criteria for use in linkage map construction, resulting in regions with large distances between markers. This was noticeable for the 'Cristobalina' parental map when compared with the C × C map, due to the use of different mapping strategies for the F_1 and F_2 populations (Tavassolian et al. 2010). In general, the use of all heterozygous markers to develop F_2 and consensus maps resulted in higher marker density maps in the F_2 populations and in the consensus maps from the F_1 crosses, than in the parental maps.

The linkage maps constructed also identified regions that are presumably homozygous in the parental cultivars and therefore would be uninformative for QTL discovery. For example, 'Vic' is presumably homozygous for the top of LGs 2 and 3 and, therefore, homozygous for any QTL alleles that fall in these regions. Likewise, 'Cristobalina' is presumably homozygous for large portions of LGs 1 and 7, and, therefore, QTL analysis would not identify any loci in these regions. In this case, the population B × C2 will be particularly useful as it will allow an investigation of 'Cristobalina' derived alleles for regions that are not segregating in the V × C and C × C populations. Since the B × C2 population resulted from self-pollination, it will be possible to compare the effects of all three allele classes for SNPs homozygous in 'Cristobalina' (i.e., AA, AB, and BB).

Comparison with the sweet cherry and peach physical maps

Comparisons of the linkage maps developed herein, with the sweet cherry genome sequence PAV_r1.0 (Shirasawa et al. 2017), supported the genetic position and marker order of most of the markers mapped. However, because almost 30% of the sweet cherry genome was not anchored to any chromosome (Shirasawa et al. 2017), a large portion of mapped SNPs were not assigned to any chromosome and temporarily located to the cherry scaffold identified as Chr_0. In addition, some inconsistencies between linkage maps and scaffold positions could be due to minor misassembles in the cherry genome or the possibility that our use of the best matching marker position on the cherry scaffolds for each SNP did not provide an accurate comparison.

Comparison between sweet cherry linkage maps and the peach genome v2.0.a1 revealed extensive collinearity, but some markers mapped in different orders. Most noticeable was a group of markers that mapped in inverse order at the top of LG5 in the 'Vic' and B × C2 maps. This apparent inversion between the sweet cherry linkage maps and peach physical map was also observed in the 'Black Tartarian' and 'Rainier' maps (Klagges et al. 2013; Guajardo et al. 2015). For the 'Cristobalina' and 'Kordia' maps, this LG5 region is presumably homozygous, and therefore, these parental maps were uninformative for this region. When the physical positions of these inverted markers were aligned with the sweet cherry genome scaffolds (Shirasawa et al. 2017), the region was not inverted. This indicates that this region may not be inverted in the cherry genome when compared to the peach genome. However, the fact that this region appears inverted in four genetic maps from unrelated sweet cherry individuals may also indicate a real inversion that has not been correctly assembled with the sweet cherry sequence.

In the maps developed herein, some SNPs were mapped to different LGs than expected based on their positions in the peach genome sequence. Similar inconsistencies were also detected in other sweet cherry linkage maps developed using the same genotyping platform (two SNPs in 'Black Tartarian', three SNPs in 'Lapins', and six SNPs in 'Regina') (Klagges et

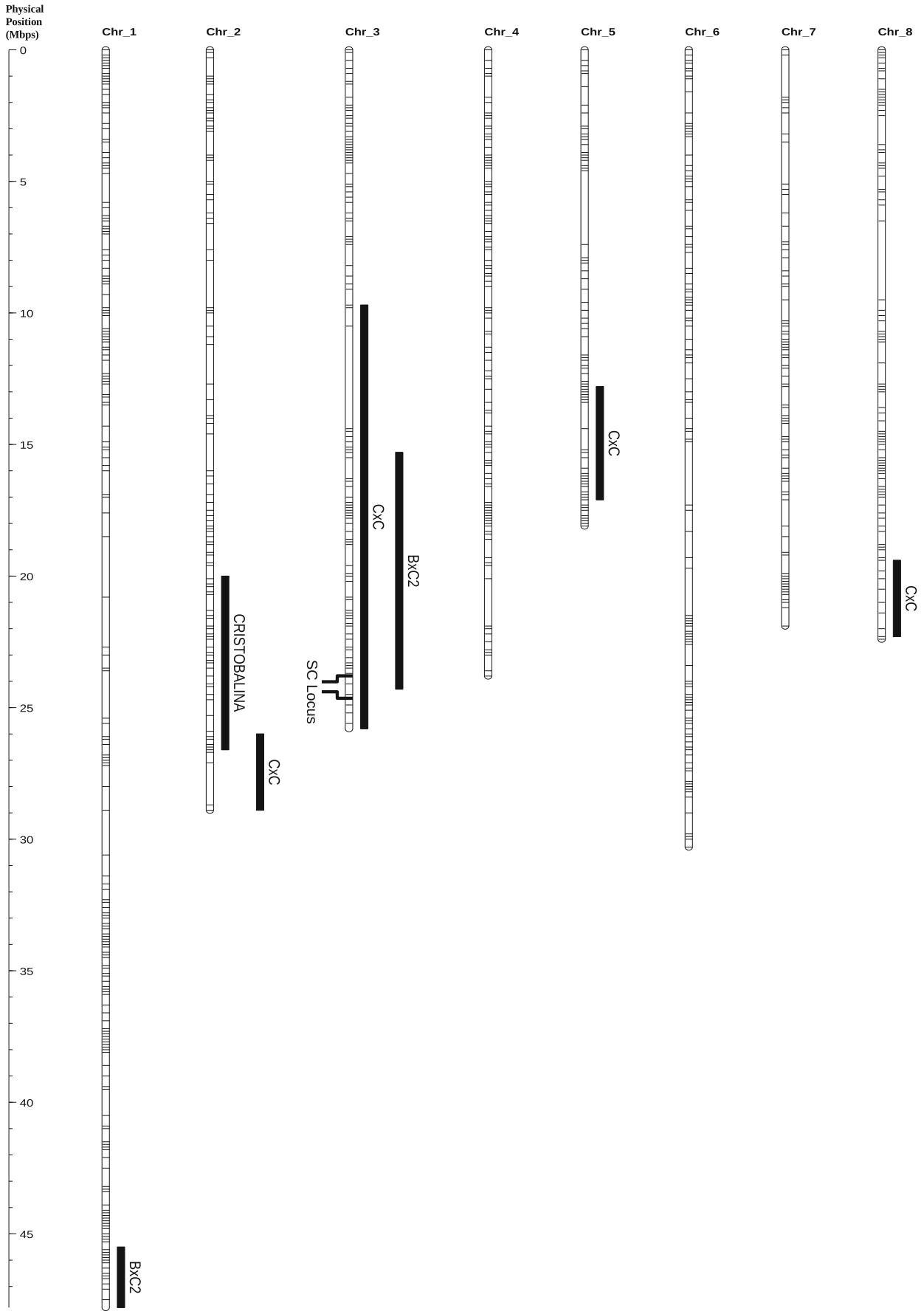
Physical Position (Mbps)
0
5
10
15
20
25
30
35
40
45
Chr_1
Chr_2
Chr_3
Chr_4
Chr_5
Chr_6
Chr_7
Chr_8
BxC2
CRISTOBALINA
CxC
SC Locus
CxC
BxC2
CxC
CxC
BxC2

◀ **Fig. 4** Physical positions of RosBREED cherry 6K SNP array v1 markers on the peach genome v2.0.a1 where segregation distortion ($p < 0.001$) was identified in 'Vic', 'Cristobalina', C × C, and B × C2 linkage maps. (SC Locus: Self-Compatibility Locus)

al. 2013). The presence of markers mapped in different LGs based on peach genome may indicate regions that are translocated from one genome to the other or duplicated (Dirlewanger et al. 2004; Fresnedo-Ramírez et al. 2013). The position of these markers could not be confirmed due to poor alignment with the current sweet cherry genome sequence. However, if these differences between the cherry and peach genome are eventually verified, they may mark species-specific genomic regions that contributed to the evolutionary differences between cherry and peach.

Segregation distortion

Skewed markers detected in this work were grouped in segregation distortion regions (SDRs). SDRs have also been detected in other species like barley (Li et al. 2010), eucalyptus (Myburg et al. 2004), oak (Bodénès et al. 2016), maize (Lu et al. 2002), or rice (Xu et al. 1997). SDRs detected in this work were also found in other sweet cherry maps. A SDR at the lower end of LG1 in B × C2 was also detected in 'Black Tartarian', 'Kordia', 'Regina', 'Lapins', and *Prunus davidiana* linkage maps (Foulongne et al. 2003; Klagges et al. 2013). Similarly, a SDR at the lower end of LG2 in 'Cristobalina' and C × C was also found in the 'Emperor Francis' and 'New York 54' maps (Olmstead et al. 2008), and a SDR at the lower region of LG8 for C × C was also detected in the 'Emperor Francis' linkage map. The presence of these SDRs in different cherry maps for LGs 1, 2, and 8 may indicate the presence of lethal and/or sub-lethal alleles in these regions that reduce viability or survival (Ward et al. 2013). The SDR identified on LG2 in this study overlaps with a QTL hotspot containing fruit and bloom time traits important for sweet cherry breeding (Cai et al. 2017); therefore, understanding the basis for segregation distortion at this region would be of interest.

Other regions with segregation distortion identified herein were specific for individual linkage maps constructed in this work. This includes the lower part of LG3 in C × C and B × C2 maps, where distorted segregation results from the pollen-expressed self-incompatibility modifier locus that is heterozygous in 'Cristobalina' that maps to this region (Cachi and Wunsch 2011; Ono et al. 2018). Only pollen containing the self-fertile allele at this locus will be able to achieve fertilization in a self-pollination, and as a result, only the self-compatible allele is inherited and segregation distortion is observed in this region. The markers with maximum distortion in this region are ss490552038, ss490552032, ss490548178, and ss490552064 in C × C (Fig. 2; Fig. 4) and are expected to map to the location of the self-incompatibility modifier locus that leads to self-compatibility. An additional region where segregation distortion was observed exclusively in C × C was the bottom region of LG5. In this region, one homozygous class was favored over the other, and therefore, for this region, deleterious recessive alleles may be selected against.

Self-pollination and chromosomal homozygosity

Sweet cherry evolved as an obligate outcrossing species due to the presence of a gametophytic self-incompatibility system. The 'Cristobalina'-derived C × C and B × C2 populations, both resulting from self-pollination, will provide a unique opportunity to investigate the impact of self-pollination on this heterozygous species. In C × C and B × C2, compared to V × C (F_1 population), a large number of individuals with one to four presumably homozygous LGs were identified in both F_2 populations, and, presumably, completely homozygous LGs were identified for all LGs in both populations. Recently, a "next-generation" RosBREED Cherry 15K Illumina Infinium® SNP Cherry Array was developed that was designed to fill gaps previously identified with the use of the 6K array (Illumina, San Diego, CA). This array was used in

Table 2 Number of heterozygous SNPs per linkage group (LG) in eight C × C progeny individuals (CC05, CC22, CC36, CC43, CC50, CC52, CC79, and CC91) identified with the RosBREED cherry 6K SNP array and the RosBREED 15K SNP array (6K/15K)

	LG1	LG2	LG3	LG4	LG5	LG6	LG7	LG8
CC05	85/168	71/142	25/55	0/0	11/30	27/95	9/51	14/26
CC22	85/162	0/0	58/148	0/7	26/58	26/83	5/35	28/76
CC36	19/48	49/93	20/59	52/124	38/80	0/11	9/36	16/26
CC43	0/8	104/193	53/138	55/143	13/30	17/55	0/25	0/0
CC50	85/167	42/72	0/1	75/171	0/0	12/56	0/13	5/16
CC52	0/0	0/0	20/62	44/87	19/40	35/108	8/48	0/0
CC79	10/25	2/11	52/142	0/2	44/106	40/131	0/17	5/22
CC91	71/133	15/33	29/87	51/124	0/2	38/134	0/17	49/10

this work to test whether the degree of homozygosity detected with the 6K array was also confirmed after analyzing a larger number of SNPs. This test revealed that the number of homozygous LGs in C × C and B × C2 was overestimated with the 6K array but confirmed the presence of large homozygous regions and homozygous LGs in the families. The finding that LG6 had the lowest level of homozygosity when considering both the C × C and B × C2 self-pollinated populations is consistent with the presence of the *S* locus on LG6. It suggests that there may be a high genetic load of presumably deleterious recessive alleles linked to the *S* locus. Taken together, these results reveal that high levels of homozygosity (up to four presumably homozygous LGs) can be tolerated in sweet cherry. The finding that 'Cristobalina' is presumably homozygous for large regions on LGs 1 and 7 and a smaller region on LG 5 suggest that it may be derived from self-pollination. If 'Cristobalina' is the result of self-pollination (S_2), then the S_2 population (C × C) would be an S_3.

Selfing in naturally outcrossing species leads to an increase in homozygosity, which may result in a decrease in fitness and fitness-related traits, characterized as inbreeding depression (Charlesworth and Charlesworth 1999). Phenotypic observations of individuals from the three mapping populations suggest that inbreeding in sweet cherry can be associated with a loss of vigor and fertility (data not presented). Trees in the C × C population are generally weak and exhibit a low vegetative vigor. The progeny only began fruiting after eight years and only 19% of the trees have fruit after 10 years. In contrast, V × C trees began fruited after five years, and 62% of trees have fruit after seven years. Furthermore, V × C is younger than C × C but shows higher vigor, measured as trunk circumference.

In conclusion, the genetic maps reported for 'Cristobalina' and its derived progeny will enable future QTL identification from this important breeding parent. In addition, the maps herein provide an opportunity to take a first look at the genome-wide impacts of self-pollination in sweet cherry. This is especially timely with the increased emphasis on the development of self-compatible cultivars using either $S_{4'}$ or naturally derived self-compatible mutations, such as the one present in 'Cristobalina'.

Acknowledgments This work was funded by the Spanish Government INIA research projects RTA2012-00103-00-00, RTA2015-00027-00-00, RFP2015-00015-00-00, and FEDER funds. A. Calle was funded by the Departamento de Industria e Innovación (Gobierno de Aragón) "Subvenciones destinadas a la contratación de personal investigador en formación 2015–2019." L. Cai was supported by the USDA-NIFA-Specialty Crop Research Initiative project, RosBREED: Enabling marker-assisted breeding in Rosaceae (2009-51181-05808) and RosBREED 2: Combining disease resistance with horticultural quality in new rosaceous cultivars (2014-51181-22378). The genotyping service was carried out at CEGEN-PRB2-ISCIII; it is supported by grant PT13/0001, ISCIII-SGEFI/FEDER.

Compliance with ethical standards

Conflict of interest The authors declare that they have no conflict of interest.

Data archiving statement Genetic linkage maps will be submitted to the Genome Database for Rosaceae (www.rosaceae.org).

References

Balas F, López-Corrales M, Serradilla MJ, Cai L, Iezzoni A, Wünsch A (in press) Firmness QTL mapping using an 'Ambrunés' x 'Sweetheart' sweet cherry population. Acta Hort

Bassil NV, Davis TM, Zhang H, Ficklin S, Mittmann M, Webster T, Mahonet L, Wood D, Alperin ES, Rosyara UR, Putten HK, Monfort A, Sargent DJ, Amaya I, Denoyes B, Bianco L, van Dijk T, Pirani A, Iezzoni A, Main D, Peace C, Yang Y, Whitaker V, Verma S, Bellon L, Brew F, Herrera R, van de Weng E (2015) Development and preliminary evaluation of a 90K Axiom® SNP array for the allo-octoploid cultivated strawberry *Fragaria* × *ananassa*. BMC Genomics 16:1

Bianco L, Cestaro A, Sargent DJ, Banchi E, Derdak S, Di Guardo M, Salvi S, Jansen J, Viola R, Gut I, Laurens F, Chagné D, Velasco R, van de Weg E, Troggio M (2014) Development and validation of a 20K single nucleotide polymorphism (SNP) whole genome genotyping array for apple (*Malus* × *domestica* Borkh). PLoS One 9(10):e110377. https://doi.org/10.1371/journal.pone.0110377

Bianco L, Cestaro A, Linsmith G, Muranty H, Denancé C, Théron A, Poncet C, Micheletti D, Kerschbamer E, Di Pierro EA, Larger S, Pindo M, Van de Weg E, Davassi A, Laurens F, Velasco R, Durel CE, Troggio M (2016) Development and validation of the Axiom® apple 480K SNP genotyping array. Plant J 86:62–74

Bodénès C, Chancerel E, Ehrenmann F, Kremer A, Plomion C (2016) High-density linkage mapping and distribution of segregation distortion regions in the oak genome. DNA Res 23:115–124

Boškovic R, Tobutt KR (1998) Inheritance and linkage relationships of isoenzymes in two interspecific cherry progenies. Euphytica 103: 273–286

Cabrera A, Rosyara UR, De Franceschi P, Sebolt A, Sooriyapathirana SS, Dirlewanger E, Quero-García J, Schuster M, Iezzoni A, van der Knaap E (2012) Rosaceae conserved orthologous sequences marker polymorphism in sweet cherry germplasm and construction of a SNP-based map. Tree Genet Genomes 8:237–247

Cachi AM, Wünsch A (2011) Characterization and mapping of non-S gametophytic self-compatibility in sweet cherry (*Prunus avium* L.). J Exp Bot 62:1847–1856

Cachi AM, Wünsch A (2014) Characterization of self-compatibility in sweet cherry varieties by crossing experiments and molecular genetic analysis. Tree Genet Genomes 10:1205–1222

Cai L, Voorrips RE, van de Weg E, Peace C, Iezzoni A (2017) Genetic structure of a QTL hotspot on chromosome 2 in sweet cherry indicates positive selection for favorable haplotypes. Mol Breed 37:85

Campoy JA, Lerigoleur-Balsemin E, Christmann H, Beauvieux R, Girollet N, Quero-García J, Dirlewanger E, Barreneche T (2016) Genetic diversity, linkage disequilibrium, population structure and construction of a core collection of *Prunus avium* L. landraces and bred cultivars. BMC Plant Biol 16:49

Chagné D, Crowhurst RN, Troggio M, Davey MW, Gilmore B, Lawley C, Vanderzande S, Hellens RP, Kumar S, Cestaro A, Velasco R, Main D, Rees JD, Iezzoni A, Mockler T, Wilhelm L, Van de Weg E, Gardiner SE, Bassil N, Peace C (2012) Genome-wide SNP

detection, validation, and development of an 8K SNP array for apple. PLoS One 7(2):e31745. https://doi.org/10.1371/journal.pone.0031745

Charlesworth B, Charlesworth D (1999) The genetic basis of inbreeding depression. Genet Res 74(3):329–340

Clarke JB, Sargent DJ, Boškovic RI, Belaj A, Tobutt KR (2009) A cherry map from the inter-specific cross *Prunus avium* 'Napoleon' × *P. nipponica* based on microsatellite, gene-specific and isoenzyme markers. Tree Genet Genomes 5:41–51

Di Guardo M, Micheletti D, Bianco L, Koehorst-Van Putten HJJ, Longhi S, Costa F, Aranzana MJ, Velasco R, Arús P, Troggio M, van de Weg EW (2015) ASSIsT: an automatic SNP scoring tool for in- and outbreeding species. Bioinformatics 31:3873–3874

Di Pierro EA, Gianfranceschi L, Di Guardo M, Koehorst-van Putten HJJ, Kruisselbrink JW, Longhi S, Troggio M, Bianco L, Muranty H, Pagliarani G, Tartarini S, Letschka T, Lozano Luis L, Garkava-Gustavsson L, Micheletti D, Bink MCAM, Voorrips RE, Aziz E, Velasco R, Laurens F, van de Weg WE (2016) A high-density, multi-parental SNP genetic map on apple validates a new mapping approach for outcrossing species. Hortic Res 3:16057

Dickson GH (1959) Vista, Venus and Vic sweet cherries. In: Ontario Hort. Expt. Sta. and Prod. Lab. Rpt. for 1957–58. Vineland Station, Ont, pp 43–44

Dirlewanger E, Graziano E, Joobeur T, Garriga-Calderé F, Cosson P, Howad W, Arús P (2004) Comparative mapping and marker-assisted selection in Rosaceae fruit crops. PNAS 101:9891–9896

Food and Agriculture Organization of the United Nations (2018). FAOSTAT database. http://www.fao.org/faostat

Foulongne M, Pascal T, Arús P, Kervella J (2003) The potential of *Prunus davidiana* for introgression into peach (*Prunus persica* (L.) Batsch) assessed by comparative mapping. Theor Appl Genet 107:227–238

Fresnedo-Ramírez J, Martínez-García PJ, Parfitt DE, Crisosto CH, Gradziel TM (2013) Heterogeneity in the entire genome for three genotypes of peach [*Prunus persica* (L.) Batsch] as distinguished from sequence analysis of genomic variants. BMC Genomics 14:750–750

Guajardo V, Solís S, Sagredo B, Gainza F, Muñoz C, Gasic K, Hinrichsen P (2015) Construction of high density sweet cherry (*Prunus avium* L.) linkage maps using microsatellite markers and SNPs detected by genotyping-by-sequencing (GBS). PLoS One 10:1–17

Hansche PE, Beres W, Doyle J, Micke WC (1988) 'Brooks' sweet cherry. Hortscience 23:664

Iezzoni A, Wünsch A, Höfer M, Giovannini D, Jensen M, Quero-García J, Campoy JA, Vokurka A, Barreneche T (2017) Biodiversity, germplasm resources and breeding methods. In: Quero-García J, Iezzoni A, Paławska LG (eds) Cherries: botany, production and uses. CAB International, Wallingford, pp 36–57

Jung S, Staton M, Lee T, Blenda A, Svancara R, Abbott A, Main D (2008) GDR (genome database for Rosaceae): integrated web-database for Rosaceae genomics and genetics data. Nucleic Acids Res 36:1034–1040

Klagges C, Campoy JA, Quero-García J, Guzmán A, Mansur L, Gratacós E, Silva H, Rosyara UR, Iezzoni A, Meisel LA, Dirlewanger E (2013) Construction and comparative analyses of highly dense linkage maps of two sweet cherry intra-specific progenies of commercial cultivars. PLoS One 8(1):e54743

Kosambi DD (1944) The estimation of map distances from recombination values. Ann Eugenics 12:172–175

Lambert P, Campoy JA, Pacheco I, Mauroux JB, Da Silva LC, Micheletti D, Bassi D, Rossini L, Dirlewanger E, Pascal T, Troggio M, Aranzana MJ, Patocchi A, Arús P (2016) Identifying SNP markers tightly associated with six major genes in peach [*Prunus persica* (L.) Batsch] using a high-density SNP array with an objective of marker-assisted selection (MAS). Tree Genet Genomes 12:121

Lewis D (1949) Structure of the incompatibility gene. II. Induced mutation rate. Heredity 3:339–355

Li H, Kilian A, Zhou M, Wenzl P, Huttner E, Mendham N, McIntyre L, Vaillancourt RE (2010) Construction of a high-density composite map and comparative mapping of segregation distortion regions in barley. Mol Gen Genomics 284:319–331

Lu H, Romero-Severson J, Bernardo R (2002) Chromosomal regions associated with segregation distortion in maize. Theor Appl Genet 105:622–628

Mahoney LL, Sargent DJ, Abebe-Akele F, Wood DJ, Ward JA, Bassil NV, Hancock JF, Folta KM, Davis TM (2016) A high-density linkage map of the ancestral diploid strawberry, *Fragaria iinumae*, constructed with single nucleotide polymorphism markers from the IStraw90 array and genotyping by sequencing. Plant Genome 9(2):1–14

Marchese A, Boškovic R, Caruso T, Raimondo A, Cutuli M, Tobutt K (2007) A new self-compatibility haplotype in the sweet cherry 'Kronio', $S_{5'}$, attributable to a pollen-part mutation in the SFB gene. J Exp Bot 58:4347–4356

Martínez-Royo A, Wünsch A (2014) Genetic structure of sweet cherry with the 6K SNP Array v1. In: 7th International Rosaceae Genomics Conference, Seattle

Myburg AA, Vogl C, Griffin AR, Sederoff RR, Whetten RW (2004) Genetics of postzygotic isolation in Eucalyptus: whole-genome analysis of barriers to introgression in a wide interspecific cross of *Eucalyptus grandis* and *E. globulus*. Genetics 166:1405–1418

Olmstead JW, Sebolt AM, Cabrera A, Sooriyapathirana SS, Hammar S, Iriarte G, Wang D, Chen CY, van der Knaap E, Iezzoni A (2008) Construction of an intra-specific sweet cherry (*Prunus avium* L.) genetic linkage map and synteny analysis with the *Prunus* reference map. Tree Genet Genomes 4:897–910

Ono K, Akagi T, Morimoto T, Wünsch A, Tao R (2018) Genome re-sequencing of diverse sweet cherry (*Prunus avium*) individuals reveals a modifier gene mutation conferring pollen-part self-compatibility. Plant Cell Physiol:pcy068. https://doi.org/10.1093/pcp/pcy068

van Ooijen JW (2006) JoinMap® 4, software for the calculation of genetic linkage maps in experimental populations. Kyazma B.V, Wageningen

Peace C, Bassil N, Main D, Ficklin S, Rosyara UR, Stegmeir T, Sebolt A, Gilmore B, Lawley C, Mockler TC, Bryant DW, Wilhelm L, Iezzoni A (2012) Development and evaluation of a genome-wide 6K SNP array for diploid sweet cherry and tetraploid sour cherry. PLoS One 7(12):e48305

Salazar J, Ruiz D, Campoy JA, Sánchez-Pérez R, Crisosto C, Martínez-García P, Blenda A, Jung S, Main D, Martínez-Gómez P, Rubio M (2014) Quantitative trait loci (QTL) and Mendelian trait loci (MTL) analysis in *Prunus*: a breeding perspective and beyond. Plant Mol Biol Report 32:1–18

Shirasawa K, Isuzugawa K, Ikenaga M, Saito Y, Yamamoto T, Hirakawa H, Isobe S (2017) The genome sequence of sweet cherry (*Prunus avium*) for use in genomics-assisted breeding. DNA Res 24(5):499–508

Soriano JM, Vera-Ruiz EM, Vilanova S, Martínez-Calvo J, Llácer G, Badenes ML, Romero C (2008) Identification and mapping of a locus conferring plum pox virus resistance in two apricot-improved linkage maps. Tree Genet Genomes 4:391–402

Stockinger EJ, Mullnix CA, Long CM, Brettin TS, Iezzoni AF (1996) A linkage map of sweet cherry based on RAPD analysis of a microspore-derived callus culture population. J Hered 87(3):214–218

Tabuenca MC (1983) Winter chilling requirements of cherry varieties. I Congreso Nacional de la Sociedad Española de Ciencias Hortícolas (Valencia). Comunicaciones, SECH: 661–667

Tao R, Iezzoni AF (2010) The S-RNase-based gametophytic self-incompatibility system in *Prunus* exhibits distinct genetic and molecular features. Sci Hortic 124:423–433

Tavassolian I, Rabiei G, Gregory D, Mnejja M, Wirthensohn MG, Hunt PW, Gibson JP, Ford CM, Sedgley M, Wu SB (2010) Construction of an almond linkage map in an Australian population Nonpareil × Lauranne. BMC Genomics 11:551

Verde I, Bassil N, Scalabrin S, Gilmore B, Lawley CT, Gasic K, Micheletti D, Rosyara UR, Cattonaro F, Vendramin E, Main D, Aramini V, Blas AL, Mockler TC, Bryant DW, Wilhelm L, Troggio M, Sosinski B, Aranzana MJ, Arús P, Iezzoni A, Morgante M, Peace C (2012) Development and evaluation of a 9K SNP array for peach by internationally coordinated SNP detection and validation in breeding germplasm. PLoS One 7(4):e35668

Verde I, Abbott AG, Scalabrin S, Jung S, Shu S, Marroni F, Zhebentyayeva T, Dettori MT, Grimwood J, Cattonaro F, Zuccolo A, Rossini L, Jenkins J, Vendramin E, Meisel LA, Decroocq V, Sosinski B, Prochnik S, Mitros T, Policriti A, Cipriani G, Dondini L, Ficklin S, Goodstein D, Xuan P, Del Fabbro C, Aramini V, Copetti D, Gonzalez S, Horner D, Falchi R, Lucas S, Mica E, Maldonado J, Lazzari B, Bielenberg D, Pirona R, Miculan M, Barakat A, Testolin R, Stella A, Tartarini S, Tonutti P, Arús P, Orellana A, Wells C, Main D, Vizzotto G, Silva H, Salamini F, Schmutz J, Morgante M, Rokhsar DS (2013) The high-quality draft genome of peach (*Prunus persica*) identifies unique patterns of genetic diversity, domestication and genome evolution. Nat Genet 45(5):487–496

Verde I, Jenkins J, Dondini L, Micali S, Pagliarani G, Vendramin E, Paris R, Aramini V, Gazza L, Rossini L, Bassi D, Troggio M, Shu S, Grimwood J, Tartarini S, Dettori MT, Schmutz J (2017) The Peach v2.0 release: high-resolution linkage mapping and deep resequencing improve chromosome-scale assembly and contiguity. BMC Genomics 18:1–18

Vilanova S, Romero C, Abbott AG, Llácer G, Badenes ML (2003) An apricot (*Prunus armeniaca* L.) F_2 progeny linkage map based on SSR and AFLP markers, mapping plum pox virus resistance and self-incompatibility traits. Theor Appl Genet 107:239–247

Voorrips RE (2002) MapChart: software for the graphical presentation of linkage maps and QTLs. J Hered 93(1):77–78

Wang J, Zhang K, Zhang X, Yan G, Zhou Y, Feng L, Ni Y, Duan X (2015) Construction of commercial sweet cherry linkage maps and QTL analysis for trunk diameter. PLoS One 10(10):e0141261

Ward JA, Bhangoo J, Fernández-Fernández F, Moore P, Swanson JD, Viola R, Velasco R, Bassil N, Weber CA, Sargent DJ (2013) Saturated linkage map construction in *Rubus idaeus* using genotyping by sequencing and genome-independent imputation. BMC Genomics 14(2):1–14

Wünsch A, Hormaza JI (2004) Genetic and molecular analysis in Cristobalina sweet cherry, a spontaneous self-compatible mutant. Sex Plant Reprod 17:203–210

Xu Y, Zhu L, Xiao J, Huang N, McCouch SR (1997) Chromosomal regions associated with segregation distortion of molecular markers in F_2, backcross, double haploid, and recombinant inbred populations in rice (*Oryza sativa* L.). Mol. Gen. Genet 253:535–545

Zhang YM (2012) F_2 designs for QTL analysis. Methods Mol Biol 871: 17–29

APPENDIX II - ABBREVIATIONS

A×C: ‘Ambrunés’ × ‘Cristobalina’
A×S: ‘Ambrunés’ × ‘Sweetheart’
AGL24: Agamous-like 24
ANOVA: Analysis of variance
B×C: ‘Brooks’ × ‘Cristobalina’
B×C2: ‘BC8’ × ‘BC8’
BAM: Binary alignment map
BF: Bayes factor
BLUP: Best linear unbiased prediction
BT: Bloom time
C×C: ‘Cristobalina’ × ‘Cristobalina’
CA: *ρ*-coumaric acid
CD: Calendar day
CICYTEX: Centro de Investigaciones Científicas y Tecnologicas de Extremadura
CITA: Centro de Investigación y Tecnología Agroalimentaria de Aragón
cM: centiMorgan
CNV: Cell number varitaion
CQA: *ρ*-coumaroylquinic acid
CR: Chilling requirement
CTIFL: Centre Technique Interprofessionnel des Fruits et Légumes
Cy3-glu: cyanidin 3-O-glucoside
Cy3-rut: cyanidin 3-O-rutinoside
DAM: Dormancy associated MADs-box
DDBJ: DNA Data Bank of Japan
DPD: *DAM* promoter deletion
DPDF: *DAM* promoter deletion forward
DPDR: *DAM* promoter deletion reverse
EVG: Evergrowing peach mutant
FAR1: Far-red impaired response 1

FD: Fruit development time
FF: Fruit firmness
FS: Fruit size
FT: Flowering Locus T
FW: Fruit weight
GBS: Genotyping by sequencing
GBV: Genome breeding value
GDH: Growing degree hours
GDR: Genome Database for Rosaceae
GFF: General File Format
H^2: Broad-sense heritability
HPLC: High-performance liquid chromatography
HR: Heat requirement
IGV: Integrative genomic viewer
INDEL: Insertion/deletion
INRA: Institut National de la Recherche Agronomique
L×C: 'Lambert' × 'Cristobalina'
LG: Linkage group
LOD: Logarithm of odds
MAS: Marker-assisted selection
MCL: Maximum composite likelihood
MCMC: Markov chain Monte Carlo
MD: Maturity date
MQM: Multiple QTL mapping
NA: neochlorogenic acid
NCBI: National Center for Biotechnology Information
NGS: Next generation sequencing
NT: Nucleotide
PARC: Pacific Agri-Food Research Centre
PCR: Polymerase chain reaction
Peo3-glu: peonidin 3-O-glucoside
Peo3-rut: peonidin 3-O-rutinoside
POD: Protected Designation of Origin
PPC: Parent-Parent-Child

PV: Phenotype variation

PVE: Percentage of variation explained

QTL: Quantitative trait locus

R×G: 'Regina' × 'Garnet'

R×L: 'Regina' × 'Lapins'

RAPD: Random amplification of polymorphic DNA

SC: Self-compatibility

SD: Segregation distortion

SDR: Segregation distortion region

SLAF: Specific-Locus Amplified Fragment

SNP: Single nucleotide polymorphism.

SSC: Solid soluble content

SSR: Simple sequence repeat

SVP: Short vegetative phase

TA: Titratable acidity

TBE: Tris-borato-EDTA

UPOV: International Union for the Protection of new Varieties of plants

V×C: 'Vic' × 'Cristobalina'

Y1: Year 1

Y2: Year 2